



Experiments in Nuclear Science

AN34 Laboratory Manual Third Edition, Revised

Introduction to Theory and Basic Applications

Alpha, Beta, Gamma, X-Ray, and Neutron
Detectors and Associated Electronics

Published September 1987.

Preface

The series of experiments included in this Laboratory Manual provide an introduction to the various techniques that are currently used to study nuclear science and a framework to help the student learn. The methodology, list of equipment, and step-by-step instructions that are needed are included in each experiment, together with sufficient reference material and theoretical information about the experiment to help the student interpret results.

EG&G ORTEC has tried to consider all major disciplines that are involved in nuclear science. These include physics, chemistry, biology, radiopharmacy, nuclear engineering, and other specialized nuclear technologies. By consulting many sources, EG&G ORTEC has determined which of these experiments are most appropriate to each discipline; the sources include university professors, appropriate texts, experimental manuals, and the published recommendations of the U.S. Department of Energy (DOE) and other government agencies. From these studies, EG&G ORTEC recommends the following basic experiment groups for each of the major disciplines:

Physics	1 through 21, and 23 through 26.
Chemistry	1 through 6, and 12, 17, 23, 24, and 26.
Biology	1 through 7, and 12, 17, 22, 23, and 24.
Radiopharmacy	1 through 6, and 17, 22, 23, and 24.
Nuclear Engineering	1 through 9, and 12, 13, 14, 15, 17, and 23 through 26.
Nuclear Technology	1 through 6, and 12, 17, 22, 23, and 24.

The series of experiments that are appropriate to nuclear technology are also appropriate for nuclear technician training. Other combinations of experiments can be derived for use in other fields of interest such as environmental studies, medical research, quality control and many more in the rapidly growing list of nuclear applications.

Most of the 26 experiments are divided into parts that can be completed in an average time of 30 to 45 minutes and can be performed independently. For example, Experiment 3 deals with gamma-ray spectroscopy and includes Experiments 3.1 through 3.10. All experiments that are to be made, however, should be done in sequence. The experiments are provided for educational purposes and can be duplicated for class use as desired.

A complete nuclear laboratory, or one that is designed to serve a given area, can be set up with the aid of the information that is furnished in this Laboratory Manual.

EG&G ORTEC hopes that this manual will benefit you in your Nuclear Science Program.

Acknowledgements

EG&G ORTEC wishes to thank the author, Professor Jerome L. Duggan, Texas State University, for writing these experiments and for his continued support of this effort from rough draft to publication. EG&G ORTEC also wishes to thank university professors all over the world for their comments and suggestions.

The author wishes to thank Professor Dollard Desmarais of the University of Alberta, Canada, for his assistance with Experiments 21, 25, and 26. He also wishes to thank the many university professors throughout the world who have performed the experiments with their students in the first two editions of this manual and were kind enough to send their comments and suggestions to us for consideration in our revisions.

Este manual é de propriedade da EG&G ORTEC tendo sido obtido a partir do endereço:

<ftp://ftp.egginc.com/divisions/iras/ORTEC/homepage/AppNotes/AN34/>

A presente reprodução objetiva fins educacionais e não possui fins comerciais ou lucrativos.

AN34 Table of Contents

[Errata](#) **Obsolete Model Replacements**

[Safe Handling of Radioactive Sources](#)

[Experiment 1](#) **Basic Identification in Electronic Measurement Systems**

- 1.1 Observing the Direct and Attenuated Outputs of the Pulser
- 1.2 Using the Pulser as the Linear Input to a Typical Counting System
- 1.3 Using a Single-Channel Analyzer

[Experiment 2](#) **Geiger Counting**

- 2.1 Operating Plateau for the Geiger Tube
- 2.2 Half-Life Determination
- 2.3 Resolving-Time Corrections for the Geiger Counter
- 2.4 Linear Absorption Coefficient
- 2.5 Inverse Square Law
- 2.6 Counting Statistics

[Experiment 3](#) **Gamma-Ray Spectroscopy Using NaI(Tl)**

- 3.1 Energy Calibration
- 3.2 Energy Analysis of an Unknown Gamma Source
- 3.3 Spectrum Analysis of ^{60}Co and ^{137}Cs
- 3.4 Energy Resolution
- 3.5 Activity of a Gamma Emitter (Relative Method)
- 3.6 Activity of a Gamma Emitter (Absolute Method)
- 3.7 Mass Absorption Coefficient
- 3.8 The Linear Gate in Gamma-Ray Spectroscopy
- 3.9 Sum Peak Analysis
- 3.10 Photoelectric Absorption

[Experiment 4](#) **Alpha Spectroscopy with Surface Barrier Detectors**

- 4.1 Simple Alpha Spectrum and Energy Calibration with a Pulser
- 4.2 Energy Determination of an Unknown Alpha Source
- 4.3 Energy Calibration with Two Alpha Sources
- 4.4 Absolute Activity of an Alpha Source
- 4.5 Spectrum Expansion with a Biased Amplifier
- 4.6 Decay Ratios for ^{241}Am

[Experiment 5](#) **Energy Loss of Charged Particles (Alphas)**

- 5.1 dE/dx for Alpha Particles in Copper Foil
- 5.2 dE/dx for Alpha Particles in Gas

[Experiment 6](#) **Beta Spectroscopy**

- 6.1 Calibration with a Pulser
- 6.2 Beta End-Point Determination for ^{204}Tl

6.3 Conversion Electron Ratios

Experiment 7 High-Resolution Gamma-Ray Spectroscopy

- 7.1 Energy Resolution with an HPGe Detector
- 7.2 Photopeak Efficiency for HPGe Detectors
- 7.3 Escape Peaks and Efficiency for HPGe Detectors
- 7.4 The Response of HPGe Detectors to High-Energy Gammas

Experiment 8 High-Resolution X-Ray Spectroscopy

- 8.1 Energy Calibration with a Pulser
- 8.2 Efficiency Measurements and Energy Calibration with Standard X-Ray Sources
- 8.3 Mass Absorption Coefficient for X Rays

Experiment 9 Time Coincidence Techniques and Absolute Activity Measurements

- 9.1 Simple Fast Coincidence
- 9.2 Fast Coincidence and the Time-to-Amplitude Converter
- 9.3 Determination of Absolute Activity by the Coincidence Method

Experiment 10 Compton Scattering

- 10.1 Simple Compton Scattering (Energy Determination)
- 10.2 Simple Compton Scattering (Cross-Section Determination)
- 10.3 Compton Scattering (Coincidence Method)
- 10.4 Compton Scattering (Electron Recoil Energy)

Experiment 11 The Proportional Counter and Low-Energy X-Ray Measurements

- 11.1 Energy Calibration
- 11.2 Mass Absorption Coefficient for Low-Energy X Rays

Experiment 12 X-Ray Fluorescence

- 12.1 X-Ray Fluorescence with a Proportional Counter
- 12.2 X-Ray Fluorescence with a Si(Li) Detector

Experiment 13 Gamma-Gamma Coincidence

- 13.1 Overlap Coincidence Method for Measuring Gamma-Gamma Coincidence of ^{22}Na
- 13.2 Linear Gate Method for Measuring Gamma-Gamma Coincidence of ^{22}Na
- 13.3 Time-to-Amplitude Converter Method for Measuring Gamma-Gamma Coincidence of ^{22}Na

Experiment 14 Nuclear Lifetimes and the Coincidence Method

- 14.1 Lifetime Measurement of the 14-keV State in ^{57}Fe Using the TAC Method
- 14.2 Lifetime Measurement of the 14-keV State in ^{57}Fe Using the Delayed Coincidence Method
- 14.3 Alternate Detectors to be Used with the Electronics in Experiments 14.1 and 14.2

- Experiment 15** **Rutherford Scattering of Alphas from Thin Gold Foil**
 15.1 The Rutherford Cross Section
 15.2 The Z^2 Dependence of the Rutherford Cross Section
- Experiment 16** **The Total Neutron Cross Section and Measurement of the Nuclear Radius**
- Experiment 17** **Neutron Activation Analysis (Slow Neutrons)**
 Neutron Flux Determination
 17.1 Measurement of the Thermal Neutron Cross Section for the $^{51}\text{V}(n, g) ^{52}\text{V}$ Reaction
 17.2
 17.3 Determination of the Half-Life for the $^{27}\text{Al}(n, g) ^{28}\text{Al}$ Reaction
 17.4 The Saturation Factor in Neutron Activation Analysis
 17.5 The Study of a Complex Sample with Two Half-Lives Present
 17.6 Thermal Neutron Shielding
 17.7 The Measurement of Thermal Neutron Activation Cross Sections of Elements with High Sensitivity Ratios
- Experiment 18** **Neutron Activation Analysis (Fast Neutron)**
 Gammas and Half-Lives from (n, p) Reactions
 18.1 Optional (n, p) Reactions that can be Studied
 18.2
- Experiment 19** **A Study of the Decay Scheme and Angular Correlation of ^{60}Co**
 19.1 Verification of the Gamma-Gamma Coincidence of ^{60}Co
 19.2 Angular Correlation of ^{60}Co
- Experiment 20** **A Study of the Decay Scheme of ^{244}Cm by an Alpha X-Ray Coincidence Experiment**
- Experiment 21** **Alpha-Induced Innershell Ionization Studies with an ^{241}Am Source**
 Innershell Ionization Induced by Alpha Particles
 21.1 Efficiency of the Si(Li) Detector
 21.2 The Innershell Ionization Measurements
 21.3
- Experiment 22** **Measurements in Radiation Biology**
 Geometrical Considerations in Radiobiological and Medical Experiments
 22.1 ^{131}I Uptake Studies in Rats
 22.2 Translocation of Radio-Phosphorus in Plants
 22.3
- Experiment 23** **Nuclear Techniques in Environmental Studies**
 A Study of Environmental Samples by Tube-Excited Fluorescence Analysis
 23.1 A Study of Environmental Samples by Source-Excited Fluorescence Analysis
 23.2 A Study of Environmental Samples Using Neutron Activation Analysis and
 23.3 High-Resolution Gamma Spectroscopy

Experiment

24

Measurements in Health Physics

- Gamma Intensity as a Function of Distance
- 24.1 Gamma Intensity Measured with a Geiger Counter
- 24.2 Shielding Effectiveness of Different Materials for Gammas
- 24.3 Attenuation of Betas in Aluminum by the Geiger Mueller Method
- 24.4 Attenuation of Betas in Aluminum by the Surface Barrier Detector Method
- 24.5 A Study of Paraffin as a Neutron Shielding Material
- 24.6 A Study of Lead as a Neutron Shielding Material
- 24.7

Experiment

25

Time-of-Flight Spectroscopy

- Alpha Particle Time-of-Flight and Energy Loss Measurements
- 25.1 Gamma Ray Time-of-Flight and the Speed of Light
- 25.2

Experiment

26

Fission Fragment Energy Loss Measurements from ^{252}Cf

- Energy Calibration for Fission Fragments
- 26.1

Appendix

- Linear and Logic Signal Standards in EG&G ORTEC NIM Instruments
- Equipment and Supplies Identified by Code
- Glossary
- Relative Sensitivities of Elements to Thermal Neutron Activation
- X-Ray Critical-Absorption and Emission Energies in KeV



AN34 Errata Model Replacements

Experiment	Model and Description	Replacement
No. 4	Model 408A Biased Amplifier	Model 444 Gated Biased Amplifier
No. 7	Model 459 5-kV Detector Bias Supply	Model 659 5-kV Detector Bias Supply
No. 8	Model 459 5-kV Detector Bias Supply	Model 659 5-kV Detector Bias Supply
No. 11	Model 904-1B Thin-Window Proportional Counter	Model 904 Proportional Detector
No. 12	Model 904-1B Thin-Window Proportional Counter	Model 904 Proportional Detector
No. 14	Model 905-1B Thin-Window NaI(Tl) Detector with PMT	Model 905-1 NaI Scintillation Detector
No. 20	Model 408A Biased Amplifier Model 905-1B Thin-Window NaI(Tl) Detector with PMT	Model 444 Gated Biased Amplifier Model 905-1 NaI Scintillation Detector
No. 21	Model 459 5-kV Detector Bias Supply	Model 659 5-kV Detector Bias Supply
No. 23	Model 459 5-kV Detector Bias Supply TEFA (Complete System) is no longer available	Model 659 5-kV Detector Bias Supply
No. 25	Model 459 5-kV Detector Bias Supply	Model 659 5-kV Detector Bias Supply

Safe Handling of Radioactive Sources

Several types of radioactive sources are used for the experiments in this manual. The simple rules given in this section will assure safe handling of these sources.

Never eat, drink, or smoke in the laboratory counting area. Wash your hands at the end of each laboratory experiment. In Experiment 22 liquid sources are used; therefore, special clothing and gloves should be worn.

Source Kits SK-1G, SK-1X, and SK-1B contain sealed sources. These sources contain activities $<1 \mu\text{Ci}$ and can be safely handled with your fingers. It is good practice to always handle these sources by the edge of the disk.

All of the alpha sources (Source Kit SK-1A) used in this manual are unsealed and should be handled very carefully to avoid wiping any of the radioactive spot onto hands, clothing, or equipment. Any source that has an activity $>10 \mu\text{Ci}$ should be handled with tongs.

Experiments 16, 17, and 18 require the use of a 1–3 Ci Am-Be neutron source. These sources are quite dangerous if not handled properly. Tongs or a 1-meter length string should be used in handling these neutron sources. For Experiment 17, the neutron source can be transferred to the Activation Howitzer and locked in position for safe activation. The complete techniques for handling neutron sources are usually included with the shipping container of the source.

Survey meters should be available in the nuclear counting laboratory to monitor all sources of activity $>5 \mu\text{Ci}$.

Handling of Sources

1. Source Kits SK-1X, SK-1G, SK-1B	$\sim 1 \mu\text{Ci}$	May be handled with fingers.
2. Source Kit SK-1A and all weak alpha sources	$\sim 1 \mu\text{Ci}$	May be handled with fingers but care must be taken not to touch the radioactive spot.
3. Any sources sealed or unsealed	$>10 \mu\text{Ci}$	Use tongs or other devices. Do not handle directly.
4. Neutron sources	1–3 Ci	Use tongs. Follow the instructions provided by the manufacturer or those required in the license application.

Measurements in Health Physics from a Practical Point of View

In order to use isotopes in a counting laboratory, it is necessary to understand and use good health physics practices. Most of the sources used in this AN 34 series of experiments are sealed, low-activity sources and hence present no real health physics problems. In many industrial, medical, and research laboratories, high-activity unsealed sources are frequently used. If a liquid source is accidentally spilled, the procedures for determining the types of radiation and the activity of the smears that are taken from the area are exactly the same as those outlined in the preceding experiments. For added safety, however, consult the local health-physics authorities for specific instructions.

If in the course of research it is necessary to use a “hot” source, it is wise to minimize exposure by: (1) staying in the area of the source a minimum amount of time; (2) staying as far away from the source as is practical for the indicated measurement; and (3) using the proper shielding material between yourself and the source.

With a knowledge of the activity of the source and a wise compromise between shielding, distance, and time, we can safely use radioisotopes in all actual laboratory situations.

Basic Identifications in Electronic Measurement Systems

EQUIPMENT NEEDED FROM EG&G ORTEC

480 Pulser

113 Scintillation Preamplifier

575A Amplifier

551 Timing Single-Channel Analyzer

875 Counter

Bin and Power Supply

ORC-1 Cable Set

Tektronix 2213A Oscilloscope or equivalent

Purpose

All of the experiments described in this manual require that some combination of electronic instrument modules be interconnected and adjusted to provide the desired information. The purpose of this experiment is to familiarize the student with the basic techniques to use in checking for proper system arrangement and responses.

Electronic Circuits

The first part of this experiment provides familiarity with the oscilloscope. This is the instrument that is used for observing the input and output pulses for the various modules in the system to determine whether the waveshapes, amplitudes, and timing are correct with respect to the rest of the equipment.

Next is an introduction to a pulse generator. This is an instrument that simulates the pulses that would originate in a nuclear radiation detector and furnishes the pulses with the known characteristics into the input of the system. The pulse generator is used for calibration, timing, and certain test operations. Used together, the oscilloscope and pulse generator can assure the student that the electronics have been set up according to the block diagrams that accompany each experiment so that the series of exercises can be completed as required.

The system that is used in this experiment includes a group of modules that are basic to many experiments: a preamplifier, an amplifier, a threshold discriminator, a single-channel

analyzer (SCA), a counter, and an oscilloscope. Each module provides a necessary function in the overall system, which, in this combination, is a simple counting system.

These electronic modules are divided into two general types, logic and linear. A more complete discussion of these devices is included in the Appendix, "Linear and Logic Signal Standards in EG&G ORTEC NIM Instruments." Briefly, a logic module is a device that generates an output pulse of fixed amplitude if its logic criteria are met. The simplest example of a logic device is a threshold discriminator, which gives an output pulse (always with the same amplitude) every time it receives an input pulse that has an amplitude greater than the threshold level. The SCA is another good example of a logic module. A linear module is one in which the output linear signal contains information such as the energy of an incident particle that has been absorbed in a detector.

Measurement of the energies of alpha particles with a surface barrier detector illustrates the use of both linear and logic modules. A simplified electronic block diagram for this measurement is shown in Fig. 1.1.

The alpha particles from the source produce pulses from the detector whose magnitudes are proportional to the energies of the alpha particles. The preamplifier and amplifier simply (at least for this discussion) amplify each pulse by an adjusted gain factor and provide some pulse shaping.

Let us assume that the alpha particles have an energy of 5 MeV and that the output of the preamplifier is a series of

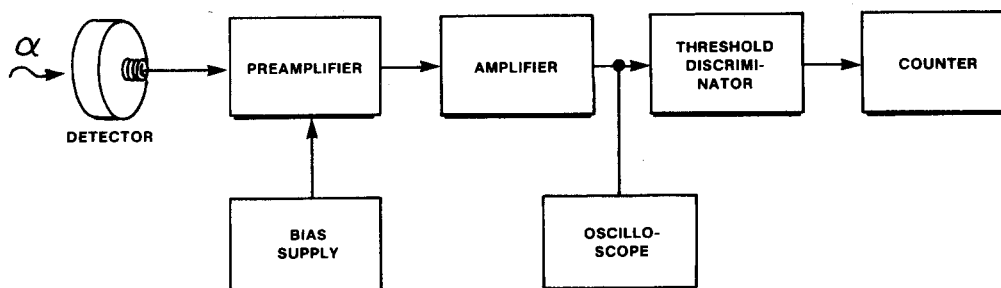


Fig. 1.1. Block Diagram for Alpha-Particle Measurements.

0.5-V pulses. Let us further assume that the gain of the amplifier is set at 10. Then the output pulses from the amplifier will have an amplitude of 5 V. If everything is left the same except that the 5-MeV alpha source is replaced with a 6-MeV alpha source, then the output pulses from the preamplifier would be 0.6 V and those from the amplifier would be 6 V. In this example the linear signal is the output of the amplifier and it contains information with regard to the energy of the alpha particle that originated the pulse. That is, the output of the amplifier is proportional to the energy of the alpha particle.

Figure 1.2 shows how the output of the amplifier might look on an oscilloscope with both 5- and 6-MeV alphas impinging on the detector.

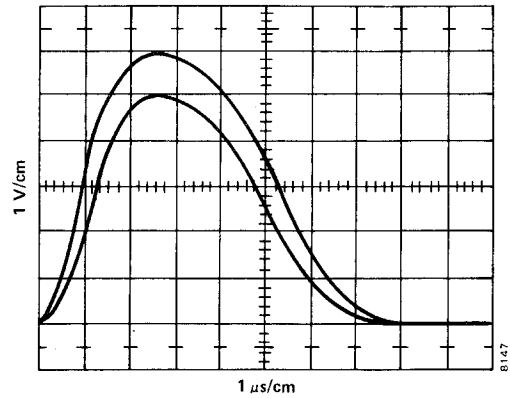


Fig. 1.2. Typical Amplifier Output.

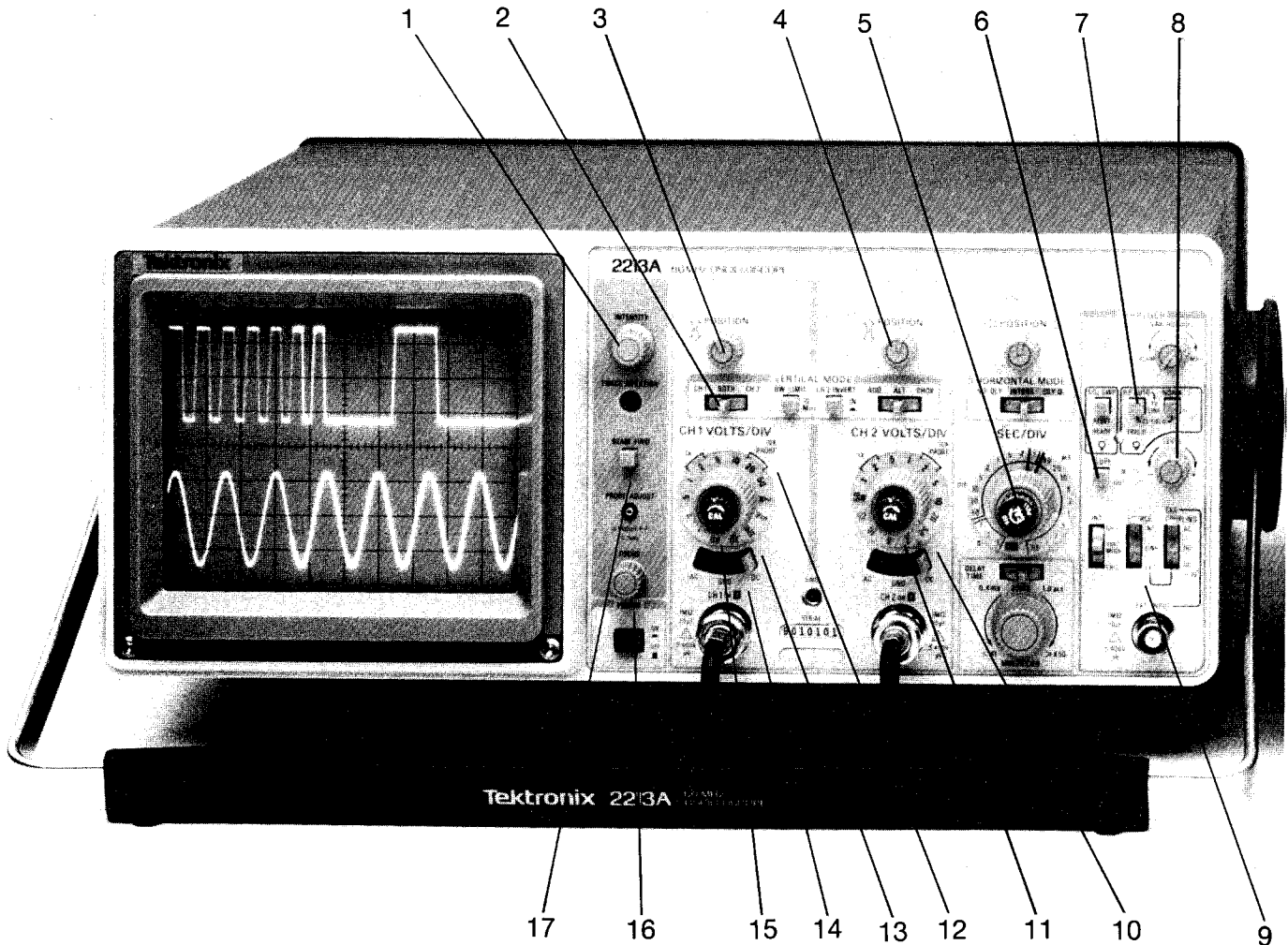


Fig. 1.3. Tektronix 2213A Oscilloscope Front Panel.
(Courtesy of Tektronix, Incorporated.)

Each time a 5-MeV alpha particle strikes the detector, a 5-V pulse is produced, etc. Therefore, in addition to the pulse-height information, the number of linear signals can also tell how many events of a given pulse height occurred per unit time. If the discriminator level is set at 5.1 V for the amplifier output in Fig. 1.2, the discriminator gives logic output pulses for only the 6-MeV alphas. These logic pulses are then fed into the counter and counted. Other examples of linear and logic arrangements are given later.

The procedure outlined in Experiment 1.1 tells the student how to operate the oscilloscope and the EG&G ORTEC 480 Pulser to observe the direct and attenuated outputs from the 480. The procedures in Experiment 1.2 consist of three parts: (1) how to apply the output signal from the 480 into the linear portion of the measurement system (the preamplifier and amplifier) and observe the linear shaping of these modules in the system; (2) how to determine whether the logic criteria have been met by observing with the oscilloscope the logic output from an integral discriminator; and (3) how to use a single-channel analyzer to replace the function of the integral discriminator.

The Oscilloscope

Most oscilloscopes in nuclear laboratories have about 30 knobs and adjustments for performing the various functions for which they were designed. Fortunately, only about 10 of these parameters are necessary for observing input and output pulses from modules or for making simple timing adjustments. In other words, you can perform virtually all the necessary operations if you can become proficient with these 10 knobs.

Since most laboratories have an oscilloscope similar to a Tektronix 2213A, this brief discussion will be concerned with these types. Familiarity with the operation of a Tektronix oscilloscope makes it quite easy to learn the functions of any other oscilloscope. For reference, Fig. 1.3 shows the details of the front panel of a Tektronix 2213A oscilloscope.

In this experiment, only one of the two channels will be used, and the settings in Table 1.1 are basic adjustments that will be adequate to operate the oscilloscope. In Experiment 1.1, the output from the pulse generator is cabled directly to the oscilloscope input and the amplification factors shown for

Table 1.1. Oscilloscope Parameters.
(Keyed to Fig. 1.3)

1. **Intensity:** mid-scale, and then readjust for desirable level; this control interacts with the Focus adjustment.
2. **Display mode selection:** select CH1 (only) for the vertical deflection.
3. **Vertical Position (Channel 1):** place baseline of trace at 0% mark on graticule, 2.5 cm below the center line.
4. **Vertical Position (Channel 2):** ineffective, channel not used.
5. **Sec/Div:** .1 ms provides a horizontal sensitivity of 100 μ s (0.1 milliseconds) per centimeter in the sweep; other available time bases will be appropriate to other applications.
6. **Triggering Slope:** + (Out) elects to trigger on the positive rise of the trigger source pulse.
7. **Triggering Mode:** NORM is appropriate to most laboratory uses; alternate settings are for other applications of this oscilloscope.
8. **Triggering Level:** set at mid-scale and then readjust when input pulses are available.
9. **Triggering Source:** INT starts a sweep on each input pulse through the Channel 1 input circuit; other settings select alternate triggering sources for other applications.
10. **Volts/Div (Channel 2):** ineffective, because the channel is not used.
11. **Variable Volts/Div (Channel 2):** ineffective, channel not used.
12. **Probe selection:** use the X1 window on the knob-skirt if the input is a direct connection, or the X10 window if through the X10 Tektronix probe that is furnished with the instrument.
13. **Volts/Div (Channel 1):** set a 1 for a vertical deflection sensitivity of 1 V/cm.
14. **Input Coupling (both channels):** select AC for this application.
15. **Variable Volts/Div (Channel 1):** full clockwise to use the selected vertical sensitivity; otherwise provides fine attenuation adjustment.
16. **Focus:** mid-scale, and then readjust for pin-point spot of light.
17. **Beam Finder:** push to center the trace if off-scale to determine the direction to adjust both vertical and horizontal position controls.

the X1 Probe are effective. For Experiments 1.2 and 1.3, the probe that is furnished with the oscilloscope is used for the circuit test connections, so the vertical amplification factors shown for the X10 Probe are effective.

If you are using a different oscilloscope, your instructor will give you the necessary modifications of the parameters listed in Table 1.1. Also, additional information and definitions of the parameters are given in the oscilloscope operator's manual.

EXPERIMENT 1.1

Observing the Direct and Attenuated Outputs of the Pulser

Introduction

The 480 Pulser generates output pulses that are used to simulate pulses from nuclear radiation detectors. Normally the output from the pulse generator will be fed into a preamplifier to become the test pulse input. It may also be fed directly into an amplifier.

The pulse generator has two output pulses that occur simultaneously: a direct output and an attenuated output. The direct output has a pulse height or full amplitude that is adjusted with a front panel dial and will usually be used to trigger the oscilloscope with a time = 0 reference. The attenuated output has a pulse height that is a selected fraction of the direct output and is the variable amplitude needed for energy calibration. The amplitude of these outputs can be varied continuously from 0 to about 5 V by the use of the pulse-height and calibration controls and the attenuator switches. The output polarity is selectable on the front panel.

As is true for almost all NIM modules, the 480 Pulser must be installed in a bin and power supply and the power supply must be turned on to provide the operating power requirements of the module. The bin and power supply can accommodate any of these instrument modules in any configuration and supply the appropriate power to all the modules. Always turn off the power before inserting or removing any instrument module.

Procedure

1. Install the 480 Pulser in the bin and power supply and turn on the power.
2. Connect a BNC tee to the input of the oscilloscope, channel 1. Connect a 93 Ω cable with BNC connectors from the direct output of the 480 to one side of the BNC tee, and connect a 100 Ω terminator to the other side of the tee. This is known as receiving-end termination and in this case simulates the input impedance of the preamplifier.
3. Set the 480 Cal (calibrate) and Pulse-Height controls fully clockwise and select a positive output polarity. Set the oscilloscope parameters as listed in Table 1.1.

4. Trigger the oscilloscope by adjusting the Triggering-Level control. If the trace will not trigger, recheck the settings of the parameters in Table 1.1. When the oscilloscope is operating properly, the output should appear approximately as that shown in Fig. 1.4. Note that in Fig. 1.4 the maximum pulse amplitude appears at the beginning and is ~ 5 V.

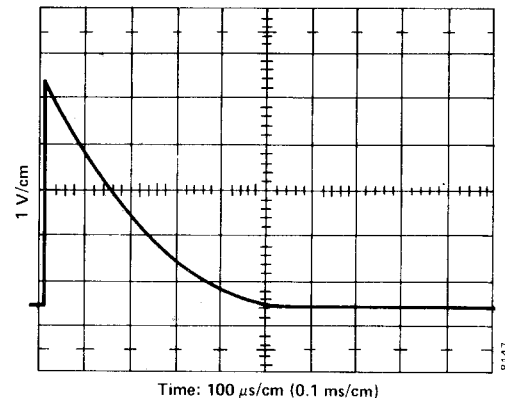


Fig. 1.4. Typical Pulse Generator Output.

EXERCISES

- a. Make a plot on centimeter graph paper of the picture that is observed. Note that the picture gives the voltage of the pulse as a function of time. The scale on the ordinate can be changed by changing parameter 13 of Table 1.1. When this is changed, it may be necessary to readjust the triggering controls. The time per centimeter can be changed by adjusting parameter 5.
- b. Set parameter 13 at 2 V/cm and parameter 5 at .2 ms/cm and make a plot on centimeter graph paper of the picture that you observe.

5. Now change the cable connection on the pulser to the attenuated output. Set all attenuation switches at X1. Leave the pulse-height and calibration controls fully clockwise. The output pulse on the oscilloscope should show a 5-V amplitude. The pulse-height dial on the 480 Pulser is a 10-turn potentiometer with a duo-dial. There are 100 division marks for each turn of the knob for a total of 1000 divisions on the dial. The settings on the pulse-height dial can then be represented as a ratio. For example, 90% of full clockwise would be 900/1000 etc.

EXERCISES

- c. In Table 1.2, record from the oscilloscope the maximum voltage values observed for the pulse-height settings.
 - d. Make a plot on linear graph paper of pulse-height dial settings vs oscilloscope voltage. Is this a straight line?
6. Return the pulse height dial to 1000/1000. Set the top attenuator switch at X2 on the pulser. The amplitude of the pulse should decrease by a factor of 2.

Table 1.2

Pulse-Height Dial Settings	Voltage Amplitude (Oscilloscope)
1000/1000	
800/1000	
600/1000	
400/1000	
200/1000	

Try various combinations of these attenuator switches and observe the output. It will be necessary to change parameter 13 of Table 1.1 and readjust the oscilloscope triggering controls when the output signals are attenuated in order to observe the pulses with reduced amplitudes. Return the attenuator switches to X1 and readjust the oscilloscope vertical sensitivity. Now with a small screwdriver slowly turn the calibrate control counterclockwise while observing the output pulse. It should linearly attenuate the output voltage as does the pulse-height dial.

EXPERIMENT 1.2

Using the Pulser as the Linear Input to a Typical Counting System

Introduction

To set up the electronics shown in Fig. 1.5:

1. Install the 480, 575A, 551, and 875 in the bin and power supply.
2. Connect the power cable for the 113 to the preamplifier power connector on the rear of the 575A.
3. Connect the attenuated output of the 480 Pulser to the test input connector on the 113 Scintillation Preamplifier (connections are always made with 93 Ω cable and BNC connectors unless otherwise specified). The 100 Ω terminator previously used is no longer required.

4. Use a BNC tee at the 575A Amplifier input and connect the output of the preamplifier to one side of the tee. Connect the oscilloscope to the other side of the tee.
5. Connect the amplifier output to the input of the 551, used as an integral discriminator.
6. Connect the positive output of the 551 to the input of the 875 Counter.

Make the following control settings:

1. Set the input capacity of the 113 Scintillation Preamplifier at 100 pF.
2. Set the 575A for a negative input and unipolar output.
3. Set the 551 mode switch at Integral, Lower Level at 50/1000, and rear panel toggle switch at Internal. This combination makes the 551 operate as a threshold discriminator.

Procedure

Adjusting the Linear Portion of the System

1. Using the 480 attenuated output, set its parameters as follows: pulse height, 1000/1000; calibrate, full clockwise; output, negative. Other adjustments will be made later.
2. Adjust the attenuator switches and the calibrate control of the 480 so that the output pulses from the preamplifier are about 0.1 V. (When using the X10 probe for the oscilloscope, use the X10 probe settings of parameter 13 of Table 1.1.)
3. Trigger the oscilloscope by the methods shown in Experiment 1.1.
4. Now move the oscilloscope cable to the output of the 575A Amplifier and adjust its gain controls until the output pulses have an 8.5-V amplitude. The oscilloscope parameters should be the same as those in Table 1.1 except that parameter 13 should be 2 V/cm and parameter 5 should be 0.1 ms/cm. The correct output pulse should look like the pulse shown in Fig. 1.6.
5. With all other settings the same, switch the 575A output to bipolar. The correct output pulse should look like the pulse shown in Fig. 1.7. (Retrigger oscilloscope if necessary.)
6. Return the switch on the amplifier to unipolar.

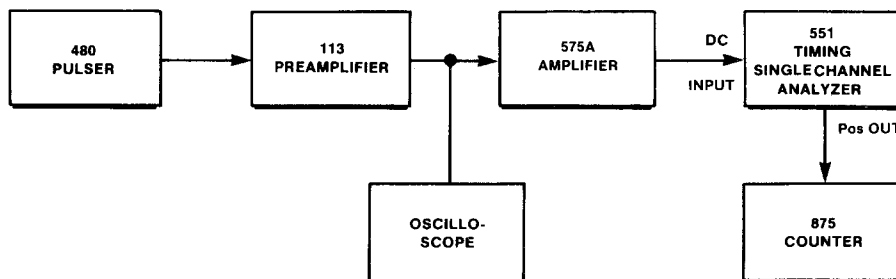


Fig. 1.5. Typical Counting System with Pulser Input.

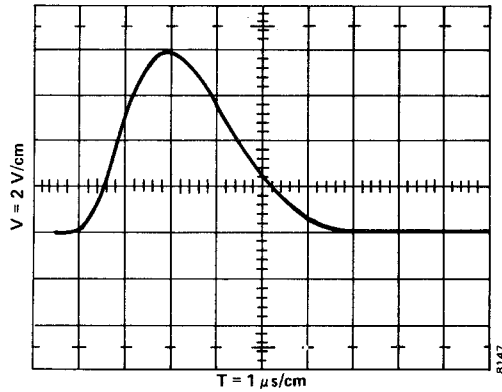


Fig. 1.6. Correct Amplifier Unipolar Output.

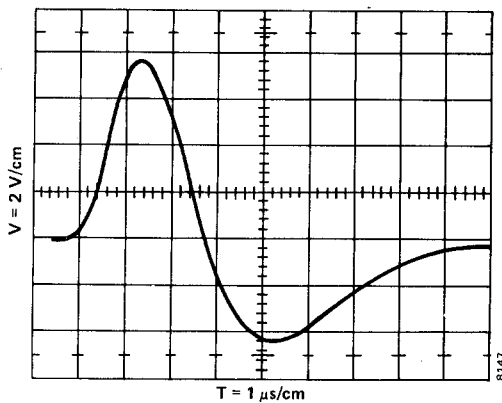


Fig. 1.7. Correct Amplifier Bipolar Output.

Determining Logic Criteria

1. Connect the oscilloscope to the test point for the Pos output of the 551.
2. Trigger the oscilloscope with the same parameters that were used for looking at the amplifier output.
3. A 5-V logic pulse should be observed in the oscilloscope.
4. Set the counter Count/Stop switch at Count. The counter should count the 551 output pulses.
5. Now, increase the setting of the 551 Lower-Level control until the counter just stops counting. Record the control setting for the first line in Table 1.3.
6. On the 480 Pulser, decrease the Pulse-Height control to 800/1000.

EXERCISES

- a. Decrease the 551 Lower-Level control until the counter just barely starts to count. Record this setting in Table 1.3, and continue for the other settings in Table 1.3.
- b. Make a plot of the data in Table 1.3 on linear graph paper. This should produce a straight line.

Table 1.3

480 Pulse Height	551 Lower Level
1000/1000	
800/1000	
600/1000	
400/1000	
200/1000	

EXPERIMENT 1.3

Using a Single-Channel Analyzer

1. Change the 551 mode switch from Integral to Normal. This changes its function from an integral discriminator to a single-channel analyzer. Connect the LL Out on the rear panel of the 551 to the 875 Counter Input.
2. Use the Lower-Level control of the 551 to adjust the discriminator levels for various settings of the 480 Pulse-Height control. With this connection, the 551 operates the same as it did for Integral mode.

EXERCISES

- a. Fill in Table 1.4.

Table 1.4

480 Pulse Height	551 Lower Level
1000/1000	
800/1000	
600/1000	
400/1000	
200/1000	

- b. Make a plot of the lower-level settings as a function of pulse height. This will prove that the lower-level portion of the SCA operates the same as the integral discriminator.
3. Move the output connection of the 551 from LL Out to either the SCA Out connector on the rear panel or the Pos Output connector on the front panel; output pulses are identical through these two connectors.
4. Set the 551 front panel toggle switch at Normal and the Upper-Level dial at 1000/1000. The operation of the 551 for this arrangement will be exactly the same as for the use of its LL Out signals, except that the output signals occur slightly later in the trace.
5. Set the SCA in the Window (Differential) mode. Set the

Lower-Level dial at 100/1000 and the Window or Upper-Level dial at 100/1000.

6. Decrease the 480 Pulse-Height control until the counter starts to count. Record this setting in Table 1.5 as ΔE Upper.

Table 1.5

Lower Level	Window or Upper Level	ΔE Upper	ΔE Lower
100/1000	100/1000		
100/1000	300/1000		
100/1000	600/1000		
100/1000	800/1000		

EXERCISES

c. Continue to decrease the 480 Pulse-Height control until the counter stops counting. Record this value as ΔE Lower in Table 1.5.

d. Make a plot of the Window settings vs ΔE Upper – ΔE Lower on linear graph paper.

e. Repeat these measurements with the Lower Level set at 200/1000 as in Table 1.6.

7. Place the toggle switch on the front panel in the Normal position. With the toggle switch in the Normal position, the Upper-Level and Lower-Level controls on the front panel of the 551 are independently variable from 0 to 10 V. Also in the

Table 1.6

Lower Level	Window or Upper Level	ΔE Upper	ΔE Lower
200/1000	100/1000		
200/1000	300/1000		
200/1000	600/1000		
200/1000	800/1000		

Normal mode, if the Upper Level is set below the Lower Level, no output will be generated from the SCA output on the 551.

With this in mind, complete Exercise f.

EXERCISE

f. Repeat the measurements for Table 1.7 with the Lower Level set at 200/1000 as in Table 1.6.

Table 1.7

Lower Level	Window or Upper Level	ΔE Upper	ΔE Lower
200/1000	100/1000		
200/1000	300/1000		
200/1000	600/1000		
200/1000	800/1000		

Geiger Counting

EQUIPMENT NEEDED FROM EG&G ORTEC

- | | |
|--|-----------------------|
| 903 End-Window Geiger Tube | OT-8 Split Source Kit |
| Source Kit SK-1B (see Appendix) | 906 GM Pulse Inverter |
| Source Kit SK-1G (see Appendix) | 719 Timer |
| Short half-life beta source or minigenerator | Absorber Kit PbAl-23 |
| 556 High Voltage Power Supply | MGM-5 Detector Holder |
| Bin and Power Supply | ORC-2 Cable Set |
| 875 Counter | Oscilloscope |

Purpose

The purpose of this experiment is to familiarize the student with the Geiger-Mueller counter. This counter is a widely used pulse-counting instrument that uses gas amplification, which makes it remarkably sensitive, but whose simple construction makes it relatively inexpensive. The experiments that are designed to accomplish this purpose deal with the operating plateau of the Geiger tube, half-life determinations, resolving-time corrections, and the basic nuclear considerations involved.

Description

Basically, the Geiger counter consists of two electrodes with a gas at reduced pressure between the electrodes. The outer electrode is usually a cylinder, while the inner (positive) electrode is a thin wire positioned in the center of the cylinder. The voltage between these two electrodes is maintained at such a value that virtually any ionizing particle entering the Geiger tube will cause an electrical avalanche within the tube. The Geiger tube used in this experiment is called an end-window tube because it has a thin window at one end through which the ionizing radiation enters.

The Geiger counter does not differentiate between kinds of particles or energies; it tells only that a certain number of particles (betas and gammas for this experiment) entered the detector during its operation. The voltage pulse from the avalanche is typically >1 V in amplitude. These pulses are large enough that they can be counted in an EG&G ORTEC 875 Counter directly, without amplification. Pulse inversion is, however, necessary (Fig. 2.1). In this experiment the properties of the Geiger counter will be studied and several fundamental measurements will be made.

EXPERIMENT 2.1

Operating Plateau for the Geiger Tube

Purpose

The purpose of this experiment is to determine the voltage plateau for the Geiger tube and to establish a reasonable operating point for the tube. Figure 2.2 shows a counts-vs-voltage curve for a typical Geiger tube that has an operating point in the vicinity of 1000 V.

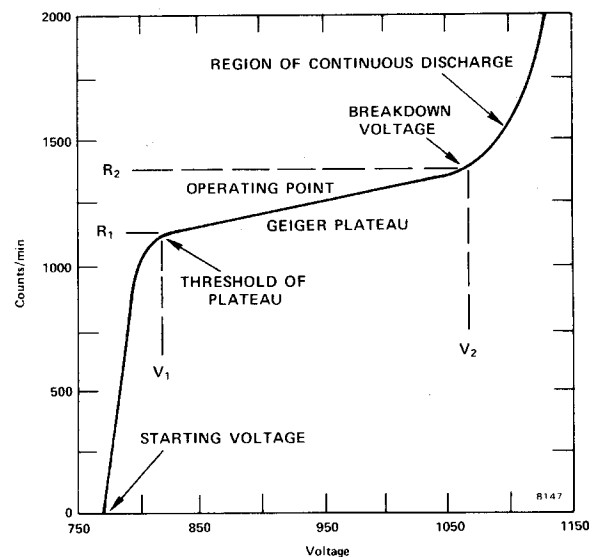


Fig. 2.2. Geiger Tube Plateau.

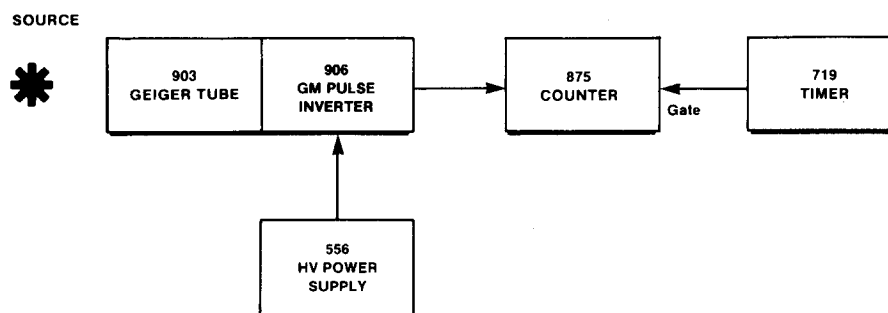


Fig. 2.1. Electronics for Geiger Counting.

The region between R_1 and R_2 , corresponding to operating voltages V_1 and V_2 , is called the Geiger region. Voltages $<V_2$ in Fig. 2.2 cause a continuous discharge in the tube and will definitely shorten the life of the tube.

Procedure

1. Set up the electronics as shown in Fig. 2.1.
2. Set the 875 Counter display at X1.
3. Place beta source ^{204}Tl from the source kit at a distance of ~ 2 cm from the window of the Geiger tube.
4. Adjust the 719 Timer for a long period of time (~ 30 min).
5. Increase the (positive) high voltage until the 875 Counter just begins registering counts. This point is called the starting voltage in Fig. 2.2. Starting voltages are rarely >900 V and can be as low as 250 V.
6. Reset the 875 Counter, set the 719 Timer for 1-min timing intervals, and count for 1 min. Increase the high voltage by 50 V and count again for 1 min.

EXERCISES

- a. Continue making measurements at 50-V intervals until you have enough data to plot a curve, on linear graph paper, similar to that in Fig. 2.2 (caution: use only values below V_2). The region between V_1 and V_2 is usually <300 V. A sharp rise in the counting rate will be observed if you go just above V_2 . When this happens, the upper end of the plateau has been reached. Reduce the voltage to V_2 immediately. Choose the operating point for your instrument at ~ 50 to 70% of the plateau range.
- b. Evaluate your Geiger tube by measuring the slope of the plateau in the graph; it should be $<10\%$. The slope of the plateau is defined as

$$\text{slope} = \left[\frac{(R_2 - R_1)}{R_1} \right] \left[\frac{100}{V_2 - V_1} \right] \% \quad (1)$$

EXPERIMENT 2.2

Half-Life Determination

Purpose

The purpose of this experiment is to construct a decay curve and determine the half-life of an unknown isotope. The instructor will provide you with the unknown short-half-life source to be used for this experiment. He will also tell you at what time intervals counts are to be made and suggest a duration for counting intervals. For example, he might tell you to take one 10-min measurement every h for the next 6 h, or one 2-min measurement every 15 min for the next 3 h.

Procedure

1. Set the Geiger counter at its operating voltage.
2. Place the unknown half-life source 2 cm away from the window of the Geiger tube and make a count as in Experiment 2.1.
3. Record the time of day, counting duration, and number of counts.
4. After the period of time recommended by the laboratory instructor, repeat the measurement. Be sure to place the sample at exactly the same distance from the window of the tube.
5. Continue the measurements at the intervals recommended by the instructor. When you are not making half-life measurements you can continue with the other parts of the experiment.

EXERCISES

- a. When you have completed your half-life measurements, correct the counting rates for dead-time losses (see Experiment 2.3), and plot the corrected counting rates as a function of time. If this is plotted on semilog paper, a straight line should result.
- b. Determine the half-life from the curve. Find λ , the decay constant for the isotope.

EXPERIMENT 2.3

Resolving-Time Corrections for the Geiger Counter

Purpose

In later experiments we will be dealing with fast electronics (\sim nanoseconds). The Geiger counter, however, is a slow device. When used for counting rates above 5000 counts/min, it is necessary to make a dead-time correction to obtain the true counting rate. In order to determine this dead time, use a split source that is provided in Source Kit OT-8. In counting the source, count the right half first, then both halves, and finally the left half.

Procedure

1. Place the right half of the split source 2 cm from the window and make a 1-min count. Record the count. Define this count to be R_1 .
2. Place the left-half of the source along with the right-half and make a 1-min count. Define this quantity to be R_T .
3. Remove the right half and count the left half for 1 min. Define this quantity to be R_2 . Calculate the resolving time of the GM tube with the following formula:

$$T_R = \frac{R_1 + R_2 - R_T}{2R_1R_2} \quad (2)$$

The answer should be in min/count.

The true counting rate, R , can then be determined for an observed counting rate, R_0 , from the following formula:

$$R = \frac{R_0}{1 - R_0 T_R} \text{ counts/min} \quad (3)$$

Equation (3) should be used to correct any counting rate that is above 5000 counts/min.

EXPERIMENT 2.4

Linear Absorption Coefficient

Purpose

When gamma radiation passes through matter, it undergoes absorption primarily by Compton, photoelectric, and pair-production interactions. The intensity of the radiation is thus decreased as a function of distance in the absorbing medium. The mathematical expression for intensity, I , is given by the following expression:

$$I = I_0 e^{-\mu x}, \quad (4)$$

where

I_0 = original intensity of the beam,

I = intensity transmission through an absorber to a distance, depth, or thickness x ,

μ = linear absorption coefficient for the absorbing medium.

If we rearrange Eq. (4) and take the logarithm of both sides, the expression becomes

$$\ln(I/I_0) = -\mu x. \quad (5)$$

The half value layer (HVL) of the absorbing medium is defined as that thickness, $x_{1/2}$, which will cut the initial intensity in half. That is, $I/I_0 = 0.5$. If we substitute this into Eq. (5),

$$\ln(0.5) = -\mu x_{1/2}. \quad (6)$$

Putting in numerical values and rearranging, Eq. (6) becomes

$$x_{1/2} = 0.693/\mu \text{ or } \mu = \frac{0.693}{x_{1/2}}. \quad (7)$$

Experimentally, the usual procedure is to measure $x_{1/2}$ and then calculate μ from Eq. (7).

Procedure

1. Set the voltage of the Geiger tube at its operating value.
2. Place the ^{60}Co source (from SK-1G) about 3 cm from the window of the GM tube and make a 2-min count. Record the number of counts.

3. Place a sheet of lead from the absorber kit between the source and the GM window and take another 2-min count and record the value.

4. Place a second sheet on top of the first and make another count.

5. Continue adding lead sheets until the number of counts is 25% of the number recorded with no absorber.

6. Make a 2-min background run and subtract this value from each of the above counts.

EXERCISE

Record the density-thickness of the lead in g/cm^2 and plot on semilog paper the corrected counts as a function of absorber density-thickness in g/cm^2 . The density-thickness is defined as the product of density in g/cm^3 times the thickness in cm of the absorber. Draw the best straight line through the points and determine $x_{1/2}$ and μ . How do your values compare with those indicated in ref. 8? See also Experiment 3 in this manual, in which this same experiment is done with a sodium iodide detector.

EXPERIMENT 2.5

Inverse Square Law

Purpose

There are many similarities between ordinary light rays and gamma rays. They are both considered to be electromagnetic radiation, and hence they obey the classical equation

$$E = h\nu, \quad (8)$$

where

E = energy of the photon in ergs,

ν = the frequency of the radiation in cycles/s,

h = Planck's constant (6.624×10^{-27} ergs \cdot s).

Therefore in explaining the inverse square law it is convenient to make the analogy between a light source and a gamma-ray source.

Let us assume that we have a light source that emits light photons at a rate N_0 photons/s. It is reasonable to assume that these photons are given off in an isotropic manner, that is, equally in all directions. If we place the light source in the center of a clear plastic spherical shell, it is quite easy to measure the number of light photons per second for each cm^2 of the spherical shell. This intensity is given by

$$I_0 = \frac{N_0}{A_0}, \quad (9)$$

where N_0 = total number of photons/s from the source, and A_0 = total area of the sphere in cm^2 .

Since $A_0 = 4\pi R_0^2$, where R_0 is the radius of the sphere, Eq. (9) can then be written

$$I_0 = \frac{N_0}{4\pi R_0^2} \quad (10)$$

Since N_0 and 4π are constants, I_0 is seen to vary as $1/R_0^2$. The purpose of this experiment is to verify Eq. (10).

Procedure

1. Place the ^{60}Co source 1 cm away from the face of the window.
2. Set the GM tube at the proper operating voltage.
3. Count for a period of time long enough to get reasonable statistics (~4000 counts).
4. Move the source to 2 cm and repeat the measurement for the same amount of time. Continue for the distances listed in Table 2.1. (Note that for the longer distances the time will have to be increased for the same statistics.)

Table 2.1

Distance	Activity (counts/min)	Corrected Activity (counts/min)
1 cm		
2 cm		
3 cm		
4 cm		
5 cm		
6 cm		
7 cm		
8 cm		

EXERCISES

a. Correct the activity for dead time and background and fill in the corrected activity in Table 2.1. On linear paper plot the corrected activity (y axis) as a function of distance. Since the intensity is proportional to the activity, this plot should have the $1/R_0^2$ characteristics exhibited by Eq. (10). From the corrected activities in Table 2.1,

$$A = \frac{K}{R^2} \quad (11)$$

where

- R = the distance for the measurement (cm),
- A = the corrected activity, and
- K = a constant which is to be determined from the individual entries in Table 2.1.

b. Find K for each entry in Table 2.1. Calculate an average

$K(\bar{K})$ from the eight values. What is the percent deviation of each individual K value from \bar{K} ?

EXPERIMENT 2.6

Counting Statistics

Purpose

As is well known, each measurement made for a radioactive sample is independent of all previous measurements, because radioactive decay is a random process. However, for a large number of individual measurements the deviation of the individual count rates from what might be termed the "average count rate" behaves in a predictable manner. Small deviations from the average are much more likely than large deviations. In this experiment we will see that the frequency of occurrence of a particular deviation from this average, within a given size interval, can be determined with a certain degree of confidence. Fifty independent measurements will be made, and some rather simple statistical treatments of the data will be performed.

The average count rate for N independent measurements is given by

$$\bar{R} = \frac{R_1 + R_2 + R_3 + \dots + R_N}{N} \quad (12)$$

where R_1 = the count rate for the first measurement, etc., and N = the number of measurements.

In summation, notation \bar{R} would take the form

$$\bar{R} = \frac{\sum_{i=1}^N R_i}{N} \quad (13)$$

The deviation of an individual count from the mean is $(R - \bar{R})$. From the definition of \bar{R} it is clear that

$$\sum_{i=1}^N (R_i - \bar{R}) = 0. \quad (14)$$

The standard deviation $\sigma = \sqrt{\bar{R}}$.

Procedure

1. Set the operating voltage of the Geiger counter at its proper value.
2. Place the ^{60}Co source far enough away from the window of the GM tube so that ~1000 counts can be obtained in a time period of 0.5 min.
3. Without moving the source, take 50 independent 0.5-min runs, and record the values in Table 2.2. (Note that you will have to extend Table 2.2; we have shown only ten entries.)

Table 2.2*

Run	R	σ	R - \bar{R}	$(R - \bar{R})/\sigma$		$(R - \bar{R})/\sigma$ (Rnd'd Off)	
				Typical	Measured	Typical	Measured
1				-0.15		0	
2				+1.06		+1.0	
3				+0.07		0	
4				-1.61		-1.5	
5				-1.21		-1.0	
6				+1.70		+1.5	
7				-0.03		0	
8				-1.17		-1.0	
9				-1.67		-1.5	
10				+0.19		0	

*Typical values of $(R - \bar{R})/\sigma$ and $(R - \bar{R})/\sigma$ rounded off; listed for illustrative purposes only.

The counter values, R, may be recorded directly in the table since for this experiment R is defined as the number of counts recorded for a 0.5-min time interval.

4. With a calculator determine \bar{R} from Eq. (12). Fill in the values of R - \bar{R} in Table 2.2. It should be noted that these values can be either positive or negative. You should indicate the sign in the data entered in the table.

EXERCISES

a. Calculate σ , and fill in the values for σ and $(R - \bar{R})/\sigma$ in the table, using only two decimal places. Round off the values for $(R - \bar{R})/\sigma$ to the nearest 0.5 and record these values in the table. Note that in Table 2.2 we have shown some typical values of $(R - \bar{R})/\sigma$ and the rounded-off values.

b. Make a plot of the frequency of the rounded-off events $(R - \bar{R})/\sigma$ vs the rounded-off values. Figure 2.3 shows this plot for an ideal case.

Note that at zero there are eight events, etc. This means that in our complete rounded-off data in Table 2.2 there were

eight zeros. Likewise, there were seven values of +0.5, etc. Does your plot follow a normal distribution similar to that in Fig. 2.3?

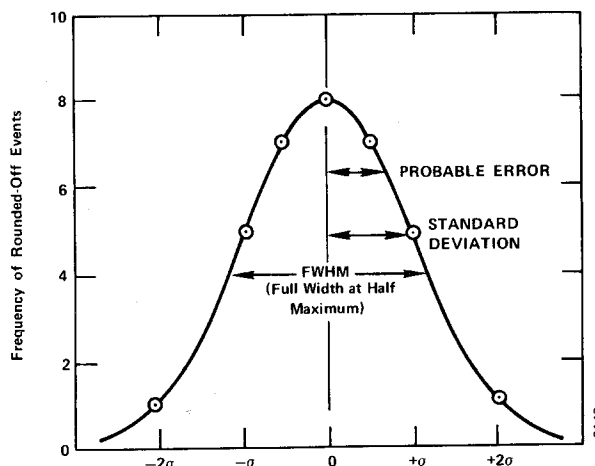


Fig. 2.3. Typical Plot of Frequency of Rounded-Off Events vs the Rounded-Off Values.

References

- G. F. Knoll, *Radiation Detection and Measurement*, John Wiley and Sons, New York (1979).
- E. W. Emery, *Geiger-Mueller and Proportional Counters in Radiation Dosimetry, II*, F. H. Attix and W. C. Roesch, Eds., Academic Press, New York (1966).
- A. Peeva and T. Karatoteva, *Nucl. Instrum. Methods* **118**, 49 (1974).
- H. L. Andrews, *Radiation Biophysics*, Prentice-Hall, New Jersey (1974).
- V. Arena, *Ionizing Radiation and Life*, The C. V. Mosby Co., Missouri (1971).
- G. D. Chase and J. L. Rabinowitz, *Principles of Radioisotope Methodology*, 3rd Edition, Burgess Publishing Co., Minnesota (1967).
- C. M. Lederer and V. S. Shirley, Eds., *Table of Isotopes*, 7th Edition, John Wiley and Sons, Inc., New York (1978).
- Radiological Health Handbook*, U.S. Dept. of Health, Education, and Welfare, PHS Publication 2016. Available from National Technical Information Service, U.S. Dept. of Commerce, Springfield, Virginia.

Gamma-Ray Spectroscopy Using NaI(Tl)

EQUIPMENT NEEDED FROM EG&G ORTEC FOR EXPERIMENTS 3.1 THROUGH 3.7, 3.9, and 3.10

Bin and Power Supply
 905-3 NaI(Tl) Crystal and Phototube Assembly
 266 Photomultiplier Tube Base
 556 High Voltage Power Supply
 113 Scintillation Preamplifier
 575A Amplifier
¹³⁷Cs gamma source, 5 μ Ci \pm 5%
 SK-1G Source Kit (see Appendix)
 Absorber Kit Model 3-Z2
 Absorber Kit PbAl-23
 M-Nal-3 Stand for Sodium Iodide Detector

ACE-2K MCA System including suitable IBM PC (other
 EG&G ORTEC MCAs may be used)
 Oscilloscope

ADDITIONAL EQUIPMENT NEEDED FROM EG&G ORTEC FOR EXPERIMENT 3.8

427A Delay Amplifier
 551 Timing Single-Channel Analyzer
 426 Linear Gate
 875 Counter

Purpose

The purpose of this experiment is to acquaint the student with some of the basic techniques used for measuring gamma rays. It is based on the use of a sodium iodide (NaI) detector that is thallium (Tl) activated.

Gamma Emission

Most isotopes that are used for gamma measurements also have betas in their decay schemes. The typical decay scheme for the isotope will include a beta decay to a particular level followed by gamma emission to the ground state of the final isotope. The beta particles will usually be absorbed in the surrounding material and not enter the scintillator at all. This absorption is normally assured with aluminum absorbers (ref. 10). For this experiment the betas offer no real problem, and so absorbers are not specified. There will be some beta absorption by the light shield over the phototube. The gammas, however, are quite penetrating and will pass easily through the aluminum light shield.

Generally there are two unknowns that we would like to investigate about a gamma source. One is the energies of the gammas from the source; the other is the number of gammas

that leave the source per unit of time. In this experiment the student will become familiar with some of the basic NaI(Tl) measurements associated with gamma-emitting unknowns.

A total time of \sim 6 h is required to complete all the parts of Experiment 3 (3.1 through 3.10). The complete series can be done in two 3-h lab periods, since each is written to be fairly independent of the others.

EXPERIMENT 3.1

Energy Calibration

Setup of Equipment

Set up the electronics in the arrangement shown in Fig. 3.1. There are two parameters that ultimately determine the overall gain of the system: the high voltage that is furnished to the phototube and the gain of the linear amplifier. The gain of the photomultiplier tube is quite dependent upon its high voltage. A rule of thumb for most phototubes is that a 10% change of the high voltage will change the gain by a factor of 2. The high-voltage value depends on the phototube being

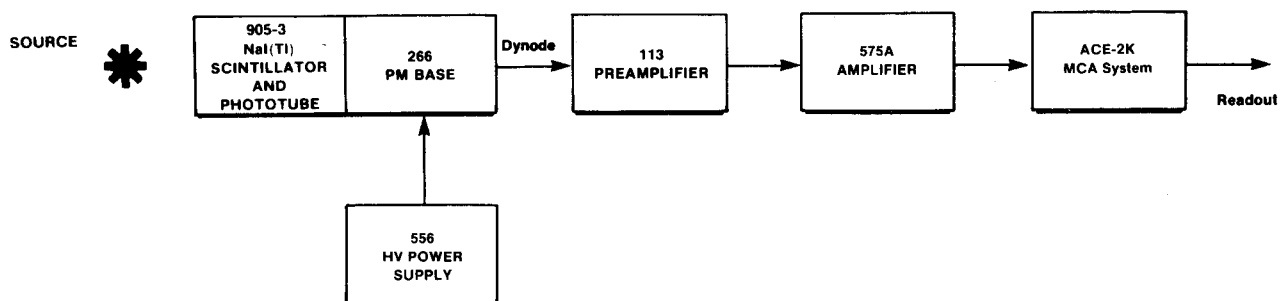


Fig. 3.1. Electronic Block Diagram for Gamma-Ray Spectroscopy System with NaI(Tl) Detector.

used; consult your instruction manual for the phototube and select a value in the middle of its normal operating range. (The instructor may wish to recommend a value.)

Set the indicated modules as follows:

556 High Voltage: See phototube instructions and set the level at about the middle of the acceptable operating range (normally about +1000 V).

113 Scintillation Preamplifier: Set the Input Capacity switch at 200 pF. The output pulses will be positive.

575A Amplifier: Positive input and Bipolar output. Shaping time set to 0.5 μ sec. The gain will be adjusted during the experiment.

Multichannel Analyzer: PHA Analysis mode; 1000 channels are adequate for this experiment.

Procedure

1. Place the ^{137}Cs source from SK-1G ($E_\gamma = 0.662$ MeV) ~ 2 cm in front of the NaI(Tl) crystal.
2. Adjust the coarse and fine gain controls of the linear amplifier so that the 0.662-MeV photopeak for ^{137}Cs falls at approximately channel 280. For the illustrations shown in Figs. 3.2 and 3.3, the gain of the system has been set so that 1 MeV falls at about channel 420 to 425. Since the system is linear, 2 MeV would therefore fall at approximately channel 840 to 850.

3. Accumulate the ^{137}Cs spectrum for a time period long enough to determine the peak position. Figure 3.2 shows a typical ^{137}Cs spectrum that has been plotted. Although these spectra are usually plotted on semilog graph paper, the figures shown in this experiment are plotted on linear paper to point out some of the features of the spectra.

4. After the ^{137}Cs spectrum has been read out of the MCA, erase it and replace the ^{137}Cs source with a ^{60}Co source from SK-1G.

5. Accumulate the spectrum for a period of time long enough for the spectrum to be similar to that in Fig. 3.3.

6. Read out the MCA.

EXERCISES

- a. Plot both the ^{137}Cs and ^{60}Co spectra and fill in items 1, 2, and 3 in Table 3.1.
- b. From items 1, 2, and 3 in Table 3.1 make a plot of energy of the photopeaks vs channel number. Figure 3.4 shows this calibration for the data taken from Figs. 3.2 and 3.3. If other calibration sources are available, additional data points can be added to Fig. 3.4. The other entries in Table 3.1 will be filled out in Experiment 3.3.
- c. Use the energy calibration feature of the MCA and compare the results with those found in Exercise b.

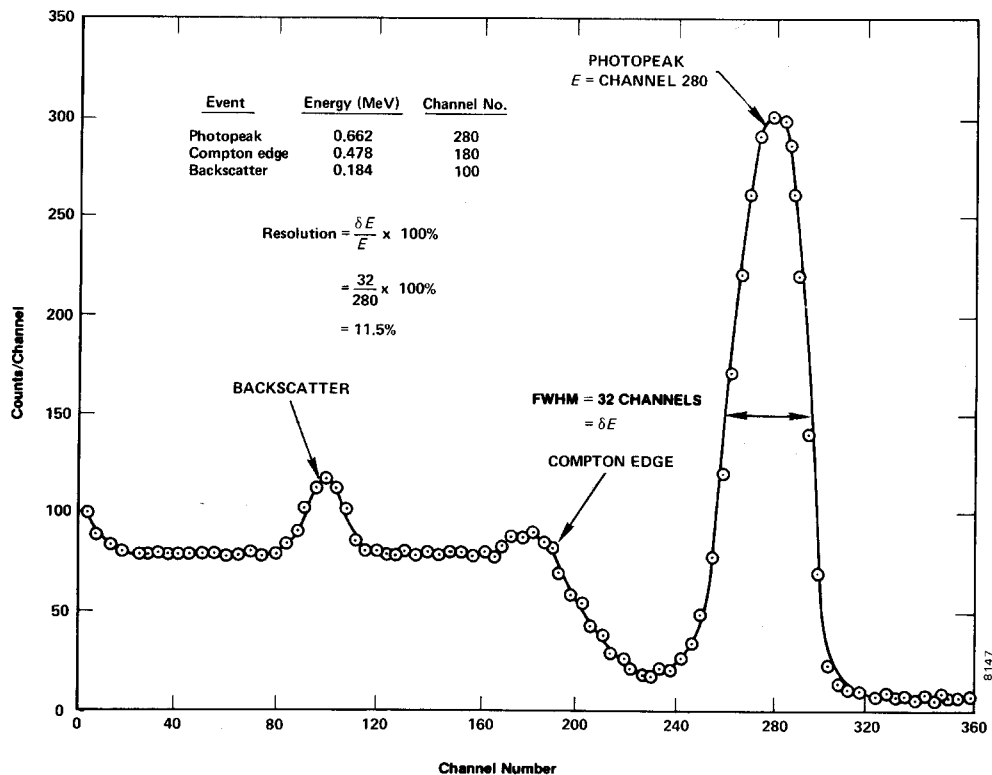


Fig. 3.2. NaI(Tl) Spectrum for ^{137}Cs .

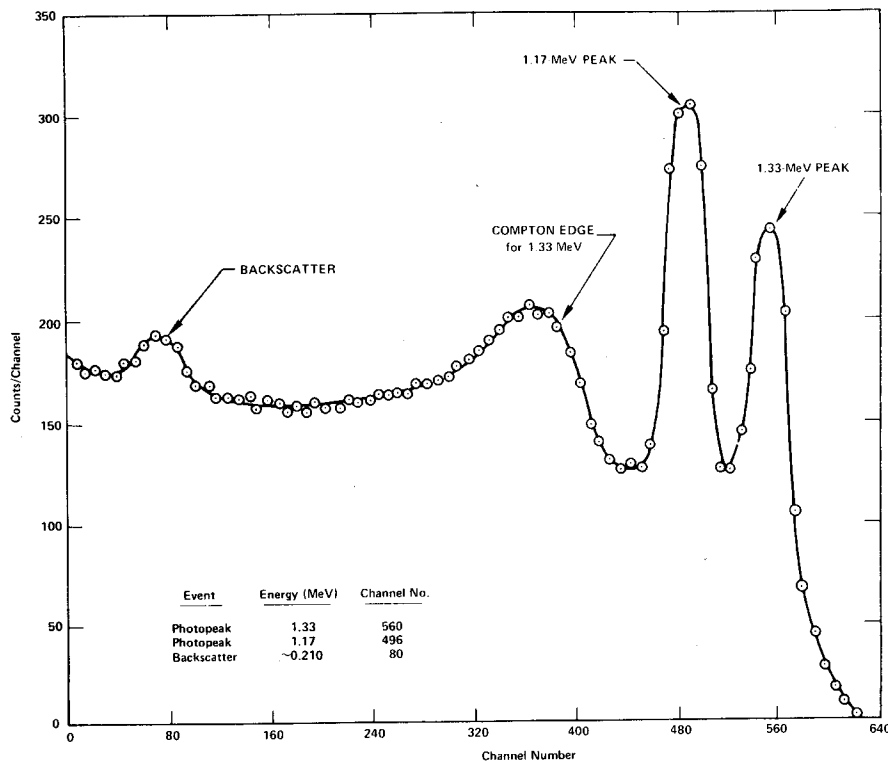


Fig. 3.3. NaI(Tl) Spectrum for ⁶⁰Co.

Table 3.1

	Event	Energy (MeV)	Channel Number
1.	0.662-MeV photopeak	0.662	
2.	1.17-MeV photopeak	1.17	
3.	1.33-MeV photopeak	1.33	
4.	Compton edge ¹³⁷ Cs		
5.	Backscatter ¹³⁷ Cs		
6.	Backscatter ⁶⁰ Co		

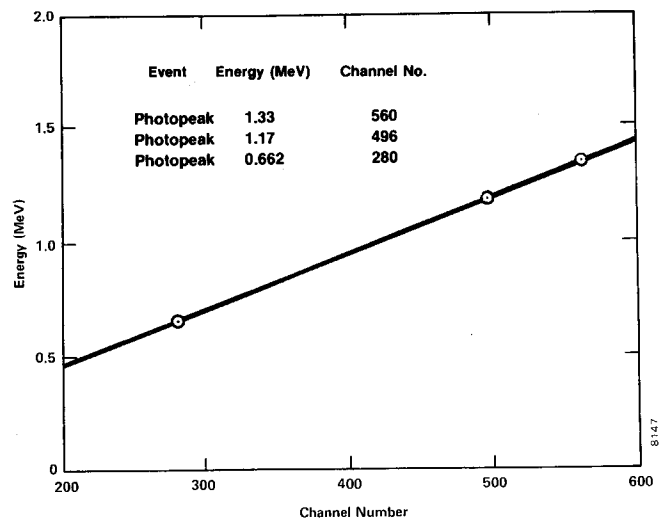


Fig. 3.4. Energy Calibration Curve for NaI(Tl) Detector.

EXPERIMENT 3.2

Energy Analysis of an Unknown Gamma Source

Purpose

The purpose here is to use the calibrated system of Experiment 3.1 to measure the photopeak energies of an unknown gamma emitter and to identify the unknown isotope.

Procedure

1. Erase the ⁶⁰Co spectrum from the MCA, but do not change any of the gain calibration settings of the system.

2. Obtain an unknown gamma source from the instructor. Accumulate a spectrum for the unknown source for a period of time long enough to clearly identify the photopeak(s) of the source. From the calibration curve, determine the energy for each photopeak.

EXERCISE

Use refs. 7 and 8 to identify the unknown isotope.

EXPERIMENT 3.3

Spectrum Analysis of ⁶⁰Co and ¹³⁷Cs

Purpose

The purpose of this experiment is to explain some of the features, other than the photopeaks, that are usually present in a pulse-height spectrum. These are the Compton edge and the backscatter peak.

The Compton interaction is a pure kinematic collision between a gamma photon and what might be termed a free electron in the NaI(Tl) crystal. By this process the incident gamma gives up only part of its energy to the electron. The amount given to the recoil electron (and the intensity of the light flash) depends on whether the collision is head-on or glancing. For a head-on collision the gamma imparts the maximum allowable energy for the Compton interaction. The energy of the scattered gamma can be determined by solving the energy and momentum equations for this billiard ball collision. The solution for these equations in terms of the scattered gamma can be written approximately as

$$E_{\gamma'} \cong \frac{E_{\gamma}}{1 + 2E_{\gamma}(1 - \cos\theta)} \quad (1)$$

where

$E_{\gamma'}$ = energy of the scattered gamma in MeV,

θ = the scattering angle for γ' ,

E_{γ} = the incident gamma-ray energy in MeV.

If $\theta = 180^\circ$ due to a head-on collision in which γ' is scattered directly back, Eq. (1) becomes

$$E_{\gamma'} \cong \frac{E_{\gamma}}{1 + 4E_{\gamma}} \quad (2)$$

As an example, we will calculate $E_{\gamma'}$ for an incident gamma energy of 1 MeV:

$$E_{\gamma'} = \frac{1 \text{ MeV}}{1 + 4} = 0.20 \text{ MeV} \quad (3)$$

The energy of the recoil electron, E_e , for this collision would be 0.80 MeV. This is true since

$$E_e = E_{\gamma} - E_{\gamma'} \quad (4)$$

Then the position of the Compton edge, which is the maximum energy that can be imparted to an electron by the Compton interaction, can be calculated by Eq. (4).

EXERCISES

a. Calculate the energy of the Compton edge for the 0.662-MeV gammas from ¹³⁷Cs. Enter this value in Table 3.1. From your plot and calibration curve, does this calculation agree with your measured value?

b. Backscatter occurs when gammas make Compton inter-

actions in the material that surrounds the detector. Figure 3.5 was taken from ref. 10 and is a good illustration of the various events that can take place in a typical source-NaI(Tl) detector-lead shield arrangement. Backscattered gammas from these interactions ($E_{\gamma'}$) make photoelectric interactions in the NaI(Tl) when they enter the crystal. The energy of the backscattered peak can be found by solving Eq. (2).

Solve Eq. (2) for the background gammas from ¹³⁷Cs and for the 1.33-MeV gammas from ⁶⁰Co. Fill in the rest of Table 3.1. How do your measured energies compare with the theoretical energies from Eq. (2)? If the backscatter peak is not very pronounced in your spectrum, it can be improved by accumulating a spectrum with a sheet of lead absorber placed slightly to the left of the source in Fig. 3.1.

EXPERIMENT 3.4

Energy Resolution

Purpose

The resolution of a spectrometer is a measure of its ability to resolve two peaks that are fairly close together in energy. Figure 3.2 shows the gamma spectrum that was plotted for the ¹³⁷Cs source. The resolution of the photopeak is found by solving the following equation:

$$R = \frac{\delta E}{E} \times 100, \quad (5)$$

where

R = the resolution in percent,

δE = the full width of the peak at half of the maximum count level (FWHM) measured in number of channels,

E = the channel number at the centroid of the photopeak.

In Fig. 3.2 the photopeak is in channel 280 and its FWHM = 32 channels. From Eq. (5) the resolution is calculated to be 11.5%.

EXERCISE

Calculate the resolution of the system from your ¹³⁷Cs spectrum. Record this value for later reference.

EXPERIMENT 3.5

Activity of a Gamma Emitter (Relative Method)

Purpose

In Experiments 3.1 and 3.3, procedures were given for determining the energy of an unknown gamma source. Another

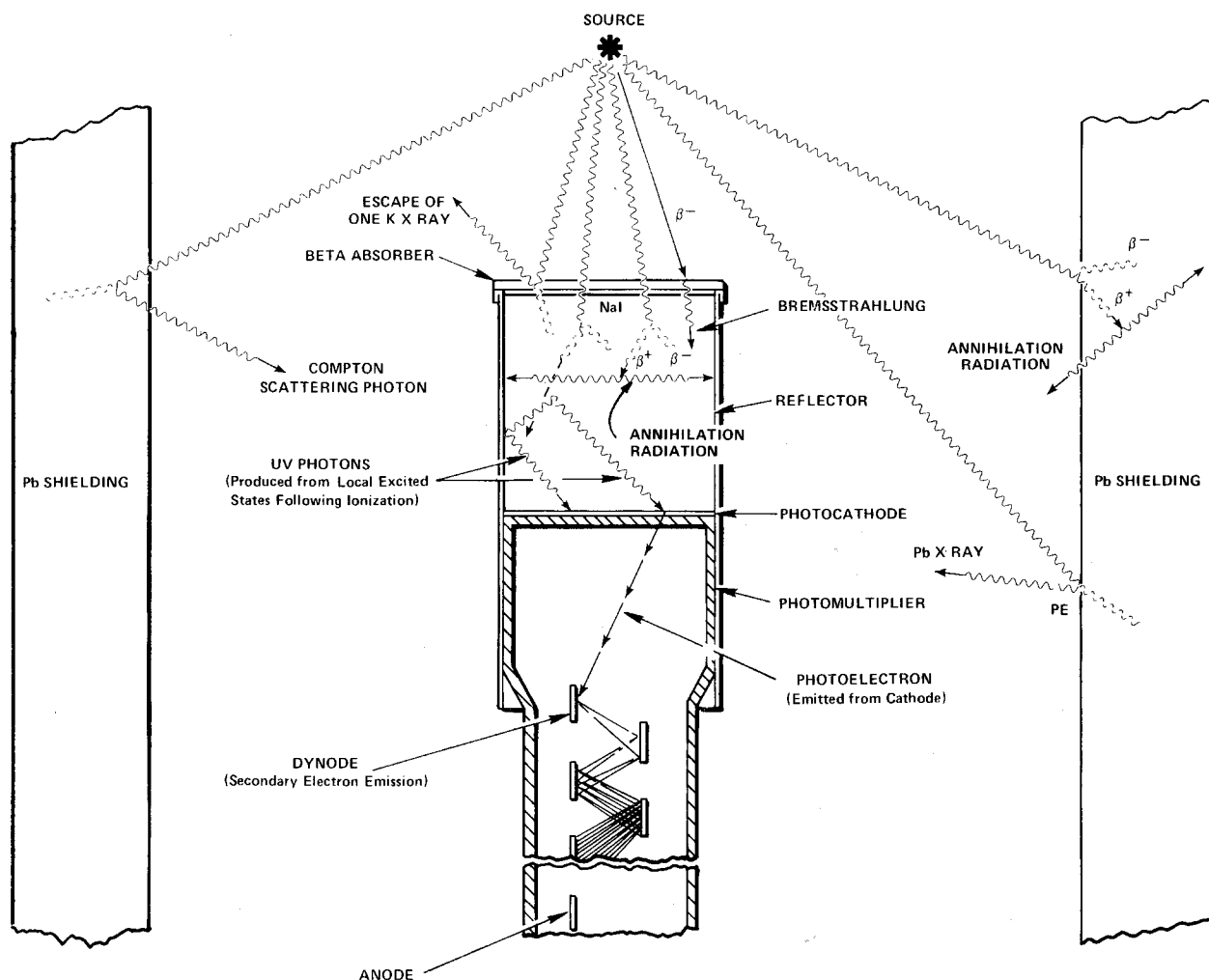


Fig. 3.5. Various Events in the Vicinity of a Typical Source-Crystal Detector-Shield Configuration.

unknown associated with the gamma source is the activity of the source, which is usually measured in curies (Ci); $1 \text{ Ci} = 3.7 \times 10^{10}$ disintegrations/s. Most of the sources that are used in nuclear laboratory experiments have activities of the order of microcuries (μCi). The purpose of this experiment is to outline one procedure by which the activity of a source can be determined, called the relative method.

In using the relative method, it is assumed that the unknown source has already been identified from its gamma energies. For this example, assume that the source has been found to be ^{137}Cs . Then all that is necessary is to compare the activity of the unknown source to the activity of a standard ^{137}Cs source that will be supplied by the laboratory instructor. For convenience, call the standard source S1 and the unknown source U1.

Procedure

1. Place the S1 source about 4 cm from the face of the detector (or closer if necessary to get reasonable statistics)

and accumulate a spectrum for a period of live time, selectable on the analyzer, long enough to produce a spectrum similar to Fig. 3.2.

2. Use the cursor to determine the sum under the photopeak. In the example shown in Fig. 3.2, this would correspond to adding up all counts in channels 240 through 320. Define this sum to be Σ_{S1} .

3. Erase the MCA spectrum. Remove source S1 and replace it with source U1, positioned **exactly** the same distance from the crystal as the S1 source was. Accumulate a spectrum for the same period of live time that was used in step 1. Sum the peak as in step 2.

4. Erase the spectrum from the MCA. Remove the U1 source and accumulate background counts for the same period of live time that was used in steps 1 and 3 above.

5. Sum the background counts in the same channels that were used for the photopeaks in steps 2 and 3 above. Call this sum Σ_b .

EXERCISE

Solve for the activity of the U1 by using the following ratio:

$$\frac{\text{activity of U1}}{\text{activity of S1}} = \frac{\Sigma_{U1} - \Sigma_b}{\Sigma_{S1} - \Sigma_b} \quad (6)$$

Since the efficiency of the detector is only energy dependent, the standard and unknown sources do not have to be the same isotope. It is only necessary that their gamma energies be approximately the same ($\pm 10\%$) in order to get a fairly good estimate of the absolute gamma activity of the unknown.

EXPERIMENT 3.6

Activity of a Gamma Emitter (Absolute Method)

Purpose

The activity of the standard used in Experiment 3.5 can be determined by the absolute method. The purpose of this experiment is to outline the procedure for this method. Here the source that is to be measured will be called U1.

Procedure

1. Place the U1 source 9.3 cm away from the face of the detector.
2. Accumulate a spectrum and note the live time that is used.
3. Use the cursor to determine the sum under the photopeak, Σ_{U1} . Then erase the spectrum, remove the source, and accumulate background for the same live time and calculate Σ_b .
4. Use the following formula to calculate the activity of U1:

$$\text{activity of U1} = \left(\frac{\Sigma_{U1} - \Sigma_b}{t} \right) \frac{1}{G \epsilon_p f} \quad (7)$$

Table 3.2. Gamma Decay Fraction, (f), for Some Common Isotopes.

Isotope	Gamma Energy (MeV)	f
^{137}Cs	0.662	0.92
^{51}Cr	0.323	0.09
^{60}Co	1.17	0.99
^{60}Co	1.33	0.99
^{22}Na	1.276	0.99
^{22}Na	0.511	0.99
^{54}Mn	0.842	1.00
^{65}Zn	1.14	0.44

where

- t = live time in seconds,
- ϵ_p = intrinsic peak efficiency for the gamma energy and detector size used (Fig. 3.6 and ref. 10),
- f = the decay fraction of the unknown activity which is the fraction of the total disintegrations in which the measured gamma is emitted (refs. 7 and 8 and Table 3.2),
- G = area of detector (cm^2)/ $4\pi s^2$,
- s = source-to-detector distance in cm.

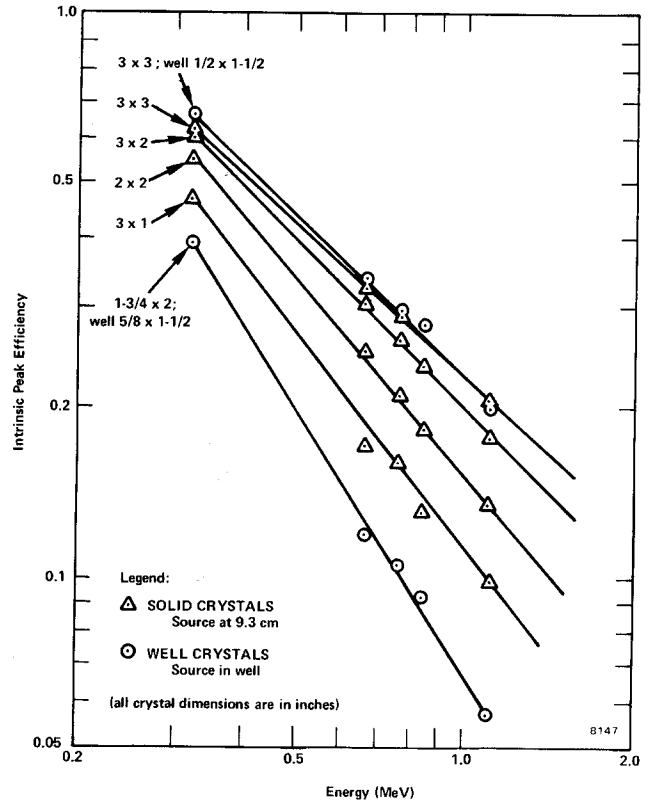


Fig. 3.6. Intrinsic Peak Efficiency of Various NaI(Tl) Crystals vs Gamma Energy.

EXPERIMENT 3.7

Mass Absorption Coefficient

Purpose

The purpose of the experiment is to measure experimentally the mass absorption coefficient in lead for 662-keV gamma rays.

References 2, 3, and 5 point out that gammas interact in matter primarily by photoelectric, Compton, or pair-production interactions. The total-mass absorption coefficient can be measured easily with a gamma-ray spectrometer. In this experiment we will measure the number of gammas that are removed from the photopeak by photoelectric or Compton

interactions that occur in a lead absorber placed between the source and the phototube.

From Lambert's law (ref. 1) the decrease of intensity of radiation as it passes through an absorber is given by

$$I = I_0 e^{-\mu x}, \quad (8)$$

where

- I = intensity after the absorber,
- I₀ = intensity before the absorber,
- μ = total-mass absorption coefficient in cm²/g,
- x = density thickness in g/cm².

The density thickness is the product of the density in g/cm³ times the thickness in cm.

The half-value layer (HVL) is defined as the density thickness of the absorbing material that will reduce the original intensity by one-half. From Eq. (8):

$$\ln I/I_0 = -\mu x. \quad (9)$$

If I/I₀ = 0.5 and x = HVL, $\ln 0.5 = -\mu(\text{HVL})$ and hence

$$\text{HVL} = \frac{0.693}{\mu} \quad (10)$$

In this experiment we will measure μ in lead for the 0.662-MeV gammas from ¹³⁷Cs. The accepted value is 0.105 cm²/g. Values for other materials can be found in ref. 8.

Procedure

1. Place the ¹³⁷Cs source about 5.0 cm from the NaI(Tl) detector and accumulate the spectrum long enough for the sum under the 0.662-MeV peak (Σ_{Cs} - Σ_b) to be at least 6000 counts. Determine (Σ_{Cs} - Σ_b).
2. Erase the MCA and insert a piece of lead from the absorber kit between the source and the detector. Accumulate the spectrum for the same period of live time as in step 1 above. Determine (Σ_{Cs} - Σ_b).
3. Erase the MCA and insert another piece of lead. Determine (Σ_{Cs} - Σ_b). Repeat with additional thicknesses of lead until the count-sum is >1000. Fill in the data in Table 3.3.

Table 3.3. Data for Mass Absorption Coefficient.

Absorber	Absorber Thickness (mg/cm ²)	Σ _{Cs} - Σ _b
1	0	
2		
3		
4		
5		
6		
7		

EXERCISES

- a. Using semilog graph paper, plot I vs absorber thickness in mg/cm², where I = (Σ_{Cs} - Σ_b)/live time. Determine the HVL from this curve and calculate μ from Eq. (10). How does your value compare with the accepted value of 0.105 cm²/g?
- b. Repeat the above experiment for the aluminum absorbers in the Absorber Kit. The μ for aluminum is 0.074 cm²/g.

EXPERIMENT 3.8

The Linear Gate in Gamma-Ray Spectroscopy

Purpose

The purpose of this experiment is to show how a linear gate can be used with an MCA in gamma-ray spectroscopy. The linear gate will limit the analysis of input pulse amplitudes to those that will be included within the photopeak.

The measurement of the mass absorption coefficient in Experiment 3.7 required the accumulation of several complete spectra, although the data of interest were included within only a fraction of the total number of channels that were used. The normal time for completing Experiment 3.7 is approximately 45 min. By using a linear gate, the same information can be obtained in about 1/3 of the time. An equivalent saving of time can also be made in Experiments 3.5 and 3.6 (Source Activity Determinations). Since the procedures are about the same as for Experiment 3.7, the student should repeat these experiments with the linear gate to see how much time will be saved.

See equipment list at beginning of Experiment 3 for additional equipment required for Experiment 3.8.

Connect the system components as shown in Fig. 3.7. Connect the bipolar output of the 575A Amplifier to both the 427A Delay and the 551 Timing Single-Channel Analyzer. Connect the Delay output to the linear Input of the 426 Linear Gate and connect the gate output to the analyzer input. Connect the SCA output to both the 875 Counter input and the Enable input of the Linear Gate.

The Linear Gate is a module that permits linear pulses to be passed only during the time interval that follows each Enable input. In normal operation the adjusted time interval will allow only one linear pulse to be furnished into the MCA.

The Timing Single-Channel Analyzer determines whether each input pulse amplitude is within the window and generates a logic output pulse for each input pulse that satisfies the criteria. By adjusting the lower and upper levels of its window, the 551 then can determine what portion of the spectrum is gated through for analysis in the MCA. This is true since it delivers the enable logic pulse to open the linear gate.

From the standpoint of timing, one would like to have the logic pulse arrive at the enable input of the linear gate just prior to the arrival of the corresponding linear pulse that is to be gated. Since the amplifier provides a bipolar output to the SCA, and since the SCA generates an output at 50% of full amplitude on the trailing edge of the positive lobe, the SCA output will occur at about $2 \mu\text{s}$ after the onset of the pulse. Thus, if the 427A Delay is set for $3 \mu\text{s}$ and the 426 Linear Gate width is adjusted to maximum, $4 \mu\text{s}$, the gate passes the input pulse for a period from $1 \mu\text{s}$ before the delayed pulse reaches the 426 until $3 \mu\text{s}$ of elapsed pulse time. This passes the positive portion of the bipolar pulse, which is all that affects the MCA measurement; the negative portion of the bipolar pulse is not used.

The inclusion of a counter in Fig. 3.7 permits a direct total of the counts to be observed, and the adjustment of the window width will limit these to the peak area. This simplifies the summing of counts for peak area integrations.

Figure 3.8 shows how Fig. 3.2 might look if the window of the SCA were set properly to just span the ^{137}Cs photopeak. Since the MCA has a live display while it is accumulating, it is quite simple to adjust the window of the SCA properly.

The single-channel principle and the control of the linear gate are examined here with individual modules. Both functions are also included in the MCA, so the separate modules are not required for other experimental applications.

Module Settings:

Use the same settings for the high-voltage power supply, preamplifier, and amplifier that were used for Experiment 3.1. Set the 426 Linear Gate for Normal with its Gate Width control fully clockwise for $4 \mu\text{s}$. Set the 875 Counter for count and use the Positive input from one of the Pos Out connectors on the 551 Timing SCA; reset the 875 Counter to zero. Set the 551 Timing SCA for Normal operation, the Lower-Level control at 030, the Upper-Level control fully clockwise

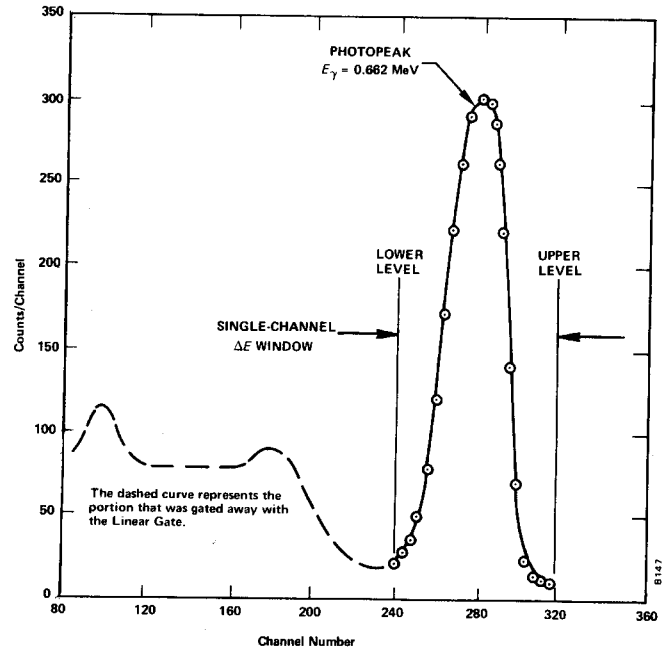


Fig. 3.8. ^{137}Cs Spectrum with the Linear Gate.

at 1000 divisions, and Delay at minimum for $0.1 \mu\text{s}$. Set the 427A Delay Amplifier for a $3\text{-}\mu\text{s}$ delay.

Procedure

1. Place the ^{137}Cs source from SK-1G about 4 or 5 cm from the crystal face. Accumulate a spectrum in the MCA while adjusting the E and the ΔE window on the 551 Timing SCA. Set the window so that it just brackets the photopeak as in Fig. 3.8. You are now ready to make the first measurements.
2. Clear the MCA and reset the counter to zero. Start both at the same time and accumulate for a period of time long enough to obtain about 6000 counts in the counter. Record

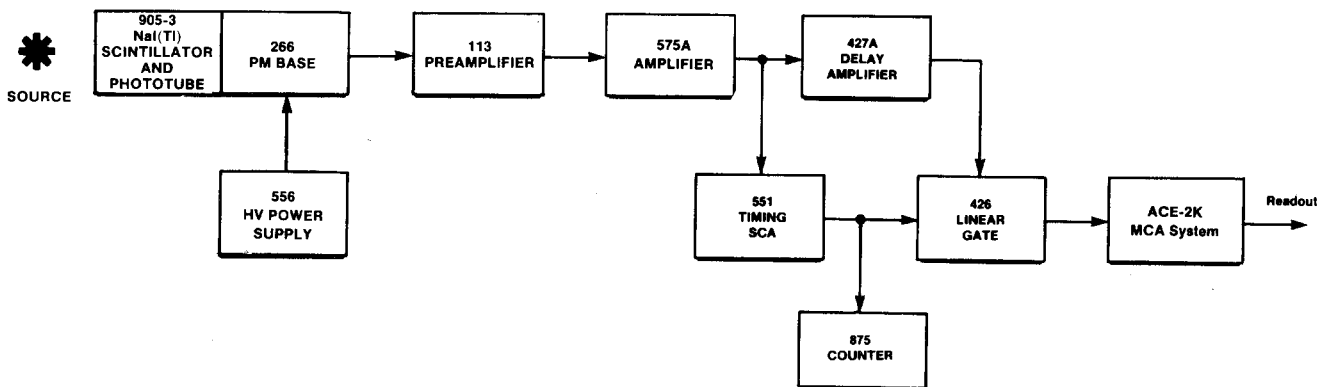


Fig. 3.7. Block Diagram of Electronics for Gamma-Ray Spectrometry System with a Linear Gate.

the total elapsed time for the measurement, the average dead time from the MCA, and the count in the counter. Read out the analyzer and then clear both the MCA and the counter.

3. Place the first lead absorber between the source and the detector as in Experiment 3.7 and accumulate for the same period of time that was used in step 2 above. Record only the counter counts and the total elapsed time. It is not necessary to read out the MCA for each spectrum since the counter is summing the counts under the photopeak. You should observe the MCA for each spectrum to make sure that the proper spectrum is being stored.

4. Repeat step 3 for each added absorber thickness that was used in Experiment 3.7. Make a background run with the source removed, and fill in Table 3.4 as in Experiment 3.7.

Table 3.4

Absorber	Absorber Thickness (mg/cm ²)	$\Sigma_{cs} - \Sigma_b$
1	0	
2		
3		
4		
5		
6		
7		

5. Calculate the same data as in Experiment 3.7, Exercises a and b.

6. In step 2 the output of the MCA was read. Sum this output spectrum and compare it with the counter sum that was taken from the same run. The counter sum should be slightly larger since it does not suffer from dead-time corrections at these counting rates. The MCA does suffer, because it requires some amount of time to measure and store each pulse and thus does not actually analyze as many pulses as have been furnished to it. The MCA sum should be equal to the counter count times the percent of live time, which is equal to the live time of the MCA divided by the clock time for the spectrum accumulation.

EXPERIMENT 3.9

Sum Peak Analysis

Figure 3.3 shows the two pronounced peaks in ⁶⁰Co. Figure 3.9 shows the decay scheme of ⁶⁰Co.

Most of the time the decay occurs by β emission to the 2.507-MeV excited state of ⁶⁰Ni. Subsequent decay to the ground state always occurs by gamma emission to the 1.3325-MeV level (a 1.174-MeV gamma) followed almost simultaneously by the 1.3325-MeV gamma to the ground state. In Experi-

ment 19 we will show that these two events are in coincidence and have an angular correlation that deviates from an isotropic distribution by only 16%. For the purposes of this experiment we can assume that each of these gammas are isotropically distributed. In other words, if γ_1 goes in a particular direction, γ_2 can go in any of the 4π steradians that it wishes. There is a certain probability that it will go in the same direction as γ_1 . If this occurs within the resolving time of the detector, γ_1 and γ_2 will be summed and hence a sum peak will show up in the spectrum. From the definitions in Experiment 3.6, the number of counts, Σ_1 , under the γ_1 peak is given by:

$$\Sigma_1 = \epsilon_1 G f_1 t A, \tag{11}$$

where A is the activity of the sample and t is the time. In a similar calculation, the sum Σ_2 for γ_2 is given by:

$$\Sigma_2 = \epsilon_1 G f_2 t A. \tag{12}$$

From Eqs. (11) and (12) the number of counts in the sum peak, Σ_s , is given by:

$$\Sigma_s = \epsilon_1 \epsilon_2 f_1 f_2 G^2 A t [W(0^\circ)], \tag{13}$$

where $W(0^\circ)$ is a term that accounts for the angular correlation function. For the case of ⁶⁰Co, Eq. (13) is quite simple. Σ_s becomes:

$$(\Sigma_s)_{60\text{Co}} \cong \epsilon_1 \epsilon_2 G^2 A t, \tag{14}$$

since $W(0^\circ) \cong 1.0$.

In this experiment we will show that the sum peak for ⁶⁰Co has an energy of 2.507 MeV and that its sum is given by Eq. (14).

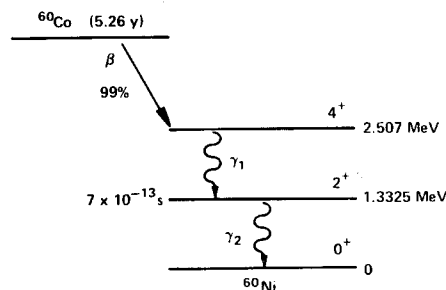


Fig. 3.9. The Decay Scheme of ⁶⁰Co.

Procedure

1. Set up the electronics as shown in Fig. 3.1.
2. Use the gammas from the source kit to calibrate the MCA so that full scale is ~ 3.0 MeV. For 1024 channels this would put the ¹³⁷Cs (0.662 MeV) peak at approximately channel 225.
3. Construct a calibration curve as in Experiment 3.1.
4. Place the ⁶⁰Co source from the source kit at exactly 9.3 cm from the face of the detector. Count for a period of time long enough so that the area under the sum peak is ~ 1000 counts. This procedure was outlined in Experiment 3.6.

EXERCISES

- a. Verify that the energy of the sum peak is 2.507 MeV. Subtract the background from the sum peak and verify its sum from Eq. (14).
- b. Repeat this sum peak analysis for the ²²Na source. Figure 3.10 shows the decay scheme for ²²Na and a typical spectrum with the sum peak.

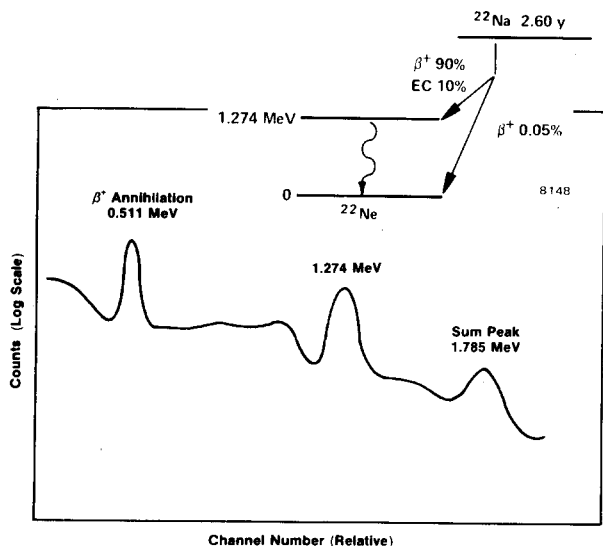


Fig. 3.10. Sum Peak for the ²²Na Source from Source Kit SK-1G.

EXPERIMENT 3.10

Photoelectric Absorption

Purpose

The purpose of this experiment is to study the photoelectric absorption of photons and verify the strong dependence of this process on the atomic number of the absorbing material.

When a gamma of energy <150 keV interacts with matter, the interaction has a high probability of being photoelectric. In the photoelectric interaction, the photon interacts with one of the tightly bound electrons in the material. The electron, in general, is knocked out of the atom with an energy given by:

$$E_e = hf - E_b,$$

where f is the frequency of the photon and E_b is the binding energy of the electron that is involved in the interaction. The probability of photoelectric interaction is dependent on the atomic number of the absorbing material and the energy of the gamma or x-ray photon. Although it is difficult to write out an exact analytic expression for this probability, it can be shown that for low energy photons

$$\mu = \frac{K \cdot Z^n}{E_\gamma^3}, \tag{15}$$

where K is a constant, Z is the atomic number, and n is usually between 4 and 5.

Procedure

The set up for this experiment is the same as for Experiment 3.7.

1. Place the ⁵⁷Co source ~3.8 cm from the NaI detector. Accumulate for a time period long enough to get reasonable statistics in the 122-keV line. As in Experiment 3.7, Σ - Σ_b should be at least 6000 counts.
2. Clear the MCA and place the thinnest aluminum absorber between the source and the detector. Count for the same period of time as in step 1. Repeat for the other two aluminum absorbers.
3. Repeat steps 1 and 2 for the other thin absorbers, Fe, Cu, Mo, Sn, Ta, and Pb, in the Model 3-Z2 source kit. Note: The counting time might have to be increased as the atomic number of the absorber is increased.

EXERCISES

- a. For the three measurements made with the thin aluminum foils, calculate and average μ, Eq. (9). Repeat for the other absorbers.
- b. Make a plot of μ vs Z^{4.5}/E_γ³ from your experimental data. How do your results compare to the theory?

References

1. G. F. Knoll, *Radiation Detection and Measurement*, John Wiley and Sons, New York (1979).
2. J. B. Birks, *The Theory and Practice of Scintillation Counting*, Pergamon Press, Oxford (1964).
3. S. M. Shafroth, Ed., *Scintillation Spectroscopy of Gamma Radiation*, Gordon and Breach, London (1967).
4. K. Siegbahn, Ed., *Alpha, Beta and Gamma Spectroscopy*, North Holland Publishing Co., Amsterdam (1968).
5. P. Quittner, *Gamma Ray Spectroscopy*, Halsted Press, New York (1972).
6. W. Mann and S. Garfinkel, *Radioactivity and its Measurement*, Van Nostrand-Reinhold, New York (1966).
7. C. M. Lederer and V. S. Shirley, Eds., *Table of Isotopes*, 7th Edition, John Wiley and Sons, Inc., New York (1978).
8. *Radiological Health Handbook*, U.S. Dept. of Health, Education, and Welfare, PHS Publ. 2016. Available from National Technical Information Service, U.S. Dept. of Commerce, Springfield, Virginia.
9. 14th Scintillation and Semiconductor Counter Symposium, *IEEE Trans. Nucl. Sci.* **NS-22**(1) (1975).
10. R. L. Heath, *Scintillation Spectrometry, Gamma-Ray Spectrum Catalog*, 1 and 2, Report No. IDO-16880. Available from the National Technical Information Center, U.S. Dept. of Commerce, Springfield, Virginia.

Alpha Spectroscopy with Surface Barrier Detectors

EQUIPMENT NEEDED FROM EG&G ORTEC

Source Kit SK-1A (see Appendix)

Surface Barrier Detector R-017-050-100

142A Preamplifier

Bin and Power Supply

575A Amplifier

807 Vacuum Chamber

428 Detector Bias Supply

408A Biased Amplifier

480 Pulser

ACE-2K MCA System including suitable IBM PC (other EG&G ORTEC MCAs may be used)

Mechanical Vacuum Pump

Oscilloscope

ORC-4 Cable Set

Purpose

The purpose of this experiment is to familiarize the student with the use of silicon charged-particle detectors and to study some of the properties of alpha-emitting isotopes.

Applicability

Semiconductor charged-particle detectors have been used extensively in experimental nuclear research for almost 20 years. In this period of time they have revolutionized nuclear particle detection. Recent publications in any of the nuclear journals indicate that semiconductor detectors are now used almost exclusively for the detection of charged particles. Semiconductor gamma- and x-ray detectors have contributed perhaps even more significantly in their own field of photon spectroscopy.

Semiconductor charged-particle detectors can be used through an extensive range of energies. These include 20-keV electrons on one end of the spectrum and 200-MeV heavy ions on the other. The inherent resolution of these surface barrier detectors is surpassed only by magnetic spectrometers. The detector output pulses rise rapidly and hence are well-suited for fast (~ 1 ns) timing with coincidence circuitry or time-to-amplitude converters (TACs).

The efficiency of these detectors for their active volume is essentially 100%, and their energy vs pulse-height curves are linear over a rather impressive range. It is fortunate that they also have good long-term pulse-height stability. This is particularly noticed when they are contrasted with scintillation counters, gas proportional counters, or ionization chambers. Finally, their small size and compactness make them easily adaptable to almost any type of counting geometry. The remaining fact of particular interest in the educational market is that they are relatively inexpensive.

It should take about 6 h to complete all parts of Experiment 4. The parts are written so that they can be completed in two 3-h laboratory periods, or certain parts can easily be omitted if equipment or time is not available.

Alpha Sources

CAUTION: Alpha sources offer a potential personal contamination problem. Never touch the face of a source with your fingers. Most alpha sources are electrodeposited onto platinum blanks. The actual radioactive source is usually a spot about 1 mm in diameter, and it has been deposited in the geometrical center of the disk. If you look carefully, you may be able to see the deposited spot. The ^{210}Po source in SK-1A has been evaporated onto a silver disk, and the disk covered with a piece of plastic with a hole through the center for transmission of the alpha particles. Always handle an alpha source by the edge of the mounting disk.

Surface Barrier Detectors

There are three main parameters that define a silicon surface barrier detector: resolution, active area, and depletion depth. The EG&G ORTEC model numbers reflect each of these three parameters in that order. The R-017-050-100 detector is a style R (Ruggedized) detector with a resolution of 17-keV FWHM for ^{241}Am alphas, an area of 50 mm^2 , and a depletion depth of $100\text{ }\mu\text{m}$.

The quoted resolution of an EG&G ORTEC detector is a measure of its quality. These resolutions can be measured only with a complete set of electronics, set for standard conditions, and the EG&G ORTEC guaranteed resolutions are measured with standard EG&G ORTEC electronics. A resolution of 20 keV or better is satisfactory for all parts of Experiment 4.

Since the shape of the detector is a circular disk, its active area is determined by the diameter of its face. At any given distance from the source a larger area will subtend a larger angle and thus intercept a greater portion of the total number of alpha particles that emanate from the source. A nominal area of 50 mm^2 is suggested for this experiment, but any area from 25 through 100 mm^2 will provide the information.

The depletion depth is synonymous with the sensitive depth of the detector. For any experiment the depth must be suf-

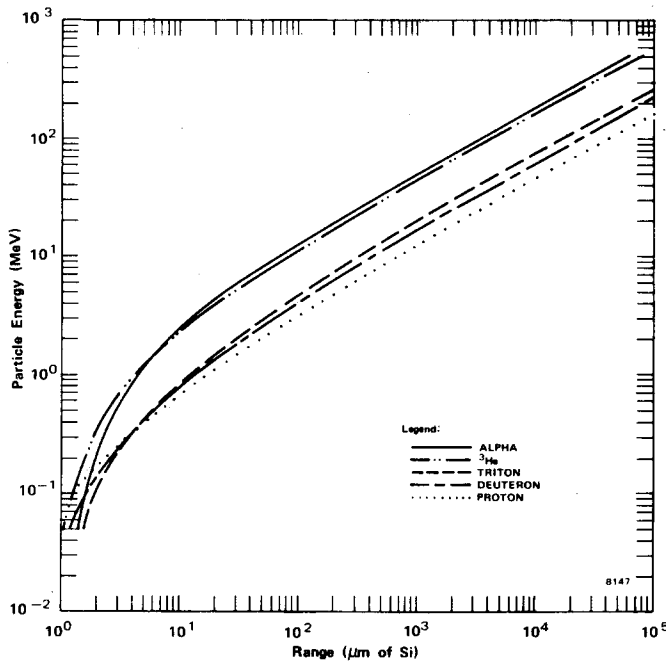


Fig. 4.1. Energy-Range Curves for Charged Particles in Silicon.
 [Data taken from C. F. Williamson, J. P. Boujot, and J. Picard, *Tables of Range and Stopping Power of Chemical Elements for Charged Particles of Energy 0.5 to 500 MeV*, CEA-R-3042 (July 1966).]

ficient to completely stop all the charged particles that are to be measured, and its ability to do this is dependent upon both the energy and the particle type. Figure 4.1 is a range-energy curve for five of the more common charged particles. From it, the minimum depth can be determined for the maximum energy of a particle type. From Fig. 4.1 note that a 5.5-MeV alpha is completely stopped with $\sim 27 \mu\text{m}$ of silicon. Since natural alphas are usually $< 8 \text{ MeV}$ in energy, a $50\text{-}\mu\text{m}$ detector is adequate to stop all natural alphas.

EXPERIMENT 4.1

Simple Alpha Spectrum and Energy Calibration with a Pulser

Procedure

1. Connect the equipment as shown in Fig. 4.2. For the examples shown below, the ^{210}Po source from Source Kit SK-1A has been selected.

2. Make the following settings: Adjust the distance from the alpha source to the detector to about 1 cm (inside the 807 Vacuum Chamber). Pump the vacuum in the chamber down to $500 \mu\text{m}$ or less. (If a vacuum gauge is not available, a pumping time of 2 min is usually adequate.) Set the 575A Amplifier for a negative input and unipolar output. Set the 480 for a positive pulse polarity and use the attenuated output. Set the 428 for a negative bias output and raise the voltage slowly to the value recommended on the detector data sheet. Voltage must be increased to compensate for voltage dropped across the high-value resistor in the Model 142A Preamplifier. Refer to Section 4.7 of the Model 428 Detector Bias Supply Manual.

3. Adjust the gain of the 575A Amplifier until the pulse amplitude observed by the oscilloscope is $\sim 5 \text{ V}$. The ^{210}Po alpha source used for this example has an alpha energy of 5.31 MeV. The source activity ($\sim 1 \mu\text{Ci}$) and the counting geometry are such that the pulse rate should be adequate for oscilloscope observation.

4. Accumulate a spectrum with the MCA long enough to have about 400 counts in the peak channel. The spectrum should resemble that of Fig. 4.3. Determine the centroid channel number for the alpha peak. Call this channel C_0 . In the example of Fig. 4.3, C_0 is channel 520, and this represents the location in the spectrum for the ^{210}Po 5.305-MeV alpha events. The FWHM, measured in number of channels, is $\delta = 16$.

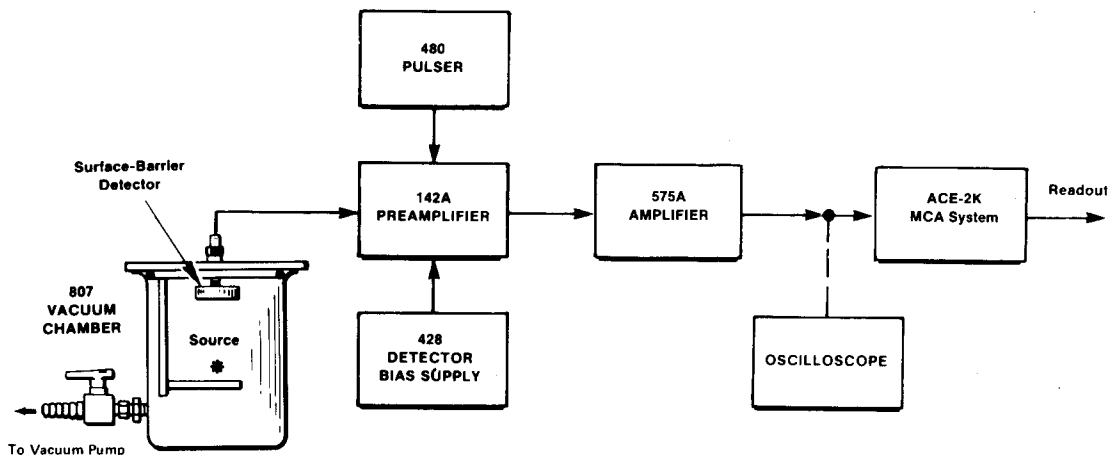


Fig. 4.2. System for Alpha Spectroscopy.

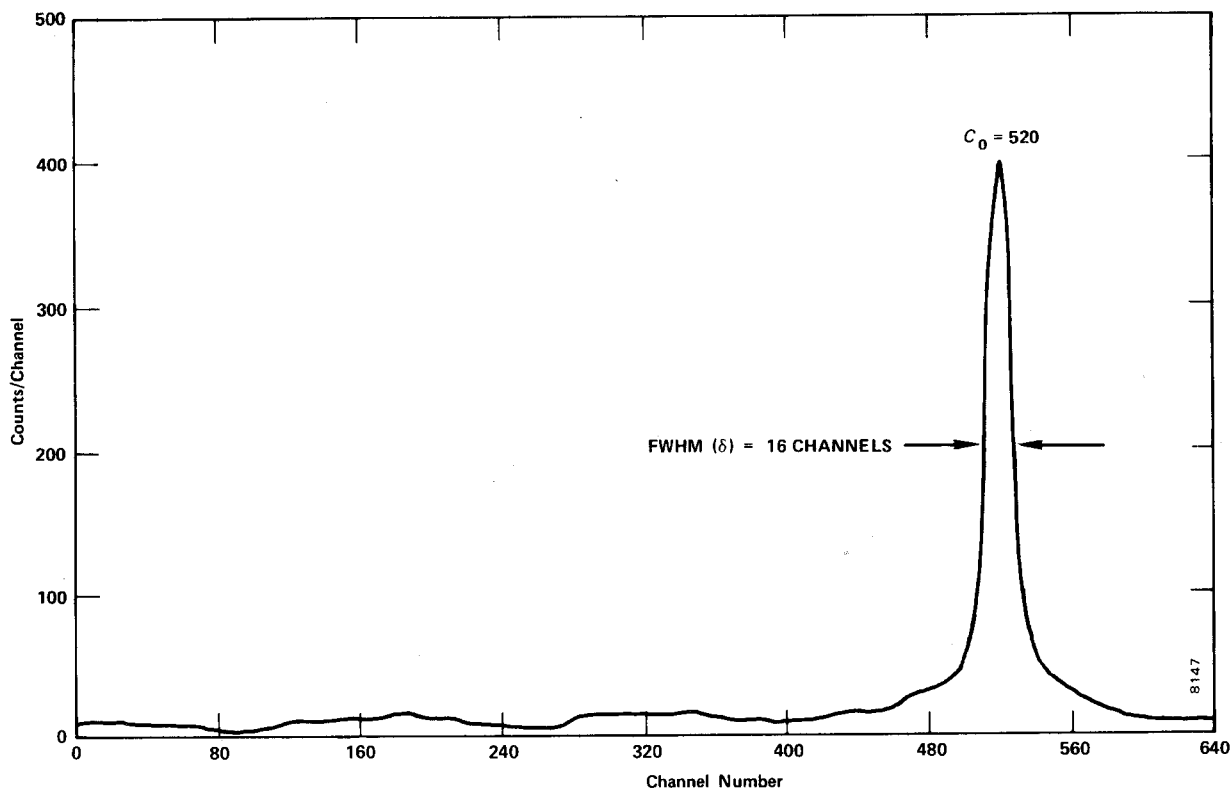


Fig. 4.3. Plot of a Typical ²¹⁰Po Alpha Spectrum.

5. Turn on the 480 Pulser and set its pulse-height dial at 531/1000. Adjust the attenuators and the calibration control until the pulse generator output is ~5 V in amplitude. The output pulses from the 575A Amplifier for the pulse generator input should now be approximately the same amplitude as the pulses from the ²¹⁰Po alphas. The pulses from both sources can be observed simultaneously on the oscilloscope.

6. Accumulate the pulser pulses in the MCA for ~20 s. Do they fall above or below channel C₀? Adjust the calibrate control on the pulse generator as necessary to locate the pulser peak exactly in channel C₀. Your pulser is now calibrated to the system so that 5.31 MeV corresponds to 531/1000 on the pulse-height dial, and therefore, any setting of the pulse-height dial represents an identified energy level. For example, 600/1000 = 6 MeV, etc.

7. Erase the MCA and accumulate the pulser pulses for ~20 s at each of the pulse-height values in Table 4.1. Determine their position with the cursor of the MCA.

EXERCISES

a. Fill in the column of data that is missing in Table 4.1. Make a plot on linear graph paper of energy (MeV) vs channel number. Compare this plot with that in Fig. 4.4. For identification purposes the 5-MeV point is accumulated for 40 s.

b. The slope of the curve in Fig. 4.4, $\Delta E/\Delta C$, is the energy per channel. For convenience this is usually expressed in

keV/channel, and in Fig. 4.4 it is ~10 keV/channel. Determine the keV/channel for the plot you made in Exercise a.

c. The resolution in a spectrum is calculated as follows:

$$\text{resolution} = \frac{\Delta E}{\Delta C} \times \delta \text{ (ch)}, \quad (1)$$

where $\delta \text{ (ch)}$ = channels FWHM. For example, in Fig. 4.3 the $\delta \text{ (ch)}$ for FWHM is 16 channels for the energy range from channel 512 through 528. It is measured at the points in the spectrum where the number of counts per channel is half the number of counts at the peak. In the example the FWHM resolution is, then, 160 keV. Calculate the $\delta \text{ (ch)}$ and the resolution of your alpha peak.

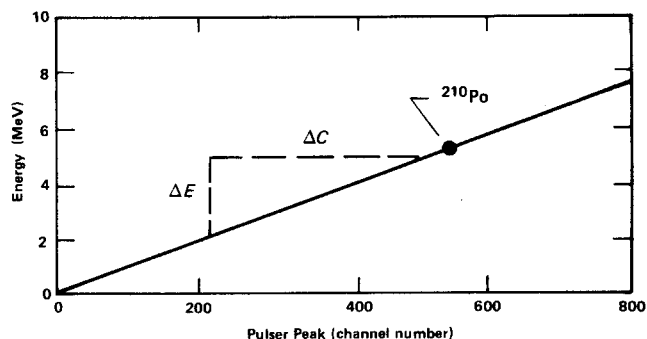


Fig. 4.4. Calibration Curve for Alpha Spectroscopy.

Table 4.1. Channel Numbers for Equivalent Energies

Accumulation Time (approx. s)	Pulse-Height Dial Setting	Equivalent Energy (MeV)	Channel Number of MCA Peak
20	100/1000	1.0	
20	200/1000	2.0	
20	300/1000	3.0	
20	400/1000	4.0	
40	500/1000	5.0	
20	600/1000	6.0	
20	700/1000	7.0	

EXPERIMENT 4.2

Energy Determination of an Unknown Alpha Source

Purpose

The purpose of this experiment is to identify the peak energy of an unknown alpha source. Its energy or energies can be determined with the system of Experiment 4.1 since the system has already been calibrated.

Procedure

1. Reduce the detector bias voltage to zero. Turn off the vacuum pump and allow the chamber pressure to come up to atmospheric pressure. Open the chamber and replace the ²¹⁰Po standard source with the unknown alpha source. Pump the vacuum back down until the pump is quiet. Increase the detector bias slowly to its proper operating level again. Turn off the 480 Pulser.
2. Accumulate the spectrum for the unknown until the more pronounced peaks in the spectrum can be identified.

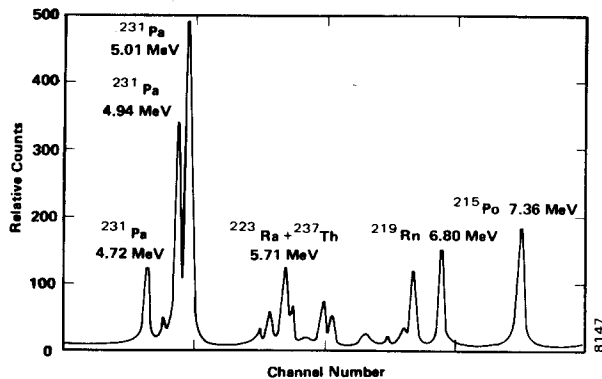


Fig. 4.5. Portion of a Typical ²³¹Pa Alpha Spectrum.

EXERCISE

Determine the energies of the peaks from your calibration curve. The source could contain just one peak, or it might have a number of alpha energies. For example, Fig. 4.5 shows a portion of a spectrum for ²³¹Pa and its daughters. Identify the source by its energy or energies. Figure 4.6 shows a ²³⁴U spectrum that was taken with a 25.5-keV resolution.

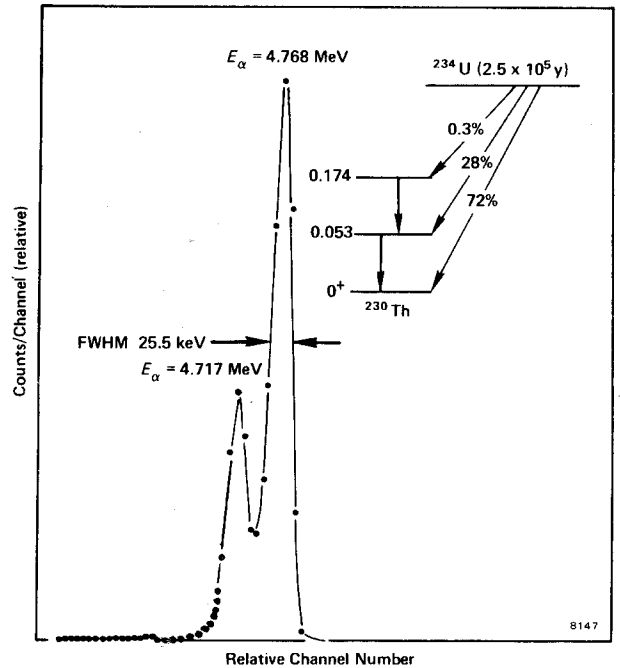


Fig. 4.6. Typical Alpha Spectrum from ²³⁴U Showing Alphas from the Two States in ²³⁰Th.

EXPERIMENT 4.3

Energy Calibration with Two Alpha Sources

An energy calibration can, of course, be made if two alpha sources are available; for example, ²⁴¹Am (E_α = 5.48 MeV) and ²¹⁰Po (E_α = 5.31 MeV).

Procedure

1. Place the ²⁴¹Am source in the vacuum chamber, pump down, and set the bias voltage. Adjust the gain of the 575A Amplifier until the ²⁴¹Am (5.48 MeV) is being accumulated in the top half of the analyzer, for example, channel 800. Record the peak channel.
2. Replace the ²⁴¹Am with the ²¹⁰Po and accumulate again for a long enough period of time to determine the peak position. If the analyzer zero level has been set so that zero energy is approximately channel zero, three points (0, 5.31, and 5.48 MeV) are now available for the calibration curve. Draw the best straight line through these three points. If the

analyzer zero level has not been set, a line through the source locations will indicate the offset of the analyzer zero.

EXERCISE

From the calibration curve determine the keV/channel and the resolution as in Experiment 4.1. Generally speaking, the pulser method outlined in Experiment 4.1 is the better way to establish the calibration for the system.

EXPERIMENT 4.4

Absolute Activity of an Alpha Source

Purpose

The purpose of this experiment is to determine the absolute activity of an alpha source, which in this case is ^{210}Po .

It was mentioned earlier that surface barrier detectors are essentially 100% efficient for their active area. It is therefore quite easy to determine an unknown source activity.

Procedure

1. Carefully place the ^{210}Po source in the vacuum chamber (exactly 4 cm from the detector's face), adjust the gain so that the 5.31-MeV alpha is in the analyzer (about midscale), and accumulate a spectrum. Store the spectrum long enough for the sum under the peak (Σ_α) to be equal to ~ 2000 counts. Determine Σ_α .

2. Calculate the activity of the source from the following expression

$$\text{activity (alpha per s)} = \left(\frac{\Sigma_\alpha}{t} \right) \left(\frac{4\pi s^2}{\pi r^2} \right) \quad (2)$$

where

s = distance from source to detector (4 cm in our example),

r = radius of the detector (cm),

t = time in seconds,

Σ_α = sum under the alpha peak.

Since $1 \mu\text{Ci} = 3.7 \times 10^4$ disintegrations/s, the answer from Eq. (2) can easily be converted to μCi 's and compared with the actual source activity. (If it is not written on the source, the laboratory instructor will supply the activity of the source.) Remember, the half-life of ^{210}Po is 138 days. If the instructor gives the activity of the source when it was made, a correction will have to be made for its present activity.

EXPERIMENT 4.5

Spectrum Expansion with a Biased Amplifier

Purpose

The purpose of this experiment is to see how the addition of a biased amplifier to the system will expand a portion of the spectrum. Connect the system as shown in Fig. 4.7.

The EG&G ORTEC 408A Biased Amplifier provides a variable bias level and a subsequent gain to the main amplifier output pulses. Each pulse that has an amplitude less than the bias level setting will be entirely eliminated from the spectrum. Each pulse that has an amplitude greater than the bias level will have the bias level subtracted from it, and the portion above the bias level can then be amplified by a factor of up to 20 using the selectable gain switch on the 408A. The bias level adjustment range is from 0 V (0/1000 on the bias level control) to ~ 10 V (1000/1000). Thus the minimum energy level of any area of interest in the spectrum can be selected, and the range above this level can be amplified, or expanded, for the desired lower keV/channel analyzer distribution. This experiment, and also Experiment 4.6, shows the advantages of this capability.

Procedure

1. Select a ^{241}Am source with a source thickness of ~ 15 keV or less. Place the source in the vacuum chamber, evacuate, and raise the detector bias gradually to the amount indicated on the detector data sheet. Adjust the gain of the 575A Amplifier for about 5 V output pulses. Set the bias level of the 408A Biased Amplifier at 0/1000 and its gain at 1; its output

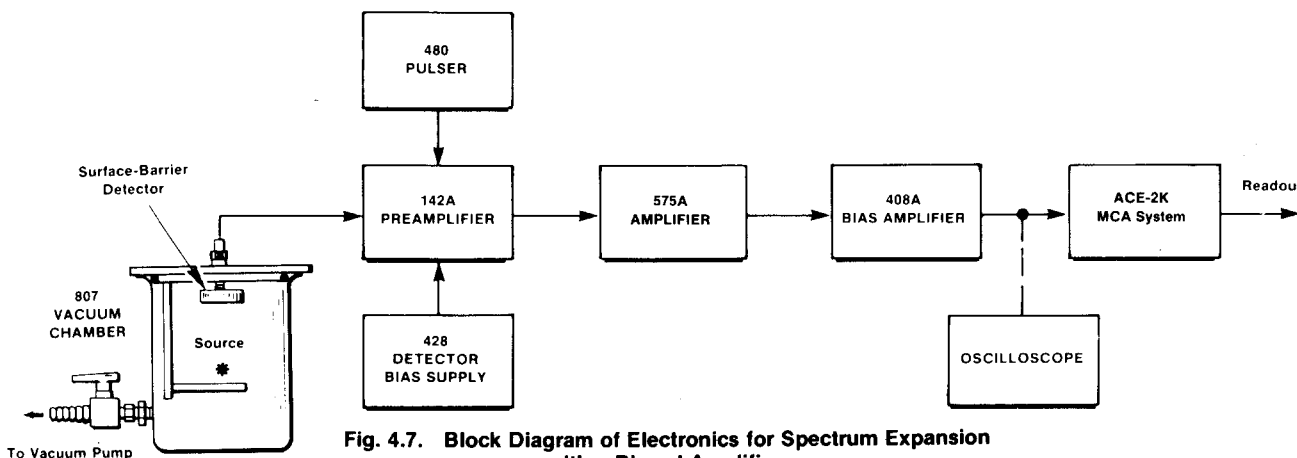


Fig. 4.7. Block Diagram of Electronics for Spectrum Expansion with a Biased Amplifier.

pulses should also be about 5 V. Accumulate a spectrum in the MCA and determine the peak channel location of the 5.48-MeV alpha from ²⁴¹Am.

2. Turn on the 480 Pulser and set its Pulse-Height control at 548/1000. Use the attenuation switches and the calibrate control to place the pulse generator pulses in the same channel location as the 5.48-MeV peak for the ²⁴¹Am source. This is the same procedure that was followed in Experiment 4.1. The pulse generator's Pulse-Height dial is now calibrated for 0 to 10 MeV.

3. Set the pulse generator at 4 MeV (400/1000). Switch the analyzer back to accumulate. Raise the bias level on the 408A while periodically observing where the pulses are being stored in the analyzer. Continue raising the bias level until the 4-MeV pulse just disappears at the low end of the MCA. The bias level is now set at 4 MeV. All pulses below 4 MeV are being blocked by the biased amplifier.

4. Set the pulse generator at 6 MeV (600/1000). Increase the gain of the 408A Biased Amplifier until the 6-MeV pulses are being stored in the top portion of the MCA. The analyzer is now roughly calibrated from 4 to 6 MeV. Clear the MCA.

Table 4.2

Time (approx. s)	Pulse Height Setting (Pulse Generator)	E (MeV)	Channel No.
20	420/1000	4.20	
20	460/1000	4.60	
20	480/1000	4.80	
40	500/1000	5.00	
20	520/1000	5.20	
20	560/1000	5.60	
20	580/1000	5.80	

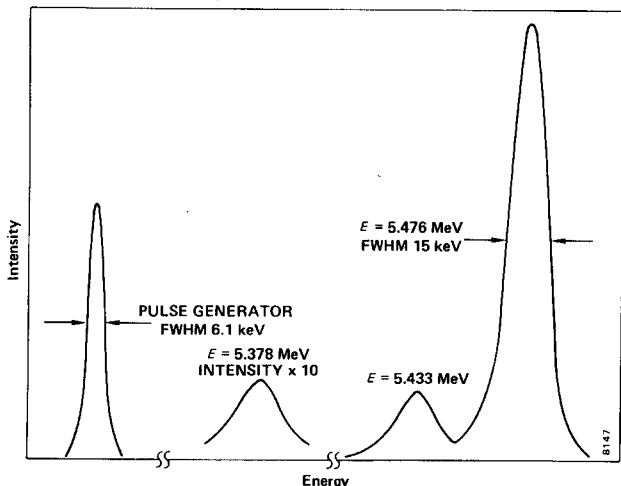


Fig. 4.8. ²⁴¹Am Alpha Spectrum.

5. Return the pulse generator to 4.20 MeV (420/1000) and accumulate in the MCA for ~20 s. Continue for the rest of the values in Table 4.2.

EXERCISE

From Table 4.2 plot E vs channel number and determine the keV/channel. This value can be used in Experiment 4.6. Compare this calibration curve with the one taken in Experiment 4.1 as shown in Fig. 4.4.

EXPERIMENT 4.6

Decay Ratios for ²⁴¹Am

This experiment is a continuation of Experiment 4.5.

Procedure

1. Clear the MCA and accumulate the ²⁴¹Am spectrum long enough to see a spectrum similar to that in Fig. 4.8.
2. From the MCA, determine the sum under the 5.476-MeV group. Call this sum Σ_2 since it comes from alpha decay to the second excited state of ²³⁷Np (Fig. 4.9). In the same manner determine Σ_4 (5.433-MeV group) and Σ_5 (5.378 MeV).

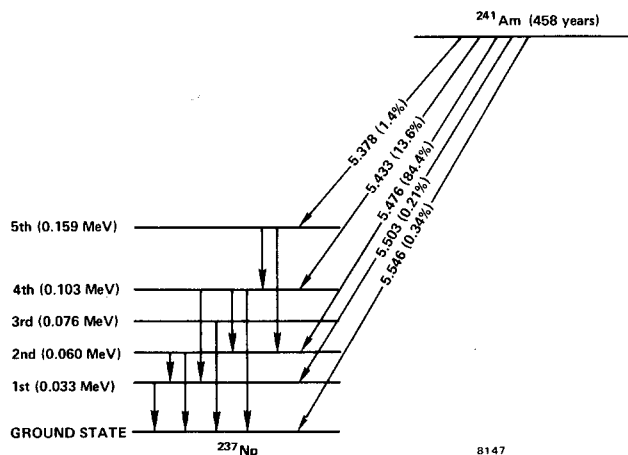


Fig. 4.9. Decay of ²⁴¹Am.

EXERCISES

a. With $\Sigma_T = \Sigma_2 + \Sigma_4 + \Sigma_5$, the decay ratio for α_2 (5.476 MeV) = Σ_2/Σ_T .

From your data, determine the decay ratios for α_2 , α_4 , α_5 . How do your values compare with those in Fig. 4.9?

b. Determine the resolution of one of the pulser peaks in Table 4.2. Define this quantity to be δ_E . From step 2 find the resolution of the 5.476-MeV alpha group. Define this resolution to be δ_T , which is the combined effect of electronics (δ_E), source thickness (δ_s), and detector resolution (δ_D).

These quantities are said to add in quadrature. That is,

$$\delta_T^2 = \delta_E^2 + \delta_s^2 + \delta_D^2. \quad (3)$$

Therefore

$$\delta_D = \sqrt{\delta_T^2 - \delta_E^2 - \delta_s^2}. \quad (4)$$

If the alpha source thickness is known, the other quantities can be measured. Find δ_D ; how does its value compare with that given on the EG&G ORTEC specification sheet for the detector?

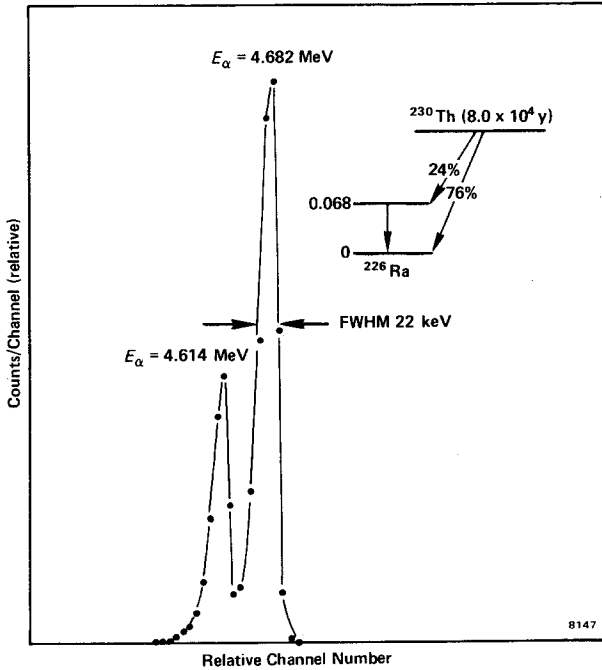


Fig. 4.10. Alpha Spectrum from the Decay of ^{230}Th Showing Alphas to the Ground and First Excited States in ^{226}Ra .

Figure 4.10 is a spectrum for ^{230}Th that has an FWHM of 22 keV.

References

1. G. F. Knoll, *Radiation Detection and Measurement*, John Wiley and Sons, New York (1979).
2. G. Bertolini and A. Coche, Eds., *Semiconductor Detectors*, American Elsevier Publishing Co., Inc. (1968).
3. G. Dearnaley, "Nuclear Radiation Detection by Solid State Devices," *J. Sci. Instrum.* **43**, 869 (1966).
4. *Surface-Barrier Radiation Detectors Instruction Manual*, available from EG&G ORTEC.
5. J. L. Duggan, W. D. Adams, R. J. Scroggs, and L. S. Anthony, "Charged-Particle Detector Experiments for the Modern Physics Laboratory," *Am. J. Phys.* **35**(7), 631 (1967).
6. C. M. Lederer and V. S. Shirley, Eds., *Table of Isotopes*, 7th Edition, John Wiley and Sons, Inc., New York (1978).
7. G. T. Ewan, "Semiconductor Spectrometers" (in progress), *Nucl. Tech. and Instrum.* **3**, F. M. Farley, Ed., Elsevier, North Holland, New York (1968).

Energy Loss of Charged Particles (Alphas)

EQUIPMENT NEEDED FROM EG&G ORTEC

Source Kit SK-1A
 Surface Barrier Detector R-017-050-100
 142A Preamplifier
 Bin and Power Supply
 575A Amplifier
 807 Vacuum Chamber
 428 Detector Bias Supply
 480 Pulser

ACE-2K MCA System including suitable IBM PC (other EG&G ORTEC MCAs may be used)
 ORC-5 Cable Set
 Mechanical Vacuum Pump
 Oscilloscope
 AuFI-x (gold foil) and NiFI-x (nickel foil) (see Appendix)
 Copper Absorber Kit MCU-5
 Nickel Foils MNI-5

Purpose

In this experiment the principal concern will be the specific ionization and rate of energy loss, dE/dx , of an alpha particle as it passes through matter. The two experiments relate to alpha particles passing through copper foil and through a gas.

Theory

As stated previously, alphas from natural sources typically have energies in the range of 3 to 8 MeV. The alpha is a relatively massive nuclear particle compared with the electron (~8000 times the mass of the electron). When an alpha particle goes through matter it loses energy primarily by ionization and excitation. Since the alpha particle is much larger than the electrons with which it is interacting, it travels through matter in a straight line. The energy required to strip one electron from a gas typically lies between 25 and 40 eV. For air, the accepted average ionization potential is 32.5 eV. The number of ion pairs that are theoretically possible can therefore be calculated easily.

Specific ionization is defined as the number of ion pairs produced per unit of path length. Specific ionization is energy dependent. The reason for this energy dependence is that it affects the rate of travel through the material that is being ionized; lower energy alpha particles spend more time per unit of path length than do the higher energy particles. Figure 5.1 is the familiar Bragg curve for alpha particles.

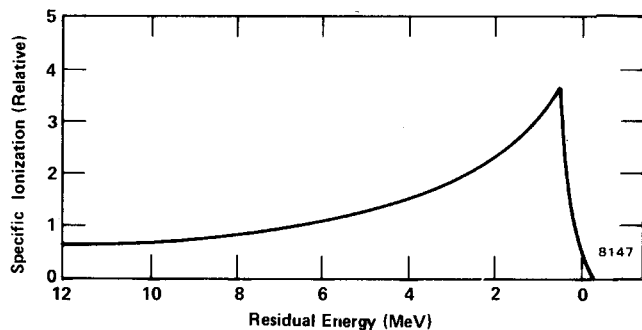


Fig. 5.1. Bragg Curve for Alpha Particles.

The dE/dx for alphas, the stopping power in ergs/cm, is given by the following expression (ref. 10).

$$\frac{dE}{dx} = \frac{2\pi Z_i^2 e^4 N Z}{m_0 c^2 \beta^2} \ln \left(\frac{2m_0 c^2 \beta^2 Q_{\max} - 2\beta^2}{I^2 (1 - \beta^2)} \right) \quad (1)$$

where

- Z_i = the atomic number of the incident particle,
- e = electronic charge (esu),
- m_0 = rest mass of electron (g),
- c = velocity of light (cm/s),
- β = ratio of incident alpha velocity divided by velocity of light,
- NZ = number of electrons per unit volume of absorber (electrons/cm³),
- Q_{\max} = maximum energy transfer from an electron to the alpha (ergs),
- I = mean ionization potential of the target (ergs),
- E = energy of the incident particle (ergs).

A careful evaluation of Eq. (1) for 5-MeV alpha particles will show that the dE/dx is approximately constant for thin absorbers in which the alpha particle will lose only 1 MeV or so

The range of an alpha particle can be found by rearranging and integrating Eq. (1) from E_0 to zero, where E_0 is the initial energy of the alpha. Figure 5.2 is an example of a graph of energy vs range. Note that the range is expressed in mg/cm² in Fig. 5.2.

In Fig. 5.2 E_0 is the initial energy of the alpha particle before it passes through the foil, R_0 is the range in copper of an alpha of energy E_0 , E_r is the energy that still accompanies the alpha after it has passed through the foil, R_r is the range of an alpha with an E_r , and ΔX is the foil thickness in mg/cm².

The theoretical energy loss that should be expected for a given foil thickness can be determined by the method shown in Fig. 5.2. In the laboratory the alpha energy from the source, E_0 , and the foil thickness, ΔX (mg/cm²), will be

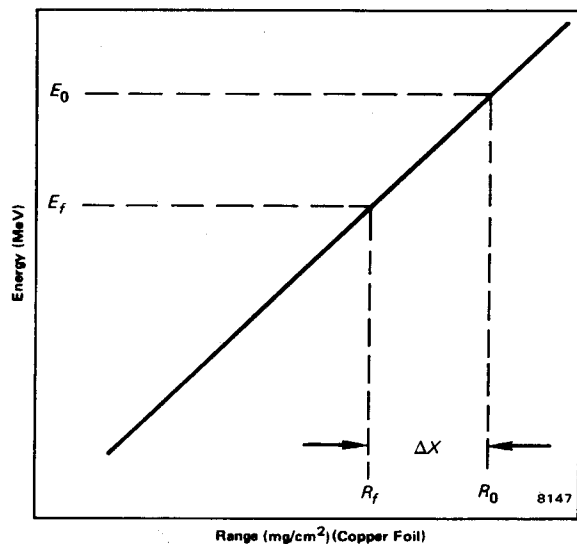


Fig. 5.2. Energy vs Range (Illustrative) for Charged Particles.

provided. It is then a simple matter to determine R_f , because $R_f = R_0 - \Delta X$. From R_f , energy E_f can be determined quickly.

Table 5.1 tabulates some range-energy information for copper, nickel, gold, and helium. Figure 5.3 shows a plot of these data for copper.

The foils that are best suited to dE/dx measurements are copper, nickel, and gold. Seven copper foils are included in Absorber Kit MCU-5.

Table 5.1. Range-Energy Values for Alpha Particles in Various Absorbers*

E_0 (MeV)	Ranges (mg/cm ²)			
	Copper	Nickel	Gold	Helium
0.25	0.79	0.74	1.31	0.181
0.50	1.09	1.02	1.90	0.245
0.75	1.38	1.29	2.50	0.316
1.00	1.69	1.58	3.12	0.399
1.25	2.01	1.88	3.79	0.490
1.50	2.36	2.21	4.47	0.601
2.00	3.11	2.91	5.97	0.850
2.50	3.93	3.68	7.59	1.14
3.00	4.82	4.50	9.34	1.48
3.50	5.80	5.44	11.0	1.86
4.00	6.81	6.39	13.1	2.29
4.50	7.9	7.40	15.2	2.76
5.00	9.1	8.51	17.4	3.27
5.50	10.3	9.66	19.7	3.82
6.00	11.6	10.87	22.1	4.41
7.00	14.3	13.46	27.1	5.70

*Data taken from ref. 10.

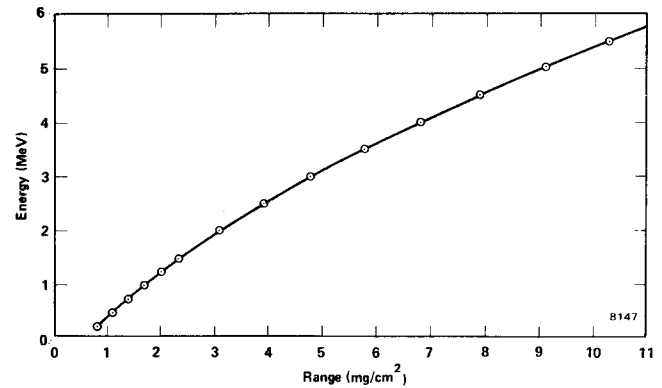


Fig. 5.3. Energy vs Range for Alpha Particles in Copper.

EXPERIMENT 5.1

dE/dx for Alpha Particles in Copper Foil

Prerequisite: Experiment 4.1.

Procedure

1. Connect the equipment as shown in Fig. 5.4. Calibrate the system with the ²¹⁰Po source from the SK-1A source kit so that the 5.31-MeV alpha particles from the ²¹⁰Po are being stored in the top quarter of the analyzer. Plot the calibration curve and determine the resolution of the pulser and of the alpha source as in Experiment 4.1.

Module Settings:

- 575A Amplifier: negative input, unipolar output.
- 480 Pulser: positive pulse polarity, attenuated output.
- 428 Detector Bias Supply: negative output; raise bias slowly to value recommended for the detector.*

2. Erase the data from the MCA. Turn off the pulse generator and store the ²¹⁰Po spectrum long enough to obtain a sum under the alpha peak of ~4000 counts.

3. Reduce the bias voltage to zero. Open the vacuum system and place the thinnest copper foil between the source and the detector. Do not change the source-detector geometry during the rest of this experiment; both the distance and the angle of incidence must remain constant.

4. Pump the vacuum back down, increase the bias voltage gradually, and accumulate the spectrum for the same time that was used in step 2. Determine the peak position and the sum.

5. Repeat steps 3 and 4 for all the foil thicknesses in the Absorber Kit. Figure 5.5 shows some typical data that were obtained for alpha particles on copper foil.

EXERCISES

- a. From the calibration curve and the MCA data, measure the energy loss, ΔE , for each foil thickness. Note that the

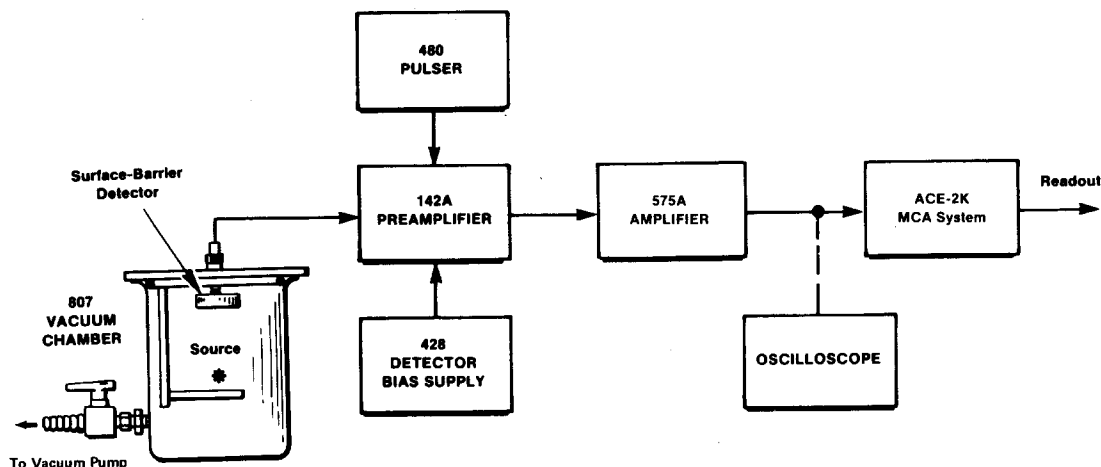


Fig. 5.4. Electronics for dE/dx Measurement.

resolution gets worse as the foil thickness and the ΔE values increase. Determine the resolution for each peak.

b. On linear graph paper plot the range vs energy for copper (Table 5.1). From the graph and the foil thicknesses find E_r by the method outlined in "Theory." Use the ΔE values and construct a table similar to that furnished for Fig. 5.5 (Table 5.2) for your data and fill it in.

c (optional). Repeat Experiment 5.1 with the nickel foils in Absorber Kit MNI-5.

absorber. The pressure can be monitored by a gauge in the vacuum/supply line. The general procedure consists of placing the source ~ 2 cm from the detector, or closer if necessary to get good statistics within a reasonable time, pumping the full vacuum, closing off the vacuum pump, and then leaking the gas (air or helium, for example) into the chamber for the desired pressure. The number of mg/cm^2 of the gas can be determined by STP conditions.

Table 5.2. Energy Loss Data for Fig. 5.5.

Curve	Foil Thickness (mg/cm^2)	Alpha Particle		ΔE (MeV)	
		Energy* (MeV)	Resolution (keV)	Measured	Calculated
A	0.00	5.47	30	0.00	0.00
B	1.23	4.95	64	0.53	0.54
C	2.06	4.55	106	0.93	0.91
D	2.50	4.36	112	1.12	1.10
E	3.74	3.69	160	1.79	1.71
F	4.22	3.44	170	2.03	1.98
G	5.00	3.03	202	2.45	2.40
H	6.24	2.33	223	3.15	3.09

*After passing through copper foil.

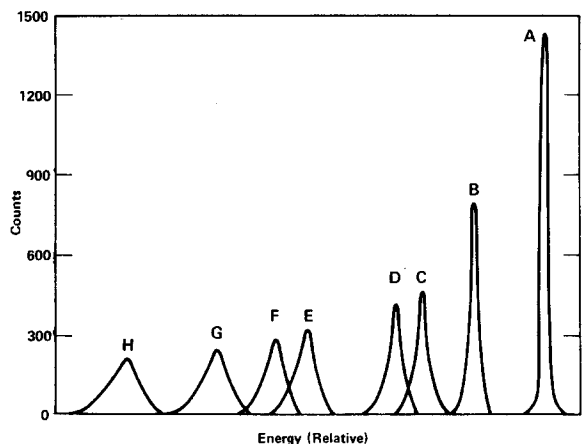


Fig. 5.5. Measured Energy Loss of Alpha Particles in Copper Foil.

EXPERIMENT 5.2

dE/dx of Alpha Particles in Gas (optional if helium is available)

There are many advantages in using gas as an absorbing medium, because the gas pressure can be varied to any value that is desired in order to regulate the thickness of the

Procedure

1. Repeat all the steps of Experiment 5.1 using helium as the absorbing medium rather than copper foils. Take enough measurements so that your measured ΔE has at least six values between no absorber and $\Delta E = 4$ MeV.
2. Repeat step 1 for air. Range-vs-energy values for air can be found in ref. 4. Compare your results with those shown in Table 5.3 and Fig. 5.6.

Table 5.3. Energy Loss Data for Fig. 5.6.

Curve	Air Thickness (mg/cm ²)	Alpha Particle		ΔE (MeV)	
		Energy* (MeV)	Resolution (keV)	Measured	Calculated
A	0.00	5.47	137	0.00	0.00
B	0.95	4.77	149	0.73	0.73
C	1.89	3.96	168	1.54	1.52
D	2.84	3.03	195	2.47	2.46
E	3.78	1.95	230	3.55	3.60

*After passing through air.

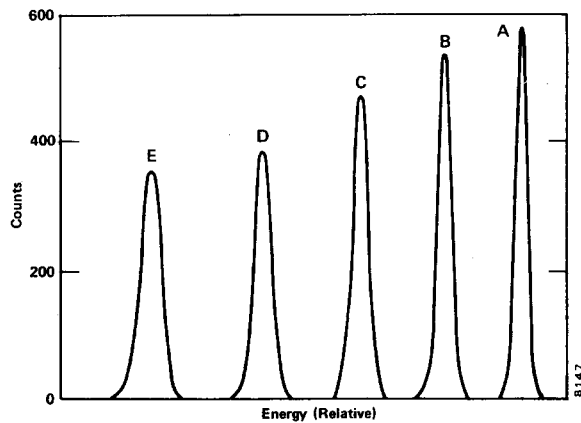


Fig. 5.6. dE/dx for Alpha Particles in Air.

References

1. L. C. Northcliffe and R. F. Schilling, *Nuclear Data Tables A7*, 233 (1970).
2. J. F. Ziegler, *The Stopping Power and Ranges of Ions in Matter*, Pergamon Press, New York (1977).
3. G. F. Knoll, *Radiation Detection and Measurement*, John Wiley and Sons, New York (1979).
4. J. B. Marion and F. C. Young, *Nuclear Reaction Analysis*, John Wiley and Sons, New York (1968).
5. G. Dearnaley and D. C. Northrop, *Semiconductor Counters for Nuclear Radiations*, 2nd Ed., John Wiley and Sons, New York (1966).
6. J. L. Duggan, W. D. Adams, and L. S. Anthony, "Charged-Particle Detector Experiments for the Modern Physics Laboratory," *Am. J. Phys.* **35**(7), 631 (1967).
7. D. J. Skyrme, *Nucl. Instrum. Methods*, **57**, 61 (1967).
8. S. Matteson, E. K. L. Chau, and D. Powers, *Phys. Rev. A* **14**, 169 (1976).
9. J. F. Janni, *Calculations of Energy Loss, Range, Pathlength, Straggling, Multiple Scattering, and the Probability of Inelastic Nuclear Collisions for 0.1- to 100-MeV Protons*, **AFWL-TR-65-150** (AD-643837), (1966). Available from Clearinghouse for Federal Scientific and Technical Information, Springfield, Virginia.
10. C. F. Williamson, J. P. Boujot, and J. Picard, *Tables of Range and Stopping Power of Chemical Elements for Charged Particles of Energy 0.5 to 500 MeV*, **CEQ-R-3042** (1966). Available from Clearinghouse for Federal Scientific and Technical Information, Springfield, Virginia.

EXPERIMENT 6

Beta Spectroscopy

EQUIPMENT NEEDED FROM EG&G ORTEC

Source Kit SK-1B
 Surface Barrier Detector (A-015-025-1500)
 142A Preamplifier
 Bin and Power Supply
 575A Amplifier
 807 Vacuum Chamber
 428 Detector Bias Supply

480 Pulser
 ACE-2K MCA System including suitable IBM PC (other EG&G ORTEC MCAs may be used)
 Mechanical Vacuum Pump
 Oscilloscope
 ORC-6 Cable Set

Purpose

This experiment demonstrates the technique of obtaining a beta-particle spectrum and outlines a method for determining β_{\max} .

Theory

The measurement of beta-particle energies can be made with surface barrier detectors, using the same techniques that were outlined in Experiment 4. Beta decay occurs when a nucleus has an excess number of neutrons compared to its more stable isobar. For example, ^{204}Tl decays to ^{204}Pb and emits a beta particle. In order to achieve stability, one of the neutrons in the nucleus of the ^{204}Tl will be converted into a proton. The process is



where $\bar{\nu}$ is a neutrino.

From Eq. (1) you can see that there are three particles in the final state. The excitation energy will be shared by the $\bar{\beta}$ and $\bar{\nu}$ particles. Theoretically, $\bar{\beta}$ could have any energy up to the maximum (β_{\max}), but the probability for any event to have this amount of energy accompany its $\bar{\beta}$ is very low.

A typical beta spectrum, shown in Fig. 6.1, indicates the distribution of relative probabilities for the portions of β_{\max} that accompany a quantity of events measured for ^{204}Tl . This is a typical continuum of $\bar{\beta}$ energies. The energy that is represented at the extrapolated baseline crossover of the curve (around channel 350 in Fig. 6.1) is β_{\max} . From ref. 7, this endpoint energy for ^{204}Tl is 0.766 MeV. The system can be calibrated with known conversion electron energies since in the internal conversion process it is possible for a nucleus to impart its energy of excitation directly to one of its nearby orbiting electrons and the electron will then leave the atom with a discrete energy (E_c). This energy is given by

$$E_c = E_x - E_B, \quad (2)$$

where

- E_c = the measured energy of the conversion electron,
- E_x = the excitation energy available in the decay,
- E_B = the binding energy of the electron in the atom.

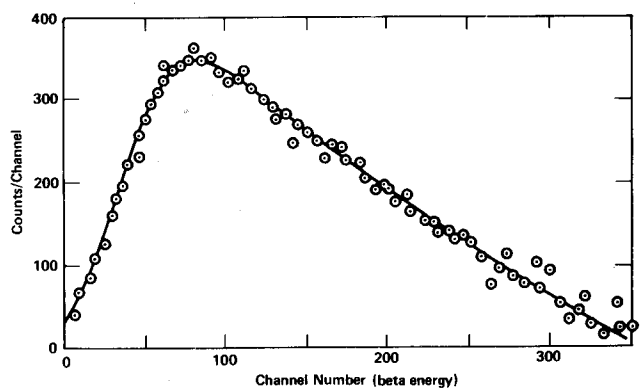


Fig. 6.1. Beta Spectrum for ^{204}Tl .

These three quantities can be found in ref. 7. Figures 6.2, 6.3, and 6.4 show the conversion electron spectra for ^{207}Bi , ^{113}Sn , and ^{137}Cs . The calibration curve for channel number vs energy is also shown in Fig. 6.2.

Application of Surface Barrier Detectors

The list of equipment specifies an appropriate EG&G ORTEC surface barrier detector for this work. The A-015-025-1500 detector has the combination of parameters that satisfies the requirements.

WARNING

Never touch the exposed surface of this non-ruggedized detector with any foreign material – especially your fingers. The surface is a layer of deposited gold that will be irreparably damaged by skin oils or any abrasive. Always handle the detector by its edges and/or its protective case.

Figure 6.5 shows a range-vs-energy curve for betas in silicon. If the maximum beta energy for an isotope is known, the required detector thickness can be determined from the curve. The maximum energy for Experiment 6 will be the 1.048-MeV conversion electron from ^{207}Bi , as shown in Fig. 6.2. According to Fig. 6.5, a 1.048-MeV beta would have a range of $\sim 1700 \mu\text{m}$. Since the path of a beta is not a straight line, it is not absolutely essential that the detector have the indicated thickness. Therefore for this experiment we are recommending a 1500- μm detector.

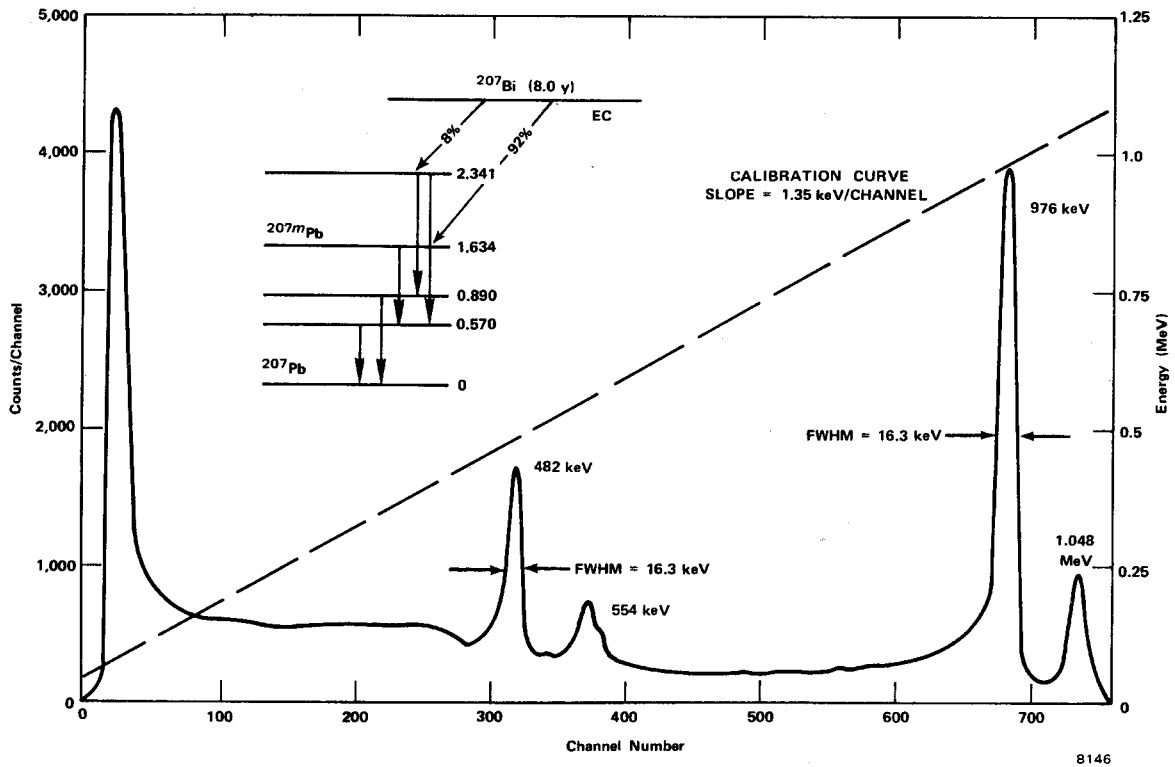


Fig. 6.2. ²⁰⁷Bi Conversion Electron Spectrum.

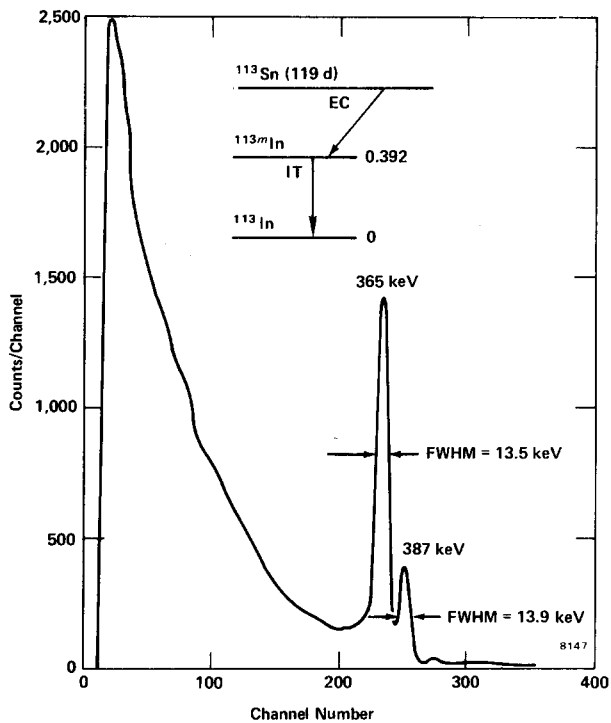


Fig. 6.3. ¹¹³Sn Conversion Electron Spectrum.

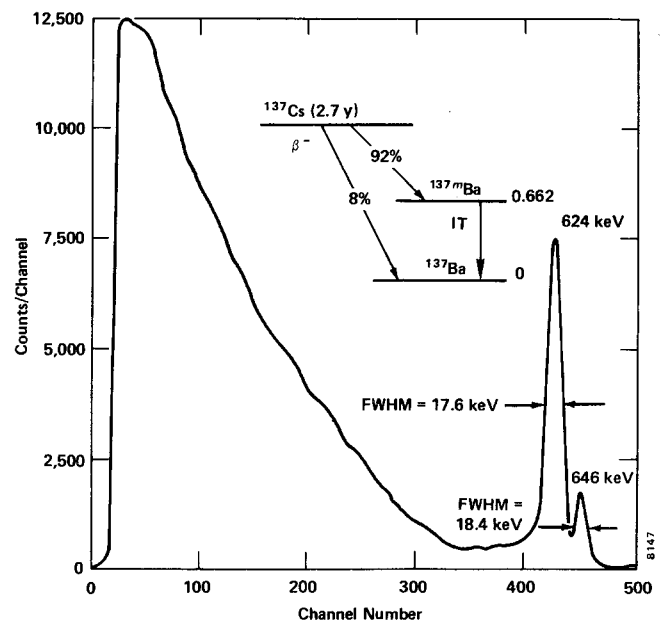


Fig. 6.4. ¹³⁷Cs Beta and Conversion Electron Spectrum.

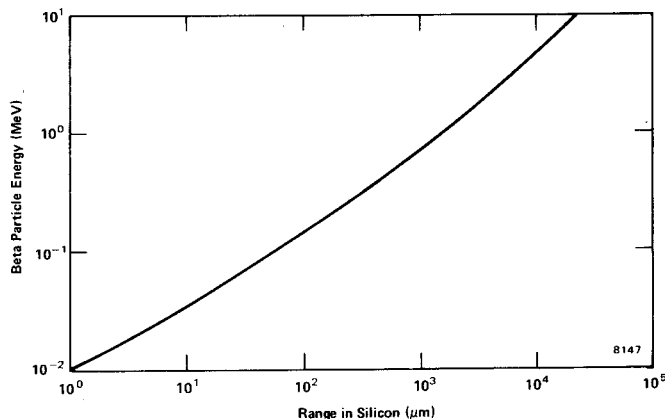


Fig. 6.5. Beta Energy vs Range in Silicon.

EXPERIMENT 6.1 Calibration with a Pulser

The equipment that will be used in this experiment is the same as the system for Experiment 4. Review the rules in Experiment 4 that explain how to apply the bias voltage properly, when the vacuum is to be pumped down, what the procedures are for exchanging a source, etc. The methods explained there are basic, but the precautions are much more important in this experiment because you are working with a more expensive detector.

Procedure

1. Connect the equipment as shown in Fig. 6.6. Use the following settings for the module controls: set the 575A Amplifier for a positive input and a unipolar output; set the 480 Pulser for a negative output and use the attenuated output; set the 428 Bias Supply for a positive polarity and increase the voltage gradually to the recommended level.
2. Position the ^{137}Cs source about 1/4 in. from the detector. Pump down the vacuum chamber and apply the proper operating bias (+) to the detector.
3. Adjust the gain of the 575A Amplifier until the pulses observed on the oscilloscope are ~ 4 V in amplitude. The most pronounced pulse amplitudes will represent the 624-keV energy of the conversion electrons.
4. Accumulate a spectrum long enough to identify the channel location in the MCA for the 624-keV line. Adjust the amplifier gain to place the 624-keV peak at about mid-scale on the MCA. In Fig. 6.4 the peak is at about mid-scale for a 1024-channel analyzer. When the gain has been adjusted properly, accumulate the spectrum long enough to have ~ 600 counts in the 624-keV peak. Record the channel number for the 624-keV peak and call this channel C_0 .
5. Turn on the 480 Pulser and adjust its Pulse-Height dial to 624/1000 divisions. Use the attenuator switches and the calibration potentiometer to position the pulser peak in channel C_0 . The pulser is now calibrated so that 1000 keV = 1000 dial divisions on the pulse-height control.

EXERCISES

- a. Fill in the information for Table 6.1.

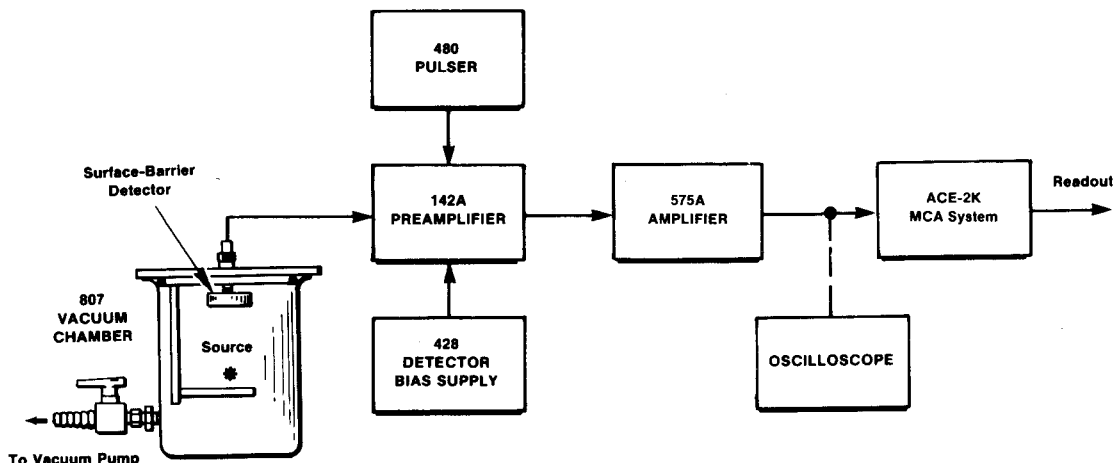


Fig. 6.6. Electronics for Calibration with a Pulser.

Table 6.1

Approximate Accumulation Time (s)	Pulse-Height Dial Setting	Equivalent Energy (keV)	Analyzer Channel No.
20	200/1000	200	
20	400/1000	400	
40	600/1000	600	
20	800/1000	800	
20	1000/1000	1000	

b. Plot the calibration points and determine the keV/channel for the curve. From your printed data for the ¹³⁷Cs spectrum, determine the resolution of the detector system at the 624-keV line. Determine the resolution of one of your pulser peaks.

c. As in Experiment 4.5, define the following:

- δ_T , the measured width of the 624-keV line.
- δ_E , the measured width of the pulser peak.
- δ_s , the source thickness (assume that this is zero).

Solve for δ_D , the resolution of the detector; $\delta_D = \sqrt{\delta_T^2 - \delta_E^2}$. How does your calculated δ_D compare with the value that the instructor has for the detector?

6. Replace the ¹³⁷Cs source with the ²⁰⁷Bi source. Accumulate its spectrum for a period of time long enough to clearly determine the locations of the pronounced peaks in the spectrum (Fig. 6.2). Read out the analyzer and erase the spectrum.

7. Replace the ²⁰⁷Bi source with the ¹¹³Sn source. Accumulate its spectrum for a period of time long enough to have ~1000 counts for the 365-keV conversion electron line (Fig. 6.3). Read out the analyzer and erase the spectrum.

EXERCISE

d. From your analyzer readouts and the calibration curve, calculate the energy levels for Table 6.2 and fill them in.

Table 6.2

Source	Energy	
	Theoretical (keV)	Calculated
¹³⁷ Cs	624	
¹³⁷ Cs	626	
¹³⁷ Cs	266	
¹³⁷ Cs	238	
²⁰⁷ Bi	1040	
²⁰⁷ Bi	972	
¹¹³ Sn	365	

8 (optional). If you have a ¹³³Ba source, obtain its spectrum and add your calculated energies for its lines to Table 6.2. Figure 6.7 shows the details of a typical spectrum for ¹³³Ba.

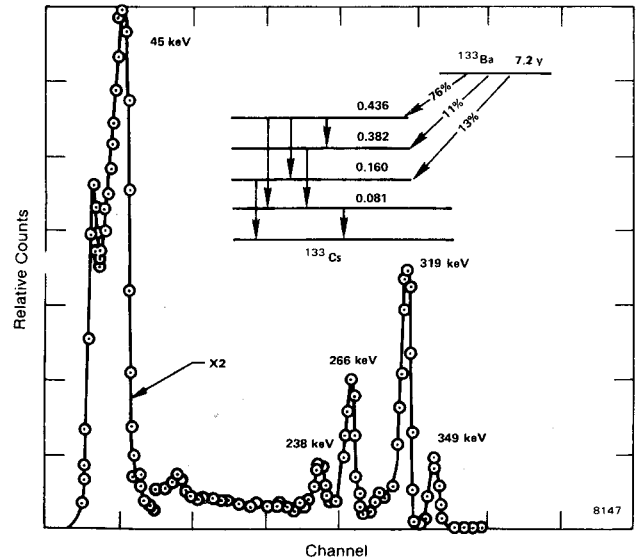


Fig. 6.7. Conversion Lines from ¹³³Ba.

EXPERIMENT 6.2

Beta End-Point Determination for ²⁰⁴Tl

Theory

The most precise method for determining maximum beta energy requires that a Kurie plot be made. This method is derived from the theory of beta decay, discussed in ref. 2. A description of a beta curve is given by

$$\left[\frac{N(W)}{F(Z,W)PW} \right]^{1/2} = K(W_0 - W) \quad (3)$$

where

- N(W) = counts in each channel being considered,
- F(Z,W) = Fermi function,
- P = momentum of beta particle,
- W = total energy of beta particle,
- W₀ = maximum end-point energy of beta spectrum,
- K = a constant that is independent of energy.

If the left side of Eq. (3) is plotted against W, an allowed spectrum will yield a straight line that may be extrapolated to the energy axis to give W₀. Forbidden β transition spectra will show an upward curvature in the low-energy region.

A somewhat easier calculation can be made by using a modified Fermi function G(Z,W) which may be calculated from

the beginning of Experiment 6. The electrons that are usually involved are in the K, L, and M shells that are closest to the nucleus. The energy of the conversion electron is given by

$$E_e = E_x - E_B, \quad (6)$$

where

E_e = the measured energy of the conversion electron,

E_x = the excitation energy available in the decay,

E_B = the binding energy of the electron in the atom.

The conversion electron spectrum for ^{207}Bi is shown in Fig. 6.2. It shows lines at 1.048 and 0.976 MeV. These are the lines that come from the K and L conversion processes, respectively.

The decay scheme of ^{207}Bi , also shown in Fig. 6.2, shows a gamma transition from the 1.634-MeV level to the 0.570-MeV level. This difference in energy is 1.064 MeV. In Eq. (6) this is the excitation energy, E_x , which is available for the conversion process.

The K binding energy, E_B , for ^{207}Pb is 88 keV. For this conversion $E_e = 1.064 - 0.88 = 0.976$ MeV or 976 keV. The L binding energy for ^{207}Pb is 15.86 keV for this conversion, $E_e = 1.064 - 0.01586 = 1.048$.

In a similar manner the conversion electron energies for the 570-keV excitation can be calculated. These are 482 and 554 keV. The binding energies for all elements are listed in ref. 7, pp. 556–569. In this experiment the K/L ratios will be measured.

Procedure

1. Use the system of Experiment 6.1, including the calibration.
2. Be sure to use a detector with 18-keV resolution or better.

3. Accumulate a spectrum for ^{207}Bi for a period of time long enough to obtain ~ 1000 counts in the 1.048-MeV peak. Print the data from the MCA.

EXERCISES

a. Find the sum under the 1.048-MeV peak. Define this quantity to be $\Sigma L_{1.064}$. Find the sum under the 976-keV peak, and define this quantity to be $\Sigma K_{1.064}$. Calculate the K/L ratio, which is $(\Sigma K / \Sigma L)_{1.064}$. Repeat these steps for the 482-keV and 554-keV lines and calculate the ratio $[\Sigma K / \Sigma(L + M)]_{0.570}$. Note that the L and M lines are not quite resolved in your spectrum. How do your values compare to those in ref. 7?

b. Repeat the measurements and calculations for ^{113}Sn and ^{137}Cs . Your spectra should look like Figs. 6.3 and 6.4, respectively. How do your values compare to those in ref. 7 for these isotopes?

References

1. G. F. Knoll, *Radiation Detection Measurement*, John Wiley and Sons, New York (1979).
2. K. Siegbahn, ed., *Alpha-, Beta-, and Gamma-Ray Spectroscopy*, 1 and 2, North Holland Publishing Co., Amsterdam (1965).
3. G. D. Chase and J. L. Rabinowitz, *Principles of Radioisotope Methodology*, 3rd Edition, Burgess Publishing Co., Minneapolis, Minnesota (1967).
4. E. Segre, *Nuclei and Particles*, The Benjamin-Cummings Publishing Co., Reading, Massachusetts (1977).
5. J. B. Marion and F. C. Young, *Nuclear Reaction Analysis*, John Wiley and Sons, New York (1968).
6. G. Bertolini and A. Coche, eds., *Semiconductor Detectors*, American Elsevier Publishing Co., Inc. (1968).
7. C. M. Lederer and V. S. Shirley, Eds., *Table of Isotopes*, 7th Edition, John Wiley and Sons, Inc., New York (1978).

EXPERIMENT 7

High-Resolution Gamma-Ray Spectroscopy

EQUIPMENT NEEDED FROM EG&G ORTEC

Source Kit SK-1G
 Other sources: 5 μCi of ^{137}Cs ; 10 μCi of ^{60}Co ; 10 μCi of ^{228}Th
 Bin and Power Supply
 GEM-10195 Coaxial Detector System (includes detector, cryostat, dewar, and preamplifier); typical specifications, 10% efficiency, 1.95-keV resolution at 1.33 MeV, 37:1 peak-to-Compton
 459 5 kV Detector Bias Supply
 572 Spectroscopy Amplifier
 444 Gated Biased Amplifier

480 Pulser
 ACE-2K MCA System including suitable IBM PC (other EG&G ORTEC MCAs may be used)
 Oscilloscope
 (Optional for Experiment 7.4) a 1- to 3-Ci americium-beryllium isotopic neutron source; if the source is not in a paraffin howitzer, place a 6-in. thickness of paraffin between the source and the HPGe detector to thermalize the source neutrons.
 ORC-7 Cable Set

Purpose

Gamma-ray energies will be measured with a high-purity germanium (HPGe) detector and research-grade electronics. The theory of response characteristics is explained, and the high-resolution results of measurement are contrasted with an NaI(Tl) scintillation detector in Experiment 3.

Introduction

Most of the experiments in this manual are written for use with EG&G ORTEC educational modules. In this experiment, which illustrates the high-resolution capabilities of HPGe detector systems, research-grade modules have been listed in order to process the pulses from the HPGe detector with a greater degree of precision to complement the detector capabilities.

Many colleges, both large and small, have Nuclear Spectroscopy Centers. In these laboratories the research efforts of the department will normally be directed in the area of high-resolution gamma-ray spectroscopy. It is possible to do a great amount of publishable research on such work as decay scheme analysis, etc., with these high-resolution systems. In many cases additional lines can be found in spectra or the improved resolution can reveal a doublet, whereas earlier measurements with NaI(Tl) detectors indicated a single energy line.

The latest decay schemes for isotopes are included in refs. 10 and 12. More recent information on certain nuclei can be obtained by writing

The Nuclear Data Project
 Building 4500
 Oak Ridge National Laboratory
 Post Office Box X
 Oak Ridge, Tennessee 37831 U.S.A.

In Experiment 3 gamma spectroscopy was studied with NaI(Tl) detectors. Typical energy resolution that can be

obtained with NaI(Tl) is $\sim 7\%$ for the 0.661-MeV ^{137}Cs gamma line. For NaI(Tl) detectors the resolution is a strong function of energy. Variation of resolution results primarily from the statistical fluctuation of the number of photoelectrons that are produced at the photocathode surface in the photomultiplier tube. Table 7.1 illustrates some typical resolutions for NaI(Tl) spectroscopy as functions of the gamma energies.

The use of germanium detectors has completely revolutionized gamma spectroscopy. Figure 7.1 illustrates the striking contrast of results obtained with these two types of

Table 7.1. Typical Resolutions of NaI(Tl) for Different Gamma Energies.

Isotope	Gamma Energy (keV)	Resolution (%)
^{166}Ho	81	16.19
^{177}Lu	113	13.5
^{133}Te	159	11.5
^{177}Lu	208	10.9
^{203}Hg	279	10.14
^{51}Cr	320	9.89
^{198}Au	411	9.21
^7Be	478	8.62
^{137}Cs	661	7.7
^{54}Mn	835	7.26
^{207}Bi	1067	6.56
^{65}Zn	1114	6.29
^{22}Na	1277	6.07
^{88}Y	1850	5.45

The information for this table was taken from *IRE Trans. Nucl. Sci.* **NS-3**(4), 57 (Nov. 1956). "Intrinsic Scintillator Resolution," by G. G. Kelley *et al.*, quoting results from F. K. McGowan, *et al.*

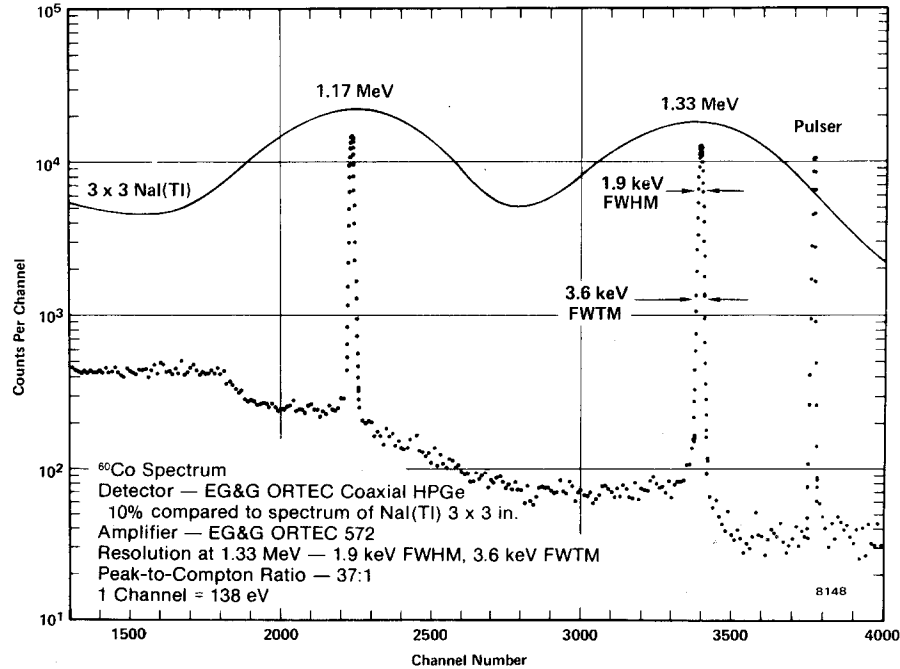


Fig. 7.1. ⁶⁰Co Spectrum Showing Resolutions and Peak-to-Compton Ratios for an HPGe Coaxial Detector and an NaI(Tl) Detector.

detectors. There is a factor of 30 improvement of the resolution of the data at the full-width at half-maximum (FWHM) count levels. As a result of the improved resolution, many nuclear energy levels that could not even be seen with NaI(Tl) detectors are identified easily with HPGe detectors.

In a parallel fashion the development of Si(Li) detectors has revolutionized x-ray spectroscopy. These Si(Li) devices will be studied in Experiment 8.

The purpose of this experiment is to study some of the properties of the HPGe detector systems. This experiment deals only with the practical aspects of making measurements with these detectors. To understand the properties of these detection systems, the following brief review of gamma-ray interactions and pair-production processes is included.

In Experiment 3 it was pointed out that the pair-production process at gamma energies >3 MeV is a very important gamma interaction. Figure 7.2 shows graphs for the three important gamma interactions for both germanium and silicon. The information for germanium is of interest in this experiment, and that for silicon will be used in Experiment 8.

When a gamma enters a detector, it must produce a recoil electron by one of three processes before it is recorded as an event: the photoelectric effect, the Compton effect, or pair production.

In the photoelectric process the gamma or x ray gives all of its energy to the recoil electron. It is the recoil electron that produces the electron-hole pairs in the detector that yield the output pulse. For the photoelectric process the output pulse from the detector is proportional to the energy of the

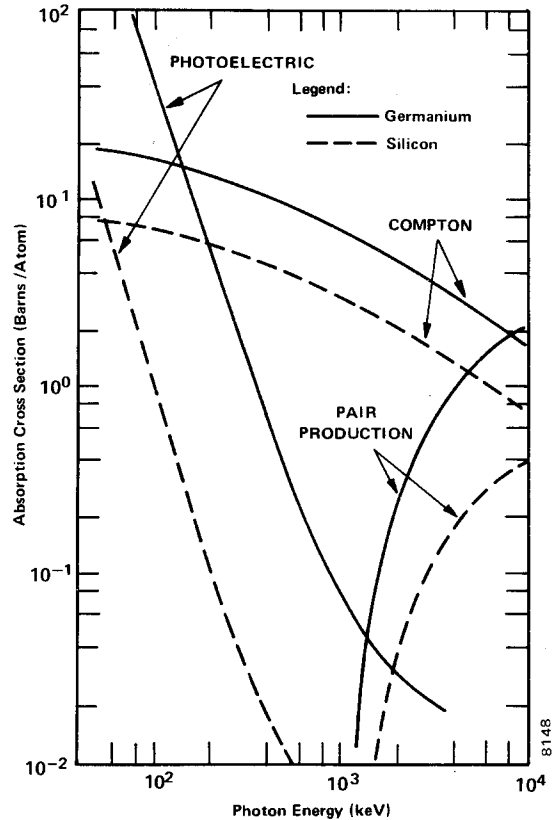


Fig. 7.2. Relative Probability of Each of the Three Types of Interactions as a Function of Energy.

gamma or x ray that produced the interaction. In the spectrum these events will show up as full-energy photopeaks.

In the Compton process there is a distribution of pulse amplitudes up to some maximum pulse height. This maximum pulse height produces the Compton edge, as explained in Experiment 3, and there is a statistical probability that each event can produce a pulse with any height up to this maximum with about an equal chance. Thus Compton events will provide a well-distributed low-energy area in the spectrum.

In modern, large detectors with high peak-to-Compton ratios, some Compton events also contribute to the full energy peak when the scattered photons undergo one or more additional interactions. This results in complete absorption.

The pair-production process can also provide a total absorption of the gamma-ray energy. The gamma enters the detector and creates an electron-positron pair. From the law of conservation of mass and energy it follows that the initial gamma must have an energy of at least 1.02 MeV because it takes that much energy to create both the negative and positive electrons. The net mass that is produced is two electron masses, and this satisfies the law of conservation of energy, $E = mc^2$.

Note that 1.02 MeV is about twice the annihilation energy that was measured from ^{22}Na (0.511 MeV). Figure 7.3 illustrates what happens in the detector in the pair-production process.

In Fig. 7.3 the e^- (ordinary electron) will produce a pulse whose magnitude is proportional to the energy of e^- (E_{e^-}). The positron will produce a pulse proportional to E_{e^+} . Since these two pulses are produced simultaneously, the output pulse from the detector would be the sum of the two pulses. When the positron annihilates in the detector, the annihilation radiation, γ_1 and γ_2 , will be produced. In Fig. 7.3 both γ_1 and γ_2 are shown escaping from the boundaries of the detector without making any further interactions. (Note: $\gamma_1 = \gamma_2 = 0.511$ MeV.) Thus, for this example, an energy of exactly 1.02 MeV escapes from the detector and is subtracted from the total energy that entered the detector. It is possible for only one, either γ_1 or γ_2 , to make a photoelectric interaction in the detector while the other escapes. In such cases the total energy absorbed is 0.511 MeV less than the original incident gamma energy. It is also possible for both

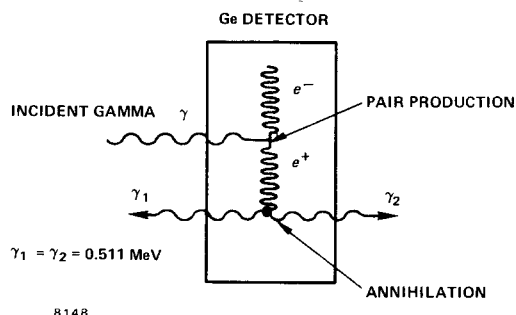


Fig. 7.3. Process of Pair Production in Germanium.

gammas to make photoelectric interactions without escaping, with all the original energy then being left in the detector. Therefore in the spectrum that is measured there will be three peaks for each gamma energy. These peaks are labeled Full-Energy Peak, Single-Escape Peak, and Double-Escape Peak, and they will be separated by 0.511-MeV increments. Figure 7.4 shows a typical spectrum that would be obtained for an incident gamma energy of 2.511 MeV. The lower end of the spectrum that includes the Compton distribution has not been included; this effect is obtained by using a biased amplifier to eliminate the lower energies and to expand the distribution of the higher-energy pulses across the range that is measured. The Single-Escape Peak occurs at $(E_\gamma - 0.511$ MeV) or 2.00 MeV, and the Double-Escape Peak occurs at $(E_\gamma - 1.02$ MeV) or 1.49 MeV. Of course, the full-energy peak represents those events for which there was a combination of pair production and photoelectric effect in which all the energy was absorbed in the detector.

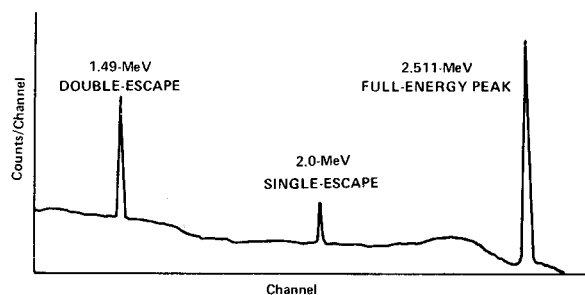


Fig. 7.4. Typical Spectrum for an Incident Gamma Energy of 2.511 MeV.

Now refer again to Fig. 7.2 and specifically to the curves for the interactions in germanium. The absorption cross section, plotted in the y direction, is a measure of the relative probability that an interaction will take place in a germanium detector. These probabilities of relative interactions, for the most part, determine the shape of the observed spectrum. For example, a photon (or gamma) with an energy of 100 keV has an absorption cross section of ~ 55 barns/atom for the photoelectric process. The corresponding Compton cross section is ~ 18 barns/atom. There is no pair production. This indicates that at 100 keV there are 3 times as many photoelectric interactions as Compton interactions, since this is the approximate ratio of the cross section. Figure 7.5 shows the shape of a spectrum that could be expected for measurement of the 100-keV energy events.

The sum of counts under the photopeak would be 3 times the sum under the Compton distribution. For larger crystals Σ_{pp} would be even >3 times Σ_c because some of the scattered gammas from the Compton interactions would make photoelectric interactions before escaping from the crystal. For an infinitely large crystal there would be no Compton distribution since the crystal would then totally absorb all of the incident gammas.

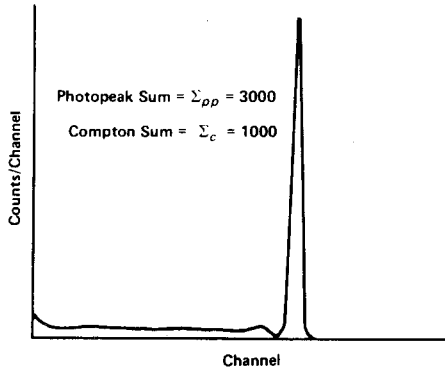


Fig. 7.5. Typical Spectrum Expected for 100-keV Energy in HPGe.

The shape of the spectrum changes drastically from 100 keV to 1 MeV. Figure 7.6 shows the gamma spectrum that could be expected for the 1-MeV gammas incident on an HPGe detector. From Fig. 7.2 the ratio of Compton cross section to photoelectric cross section is ~ 90 ; so in Fig. 7.6, Σ_c is 90,000 and Σ_{pp} is 1000. The variation of cross sections for HPGe and Si(Li) detectors can also be approximated from Fig. 7.2. For example, at $E_\gamma = 400$ keV the photoelectric cross section for germanium is 6 barns/atom and that for silicon is ~ 0.1 barn/atom. This is a ratio of 60:1 and indicates that there will be 60 times as many counts under the photopeak for a germanium detector as for a silicon detector at 400 keV, assuming that the detectors are the same size. The reason for this is that the photoelectric cross section varies as Z^5 , where Z is the atomic number of the absorbing material. The atomic number of Ge is 32 and is 14 for Si. The ratio of these two numbers raised to the 5th power is 62.22, and this is within remarkable agreement with the above cross-section ratios.

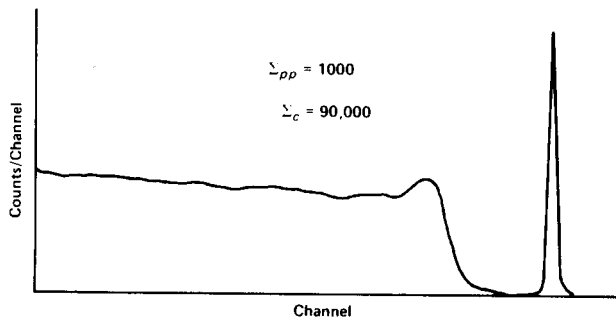


Fig. 7.6. Typical Spectrum Expected for 1-MeV Energy in HPGe.

EXPERIMENT 7.1

Energy Resolution with an HPGe Detector

The instructor will provide the HPGe detector and the instructions for its use. Read the instruction manual carefully before attempting to use the detector. This is a very expensive detector system and must be handled carefully.

Procedure

1. Install the 459, 480, 572, and 444 in the bin and power supply and interconnect the modules as shown in Fig. 7.7. The preamplifier will be mounted on the HPGe detector and the interconnection for the signal connections to the detector is made through the preamplifier. Connect the 459 to the Detector Bias Input and connect the 480 to the Test Input on the preamplifier. Connect the power cable for the preamplifier to the Preamplifier Power connector on the 572. Connect a signal output from the preamplifier to the 572 input. Connect the Unipolar Out from the 572 to the linear input of the 444, and connect the 444 output to the input of the MCA. Set the module controls as follows:

572 Amplifier: Positive input (verify with instructor); Unipolar Output; Shaping time 6 μ s; Delay Out.

444 Gated Biased Amplifier: Coarse Gain X2; Fine Gain 1/2; Bias Level 20/1000; Normal mode; DC-Couple; Pulse Duration 6 μ s (internal control); Anticoincidence and Internal Strobe (rear-panel controls).

480 Pulser: Attenuated output.

459 5 kV Detector Bias Supply: Leave at zero until all other connections and adjustments have been made; consult the instructions for the HPGe detector to determine both the polarity and the amplitude of bias that are to be used, and apply the correct amount of bias in the correct polarity when ready to operate.

2. Place the ^{60}Co source from source kit SK-1G ~ 1 cm from the face of the detector. Adjust the gain of the 572 Amplifier so that the 1.33-MeV gamma has an amplitude of 6 V at the amplifier output. The two lines for 1.17 and 1.33 MeV should be quite easily seen on the oscilloscope. Check the output from the 444 Gated Biased Amplifier to make sure it looks reasonable.

3. Observe the display of the spectrum on the MCA. Adjust the bias level and gain on the 444 and the gain on the 572 until the two sharp photopeaks are positioned as shown in Fig. 7.8. In this measurement the two photopeaks should be separated by at least 200 channels, based on 1024 channels total.

4. From the positions of the two photopeaks make a calibration curve of energy (y direction) vs channel number (x direction) and determine the keV/channel.

EXERCISES

- a. What is the resolution in keV for the two photopeaks? How does this compare in value with the detector's resolution specifications?

- b. From the data, determine the energies of the Compton edges for the two gammas. How do these compare with the values that were calculated from the formula used in Experiment 3?

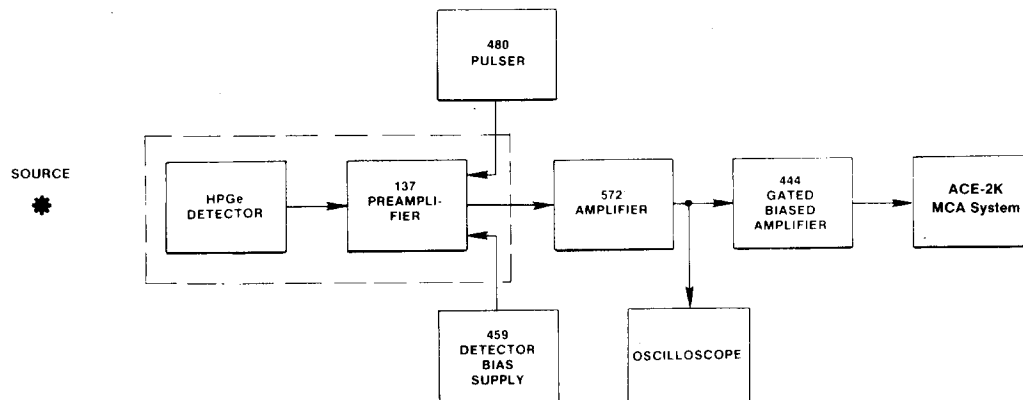


Fig. 7.7. Electronic Interconnections for Experiment 7.1.

5. Turn on the 480 Pulser and adjust the output so that the pulser peak falls about half-way between the 1.17- and 1.33-MeV peaks. After the pulser has produced enough counts for its peak channel to have 1000 counts, read that portion of the analyzer memory and determine the resolution of the pulser. This is the electronic resolution, $R(E)$. The contribution from the detector to the overall resolution can be calculated from the formula

$$\text{system resolution} = \sqrt{[R(d)]^2 + [R(E)]^2} \quad (1)$$

where $R(d)$ is the detector resolution and $R(E)$ is the electronic resolution. These resolutions are said to add in quadrature. There is a lower limit to $R(d)$ which is energy-dependent. The recoil electron that is produced in the gamma interaction loses energy in the HPGe detector by dE/dx . The average energy required to produce an ionization in germanium is 2.95 eV/electron-hole pair. Thus for a 1.5-MeV recoil electron there would be 5.08×10^5 electron-hole pairs produced. The production of electron-hole pairs is a process that is statistical in nature, and hence there are fluctuations in the actual number produced. When the proper statistics are used, the theoretical lower limit to $R(d)$ is given by

$$R(d) = K \sqrt{F \cdot E} \quad (2)$$

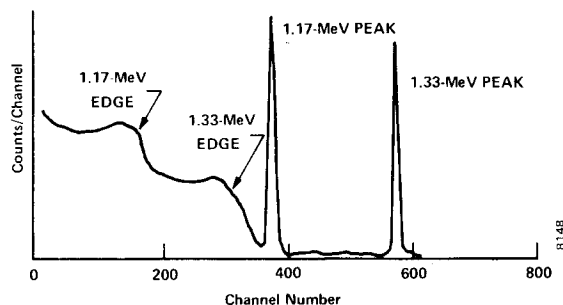


Fig. 7.8. Locating the Two Photopeaks for ^{60}Co in the HPGe Spectrum.

where K is a constant, E is the energy of the photon in MeV, and F is the statistical Fano factor. To a very good approximation this equation reduces to

$$R(d) \text{ (in keV)} = 1.35 \sqrt{E \text{ (in MeV)}}. \quad (3)$$

Solving Eq. (3), the theoretical lower limit of detector resolution is 1.44 keV for a 1-MeV gamma and is 4.5 keV for a 10-MeV gamma.

EXERCISES

c. Calculate the values of $R(d)$ from Eq. (3) for the values of E in Table 7.2.

Table 7.2

Energy (MeV)	Theoretical $R(d)$ (keV)
0.1	
0.3	
0.5	
1.0	
3.0	
6.0	
8.0	
10.0	

d. Make a plot of the values from Table 7.2 on linear graph paper. From Eq. (1) calculate the experimental $R(d)$ for the 1.33-MeV peak of ^{60}Co . How does this compare with the theoretical limit? Remember that the $R(d)$ theory is the absolute lower limit of the resolution value.

EXPERIMENT 7.2

Photopeak Efficiency for HPGe Detectors

Resolution with HPGe detectors is better by a factor of 30 or more than that obtained with NaI(Tl) conventional detectors. Coupled with this dramatic increase in resolution is a compromise of the photopeak efficiency. The pricing of HPGe detectors is related to their photopeak efficiency. The standard method for comparing the efficiencies of HPGe detectors with NaI(Tl) detectors is to compare their counting rates at the 1.33-MeV line of ⁶⁰Co, using a standard distance of 25 cm from the source to the detector face and placing the source on the detector axis.

The resolution of the HPGe detectors is so many times better than that of the NaI(Tl) that the ability to see a photopeak above the Compton distribution is considerably enhanced. Consider a simple example in which the efficiencies of the HPGe and NaI(Tl) are assumed to be the same. In a particular experiment we observe 10,000 counts under the photopeak for each detector. If the resolution of the HPGe detector is only 10 times that of the NaI(Tl) detector, the HPGe photopeak will have 10 times the maximum number of counts that the NaI(Tl) detector has, because the area under the photopeak (10,000 for this example) is approximately proportional to the width times the height of the peak. Since the width of the HPGe peak is only 1/10 the width of the NaI(Tl) peak, its height must be 10 times as great.

This example can easily be extrapolated to real situations where the advantages of superior resolution are very important. For example, Fig. 7.9 shows the striking differences for a spectrum obtained on a mixed sample of ⁷⁶As, ¹²²Sb, and ¹²⁴Sb with each of the two types of detectors. Each of the closely spaced energy lines is shown separately in the HPGe spectrum and are all included in a single broad photopeak in the NaI(Tl) spectrum.

In this experiment, we will measure some of these photopeak efficiencies and also determine the peak-to-Compton ratio for an HPGe detector.

Procedure

1. Use the same equipment setup that was used for Experiment 7.1. Adjust the gain of the 572 and bias level and gain of the 444 for a ⁶⁰Co spectrum similar to that of Fig. 7.10.
2. Accumulate the spectrum in the MCA for a time period long enough to determine heights h_1 and h_2 to a fair degree of accuracy. In Fig. 7.10, h_1 is the 1.33-MeV photopeak and h_2 is the maximum for the comparable Compton distribution, normally located just below the Compton edge. Read the data from the analyzer.

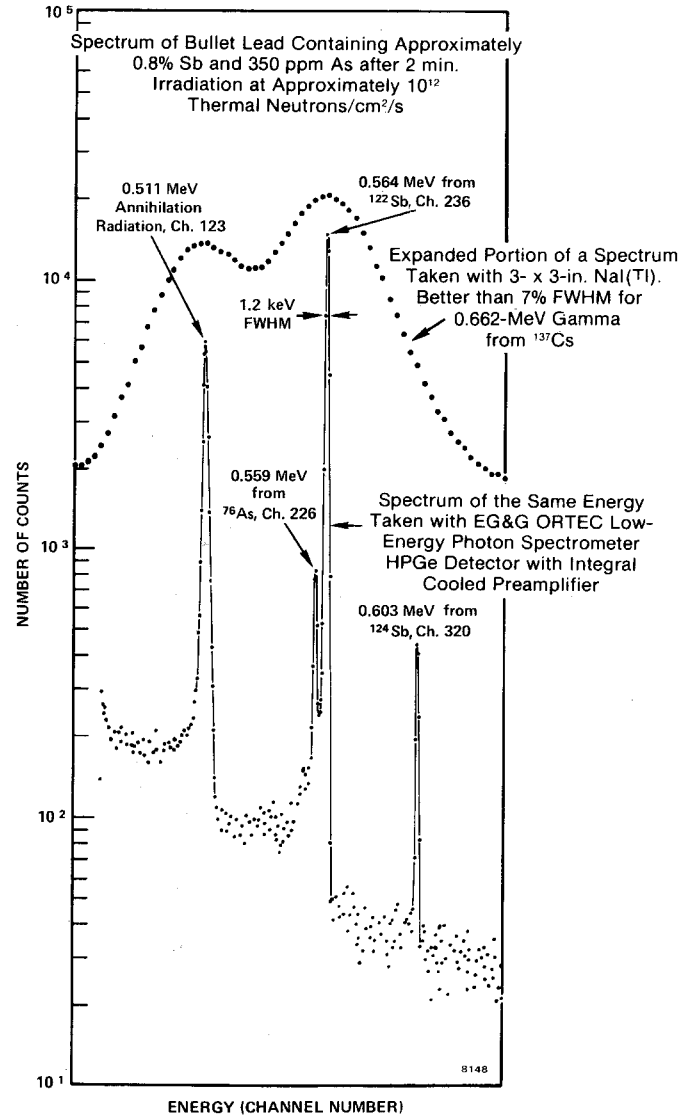


Fig. 7.9. Comparative Spectra Taken with HPGe and NaI(Tl) Detectors.

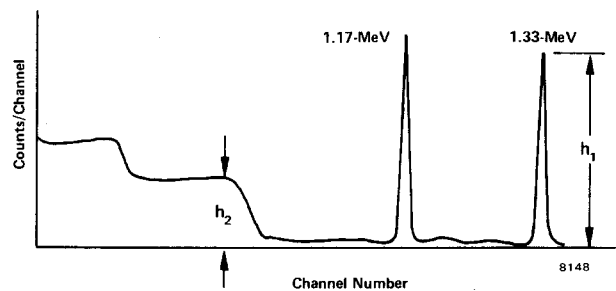


Fig. 7.10. Typical Distribution of ⁶⁰Co Spectrum for Experiment 7.2.

EXERCISE

a. Calculate the peak-to-Compton ratio, which is h_1 divided by h_2 in Fig. 7.10. Compare your value with the value for this ratio for the detector; check with your laboratory instructor for the record of the ratio.

3. Clear the spectrum from the MCA. Place a $10\text{-}\mu\text{Ci } ^{60}\text{Co}$ source at a distance of exactly 25.0 cm from the face of the detector.

4. Accumulate a spectrum for this source for a time period long enough for the sum of counts under the 1.33-MeV photopeak to be about 3000. Read the data from the analyzer and be sure to record the live time for the measurement.

EXERCISES

b. Calculate the number of counts per second for the events that were recorded in the 1.33-MeV photopeak; call this R_1 :

$$R_1 = \frac{\Sigma_{pp}}{\text{time in seconds}} \quad (4)$$

c. The rate, R_1 , from Eq. (4) is to be compared with the rate, R_2 , that is expected for the same source when it is located 25.0 cm from the face of a 3- x 3-in. NaI(Tl) detector. The efficiency of this size NaI(Tl) detector for a source-to-detector distance of 25.0 cm is given as 1.2×10^{-3} , which is from the "Gamma Ray Spectrum Catalog," by R. L. Heath, Idaho Falls Report IDO-16880. Using ϵ_1 for this number, the number of counts, (N), that you would observe under the photopeak for a 3- x 3-in. NaI(Tl) detector at 25.0 cm source distance is given by

$$N = \epsilon_1 A t, \quad (5)$$

where A is the gamma activity of the source in counts per second and t is the live time in seconds. The rate R_2 will then be

$$R_2 = \frac{N}{t} = \epsilon_1 A. \quad (6)$$

Since ^{60}Co has a 1.33-MeV gamma ray for each decay, A is given by

$$A = 3.7 \times 10^4 (x), \quad (7)$$

where x is the source strength in microcuries (μCi).

Calculate R_2 from Eq. (6). The relative photopeak efficiency is obtained for the detector by

$$\text{relative photopeak efficiency} = \frac{R_1}{R_2} \times 100. \quad (8)$$

Calculate this value for your measurement and compare it with the value that is recorded for the detector; check with your laboratory instructor for the record of the detector's efficiency.

EXPERIMENT 7.3

Escape Peaks and Efficiency for HPGe Detectors

As discussed earlier, when an incident gamma with sufficient energy enters the crystal it can create an electron-positron pair. When the positron annihilates, two gammas with equal energy at 0.511 MeV are produced and these leave with an angular separation of 180° . In Fig. 7.3 these two gammas are shown as γ_1 and γ_2 . For small detectors it is very probable that both γ_1 and γ_2 will escape from the detector before they make any further interactions in the crystal. The energy thus absorbed would be $E_\gamma - 1.02$ MeV and is shown as the Double-Escape Peak in Fig. 7.4. As the detector size is increased, the probability is greater that either γ_1 or γ_2 will make a photoelectric interaction within the crystal. If one of these gammas does make a photoelectric interaction, the energy of the event that is recorded in the detector is the Single-Escape Peak in Fig. 7.4. For even larger detectors the probability of photoelectric interactions is further increased when both γ_1 and γ_2 interact and the total energy of the gamma is absorbed in the crystal. Figure 7.11 shows some measurements that have been made for coaxial and planar HPGe detectors. From this figure the ratios of Full-Energy, Double-Escape Peak, and Single-Escape Peak efficiencies can be determined by inspection for the size of detector that is identified in the figure.

To see how the measurements were made for Fig. 7.11, consider the E_γ of 2.511 MeV shown in Fig. 7.4. Assume that the

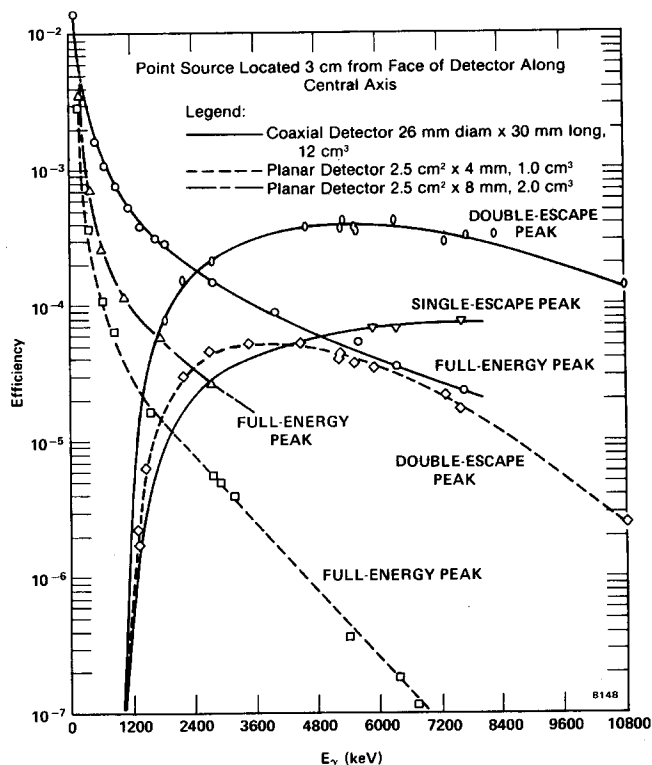


Fig. 7.11. Measured Efficiencies for HPGe Detector.

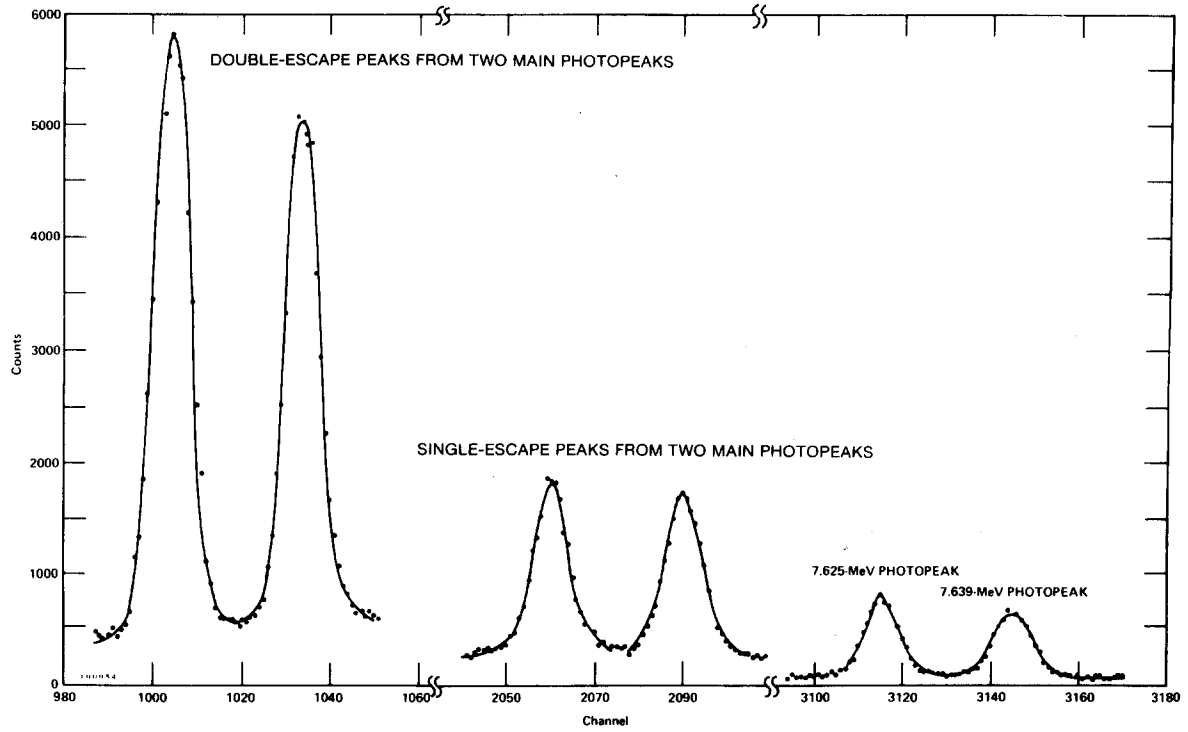


Fig. 7.12. Typical High-Energy Gamma Spectrum from a Neutron Source with Iron Scatterer.

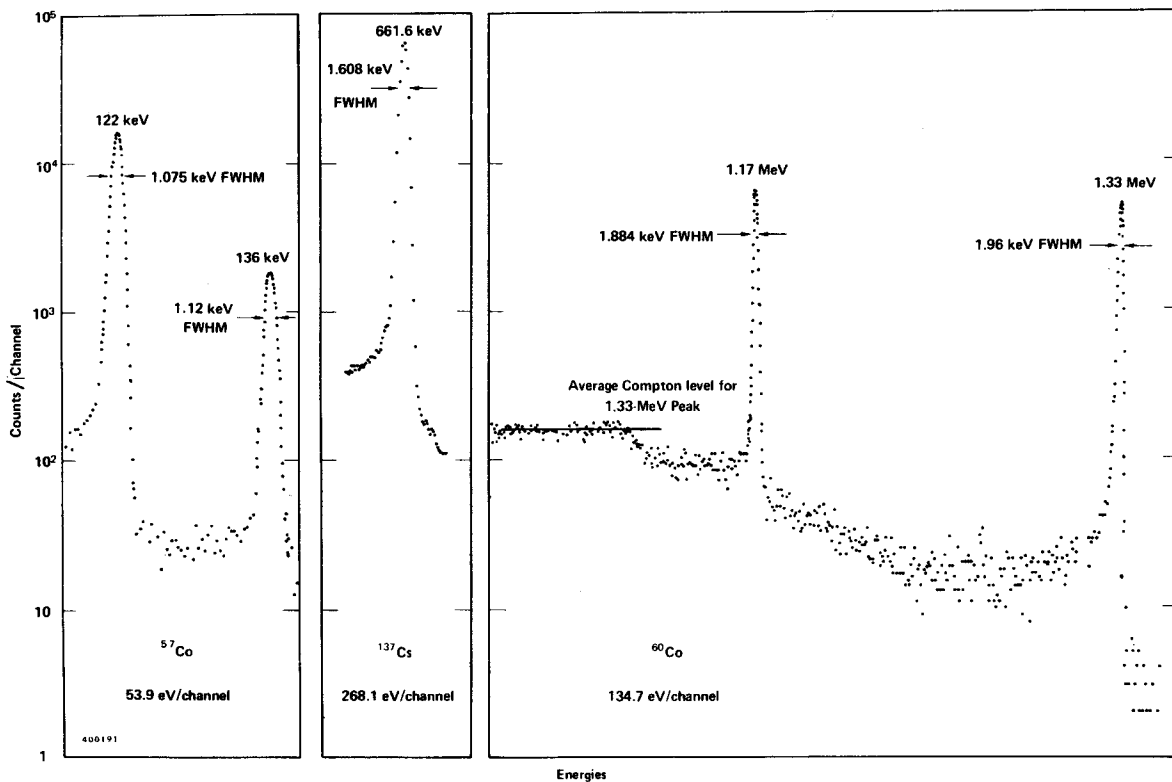


Fig. 7.13. Typical Spectral Response of an EG&G ORTEC HPGe Detector to Various Gamma-Ray Energies.

Compton distribution has been subtracted for each peak in Fig. 7.4 and that the following sums have been measured:

- Σ at Full Energy, 2.511 MeV = 6000,
- Σ at Single-Escape, 2.00 MeV = 1000,
- Σ at Double-Escape, 1.489 MeV = 3000.

From these numbers the simple ratios can be obtained.

Procedure

1. Use the same equipment setup that was used for Experiment 7.1. Use the ^{60}Co and ^{137}Cs gamma sources from SK-1G. Adjust the system gain and bias on the 572 and 444 to calibrate the analyzer roughly from 1 to 3 MeV.

2. Remove the energy calibration sources and use a ^{228}Th (or other high-energy) source to accumulate a spectrum. Accumulate for a period of time long enough to see all the pronounced peaks in the spectrum. Read the data from the analyzer.

EXERCISES

a. Plot the spectrum on semilog graph paper. On the plot identify all the major peaks and the corresponding escape peaks. Compare the energies at these peaks with those that are identified with the source.

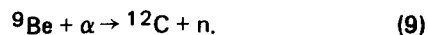
b. Calculate the escape-peak ratios. Define Σ_f as the sum of counts under the full-energy peak, Σ_1 as the sum under the single-escape peak, and Σ_2 as the sum under the double-escape peak. Be sure to subtract the Compton distribution from these sums. Then determine the ratios Σ_f/Σ_1 , Σ_f/Σ_2 , and Σ_2/Σ_1 . How do these ratios compare with those the laboratory instructor has for the ^{228}Th source and the detector you are using?

EXPERIMENT 7.4

(Optional, recommended if Experiments 16, 17, or 18 are to be done)

The Response of HPGe Detectors to High-Energy Gammas

If an isotopic neutron source of the Am-Be type is available, it is possible to obtain high-energy gammas from this source. The neutrons from the source are produced by



The Q value for the reaction is ~ 5 MeV. Since the alpha energies from most sources are also ~ 5 MeV, it is possible to produce neutrons with these sources up to 10 MeV. The neutron spectrum from these sources shows a distribution of neutron energies up to this maximum energy of ~ 10 MeV. What is of more importance is that in the reaction it is also possible for ^{12}C to be left in an excited state. The de-excitation of ^{12}C is by gamma emission. Gammas from the second excited state of ^{12}C have an energy of 7.656 MeV and make an excellent source of high-energy gammas.

Procedure

1. Use the same equipment setup that was used for Experiment 7.1. Use the ^{60}Co source and the pulse generator to adjust the gain and bias of the system so that the MCA range is ~ 3 to 8 MeV.

2. Use a block of paraffin ~ 6 in. thick between the detector and the neutron source, and place the source ~ 12 in. from the detector. The paraffin will thermalize the neutrons from the source without attenuating the high-energy gammas. In some cases the neutron source is in a paraffin howitzer; if this is the case, place the source close to the outside of the howitzer.

3. Accumulate a spectrum. This will require several hours, and sometimes overnight runs are necessary. Read the data from the analyzer.

EXERCISE

Plot the spectrum on semilog paper and identify all the peaks. As in Experiment 7.3, calculate the ratios Σ_f/Σ_1 , Σ_f/Σ_2 , and Σ_2/Σ_1 .

For your reference, Fig. 7.12 is a plot on linear graph paper for a typical neutron source with an iron scatterer. The reaction is ${}^{56}\text{Fe}(n,\gamma){}^{57}\text{Fe}$, which yields two high-energy gammas from the ${}^{56}\text{Fe}$ scatterer. The main photopeak energies are 7.639 and 7.625 MeV.

The resolution of a gamma line is dependent on the gamma energy of the peak. The student can easily verify this by measuring the resolution of the detector for the sources available in the laboratory. Figure 7.13 shows the spectral response and resolution of several common sources for an HPGe detector.

References

1. A. Coche and P. Siffert, *Lithium Drifted Silicon and Germanium Detectors in Semiconductor Detectors*, G. Bertolini and A. Coche Eds., Elsevier-North Holland, Amsterdam (1968).
2. J. C. Phillpott, *IEEE Trans. Nucl. Sci.* **NS-17**(3), 446 (1970).
3. F. Adams and R. Dams, *Applied Gamma Ray Spectrometry*, 2nd Edition, Pergamon Press, Ltd. (1970).
4. U. E. P. Berg, H. Wolf, et al., *Nucl. Instrum. Methods* **129**, 155 (1975).
5. C. Meixner, *Nucl. Instrum. Methods* **119**, 521 (1974).
6. D. M. Walker and J. M. Palms, *IEEE Trans. Nucl. Sci.* **NS-17**(3), 296 (1970).
7. M. L. Stelts and J. C. Browne, *Nucl. Instrum. Methods* **133**, 35 (1976).
8. 20th Nuclear Science Symposium, *IEEE Trans. Nucl. Sci.* **NS-21**(1) (1974).
9. 19th Nuclear Science Symposium, *IEEE Trans. Nucl. Sci.* **NS-20**(1) (1973).
10. C. M. Lederer and V. S. Shirley, Eds., *Table of Isotopes*, 7th Edition, John Wiley and Sons, Inc., New York (1978).
11. G. F. Knoll, *Radiation Detection and Measurement*, Wiley, New York (1979).
12. Nuclear Data Sheets, Edited by the Nuclear Data Project, Academic Press, New York and London.

High-Resolution X-Ray Spectroscopy

EQUIPMENT NEEDED FROM EG&G ORTEC

Source Kit SK-1X

~1 μCi each of ^{65}Zn , ^{137}Cs , ^{55}Fe , and ^{57}Co (see Table 8.2 for other possibilities)

Bin and Power Supply

SLP-06175 Series Si(Li) X-Ray Detector System; typical specifications: 6 mm diam, 175 eV resolution at 5.9 keV, and 1-mil Be window

572 Amplifier

480 Pulser

459 5-kV Detector Bias Supply

ACE-2K MCA System including suitable IBM PC (other EG&G ORTEC MCAs may be used)

12 each AIFI-2 aluminum and 12 each NIFI-1 nickel absorbers (see Appendix)

ORC-8 Cable Set

Model 311 Chamber (optional)

Oscilloscope

Purpose

X-ray energies in a range below 35 keV will be measured with a Si(Li) X-Ray Detector System, and x-ray spectra will be obtained for different samples.

Introduction

In Experiment 7 it was indicated that high-resolution gamma spectroscopy is a rewarding research area. High-resolution x-ray spectroscopy is an equally challenging research field. The Nuclear Spectroscopy Centers suggested in Experiment 7 can be duplicated for the area of x-ray spectroscopy. The state-of-the-art in x-ray spectroscopy with solid-state detector systems is changing almost every day. Both Si(Li) and germanium systems can be used for x-ray spectroscopy although this experiment is written for the use of a Si(Li) system. High-purity germanium (HPGe) detectors are also available for this discipline.

Figure 8.1 shows the spectral response of the 22.162-keV K_{α} line from silver (Ag) as it is measured with three different types of detectors: an NaI(Tl) detector, a proportional counter, and a Si(Li) x-ray detector system. The amplifier gains were carefully matched so that the width of each peak would be a true indication of the relative resolution for that type of detector. Note that the high resolution of the Si(Li) detector not only defines the $K_{\alpha 1}$ peak to advantage but also provides a definite valley below the adjacent $K_{\beta 1}$ peak. Silicon systems have been developed that will give a resolution of 148 eV and better on the 5.9 keV line from ^{55}Fe . With the resolution capabilities of these systems it is possible to study the K_{α} and K_{β} fluorescence x rays for most elements above ^{16}O . The subject of x-ray fluorescence is treated in Experiment 12.

In general, Si(Li) systems provide a little better resolution than can be obtained with HPGe systems. In contrast, the efficiencies of the HPGe systems are better at higher x-ray energies (>30 keV).

Most Si(Li) x-ray detector systems are equipped with a beryllium window over the detector element. The x-ray proportional counters used in Experiment 11 also have beryl-

lium windows. Figure 8.2 shows typical photopeak counting efficiency as a function of the x-ray wave length (reciprocal of energy) and the effects of a 2-mil and a 5-mil beryllium window on the efficiency. From the figure it can be seen that the window becomes important for energies below 6 keV, with comparable wave lengths >1 Å. The curve drops off at higher energies (>15 keV) because the 3-mm-thick Si(Li) detector starts to become more transparent to the x rays.

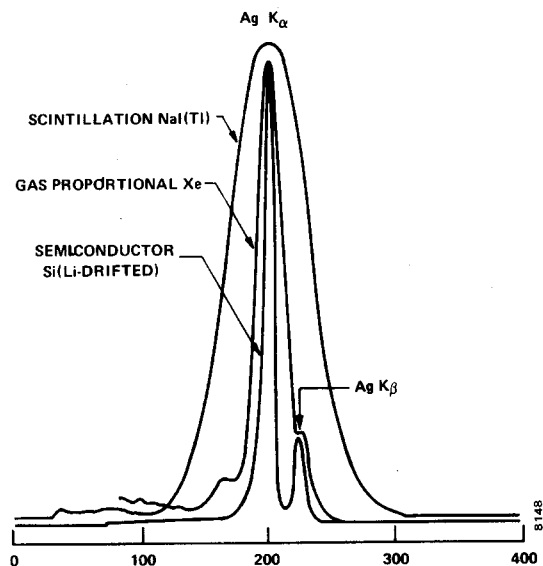


Fig. 8.1. Demonstration of the Resolution Capability of the Three Types of X-Ray Detectors for the Silver K Spectra Obtained from ^{109}Cd Source.

(Courtesy Philip G. Burkhalter and William J. Campbell, U.S. Bureau of Mines, College Park, Maryland.)

EXPERIMENT 8.1

Energy Calibration with a Pulser

Procedure

1. Install the EG&G ORTEC 459, 480, and 572 in the Bin and Power Supply. Interconnect the modules, the preamplifier on the detector, and the MCA as shown in Fig. 8.3. The preamplifier is mounted on the detector, and the signal con-

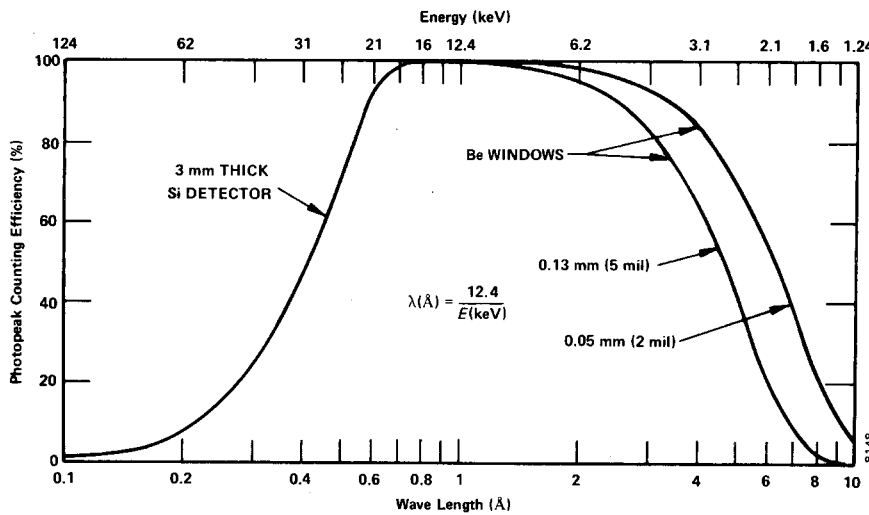


Fig. 8.2. Spectral Response of Si Detector with Be Windows.

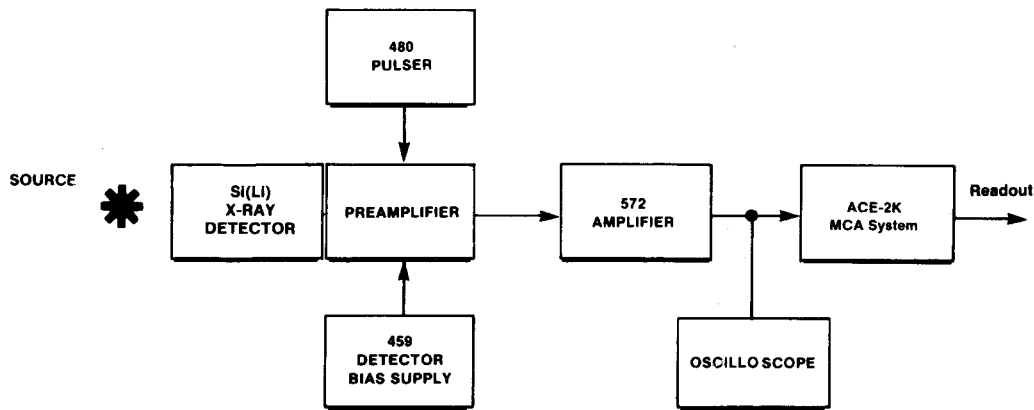


Fig. 8.3. Equipment Interconnections for Experiment 8.1.

nection from the detector to the preamplifier is made internally in the mounting. Check the detector data sheet for the correct polarity and high voltage level, and select the correct polarity with the 459 while its amplitude controls are set at zero. The oscilloscope will be used to check the waveform at the output of the 572 Amplifier.

2. Raise the voltage output of the 459 to the recommended value.
3. Place a ¹³⁷Cs source ~2 cm from the detector window.
4. Adjust the gain of the 572 Amplifier so that the 32.1-keV K_α line for ¹³⁷Cs falls in the upper portion of the analyzer.
5. Accumulate a spectrum for a time period long enough to have 2000 counts in the peak for the 32.1 K_α line.
6. Determine the channel number at the centroid location of the 32.1-keV peak and call this channel C₀.
7. Turn on the 480 Pulser and set the Pulse-Height dial at 321/1000. Adjust the Attenuation switches and the Calibrate control to place the pulser peak in the same channel (C₀), as

the ¹³⁷Cs x-ray peak. The pulser is now calibrated so that full scale (1000/1000) is equal to 100 keV. Lock the dials on the pulser.

8. Clear the analyzer and accumulate pulser peaks for the values in Table 8.1. Store at least 1000 counts in each peak channel. Record the corresponding channel numbers in Table 8.1.

Table 8.1

Pulser (Pulse Height)	Equivalent Energy (keV)	MCA Channel Number
300/1000	30	
250/1000	25	
200/1000	20	
150/1000	15	
100/1000	10	
50/1000	5	

EXERCISE

From the data in Table 8.1, plot an energy vs channel number calibration curve. Determine the keV/channel and the resolution of both the pulser and the 32.1-keV line from the ¹³⁷Cs source. Compare these resolutions with those which the instructor has recorded for the detector being used.

9. Obtain an unknown x-ray source from the instructor and accumulate a spectrum for a period of time long enough to determine the channel numbers for each pronounced peak in the spectrum.

For example, Fig. 8.4 shows the K_α and K_β peaks for an ⁵⁵Fe x-ray source. This source, which is listed in Table 8.2, decays by electron capture. The daughter nucleus for the decay is ⁵⁵Mn, and this accounts for the Mn K_α at 5.9 keV and the Mn K_β at 6.49 keV. If this had been one of the unknowns, there would be no question as to the daughter nucleus. Figure 8.5 shows an ²⁴¹Am spectrum with the Np L x rays and the single 26.36-keV gamma line. As in the case for ⁵⁵Fe, the parent nucleus ²⁴¹Am could be identified easily. These isotope decay schemes are shown in ref. 10.

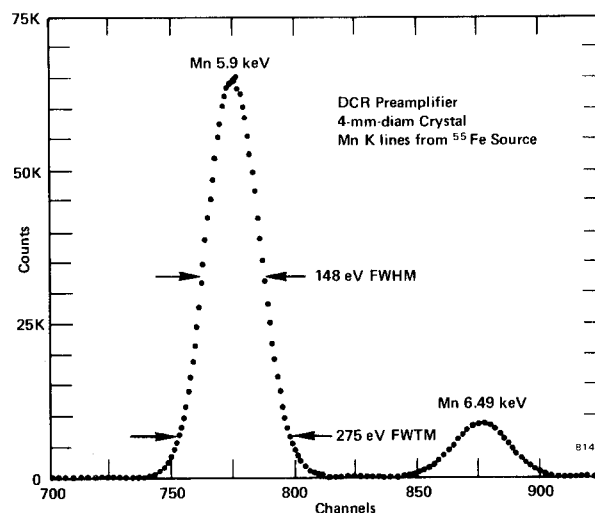


Fig. 8.4. K_α and K_β X-Ray Lines from an ⁵⁵Fe Source.

EXPERIMENT 8.2

Efficiency Measurements and Energy Calibration with Standard X-Ray Sources

This experiment will be similar to Experiment 8.1 except that standard x-ray sources of known activity will be used to measure the efficiency of the detector while the energy calibration curve is being determined. The x-ray sources that are used for all of these experiments should be sources that are manufactured specifically for x-ray studies. For x-ray sources, most manufacturers will deposit a spot of the radioactive material onto 2.5 x 10⁻⁴ in. thick (0.25-mil) Mylar foil. The back side of the source is then covered with another piece of Mylar of approximately the same thickness. The spot size is usually maintained at ~1 mm. The sources used for this experiment are standard sources whose activities are known to ±5%. Thin electrodeposited sources can also be used for x-ray studies.

Procedure

1. Set up the electronics as shown in Fig. 8.3 and adjust the various parameters exactly as described in Experiment 8.1.
2. Place the ¹³⁷Cs standard activity source at a distance of exactly 2 cm from the detector window (for this experiment, all sources must be placed at exactly the same distance from the detector).
3. Adjust the gain of the 572 Amplifier so that the 32.1-keV K_α line is in the upper portion of the 1024-channel analyzer

Table 8.2. Recommended Calibration Sources for Si(Li) Detectors
(Taken from ref. 7)
(Calibration sources for x-ray studies should be deposited on 0.25-mil Mylar or be electrodeposited.)

Nuclide	Energy of X-Rays and Low-Energy Gamma (keV)	Energy of High-Energy Gamma (keV)	Intensity Ratio X/γ
⁵⁴ Mn	5.414 (K _α)	834.8	0.2514 (±0.5%) K _α + K _β
	5.946 (K _β)		
⁵⁷ Co	6.40 (K _α)	122.1	0.5727 (±2.0%) 0.7861 (±2.9%) 0.112 (±1.8%)
	7.06 (K _β)		
	14.41 (γ)		
⁶⁵ Zn	8.04 (K _α)	1115.5	0.6596 (±0.8%) 0.0911 (±2.0%)
	8.9 (K _β)		
⁸⁵ Sr	13.38 (K _α)	514.0	0.5020 (±0.65%) 0.0880 (±1.4%)
	15.0 (K _β)		
88Y	14.12 (K _α)	898.0	0.5491 (±1.2%) 0.0989 (±1.9%)
	15.85 (K _β)		
¹⁰⁹ Cd	22.10 (K _α)	88.0	22.02 (±4.9%) 4.68 (±5.0%)
	25.0 (K _β)		
¹¹³ Sn	24.14 (K _α)	391.7	1.219 (±3.5%) 0.267 (±3.6%)
	27.4 (K _β)		
¹³⁷ Cs	32.1 (K _α)	661.6	0.0666 (±3.0%) 0.0159 (±3.1%)
	36.6 (K _β)		
¹³⁹ Ce	33.29 (K _α)	165.9	0.808 (±11%) 0.195 (±11%)
	38.0 (K _β)		
¹⁹⁸ Au	70.15 (K _α)	411.8	0.0229 (±2.3%) 0.00635 (±2.4%)
	80.7 (K _β)		
²⁰³ Hg	72.11 (K _α)	279.2	0.1247 (±2.1%) 0.0348 (±2.3%)
	83.0 (K _β)		

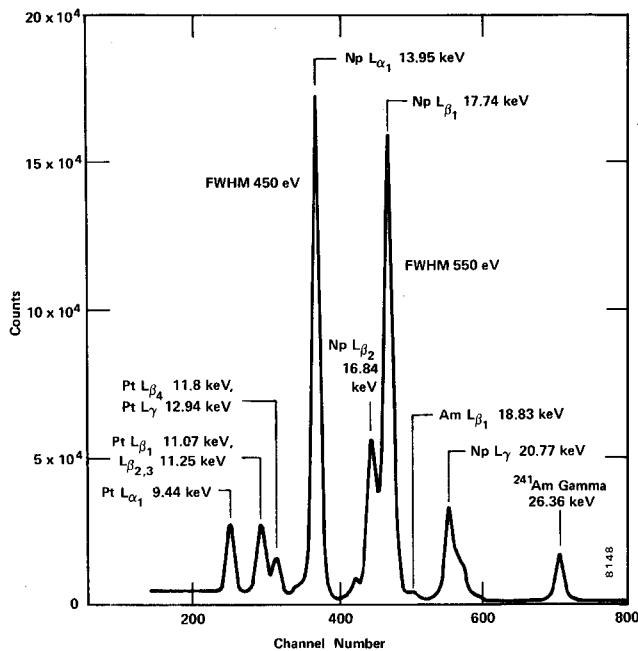


Fig. 8.5. Typical ^{241}Am Spectrum Taken with Si(Li) X-Ray Detector.

range. Accumulate for a time period long enough to obtain ~ 6000 counts in the K_{α} peak. Record the live time and readout the MCA. Since the efficiency of the detector is being determined, the live time must be recorded for each part of this experiment.

4. Replace the ^{137}Cs standard with the ^{109}Cd standard and accumulate for good statistics. Readout the MCA and record the live time.

5. Repeat for as many standard x-ray sources as you wish to use for the calibration and efficiency measurements (see Table 8.2 for suggested sources).

EXERCISES

a. From the MCA readouts and the recorded live times, determine the centroids and the measured number of x rays/second for each of the lines used in Table 8.2. Record the information in Table 8.3.

b. Plot a curve of energy vs channel number for the data that have been recorded in Table 8.3. Determine the slope of the calibration curve in eV/channel. For each peak, multiply the slope of the calibration curve by the FWHM (in channels) of each peak, and from this determine the resolution of each line. Record these values in Table 8.3 and plot a curve of resolution vs energy for the data in Table 8.3. Why does the resolution appear to get better at lower x-ray energies? Recall from Experiment 3 that for gamma-ray measurements with NaI(Tl) detectors, the resolution got considerably worse at the lower gamma energies.

c. Determine the theoretical number of x rays for each line by multiplying the activity of the source in gammas/s by the x ray/gamma intensity ratio shown in Table 8.2. Remember

the intensity of the gamma source should be determined at the calibration gamma energy shown in Table 8.2. From these data, determine the efficiency of the detector for each line and record in Table 8.3. The efficiency is defined as the ratio of the measured x-ray intensity to that which would theoretically be possible for the source. Plot the efficiency vs energy curve for the detector. Figure 8.2 shows the shape of this efficiency curve for various Be window thicknesses.

EXPERIMENT 8.3

Mass Absorption Coefficient for X Rays

In this experiment the attenuation of the ^{55}Zn K_{α} x rays at 8.04 keV will be measured as they pass through aluminum and nickel foils.

Procedure

1. Set up the electronics as shown in Fig. 8.3. Adjust the ROI (Region of Interest) of the MCA to select the channels that make up the peak for the 8.04-keV line from the ^{65}Zn source. For this measurement, the source should be placed ~ 1 cm from the face of the detector. Be sure there is plenty of space between the source and the detector for insertion of the foils without threatening the thin Be window. The Model 311 Chamber, which is optional for this experiment, can conveniently be used for these measurements. With this chamber, four foils can be loaded at one time and then sequenced as desired.

2. Accumulate the Zn K_{α} peak for a long enough analyzer live time to acquire ~ 6000 counts in the peak. From the analyzer data, determine the number of Zn K_{α} x rays detected per second. From this point on, record only the integrated total number of counts accumulated in the peak.

3. Insert the first foil thickness from Table 8.4. Clear the analyzer and set it for enough preset time to get reasonable statistics in the peak.

4. Count for the preset time interval. Record the integrated count total in Table 8.4. Then repeat for each of the other foil thicknesses listed in Table 8.4.

EXERCISE

Make a plot of counts vs absorber thicknesses. Determine the half-value thicknesses and the mass attenuation coefficients for aluminum and nickel. Refer to Experiment 11 for examples of these plots as they were obtained when using a proportional counter rather than a Si(Li) detector. How do your data compare to Figs. 11.5 and 11.6 in Experiment 11?

Table 8.3. X-Ray Efficiency and Calibration Data

Isotope	X-Ray Energy (keV)	Channel Number	X-Rays/s Measured	X-Rays/s Theory	E (Efficiency)	Resolution of Peak
⁵⁴ Mn	5.414 K _α					
	5.946 K _β					
⁵⁷ Co	6.40 K _α					
	7.06 K _β					
	14.41 γ					
⁶⁵ Zn	8.04 K _α					
	8.90 K _β					
⁸⁵ Sr	13.38 K _α					
	15.00 K _β					
⁸⁸ Y	14.12 K _α					
	15.85 K _β					
¹⁰⁹ Cd	22.10 K _α					
	25.00 K _β					
¹¹³ Sn	24.14 K _α					
	27.40 K _β					
¹³⁷ Cs	32.1 K _α					
	36.6 K _β					
¹³⁹ Ce	33.29 K _α					
	38.0 K _β					
¹⁹⁸ Au	70.15 K _α					
	80.7 K _β					
²⁰³ Hg	72.11 K _α					
	83.0 K					

Table 8.4

Aluminum Thickness (mg/cm ²)	Counts	Nickel Thickness (mg/cm ²)	Counts
5		5	
10		10	
15		15	
20		20	
25		25	
30		30	
35		35	
40		40	
45		45	
50		50	
55		55	
60		60	

References

1. R. E. Wood, P. V. Rao, *et al.*, *Nucl. Instrum. Methods* **94**, 245 (1971).
2. Z. Moroz and M. Moszynski, *Nucl. Instrum. Methods* **68**, 261 (1969).
3. G. F. Knoll, *Radiation Detection and Measurement*, John Wiley and Sons, New York (1979).
4. R. J. Gehrke and R. A. Lokken, *Nucl. Instrum. Methods* **97**, 219 (1971).
5. J. C. Russ, Coordinator, *Energy Dispersion X-Ray Analysis, X-Ray and Electron Probe Analysis*. Available as ASTM Special Technical Publication 485, 1970, 04-485000-39 from American Society for Testing and Materials, 1916 Race Street, Philadelphia, Pennsylvania.
6. R. D. Giauque and J. M. Jaklevic, "Rapid Quantitative Analysis

by X-Ray Spectrometry," *Adv. in X-Ray Analysis* **15**, 266, Plenum Press, New York (1972).

7. J. M. Jaklevic and F. S. Goulding, "Semiconductor Detector X-Ray Fluorescence Spectrometry Applied to Environmental and Biological Analysis," *IEEE Trans. Nucl. Sci.* **NS-19** (1972).

8. J. L. Campbell and L. A. McNelles, "An Intercomparison of

Efficiency Calibration Techniques for Semiconductor X-Ray Detectors," *Nucl. Instrum. Methods* **125**, 205-223 (1975).

9. 14th Scintillation and Semiconductor Counter Symposium, *IEEE Trans. Nucl. Sci.* **NS-22**(1) (1975).

10. C. M. Lederer and V. S. Shirley, Eds., Table of Isotopes, 7th Edition, John Wiley and Sons, Inc., New York (1978).

Time Coincidence Techniques and Absolute Activity Measurements

EQUIPMENT NEEDED FROM EG&G ORTEC

^{60}Co Radioactive Source, 1 to 5 μCi (beta source)
 Two Bins and Power Supplies
 Two 113 Scintillation Preamplifiers
 142A Preamplifier
 A-015-025-1500 Surface Barrier Detector
 266 Photomultiplier Tube Base
 Two 551 Timing Single-Channel Analyzers
 425A Nanosecond Delay
 428 Detector Bias Supply
 567 Time-to-Amplitude Converter and SCA
 556 High Voltage Power Supply
 480 Pulser
 418A Universal Coincidence

Three 875 Counters
 Two 575A Amplifiers
 719 Timer
 305 Vacuum Chamber
 905-3 NaI(Tl) Detector and Photomultiplier
 ACE-2K MCA System including suitable IBM PC (other EG&G ORTEC MCAs may be used)
 Vertical Phototube Stand MPM-9
 Oscilloscope
 Mechanical Vacuum Pump
 Source Kit SK-1G
 ORC-9 Cable Set

Purpose

This experiment will utilize some of the basic instrument configurations for time coincidence studies, including time spectroscopy. It includes a short discussion of typical decay schemes because these include sources of coincident events on which measurements can be made.

Introduction

Time coincidence counting is defined as a method for detecting and identifying radioactive materials and for calibrating their disintegration rates. The absolute activity measurement can be made by counting two or more characteristic radiation events, such as beta and gamma, that occur either together or within a specified time relationship to each other. The isotope that is used in this experiment is ^{60}Co .

Many beta and gamma sources that are used in nuclear training laboratories are produced with nuclear reactors. Typically, a certain stable isotope is placed in the reactor core for a specified time period. The neutron flux in the reactor core could be as much as 10^{14} neutrons per cm^2 per second. This means that 10^{14} thermal neutrons bombard each cm^2 of the sample per second. As a result of the bombardment the sample becomes radioactive.

At thermal neutron energies the most probable neutron reaction is the so-called (n,γ) reaction. A simplified explanation of this reaction is that a neutron from the reactor collides with one of the stable nuclei in the sample and in so doing is absorbed into the nucleus, causing a new nucleus to be formed. The new nucleus is most probably unstable and will get rid of this excess energy by emitting a radioactive particle. For (n,γ) neutron activation the excited nucleus is neutron-rich and the most probable decay mode for a neutron-rich isotope is beta decay. The beta decay is usually

followed by gamma emission. In order to see this, consider the simple decay scheme shown in Fig. 9.1.

This decay scheme is really quite simple to understand. It was pointed out earlier that in a decay scheme the energy of excitation of a nucleus is plotted in the vertical direction. The possible energy levels available in the decay are shown as horizontal lines in the figure. We have drawn the lines to the right in Fig. 9.1 to point out the significance of these levels. X_1 decays by beta emission to Y_1 . There are two possible modes to this decay, which in the figure are labeled β_0 and β_1 . In other words, the excited X_1 nucleus has two possible routes to become de-excited.

In the diagram, C is the zero energy of Y_1 . This zero energy is called the ground state of Y_1 . Another possible state of Y_1 is the 0.570-MeV state, labeled B in the diagram. The second decay mode for X_1 , consists of the emission of a beta particle, β_1 , followed promptly by a gamma. Prompt means that the lifetime of the state is very short. These lifetimes usually range from 10^{-8} to 10^{-21} s. The gamma energy is exactly the same as the first excited state of Y_1 . In the diagram, it is seen that this energy is 0.570 MeV. In other words, for this decay mode β_1 is emitted to the first excited state of Y_1 , which immediately decays to the ground state of Y_1 . If the beta spectrum from X_1 is studied as in Experiment 6, the two betas will be observed. However, a (β,γ) coincidence experiment

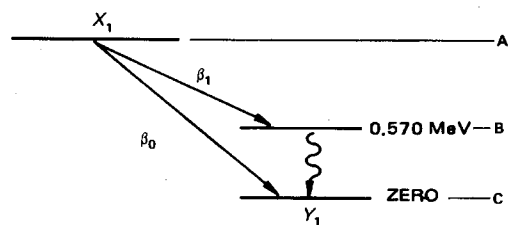


Fig. 9.1.

will quickly show that only β_1 is in coincidence with the 0.570-MeV gamma. This technique will be used later in the experiment to determine the absolute activity of a sample.

(α, γ) Coincidence

In order to understand (α, γ) coincidence, a simple example will be used. Let us assume that we have an alpha source (A) that decays by alpha emission to a stable isotope (B) with the scheme in Fig. 9.2. From the decay scheme it can be seen that 50% of the time (A) goes directly to the ground state

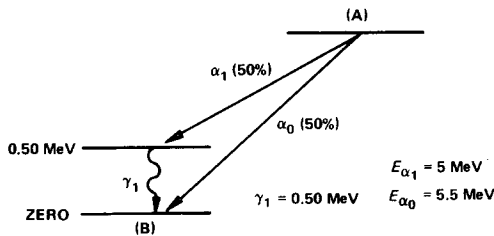


Fig. 9.2.

of (B) with the emission of an alpha, (α_0), whose 5.5-MeV energy is the difference between (A) and (B). The other 50% of the time, decay is by an (α, γ) branch, which is similar to the (β, γ) branch in the previous example. The decay is by a 5-MeV alpha (α_1) followed immediately by a 0.50-MeV gamma. Thus the α_1 and γ_1 are in coincidence. For this example, every α_1 is followed by a γ_1 . Figure 9.3 shows the alpha and gamma spectra for the source as they would have been measured in the previous experiments.

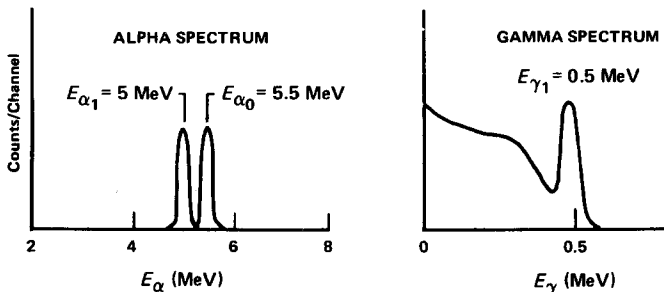


Fig. 9.3.

If the electronics are set up with a surface barrier detector to look at the alphas and with an NaI(Tl) detector to look at the gammas, it will be observed that there are no gammas in coincidence with α_0 .

(γ, γ) Coincidence

In all the examples we have shown thus far in this experiment, gamma decay occurs directly to the ground state of the final stable nucleus. It is possible for a nucleus to de-excite with the emission of several gammas. In order to understand this, let us consider the simple decay scheme shown in Fig. 9.4.

In Fig. 9.4 the nucleus (C) decays to the nucleus (D) by beta emission followed by gamma decay. A simple way to look at the decay is as follows: the beta emission of (C) results in the nucleus (D), which is left with an excess energy of excitation

of 1.0 MeV. The excited (D) nucleus gives off its energy of excitation by the emission of, first, γ_1 , which has an energy of 0.4 MeV, and then promptly by the emission of γ_2 , which has an energy of 0.6 MeV. In other words, for every γ_1 we also have a γ_2 . For this simple example the gamma spectrum of isotope (C) is shown in Fig. 9.5. Of course, as we pointed out earlier, there would also be a coincidence between the beta particle and either of the gammas. Sometimes an isotope will branch directly to the ground state without going through the intermediate states.

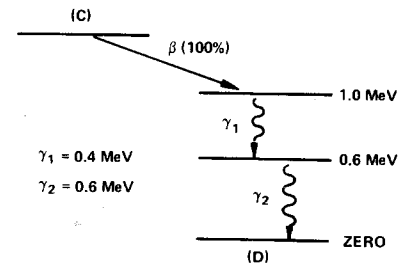


Fig. 9.4.

If this happened in the above example, a gamma of energy 1 MeV would also be seen in the spectrum. These probabilities of gamma decay from a given state to the ground state (stable state) through the intermediate states are called gamma-ray branching ratios.

In later experiments (γ, γ) and (α, γ) coincidence measurements will be made. In this experiment several possible elec-

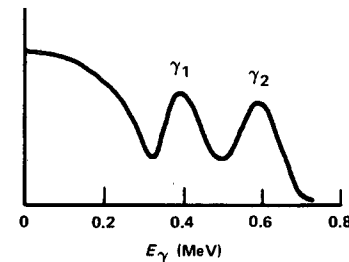


Fig. 9.5.

tronic configurations will be considered for coincidence measurements, and a (β, γ) coincidence setup will be used to determine the absolute activity of a sample.

EXPERIMENT 9.1

Simple Fast Coincidence

- In the circuit of Fig. 9.6, make the following module settings:
- 113 Preamplifiers: 0 pF Input Capacitance.
- 575A Amplifiers: Negative Input, Bipolar Output.
- 551 Timing Single-Channel Analyzers: Integral mode, Lower Level = 50/1000, Delay 0.5 μ s; adjust walk (see manual).
- 418A Universal Coincidence: Inputs A and B Coinc; C, D, and E Off; Coincidence Requirements 2; Resolving Time maximum, 2 μ s.
- 480 Pulser: Negative Output, Power On, Attenuated Output \sim 0.5 V (measured with an oscilloscope).

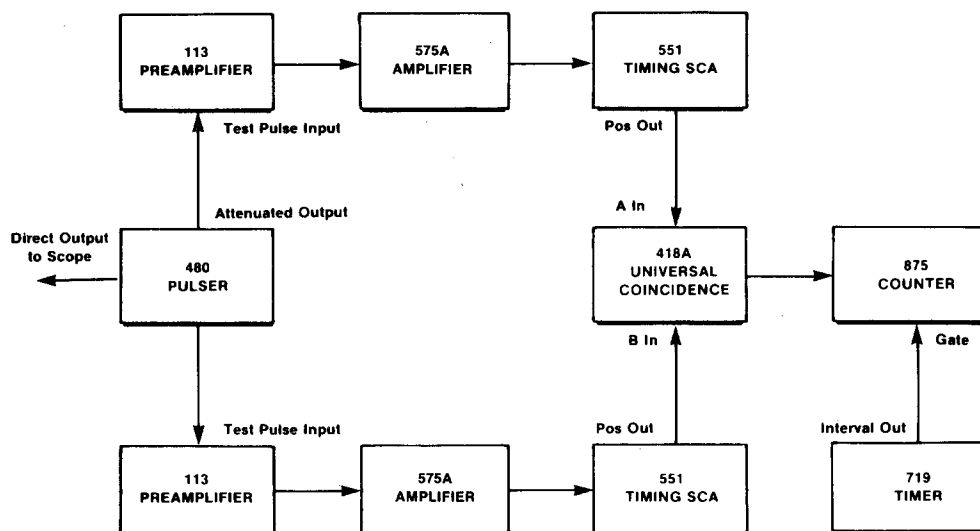


Fig. 9.6. Electronics Interconnections for Experiment 9.1.

Procedure

1. Adjust the gain of each 575A Amplifier so that the output pulse is ~5 V.
2. Set the 719 Timer for a long time (100 s). Vary the delay on either 551 until the maximum counting rate is observed on the 875 Counter. The two branches are now approximately coincident.
3. Clear the counter. Set the timer for 10 s and count. If the maximum counting rate was set properly in step 2, the counter should read ~600 (60 Hz for 10 s). Change the delay in either 551 by 10 ns (10 dial divisions) and repeat the 10-s count.

EXERCISES

- a. Continue changing the delay for enough readings to plot a time coincidence curve similar to that shown in Fig. 9.7.
- b. Narrow the resolving time of the 418A to 1 μ s and plot the coincidence curve which is similar to Fig. 9.7 (note: take readings every 100 ns).
- c. Narrow the resolving time of the 418A to 100 ns and measure the coincidence curve (take readings every 10 ns).

The student should now begin to understand the concept of simple fast time coincidence spectroscopy.

EXPERIMENT 9.2

Fast Coincidence and the Time-to-Amplitude Converter

The 567 Time-to-Amplitude Converter (TAC) can also be used when fast coincidence requirements are needed in an experiment. The TAC basically is a module that gives an output pulse whose amplitude is proportional to the time dif-

ference (Δt) between the start and stop input pulses to the converter. It is, therefore, an electronic clock that can be used to measure time differences that are very short ($\sim 10 \times 10^{-12}$ s). The TAC will not only indicate that two events are in coincidence but will also tell how the coincidence events are distributed with respect to time. The purpose of this experiment is to study some of the properties of the TAC.

In the circuit of Fig. 9.8, make the following module settings:

- 113 Preamplifiers: 0 pF Input Capacitance.
- 575A Amplifiers: Negative Input, Bipolar Output.
- 551 Timing Single-Channel analyzer on Start Side: Integral mode, Lower Level = 50/1000, Delay 100 ns; adjust walk (see manual).
- 551 Timing Single-Channel Analyzer on Stop Side: Integral mode, Lower Level = 50/1000, Delay 100 ns; adjust walk (see manual).
- 480 Pulser: Negative Output, Power On, Attenuated Output ~0.5 V (measured with an oscilloscope).
- 567 Time-to-Amplitude Converter: 0.2 μ s; single-channel controls not used.
- 425A Delay: 32 ns In, all others Out.

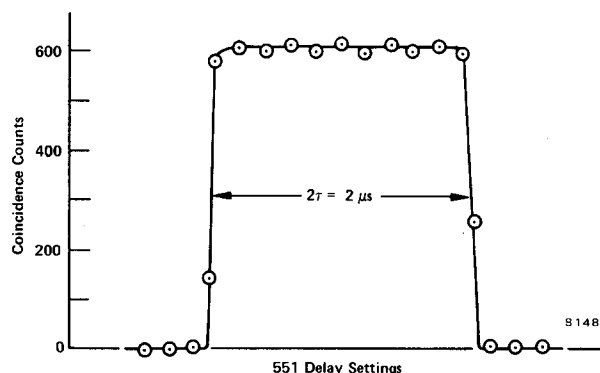


Fig. 9.7. Typical Time Coincidence Curve.

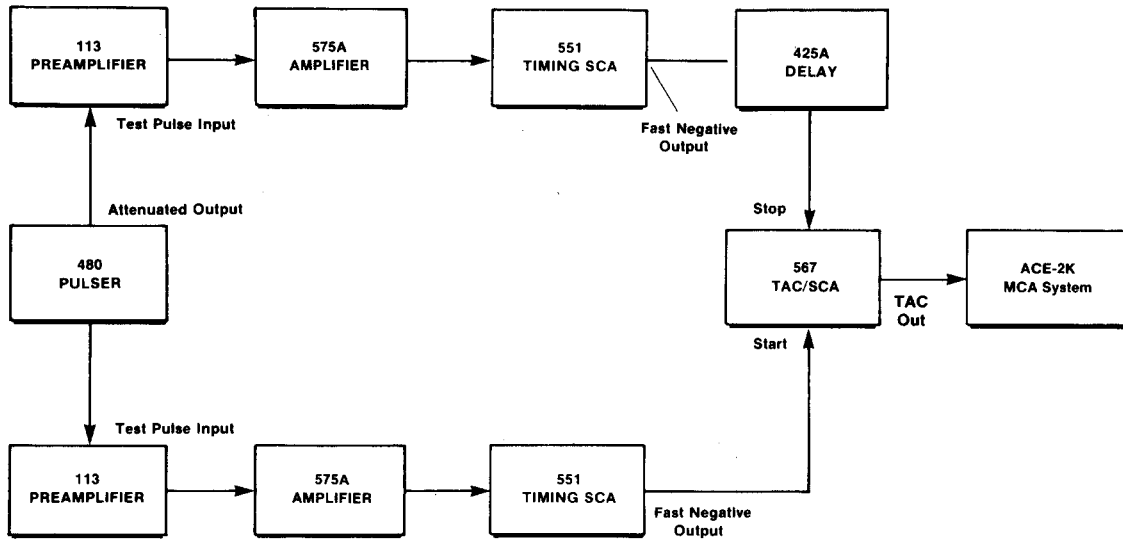


Fig. 9.8. Electronics Interconnections for Experiment 9.2.

Procedure

1. Adjust the gain of each 575A Amplifier so that its Bipolar Output has an amplitude of ~5 V.
2. Accumulate a spectrum in the analyzer. A single isolated group of signals should be observed above midscale on the analyzer display.
3. Set the 1, 2, 4, 8, and 16 ns switches of the 425A Delay unit all at In. This should move the position where signals are being accumulated in the analyzer display, and they should accumulate in the upper quarter of the display. Record the channel number of the peak.
4. Switch the 16-ns switch to Out and observe the movement of the peak in the analyzer. Record the new peak position.
5. Set all the switches in the 425A Delay module at Out, for 0 delay. Record the channel number of the peak in Table 9.1.

Table 9.1

Stop Signal Delay (ns)	Peak Location (Channel No.)	Stop Signal Delay (ns)	Peak Location (Channel No.)
0		35	
5		40	
10		45	
15		50	
20		55	
25		60	
30		65	

EXERCISES

- a. Use the 425A Delay module to increase the Stop signal delay in 5-ns steps and fill in the peak location channel numbers in Table 9.1.
- b. Plot the data from Table 9.1 on linear graph paper. The plot should be similar to that in Fig. 9.9.
- c. Determine the slope of your calibration curve.
- d. Determine the time resolution for your system. This is defined as δT in the formula

$$\delta T = (\text{FWHM}) \frac{\delta D}{\delta \text{ch}} \quad (1)$$

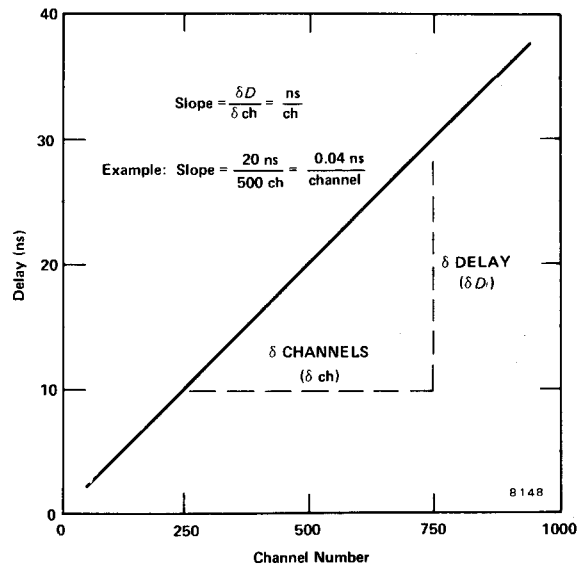


Fig. 9.9. Typical Delay vs Pulse-Height Curve.

where the (FWHM) factor is the number of channels across the half-height of the spectrum as defined earlier.

6. Switch the 567 TAC range to 400 ns. The TAC now has a full-scale output range that corresponds to 0–0.4 μ s. Change the Delay on the Start 551 to 0.1 μ s. Adjust the Delay in the Stop 551 until the TAC output is being stored in the upper quarter of the analyzer. Record the position of the peak.

7. Decrease the Delay in the Stop 551 by 100 ns (100 dial divisions). Record the new location of the peak.

EXERCISE

e. Continue to change the values of Delay in the Stop 551 and record the resulting channel locations. Use enough settings to establish a delay vs pulse-height curve for this new range of the TAC and calculate its measured resolution.

EXPERIMENT 9.3

Determination of Absolute Activity by the Coincidence Method

Introduction

Some of the coincidence techniques that were outlined above will now be used to determine the absolute activity of a ⁶⁰Co sample. The method consists of counting in the following order:

1. the gamma spectrum for the sample as in Experiment 3,

2. the beta spectrum as in Experiment 6,
3. the (β, γ) coincidence for the sample.

From step 1 the gamma counting rate, R_γ , is determined:

$$R_\gamma = A_0 \epsilon_\gamma \quad (2)$$

where A_0 is the true disintegration rate of the sample and ϵ_γ is the efficiency of the NaI(Tl) detector.

From step 2 the same information is determined for the betas:

$$R_\beta = A_0 \epsilon_\beta \quad (3)$$

where ϵ_β is the efficiency of the beta detector.

The coincidence counting rate measured in step 3 would be

$$R_c = A_0 \epsilon_\gamma \epsilon_\beta \quad (4)$$

From Eqs. (2), (3), and (4) A_0 is given by

$$A_0 = \frac{R_\gamma R_\beta}{R_c} \quad (5)$$

The purpose of the experiment is to determine A_0 for the ⁶⁰Co sample.

In the circuit of Fig. 9.10, make the following settings on the modules:

- 113 Preamplifier: 0 pF Input Capacitance.
- 575A Amplifier (from 113): Negative Input, Bipolar Output.

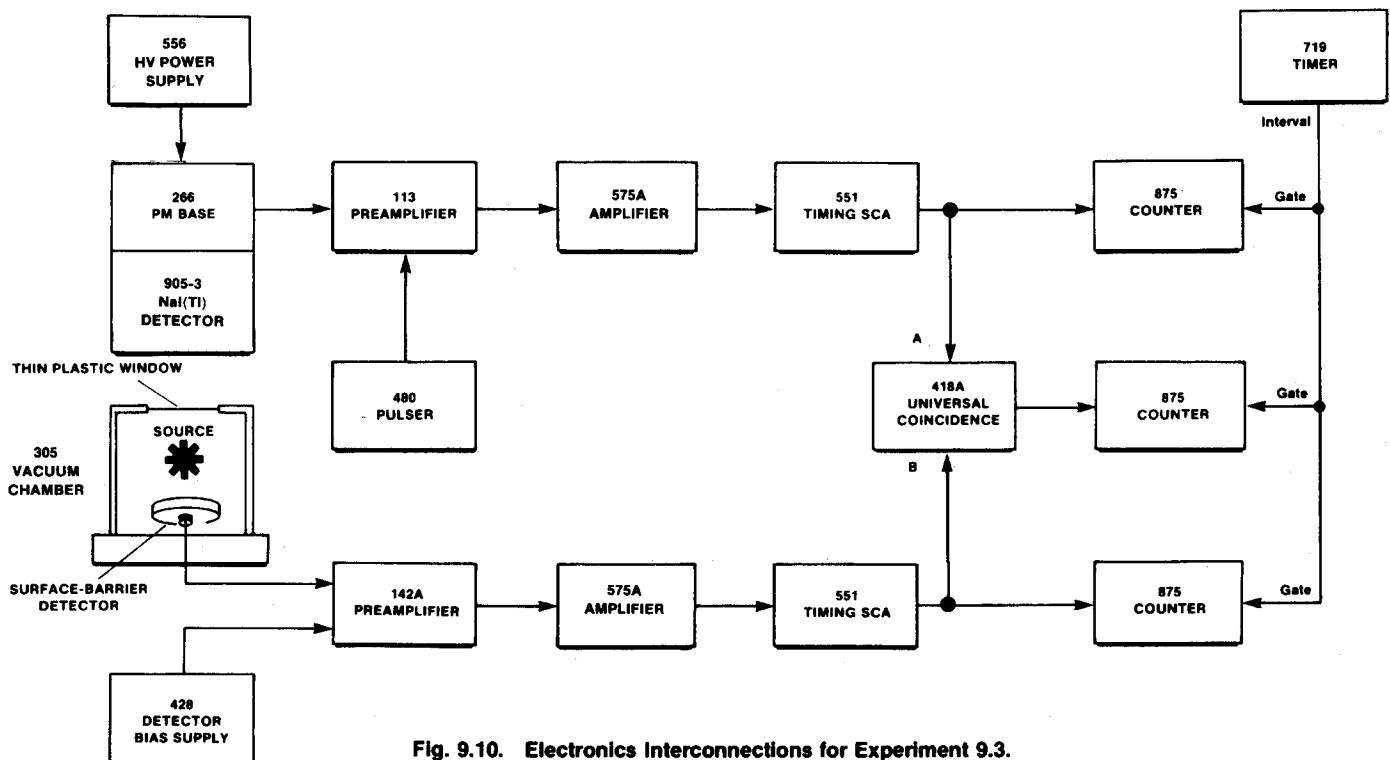


Fig. 9.10. Electronics Interconnections for Experiment 9.3.

575A Amplifier (from 142A): Positive Input, Bipolar Output.
551 Timing Single-Channel Analyzers: Integral mode, Lower Level N 40/1000, Delay minimum.

418A Universal Coincidence: Coincidence Requirements 2, Resolving Time maximum, 2 μ s, Switch A Coinc, Switch B Coinc, Switches C, D, and E Off.

Turn on the mechanical vacuum pump.

Procedure

1. Adjust the 556 high voltage to the polarity and value recommended for the phototube.
2. Adjust the gain of the 575A Amplifier on the 113 side of the circuit so that the 1.33-MeV gammas from the ^{60}Co source are ~ 6 V at the Bipolar output.
3. Raise the 428 Bias Supply voltage gradually to the value recommended for the surface barrier detector.
4. Adjust the gain of the 575A Amplifier on the 142A side of the circuit so that the maximum pulse amplitude from the beta continuum is ~ 7 V.
5. All three 875 Counters should be counting.
6. Stop the 719 Timer and clear all counters to zero.
7. Start counting in all three counters by starting the 719. Count for a time interval long enough to accumulate ~ 600 counts in the R_c counter (for the coincidence events).

EXERCISE

Calculate A_0 from Eq. (5). How does your value compare with the value indicated for the sample, considering its current rate of decay?

References

1. G. F. Knoll, *Radiation Detection and Measurement*, John Wiley and Sons, New York (1979).
2. V. Acosta, C. L. Cowan, and B. J. Graham, *Essentials of Modern Physics*, Harper and Row, New York (1973).
3. V. Arena, *Ionizing Radiation and Life*, The C. V. Mosby Co., St. Louis, Missouri (1971).
4. H. L. Andrews, *Radiation Biophysics*, Prentice-Hall, Englewood Cliffs, New Jersey (1974).
5. P. Quittner, *Gamma Ray Spectroscopy*, Halsted Press, New York (1972).
6. W. Mann and S. Garfinkel, *Radioactivity and Its Measurement*, Van Nostrand-Reinhold, New York (1966).
7. *Radiological Health Handbook*, U.S. Dept. of Health, Education, and Welfare, PHS Publication 2016. Available from National Technical Information Service, U.S. Dept. of Commerce, Springfield, Virginia.
8. A. C. Melissinos, *Experiments in Modern Physics*, Academic Press, New York (1966).
9. K. Siegbahn, Ed., *Alpha-, Beta-, and Gamma-Ray Spectroscopy 1 and 2*, North Holland Publishing Co., Amsterdam (1965).
10. A. H. Wapstra, *et al.*, *Nuclear Spectroscopy Tables*, North Holland Publishing Co., Amsterdam (1959).

EXPERIMENT 10

Compton Scattering

EQUIPMENT NEEDED FROM EG&G ORTEC

- 1-10 mCi sealed ^{137}Cs source
- Two 113 Scintillation Preamplifiers
- Two 266 Photomultiplier Tube Bases
- Bin and Power Supply
- Two 556 High Voltage Power Supplies
- 480 Pulser
- Two 575A Amplifiers
- 551 Timing Single-Channel Analyzer
- 427A Delay Amplifier
- 905-3 NaI(Tl) Detector and Photomultiplier

- 905-23 Plastic Scintillator 1/2 x 4 in., mounted to photo-multiplier tube
- Source Kit SK-1G
- AlRd-1 aluminum scattering rod (see Appendix)
- ACE-2K MCA System including suitable IBM PC (other EG&G ORTEC MCAs may be used)
- Oscilloscope
- 309 Complete Compton Scattering Apparatus
- ORC-10 Cable Set

Purpose

In this experiment the techniques for studying the effects of Compton scattering will be studied. The source will be ^{137}Cs , and the scattering will be caused by its gamma rays striking an aluminum rod and an organic scintillator.

Introduction

The collision of a gamma ray with a free electron is explained by the Compton interaction. The kinematic equations that describe this interaction are exactly the same equations as for two billiard balls colliding with each other, except that the balls are of different size. Figure 10.1 shows the interaction.

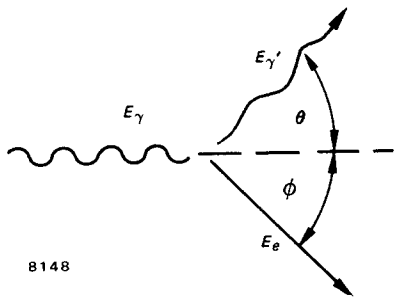


Fig. 10.1. Scattering Caused by Compton Interaction.

In Fig. 10.1 a gamma of energy, E_γ , scatters from an electron with an energy E_γ' . (For convenience, all energies are expressed in MeV.) The energy that the electron gains in the collision is E_e . In Fig. 10.1, θ and ϕ are the scattering angles for γ' and the electron respectively. The laws of conservation of energy and momentum for the interaction are as follows:

Conservation of energy,

$$E_\gamma = E_\gamma' + E_e \quad (1)$$

Conservation of momentum,

$$x \text{ direction } \frac{hf}{c} = \frac{hf'}{c} (\cos\theta) + mv (\cos\phi) \quad (2)$$

Conservation of momentum,

$$y \text{ direction } 0 = \frac{hf'}{c} (\sin\theta) - mv (\sin\phi) \quad (3)$$

In the above equations, $E_\gamma = hf$, $E_\gamma' = hf'$, $E_e = mc^2 - m_0c^2$, $m = m_0/(1 - v^2/c^2)^{-1/2}$ when $m_0 =$ rest mass of the electron, and $v =$ the velocity of the recoil electron.

Solving Eqs. (1), (2), and (3) for E_γ' results in the following:

$$E_\gamma' = \frac{E_\gamma}{1 + \frac{E_\gamma}{m_0c^2} (1 - \cos\theta)} \quad (4)$$

Note that Eq. (4) is easy to use if all energies are expressed in MeV. From Experiments 3 and 7, m_0c^2 is equal to 0.511 MeV. In this experiment E_γ is the energy of the source (0.662 MeV for ^{137}Cs), and θ is the measured laboratory angle.

Figure 10.2 shows the geometry that will be used for the experiments outlined for Compton scattering. Experiments

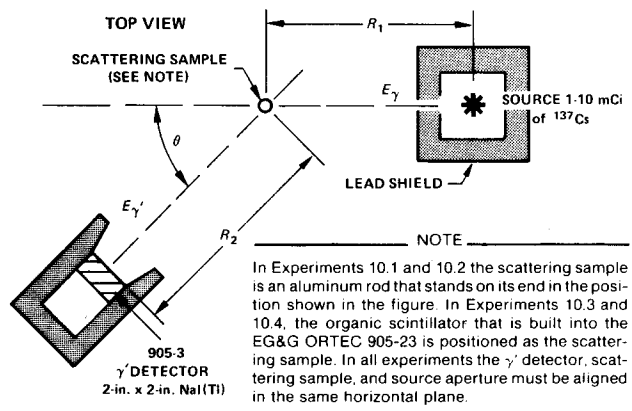


Fig. 10.2. Arrangement of Source, Sample, and Detector for Experiment 10 Using an EG&G ORTEC 309 Compton Scattering Apparatus.

10.1 and 10.2 are simple scattering experiments using an aluminum scattering sample. In Experiments 10.3 and 10.4 the aluminum sample is replaced with an organic scintillator coupled to a phototube, and a coincidence is required between the pulse in the organic scintillator and a pulse in the NaI(Tl) crystal.

EXPERIMENT 10.1

Simple Compton Scattering (Energy Determination)

Procedure

- Using $E_\gamma = 0.662$ MeV for ^{137}Cs in Eq. (4), calculate the values for $E_{\gamma'}$ and enter them in Table 10.1 for the angles that are to be used in the experiment.
- Set up the electronics as shown in Fig. 10.3. Calibrate the MCA so that the ^{137}Cs line is in approximately channel 800. This procedure was outlined in Experiment 3.
- Plot the energy vs channel number for your calibration. This calibration will be used to determine the $E_{\gamma'}$ (Measured) values in Table 10.1.
- Set $\theta = 20^\circ$ (Fig. 10.2) and accumulate for a period of time long enough to determine the position of the photopeak. (Note: if you also plan to do Experiment 10.2, the sum under each photopeak should be at least 1000 counts.) From your calibration curve fill in $E_{\gamma'}$ (Measured) in Table 10.1. Continue for the other values in the table. Figure 10.4 shows spectra at 20° and 120° .

EXERCISES

- Plot $E_{\gamma'}$ (Calculated) vs θ on linear graph paper. Put the experimental points with the estimated error on the curve. Do your experimental values agree with the theory?
- For ^{137}Cs , $E_\gamma = 0.662$ MeV, and since $m_0c^2 = 0.511$, Eq. (4) becomes:

$$E_{\gamma'} = \frac{E_\gamma}{1 + 1.956E_\gamma} (1 - \cos\theta). \quad (5)$$

This can be written:

$$\frac{1}{E_{\gamma'}} = 1.51 + 1.956 (1 - \cos\theta). \quad (6)$$

Therefore, a plot of $1/E_{\gamma'}$ vs $(1 - \cos\theta)$ should be a straight line with intercept 1.51 and a slope equal to 1.956. Table 10.2 shows θ , $1/E_{\gamma'}$, and $(1 - \cos\theta)$ for ^{137}Cs .

Make a plot of $1/E_{\gamma'}$ vs $(1 - \cos\theta)$ and put your experimental points from Table 10.1 on the graph. Figure 10.5 shows a typical graph of this function and the experimental data points.

Table 10.1

θ (deg)	$E_{\gamma'}$ (Calculated)	$E_{\gamma'}$ (Measured)
20		
40		
60		
80		
100		
120		
140		
160		

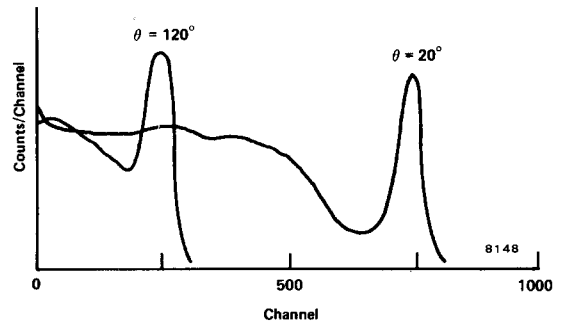


Fig. 10.4. Overlapped Spectra Obtained at Two Scattering Angles.

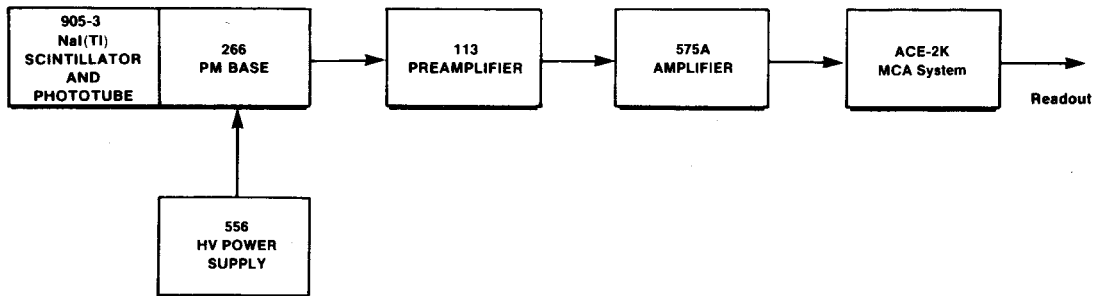


Fig. 10.3. Instrument Interconnections for Experiments 10.1 and 10.2.

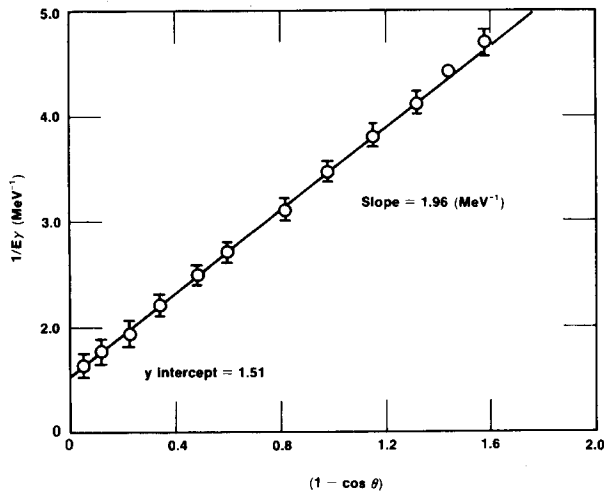


Fig. 10.5. $1/E_{\gamma'}$ vs $(1 - \cos\theta)$ for ^{137}Cs .

Table 10.2

Angle (θ)	$1/E_{\gamma'}$ (MeV^{-1})	$1 - \cos\theta$
0	1.51	0
10	1.54	0.015
20	1.63	0.060
30	1.77	0.133
40	1.97	0.234
50	2.20	0.357
60	2.49	0.500
70	2.79	0.658
80	3.12	0.826
90	3.46	1.00
100	3.80	1.17
110	4.13	1.34
120	4.44	1.50
130	4.72	1.64

EXPERIMENT 10.2

Simple Compton Scattering
(Cross-Section Determination)

The differential cross section for Compton scattering was first proposed by Klein and Nishina. This formulation is discussed in ref. 1. The expression has the following form:

$$\left(\frac{d\sigma}{d\Omega}\right)_{\text{theory}} = \frac{r_0^2}{2} \left\{ \frac{1 + \cos^2\theta}{[1 + \alpha(1 - \cos\theta)]^2} \right\} \times \left\{ 1 + \frac{\alpha^2(1 - \cos\theta)^2}{[1 + \cos^2\theta][1 + \alpha(1 - \cos\theta)]} \right\} \cdot \left(\frac{\text{cm}^2}{\text{sr}}\right) \quad (7)$$

where

$$r_0 = 2.82 \times 10^{-13} \text{ cm (classical electron radius),}$$

$$\alpha = \frac{E_{\gamma}}{m_0c^2} = \frac{0.662 \text{ MeV}}{0.511 \text{ MeV}} = 1.29 \text{ for } ^{137}\text{Cs},$$

$d\Omega$ = the measured solid angle in steradians.

In this experiment we will verify Eq. (7) from the experimental measurements.

Procedure

The procedure here is the same as that for Experiment 10.1 except that for each run the sum under the photopeak should be at least 1000 counts.

1. Solve Eq. (7) for the values of θ used in Table 10.1. (A computer is quite valuable at this point, although not absolutely necessary.)

EXERCISE

- a. Plot $(d\sigma/d\Omega)_{\text{theory}}$ vs θ on linear graph paper.
2. Find the measured differential cross section by solving the following expression:

$$\left(\frac{d\sigma}{d\Omega}\right)_{\text{measured}} = \frac{\Sigma_{\gamma'}}{N\Delta\Omega I} \quad (8)$$

where

$\Sigma_{\gamma'}$ = sum under the photopeak divided by the intrinsic peak efficiency (see Experiment 3),

$$N = \text{number of electrons in the scattering sample} = \frac{(\text{volume}) (\text{density}) (\text{atomic no.}) (\text{Avogadro's no.})}{\text{atomic weight}}$$

$\Delta\Omega$ = solid angle in steradians of detector

$$= \frac{\text{area of detector (cm}^2\text{)}}{[R_2 \text{ (cm)}]^2}$$

I = the number of incident γ 's per cm^2 per s at the scattering sample; this number can be calculated if the activity of the source is known.

EXERCISE

- b. Solve Eq. (8) for the measured values. Put the measured values with their estimated errors on the theoretical curve for the Klein-Nishina formula.

EXPERIMENT 10.3

Compton Scattering
(Coincidence Method)

Procedure

1. Set up the electronics as shown in Fig. 10.6. The 905-23 is an organic scintillation detector that will be used as the

scatterer and should be placed in sample position as shown in Fig. 10.2. It will also provide a coincident enable signal to the MCA to permit the energy analysis of the simultaneous scattered signal from the 905-3 NaI(Tl) detector.

2. For the 905-3 circuit, adjust its 556 high voltage and then adjust the gain of its 575A Amplifier so that the ¹³⁷Cs photopeak is near the top of the analyzer range. Set the MCA Gate toggle switch at Off during this adjustment.

3. For the 905-23 circuit, adjust its 556 high voltage and then adjust the gain of its 575A Amplifier so that the Compton edge of the ¹³⁷Cs signal is ~6 V in amplitude at the 575A output, measured with an oscilloscope.

4. Set the 551 Timing SCA Lower-Level dial at 50/1000 or as low as possible without counting noise. Set the Window or Upper-Level dial at 10 V. Adjust the Delay to 0.1 μs.

5. Turn on the 480 Pulser and adjust its attenuated output so that the amplitude at the 575A output in the 905-23 circuit is ~5 V.

6. Set the MCA Gate toggle switch at Coinc (coincidence mode). The analyzer should now store the pulser output pulses. Turn off the 480. The experimental arrangement is now ideal for measuring E_γ' vs θ, because the coincidence requirement from the 905-23 organic scintillator eliminates virtually all the undesired background.

EXERCISE

Repeat all the measurements made in Experiment 10.1 with this coincidence technique. Plot the experimental and theoretical values as in Experiment 10.1.

EXPERIMENT 10.4

Compton Scattering (Electron Recoil Energy)

Procedure

1. Set up the electronics as shown in Fig. 10.7. The equipment is the same as was used for Experiment 10.3. The 905-23 plastic scintillator is used as the scatterer, set in the sample position on the EG&G ORTEC 309 table, and also provides the source used for energy measurements. The 905-3 will be used to provide the coincident enable signal to the MCA to permit energy analysis of the recoil electrons from the 905-23.

2. Adjust the gain of the 575A Amplifier in the 905-3 circuit so that its output for the 0.662-MeV line of the ¹³⁷Cs is ~6 V, measured with an oscilloscope. Set the 551 Timing SCA controls as in Experiment 10.3.

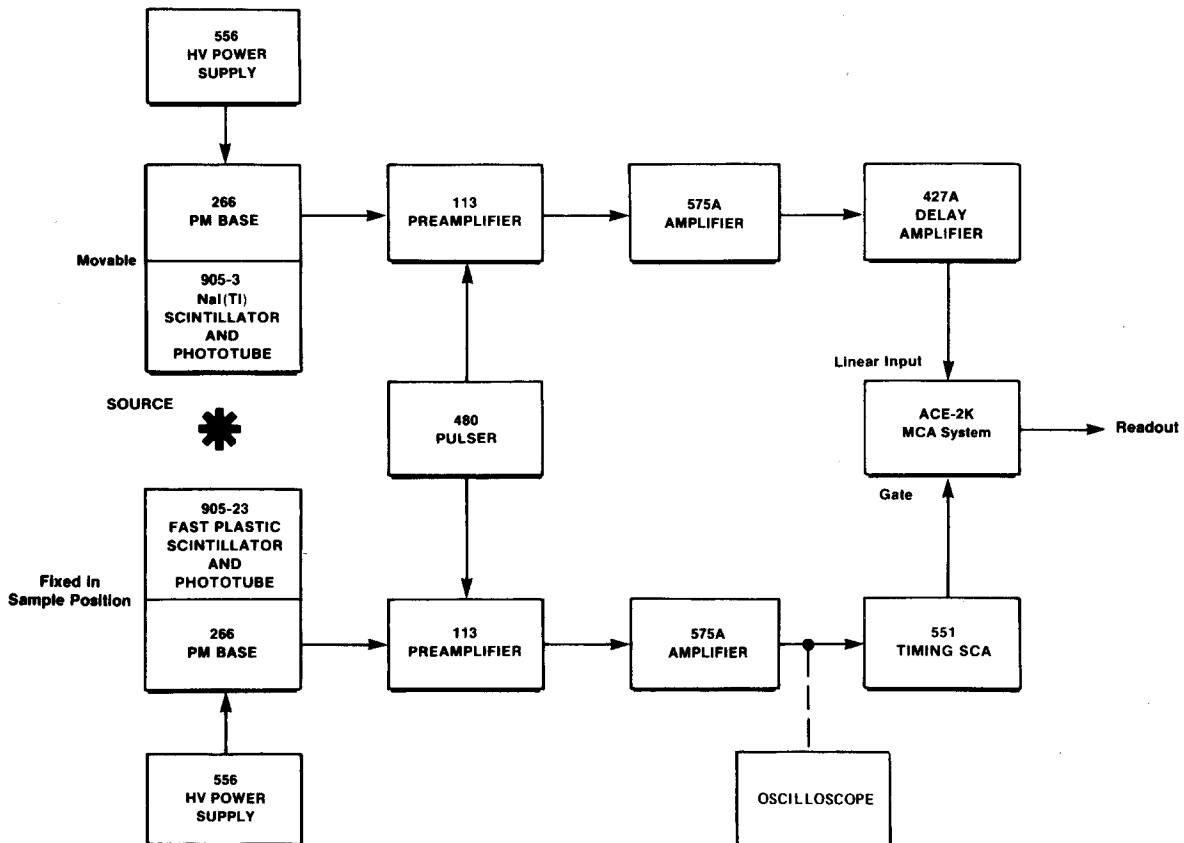


Fig. 10.6. Instrument Interconnections for Experiment 10.3.

- For the 905-23 circuit, adjust the gain of the 575A Amplifier so that the Compton edge from the 0.662-MeV line of ^{137}Cs is stored in the upper channels in the analyzer.
- Use Eqs. (1) and (4) to calculate the values for E_c in Table 10.3 and fill in this column of the table.

Table 10.3

θ (deg)	E_c (Calculated)	E_c (Measured)
0		
20		
40		
60		
80		
100		
120		
140		
160		

- Set the pulse generator for the value of E_c at 0° . Adjust the Calibrate control and the Attenuator switches to place the pulser pulses in about the same analyzer channel as the Compton edge. The pulser is now approximately calibrated.

- Store pulses from the pulser for simulated energy levels of 0.100 MeV, 0.200 MeV, 0.300 MeV, 0.400 MeV, and 0.500 MeV. Read the data out of the analyzer and plot the calibration curve. Turn off the pulser.
- Set the 905-3 detector at 20° and store a coincidence spectrum for the 905-23 output for a period of time long enough to determine the position of the recoil electron energy; record the value in Table 10.3.
- Repeat the measurements for the other angles in Table 10.3. Figure 10.8 shows a typical pair of spectra taken at $\theta = 160^\circ$ and 40° .

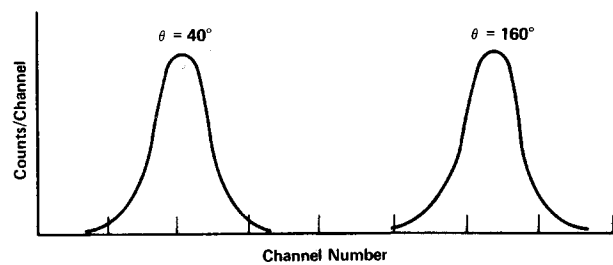


Fig. 10.8. Typical Recoil Electron Spectra Taken at Two Different Angles.

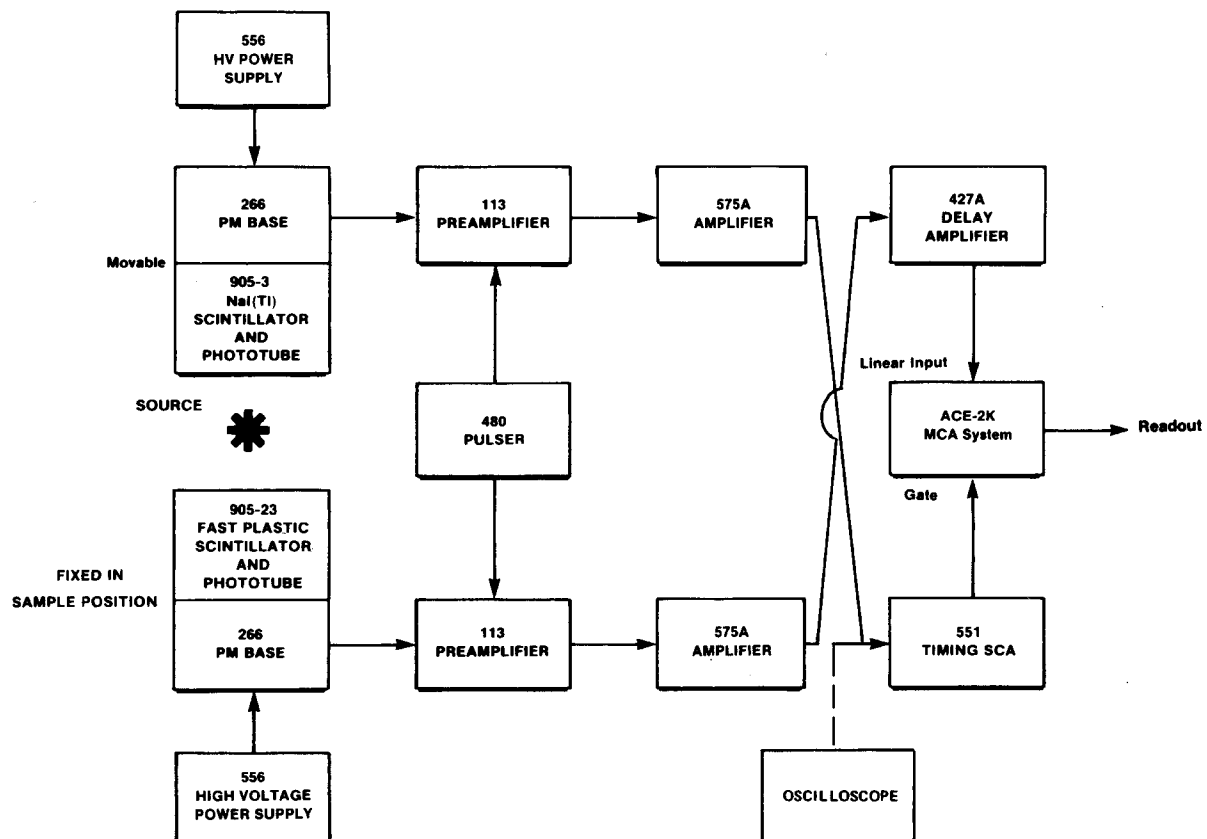


Fig. 10.7. Instrument Interconnections for Experiment 10.4.

EXERCISE

Plot E_c (Calculated) vs θ from Table 10.3. From the calibration curve and the data taken in steps 6 and 7, put the experimental points on the curve with the estimated error. How do your values agree?

References

1. A. C. Melissinos, *Experiments in Modern Physics*, Academic Press, New York (1966).
2. G. F. Knoll, *Radiation Detection and Measurement*, John Wiley and Sons, New York (1979).
3. P. Quittner, *Gamma Ray Spectroscopy*, Halsted Press, New York (1972).
4. W. Mann and S. Garfinkel, *Radioactivity and its Measurement*, Van Nostrand-Reinhold, New York (1966).
5. K. Siegbahn, Ed., *Alpha-, Beta-, and Gamma-Ray Spectroscopy*, 1, North Holland Publishing Co., Amsterdam (1965).
6. C. M. Lederer and V. S. Shirley, Eds., *Table of Isotopes*, 7th Edition, John Wiley and Sons, New York (1978).
7. R. L. Heath, "Scintillation Spectrometry," *Gamma-Ray Spectrum Catalog*, 2nd Edition 1 and 2, IDO 16880, August (1964). Available from Clearinghouse for Federal Scientific and Technical Information, Springfield, Virginia.
8. G. Marion and P. C. Young, *Tables of Nuclear Reaction Graphs*, John Wiley, New York (1968).

The Proportional Counter and Low-Energy X-Ray Measurements

EQUIPMENT NEEDED FROM EG&G ORTEC

Low-energy x-ray calibration sources SK-1X
(see Table 11.1)
Bin and Power Supply
904-1B Thin-Window Proportional Counter
556 High Voltage Power Supply
142PC Preamplifier
575A Amplifier
ACE-2K MCA System including suitable IBM PC (other EG&G ORTEC MCAs may be used)

12 AIFI-2 aluminum and 12 NiFI-1 nickel absorbers
(see Appendix)
Absorber Kit 3-Z2
310 Special Chamber, designed for source, absorbers, and proportional counter geometry
Oscilloscope
ORC-11 Cable Set
Optional ²⁴¹Am 0.1 μCi for Experiment 11.1, Exercise b

Purpose

The technique for operating a thin-window proportional counter is demonstrated in this experiment, and some typical spectra are obtained with this instrument.

CAUTION: The thin beryllium window that is typically built into these proportional counters is very fragile. Do not permit any material to contact the window and do not touch it.

Introduction

The photoelectric interaction is the most pronounced type of gamma interaction for gamma energies below 100 keV, as discussed in Experiments 3 and 7. In this experiment the proportional counter will be used to detect x-ray energies below 50 keV.

The typical proportional counter is basically a metal cylinder that has a concentric electrode in the center of the cylinder. The tube is filled with a counting gas mixture (e.g., 760 Torr of Xe-CH₄), and a positive high voltage of ~2000 V is applied to the central electrode. A thin beryllium window is built into the cylinder wall or end to permit the low-energy x rays to enter into the counting region with a minimum absorption. Beryllium is used because it has a Z value (atomic number) of only 4, and the photoelectric cross section varies as Z⁵ (as discussed in Experiments 3 and 7). When the x rays enter the tube, they make photoelectric interactions in the counting gas and the pulse that is detected is proportional to the recoil electron energy. Proportional counters are normally ~10% efficient for 5-keV x rays, and resolutions around 1.5 keV are common with these devices for 20-keV x rays.

EXPERIMENT 11.1

Energy Calibration

Procedure

1. Connect the instruments as shown in Fig. 11.1. Be careful to prevent touching the beryllium window on the

Table 11.1. Low-Energy X-Ray Calibration Sources Recommended (~1 μCi).

Isotope	X-Ray Energy (keV)
⁵⁴ Mn	5.414 K _α
	5.946 K _β
⁵⁷ Co	6.40 K _α
	7.06 K _β
	14.41 γ
⁶⁵ Zn	8.04 K _α
	8.90 K _β
⁸⁵ Sr	13.38 K _α
	15.00 K _β
⁸⁸ Y	14.12 K _α
	15.85 K _β
¹⁰⁹ Cd	22.10 K _α
	25.00 K _β
¹¹³ Sn	24.14 K _α
	27.40 K _β
¹³⁷ Cs	32.1 K _α
	36.6 K _β

proportional counter. Set the high voltage at the level recommended for the counter tube. Set the 575A Amplifier for a positive input. Place the ¹³⁷Cs source at a distance of ~1 cm from the window of the proportional counter.

2. Adjust the gain of the 575A Amplifier so that the 32.1-keV x ray is being stored in the middle channels of the 1024-channel range in the analyzer. Accumulate for a period of time long enough to determine the channel at which the centroid is being stored. Read out the data from the MCA and clear its memory to zero.

3. Replace the ¹³⁷Cs source with ⁵⁷Co and accumulate for a

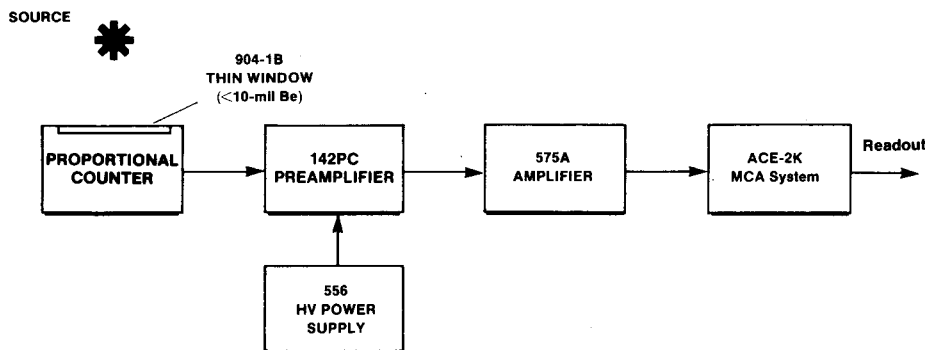


Fig. 11.1. Interconnections of Electronics for Experiment 11.1.

period of time long enough to accurately determine the locations of the 14.4- and 6.4-keV peaks. Read out the data, clear the MCA, and repeat with ^{65}Zn . For your reference, Fig. 11.2 is a typical ^{57}Co spectrum.

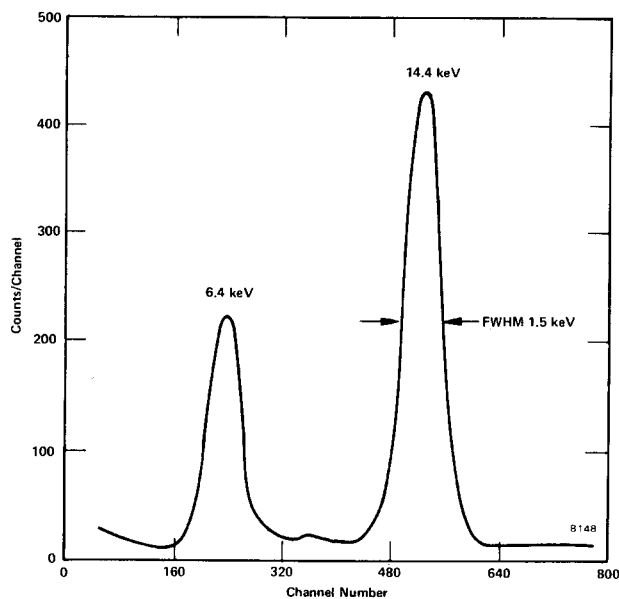


Fig. 11.2. ^{57}Co Spectrum (Proportional Counter).

EXERCISES

- Plot a calibration curve for the data and determine the slope in keV/channel. Measure the resolution, (FWHM in keV), of all the peaks and make a plot of resolution vs energy.
- (optional). Place a ^{241}Am source in front of the detector and accumulate for a period of time long enough to determine the locations of the most pronounced peaks. From the calibration curve, determine the energy of each peak. Figure 11.3 is a typical ^{241}Am x-ray spectrum that was made with a xenon-filled proportional counter.

- Obtain an unknown x-ray source from the instructor. Accumulate its spectrum and determine what it is from the tabulation in ref. 6.

EXPERIMENT 11.2

Mass Absorption Coefficient for Low-Energy X Rays

The mass absorption coefficient was measured for 0.662-MeV gammas from ^{137}Cs in Experiment 3.7. These same measurements will be repeated in this experiment for the 8.05-keV x rays from ^{65}Zn . The procedure will be similar, but the source and absorber thicknesses will differ.

Procedure

- Connect the instruments as shown in Fig. 11.4. Place the ^{65}Zn source ~ 2 cm from the window of the proportional counter. During the experiment, absorbers will be placed between the source and the detector as shown in Fig. 11.4. Adjust the gain of the 575A Amplifier so that the 8.05-keV peak from the ^{65}Zn has an amplitude of ~ 6 V at the amplifier output.
- Accumulate a spectrum in the MCA for a period of time long enough to identify the peak location. Adjust the Region of Interest, (ROI), controls of the MCA to select the channels that make up the peak for the 8.05-keV line from the ^{65}Zn source.
- When the ROI is set properly, stop the accumulation and clear the MCA. From the analyzer data, determine the number of Zn K α x rays detected per second. From this point on, record only the integrated total number of counts in the peak.
- Set the MCA to operate for a preset time interval that is long enough to obtain reasonable statistics. Clear it after each run, and then accumulate for the preset live time for each set of data. After the initial accumulation interval,

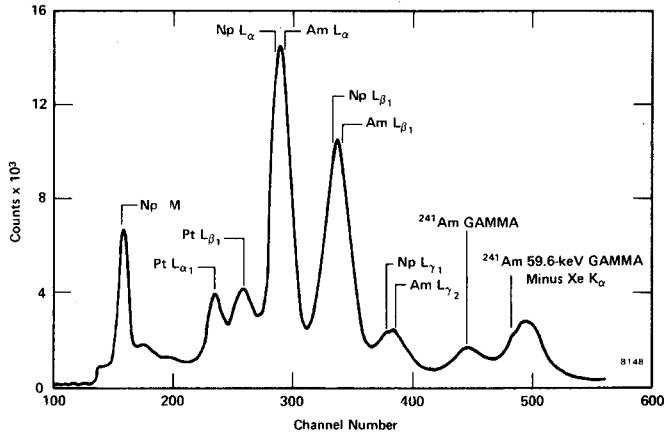


Fig. 11.3. ²⁴¹Am Spectrum Using Xenon-Filled Proportional Counter.

Table 11.2

Absorber Thickness (mg/cm ²)	Counts with Aluminum Absorber	Counts with Nickel Absorber
0		
5		
10		
15		
20		
25		
30		
35		
40		
45		
50		
55		
60		

record the integrated count total for zero absorber thickness in Table 11.2.

5. Place the first 5-mg/cm² AIFI-2 aluminum absorber between the source and the detector and accumulate for the preset time. Continue and repeat for each of the aluminum and nickel thicknesses indicated in Table 11.2.

EXERCISES

a. Make a plot on semilog paper of counts vs absorber thickness (mg/cm²) for both aluminum and nickel. Figures 11.5 and 11.6 show some typical data that were taken under conditions similar to those described.

b. From your plots and the discussion in Experiment 3, determine the half-value thicknesses and the mass attenuation coefficients.

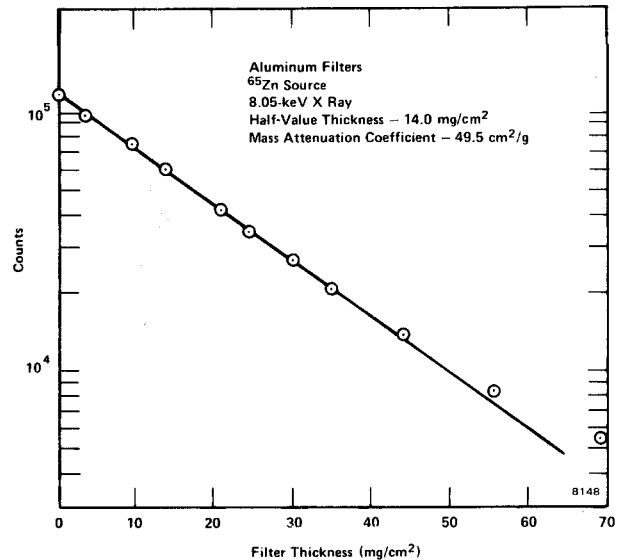


Fig. 11.5. Counts vs Aluminum Absorber Thickness for ⁶⁵Zn X Rays.

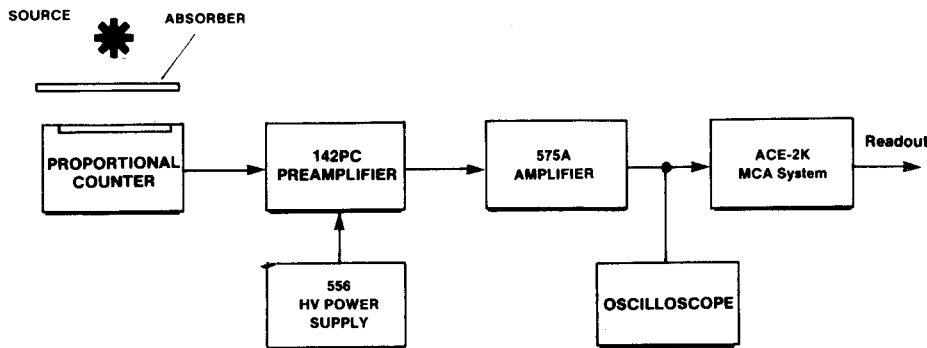


Fig. 11.4. Electronics Interconnections for Experiment 11.2.

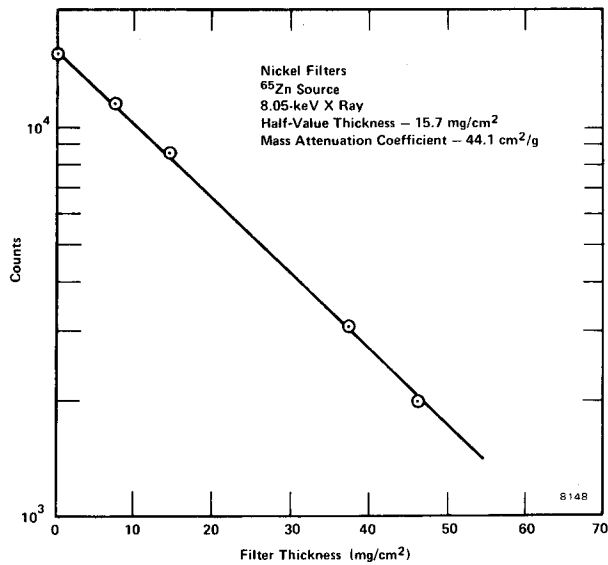


Fig. 11.6. Counts vs Nickel Absorber Thickness for ^{65}Zn X Rays.

References

1. G. F. Knolls, *Radiation Detection and Measurement*, John Wiley and Sons, New York (1979).
2. R. W. Hendriks, *Nucl. Instrum. Methods* **102**, 309 (1972).
3. M. W. Charles and B. A. Cooke, *Nucl. Instrum. Methods* **88**, 317 (1970).
4. R. Gott and M. W. Charles, *Nucl. Instrum. Methods* **72**, 157 (1969).
5. B. E. Fischer, *Nucl. Instrum. Methods* **141**, 173 (1977).
6. C. M. Lederer and V. S. Shirley, Eds., *Table of Isotopes*, 7th Edition, John Wiley and Sons, Inc., New York (1978).
7. C. E. Crouthamel, *Applied Gamma-Ray Spectrometry*, Pergamon, New York (1960).

X-Ray Fluorescence

EQUIPMENT NEEDED FROM EG&G ORTEC

Low-energy x-ray calibration sources SK-1X (Table 12.1)
 142PC Preamplifier
 Bin and Power Supply
 480 Pulser
 444 Gated Biased Amplifier
 572 Spectroscopy Amplifier
 556 High Voltage Power Supply
 Si(Li) X-Ray Detector System (SLP-06175); typical specifications, 6 mm diam, 175 eV resolution at 5.9 keV, 1-mil Be window
 459 5 kV Detector Bias Supply

ACE-2K MCA System including suitable IBM PC (other EG&G ORTEC MCAs may be used)
 Oscilloscope
⁵⁷Co excitation source with shield ≥ 5 mCi)
 904-1B Thin-Window Proportional Counter
 Target Kit M-12
 Absorber Kit 3-Z2
 ORC-12 Cable Set
 311 Chamber for X-Ray Fluorescence with a Si(Li) Detector
 312 Chamber for X-Ray Fluorescence with a Proportional Counter

Purpose

The characteristic x rays of several metallic samples will be excited by the x rays or gamma rays from a radioactive source, and a spectrum will be analyzed for each sample.

Introduction

X-ray fluorescence experiments are quite easy to perform. The technique of exciting characteristic x rays of elements has been known and used for many years. Figure 12.1 shows a typical arrangement of the detector and electronics for this experiment.

X rays from the excitation source are allowed to impinge on the sample, and these x rays make photoelectric interactions in the sample. The characteristic x rays that are then produced by the photoelectric interactions are counted by a low-energy x-ray detector. The detector in Fig. 12.1 is a proportional counter. As discussed in Experiment 8, the detector could be a high-resolution Si(Li) X-Ray Detector, which is the type used for Experiment 12.2.

Excitation Sources

The excitation sources to be used in this experiment should have activities of several millicuries, (mCi). Weaker sources can be used, but the counting times required for reasonable statistics are increased. Licenses are required before the sources can be obtained.

A general rule for the selection of an appropriate excitation source is that it should have a gamma, x ray, or Bremsstrahlung continuum slightly above the highest characteristic x ray that is to be excited. The reason is that the photoelectric cross section (Experiments 3 and 7) decreases rapidly as energy increases. The most commonly used sources for x-ray fluorescence measurements and their characteristic x-ray energies are: ⁵⁵Fe, <6 keV; ¹⁰⁹Cd, <9 keV; ⁵⁷Co, between 15 keV and 5 keV; and ²⁴¹Am, for a wide range from 60 keV down. Figure 12.2 shows the decay schemes for ⁵⁵Fe, ¹⁰⁹Cd, and ⁵⁷Co. The decay scheme for ²⁴¹Am was shown in Experiment 4.

Characteristic X Rays

The expected characteristic x rays that are excited by fluorescence are listed in refs. 1, 2, and 9. Unfortunately, not all references use the same nomenclature for binding energies and x-ray energies. (Ref. 2 is a list of binding energies given in the Appendix.) The list includes binding energies for the following energy levels: K, L_I, L_{II}, L_{III}, M_I, M_{II}, M_{III}, M_{IV}, M_V, N_I, N_{II}, . . . P_{III}. The most commonly observed x rays are the K _{α} and K _{β} lines, and these are calcu-

Table 12.1. Low-Energy (~1 μ Ci) X-Ray Calibration Sources

Isotope	X-Ray Energy (keV)	
⁵⁴ Mn	5.414	K _{α}
	5.946	K _{β}
⁵⁷ Co	6.40	K _{α}
	7.06	K _{β}
	14.41	γ
⁶⁵ Zn	8.04	K _{α}
	8.90	K _{β}
⁸⁵ Sr	13.38	K _{α}
	15.00	K _{β}
88Y	14.12	K _{α}
	15.85	K _{β}
¹⁰⁹ Cd	22.10	K _{α}
	25.00	K _{β}
¹¹³ Sn	24.14	K _{α}
	27.40	K _{β}
¹³⁷ Cs	32.1	K _{α}
	36.6	K _{β}

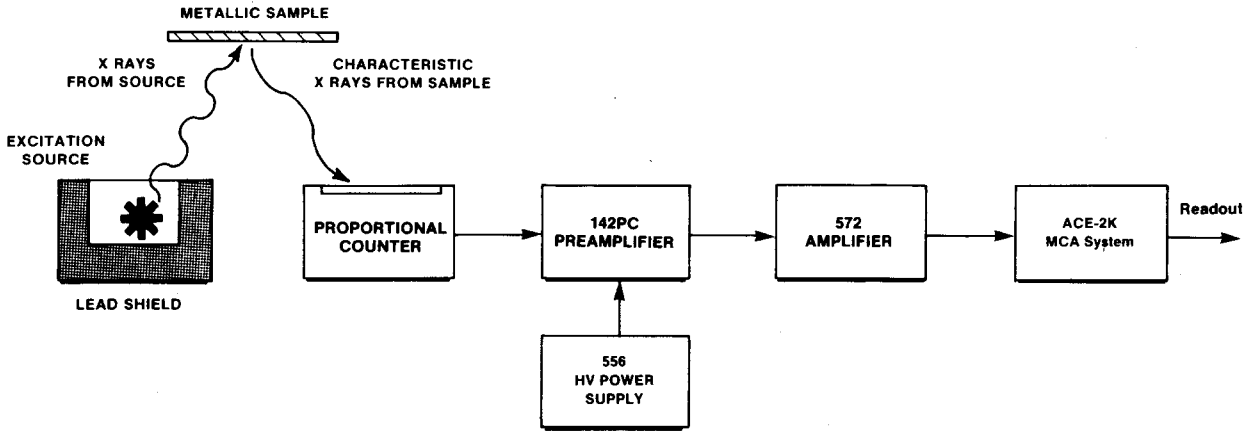


Fig. 12.1. Equipment Arrangement for Experiment 12.1.

lated from the binding energies, (BE), in the following manner:

$$K_{\alpha_1} \text{ (energy)} = BE(K) - BE(L_{III}), \quad (1)$$

where BE(K) is the binding energy of the K level, etc.,

$$K_{\beta_1} \text{ (energy)} = BE(K) - BE(M_{III}). \quad (2)$$

The method for calculating other characteristic x-ray energies is listed on page 570 of ref. 9.

EXPERIMENT 12.1 X-Ray Fluorescence with a Proportional Counter

Procedure

1. Set up the equipment shown in Fig. 12.1. Adjust the 556 to the high-voltage level required for the proportional counter. Calibrate the system as in Experiment 11 so that the 32.2-keV x ray from ^{137}Cs is being stored in the upper channels of the analyzer. Use as many sources from Table 12.1 as are necessary to establish the calibration for the system. Determine the slope of the calibration line and the resolution of the 32.2-keV line of ^{137}Cs .

2. Remove the calibration sources and place a cadmium sample and the ^{57}Co fluorescence source in position in the Model 312 Chamber. Accumulate a spectrum for a period of time sufficient to identify the characteristic x rays from the cadmium sample. Read the data out of the MCA and plot the spectrum. Figure 12.3 shows a typical cadmium spectrum using a krypton-filled proportional counter. In this device the krypton K_{α_1} at 12.651 keV can escape from the proportional counter before it makes a photoelectric interaction in the gas. The second pronounced peak in Fig. 12.3 is therefore the cadmium K_{α_1} minus the krypton K_{α_1} escape peak, etc.

Figure 12.4 shows the cadmium characteristic x rays measured with a xenon-filled proportional counter. The xenon K_{α_1} escape peak is not present in this spectrum because its energy is 29.78 keV and thus it is not energetically possible to produce this peak with the cadmium sample and the ^{57}Co source.

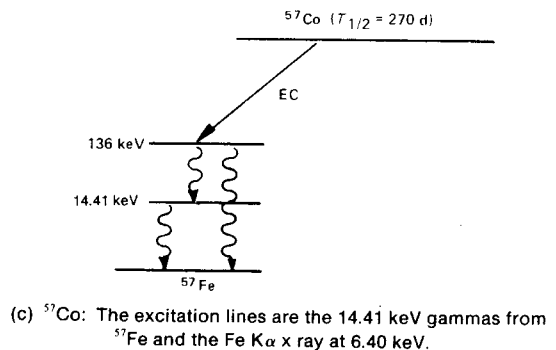
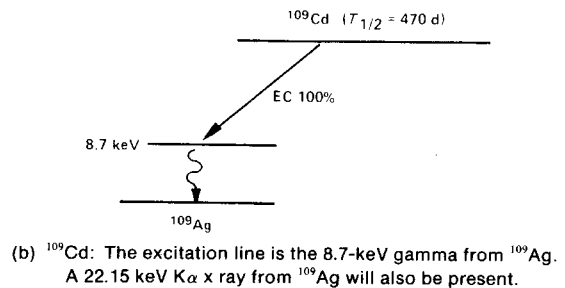
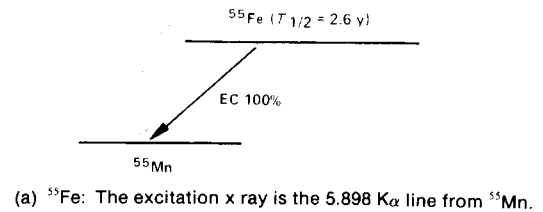


Fig. 12.2. Decay Schemes for Common X-Ray Fluorescence Excitation Sources.

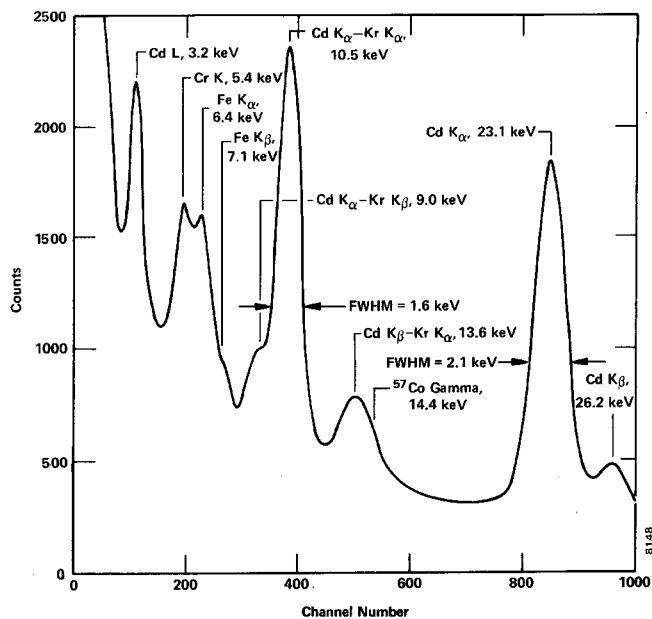


Fig. 12.3. Cadmium X-Ray Spectrum Obtained with a Krypton-Filled Proportional Counter.

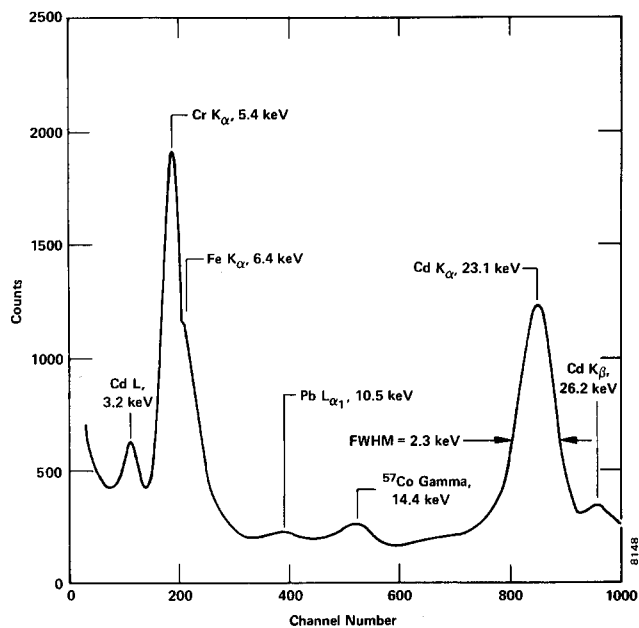


Fig. 12.4. Cadmium X-Ray Spectrum Obtained with a Xenon-Filled Proportional Counter.

3. Remove the cadmium and replace it with one of the other samples in Target Kit M-12. Accumulate a spectrum and read out the MCA. Identify the groups in the spectrum. Repeat for the other elements in the kit.

4. Place the composite sample from the target kit in the irradiation position. Accumulate a spectrum and identify all peaks. Figure 12.5 shows a composite spectrum that was taken for a clad-type U.S. quarter. This can be contrasted with Fig. 12.6 which shows one of the older type U.S. silver quarters.

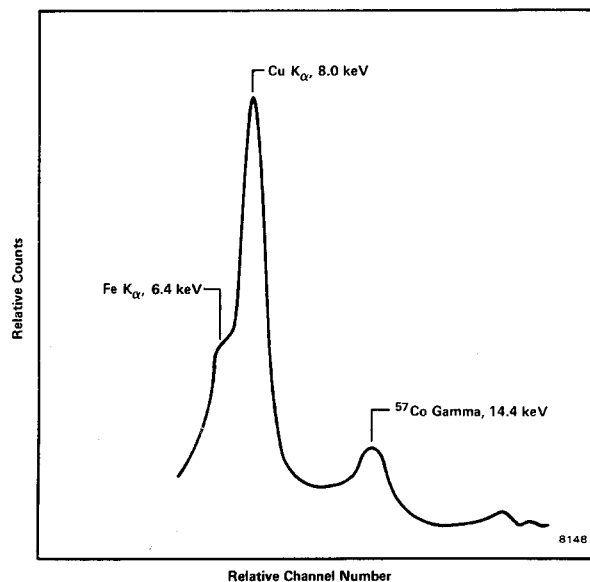


Fig. 12.5. X-Ray Spectrum for a Clad-Type U.S. Quarter.

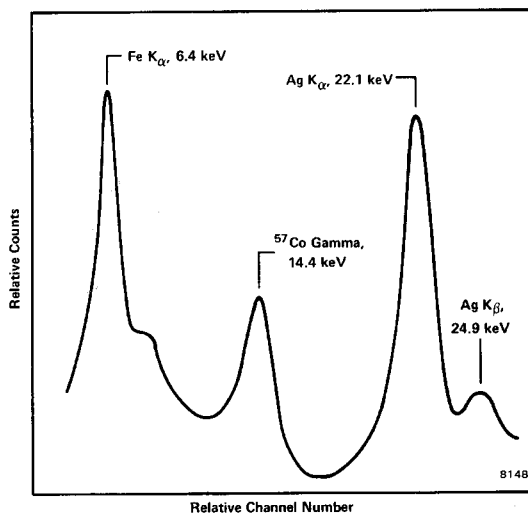


Fig. 12.6. X-Ray Spectrum for an Older U.S. Silver Quarter.

EXPERIMENT 12.2 X-Ray Fluorescence with a Si(Li) Detector

Introduction

Si(Li) x-ray detectors have been developed that will have a resolution of 150 eV for the 6.4-keV line of ⁵⁷Co, as discussed in Experiment 8. It is possible, with resolutions of this order, to distinguish between adjacent energy lines that can come from various metallic elements in a sample. In other words, if the K_α lines of the elements in the sample are resolvable from each other, the elemental constituents of the target can be determined.

Experiment 8 should be completed before this experiment is started.

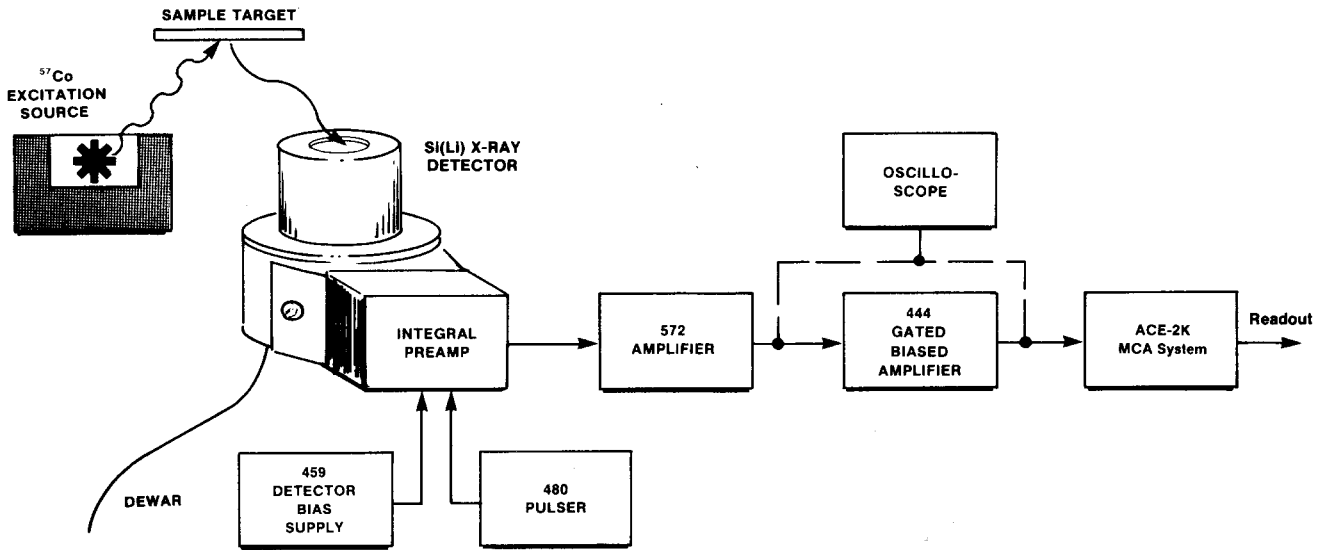


Fig. 12.7. Equipment Arrangement for Experiment 12.2.

Procedure

1. Set up the equipment as shown in Fig. 12.7. The Model 311 Chamber is used for this experiment. Use the pulse generator and any of the sources listed in Table 12.1 to calibrate the system from 2 keV to 25 keV, as outlined in Experiment 8. Plot the calibration line, determine the slope in eV/channel, and measure the resolution for the 6.4-keV line of ⁵⁷Co.
2. Use a piece of copper from the target kit as the first target and position it as shown in Fig. 12.7. Determine the energies of the Cu K_α and K_β lines from your calibration curve. Compare these with the calculated values for Cu shown in the Appendix.
3. Repeat for the other elements in Target Kit M-12. For comparison, Figs. 12.8, 12.9, and 12.10 show x rays from iron, copper, and molybdenum samples.

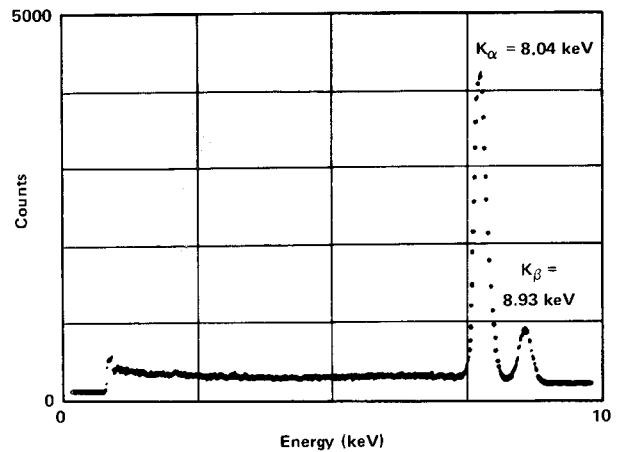


Fig. 12.9. Copper Fluorescence Spectrum.

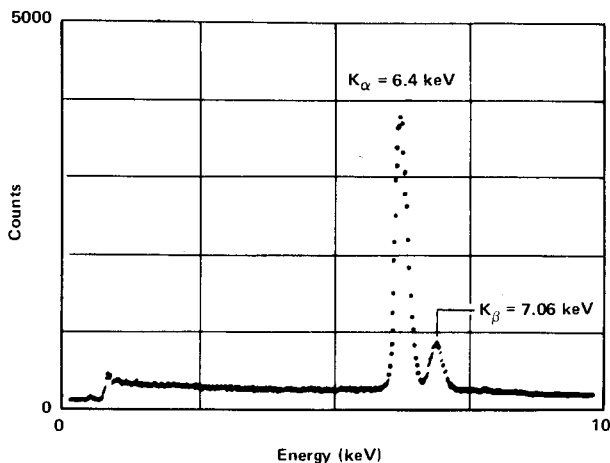


Fig. 12.8. Iron Fluorescence Spectrum.

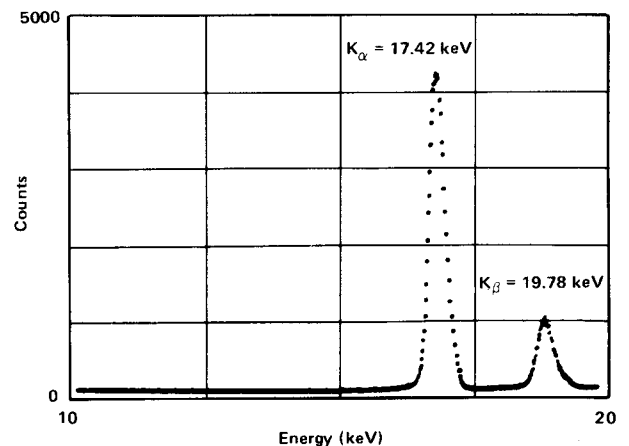


Fig. 12.10. Molybdenum Fluorescence Spectrum.

4. Place the composite sample from the target kit as the target. Determine the elements present in the sample by identifying each set of characteristic x rays. Figure 12.11 shows a spectrum for a composite metallic sample of Fe, Co, Ni, and Cu. Adjacent elements of the heavier metals can easily be identified by x-ray fluorescence as shown in Fig. 12.11. This technique is being widely accepted in industry as a method by which surface elemental analysis can be performed quickly.

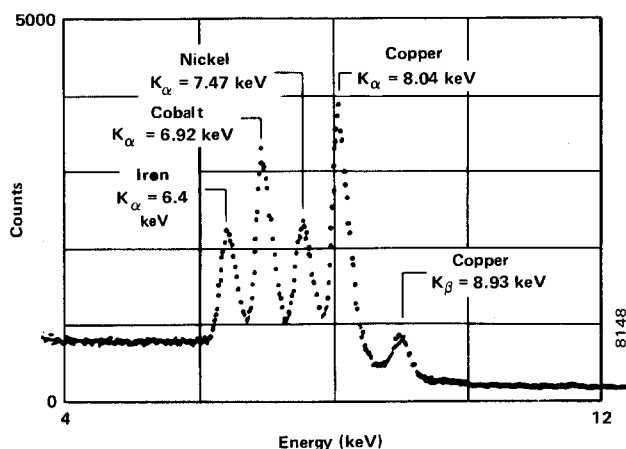


Fig. 12.11. Fluorescence Spectrum of Fe, Co, Ni, and Cu.

References

1. X-Ray Critical-Absorption and Emission Energies Chart, available from EG&G ORTEC (Slide Rule).
2. X-Ray Critical-Absorption and Emission Energies in keV (Appendix in this manual).
3. J. C. Russ, Coordinator, *Energy Dispersion X-Ray Analysis, X-Ray and Electron Probe Analysis*, available from ASTM Special Technical Publication 485, 1970, 04-485000-39 from American Society for Testing and Materials, Philadelphia, Pennsylvania.
4. R. D. Giaque and J. M. Jaklevic, "Rapid Quantitative Analysis by X-Ray Spectrometry," *Adv. in X-Ray Analysis* **15**, 266 Plenum Press, New York (1972).
5. J. M. Jaklevic and F. S. Goulding, "Semiconductor Detector X-Ray Fluorescence Spectrometry Applied to Environmental and Biological Analysis," *IEEE Trans. Nucl. Sci.* **NS-19** (1972).
6. J. S. Hansen, et al., "Accurate Efficiency Calibration and Properties of Semiconductor Detectors for Low Energy Photons," *Nucl. Instrum. Methods* **106**, 365 (1973).
7. 14th Scintillation and Semiconductor Counter Symposium, *IEEE Trans. Nucl. Sci.* **NS-22**(1) (1975).
8. J. L. Campbell and L. A. McNelles, "An Intercomparison of Efficiency Calibration Techniques for Semiconductor X-Ray Detectors," *Nucl. Instrum. Methods* **125**, 205-223 (1975).
9. C. M. Lederer and V. S. Shirley, Eds., *Table of Isotopes*, 7th Edition, John Wiley and Sons, Inc., New York (1978).

Gamma-Gamma Coincidence

EQUIPMENT NEEDED FROM EG&G ORTEC

Two 113 Scintillation Preamplifiers
 Two 266 Photomultiplier Tube Bases
 Two Bins and Power Supplies
 Two 551 Timing Single-Channel Analyzers
 426 Linear Gate
 567 Time-to-Amplitude Converter and SCA
 Two 556 High Voltage Power Supplies
 480 Pulser
 418A Universal Coincidence
 875 Counter
 Two 575A Amplifiers

427A Delay Amplifier

719 Timer

Two 905-3 NaI(Tl) 2- x 2-in. Scintillation Detectors
 and PM Tubes

ACE-2K MCA System including suitable IBM PC (other
 EG&G ORTEC MCAs may be used)

Oscilloscope

10- μ Ci ^{22}Na source

Source Kit SK-1G

306 Gamma-Gamma Angular Correlation Table with
 rotating detector and shields

ORC-13 Cable Set

Purpose

Two annihilation quanta are radiated from a ^{22}Na source in coincidence with each other for each radiation event that will be measured in this experiment. The purpose of the experiment is to verify that these quanta emanate from the source with an angular separation of 180° .

Introduction

Sodium-22 is an excellent source for a simple gamma-gamma coincidence experiment. The decay scheme for this isotope is shown in Fig. 13.1. From the decay scheme it can be seen that 99.95% of the time the decay occurs by positron emission and electron capture through the 1.274-MeV state of ^{22}Ne . Ninety percent of these decay events occur with positron emission, which then annihilate and produce a pair of 0.511-MeV gamma rays that can be seen in the gamma spectrum.

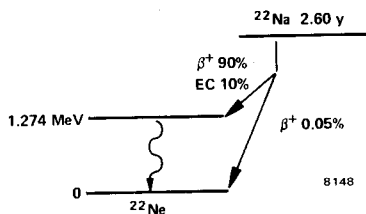


Fig. 13.1. Decay Scheme for ^{22}Na .

Figure 13.2 shows a typical gamma spectrum for ^{22}Na that was obtained with an NaI(Tl) detector. The 0.511-MeV peak will usually be quite a bit more intense than the 1.274-MeV peak, primarily because of the detector efficiency differences at the two energy levels (see Experiment 3) and the annihilation process.

Figure 13.3 shows a typical instrument configuration for measuring a gamma-gamma coincidence. The ^{22}Na source is usually covered with a thin absorber such as a thin piece of metal or plastic. Positrons from the source will lose energy in the absorber by dE/dx and will be annihilated in the ab-

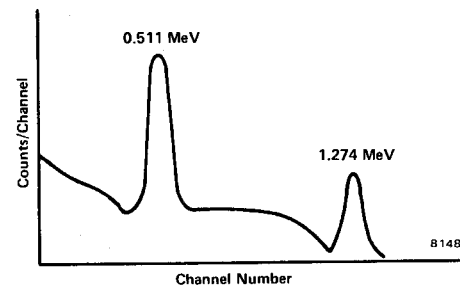


Fig. 13.2. NaI(Tl) Spectrum of ^{22}Na .

sorber. The NaI(Tl) detectors will see an approximate point source of radiation. When the positrons are annihilated, two 0.511-MeV gammas will leave the source with an angular separation of 180° .

Experimentally this pair of gamma rays is detected and measured with one detector that is fixed and another detector that can rotate about the source. Figure 13.4 shows some of the details of a rotating assembly that is used for the experiment.

The ^{22}Na coincidence experiment will use three different electronic system configurations. In the first, the events that enter the two detectors will have to produce pulses that overlap each other to indicate that a coincidence exists, and the counter will then count the number of coincidences that are sensed during its timed counting interval. In the second, a pulse from the movable detector will enable the gate of the 426 Linear Gate, and any corresponding pulse from the fixed detector that arrives within the adjusted gate width interval will be considered coincident and will be counted in the counter. In the third setup, the 567 Time-to-Amplitude Converter, (TAC), and SCA will be used to measure the variations in time at which the coincident events are sensed by the two detectors; a counter can count all of the coincidences that occur within about a 500-ns range, and then an MCA can be used to obtain a spectrum of the precise timing variations.

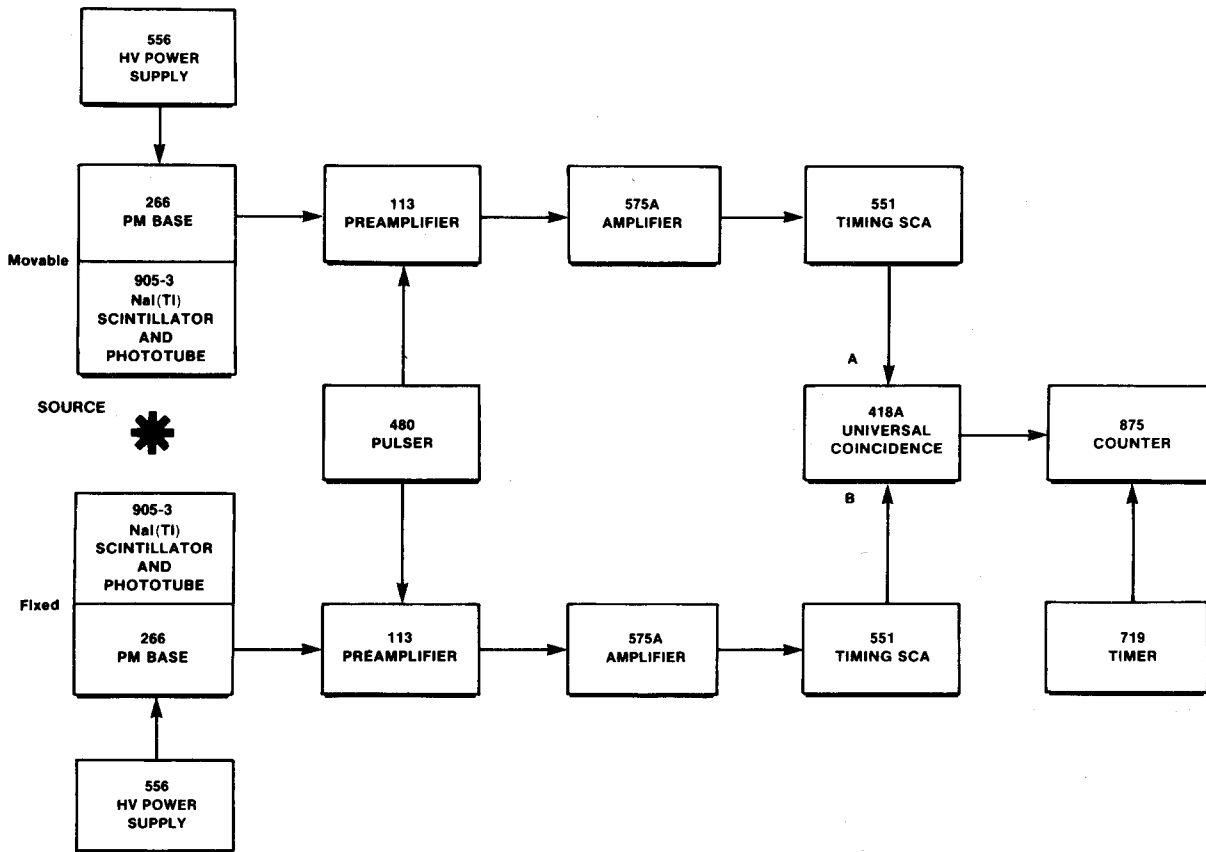


Fig. 13.3. Electronics for Experiment 13.1.

The student should complete Experiment 9 before starting this experiment and should be somewhat familiar with the principles of coincidence measurements.

EXPERIMENT 13.1

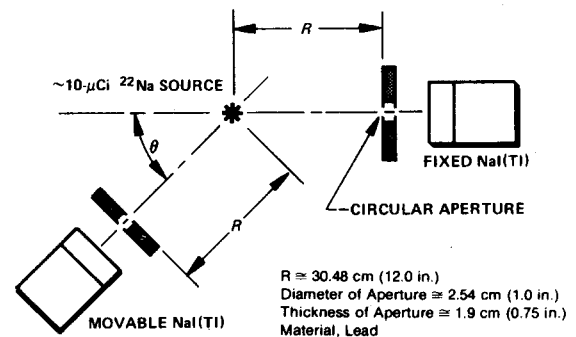
Overlap Coincidence Method for Measuring Gamma-Gamma Coincidence of ²²Na

Procedure

1. Set up the electronics as shown in Fig. 13.3. Use Fig. 13.4 as a guide to arranging the two detectors.
2. Set the 575A Amplifiers for negative input and unipolar output. Adjust the gain of both amplifiers so that the 1.274-MeV line of ²²Na results in ~6 V pulses at the outputs.
3. Set the 551 Timing SCAs for Integral mode. Set the Delay controls at minimum and the Lower-Level dials at 40/1000. Use the SCA outputs.
4. Connect the SCA Out from one of the 551 Timing SCAs to the A input of the 418A and connect the output from the other 551 to the B input of the 418A. Set the 418A Coincidence Requirements switch at 2 and the Resolving Time at

maximum (2 μs). Set the A and B toggle switches at Coinc and set the C, D, and E toggle switches at Off. With the source removed and the 480 Pulser turned on, the 418A output will indicate coincidence for the two signal paths. Turn off the 480 and return the source.

5. Set the 719 Timer for a long timing period, such as 8 min, and permit the 875 Counter to operate while the movable detector is rotated slowly to both sides of 0°. The counting rate should be maximum at θ = 0°.



8148

Fig. 13.4. Mechanical Arrangement of Detectors on EG&G ORTEC 306 Angular Correlation Table.

6. Set the timer for a long enough accumulation period to provide reasonable statistics at the points of interest and fill in the values in Table 13.1.

EXERCISE

Plot the data in Table 13.1 on linear graph paper. For each counting rate, (N), the statistical variation $\pm\sqrt{N}$ should be included on the graph. Figure 13.5 shows a typical set of data for this experiment.

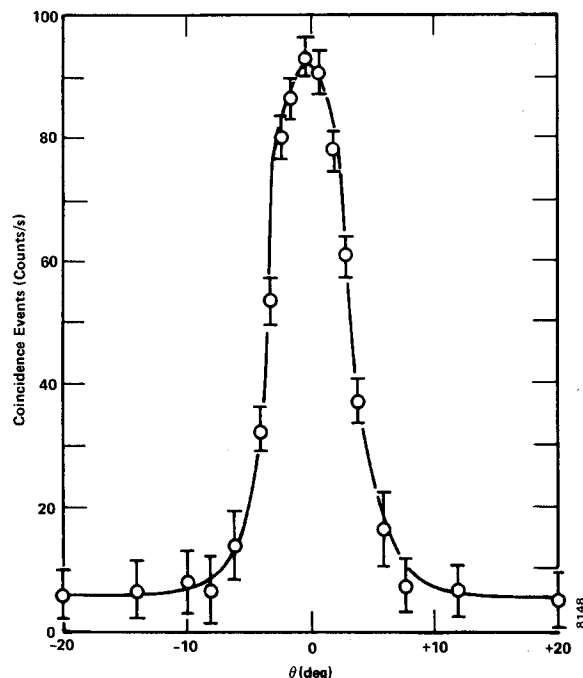


Fig. 13.5. Coincidence Data.

EXPERIMENT 13.2

Linear Gate Method for Measuring Gamma-Gamma Coincidence of ^{22}Na

Procedure

1. Set up the electronics as shown in Fig. 13.6. Use the same mechanical detector placement as in Experiment 13.1.
2. Using the ^{22}Na source, adjust the gain of each 575A Amplifier for an output of ~ 6 V for the 1.274-MeV gamma line.
3. Remove the source. Turn on the pulse generator and adjust the Pulse-Height dial, the Cal control, and the attenu-

Table 13.1

θ (deg) Positive	Counts/s	θ (deg) Negative	Counts/s
0		0	
1		1	
2		2	
3		3	
4		4	
5		5	
6		6	
7		7	
8		8	
10		10	
14		14	
20		20	
25		25	

ators so that the amplifier output pulses are the same as in step 2.

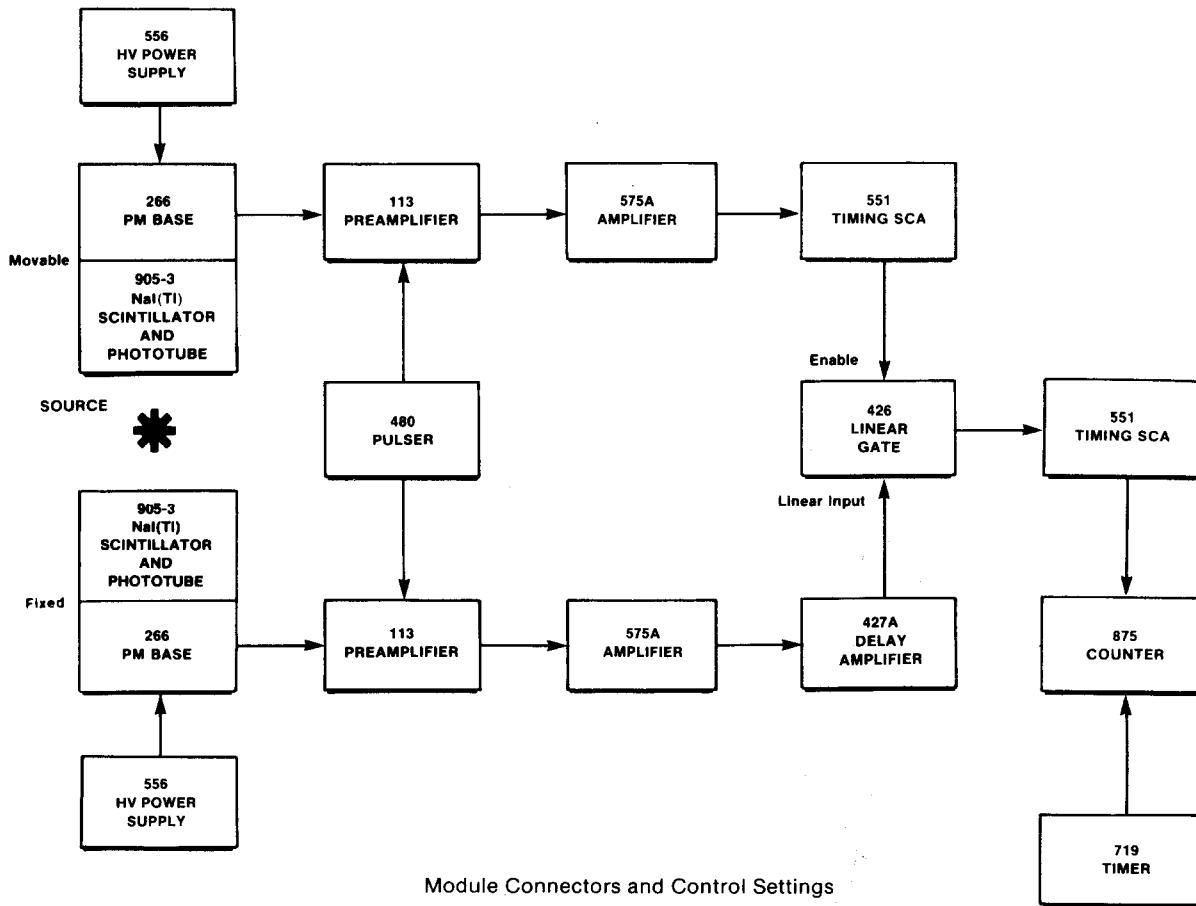
4. Look at the output of the 426 Linear Gate with the oscilloscope. If the timing is correct, a unipolar pulse should be observed whose amplitude is proportional to the pulse-height dial setting on the 480. Vary the pulse height and see that there is a linear response. If no output pulses are seen from the 426, adjust the Delay time of the 551 on the movable detector side and recheck the Gate Width control on the 426 until output pulses are seen normally.

5. Turn off the pulser and return the ^{22}Na source to its proper position as shown in Fig. 13.4. Measure the angular distribution of pulse rates from the system as in Experiment 13.1, using the angles in Table 13.1.

6. (Alternate) The output of the Linear Gate can be fed into an MCA. The spectrum should resemble Fig. 13.2 except that the 1.274-MeV peak will not be present. The coincidence requirement has virtually eliminated this peak from the spectrum.

EXERCISE

Plot the data on linear graph paper as in Experiment 13.1. Compare the count rates at $\theta = 0^\circ$.



Module Connectors and Control Settings

575A Amplifiers: Negative Input, Bipolar Output.
 551 Timing Single-Channel Analyzer on movable detector side: Lower Level = 40/1000, Integral mode, SCA Output, Delay minimum.
 551 Timing Single-Channel Analyzer following the Linear Gate: same settings.
 426 Linear Gate: Normal mode, Gate Width maximum (4 μ s).
 480 Pulser: Attenuated output, negative polarity, power switch Off.
 875 Counter: Input from the 551, Gate from the 719 Interval Out.

Fig. 13.6. Arrangement of Electronics for Experiment 13.2.

EXPERIMENT 13.3

Time-to-Amplitude Converter Method for Measuring Gamma-Gamma Coincidence of ²²Na

Procedure

1. Set up the electronics as shown in Fig. 13.7. Use the same mechanical detector placement as in Experiment 13.1.
2. Using the ²²Na source, adjust the gain of each 575A Amplifier for an output of ~6 V for the 1.274-MeV gamma line.
3. Remove the source. Turn on the pulser and adjust the Pulse-Height dial, the Cal control, and the attenuators so that the amplifier output pulses are the same as in step 2.
4. Observe the output pulses of the 567 with the oscilloscope. They should be ~6 V in amplitude. Change the delay on either 551 SCA while observing these output pulses (they can also be observed with the MCA).

5. Determine a delay vs pulse-height curve for the 567 TAC. This procedure is outlined in Experiment 9.2.

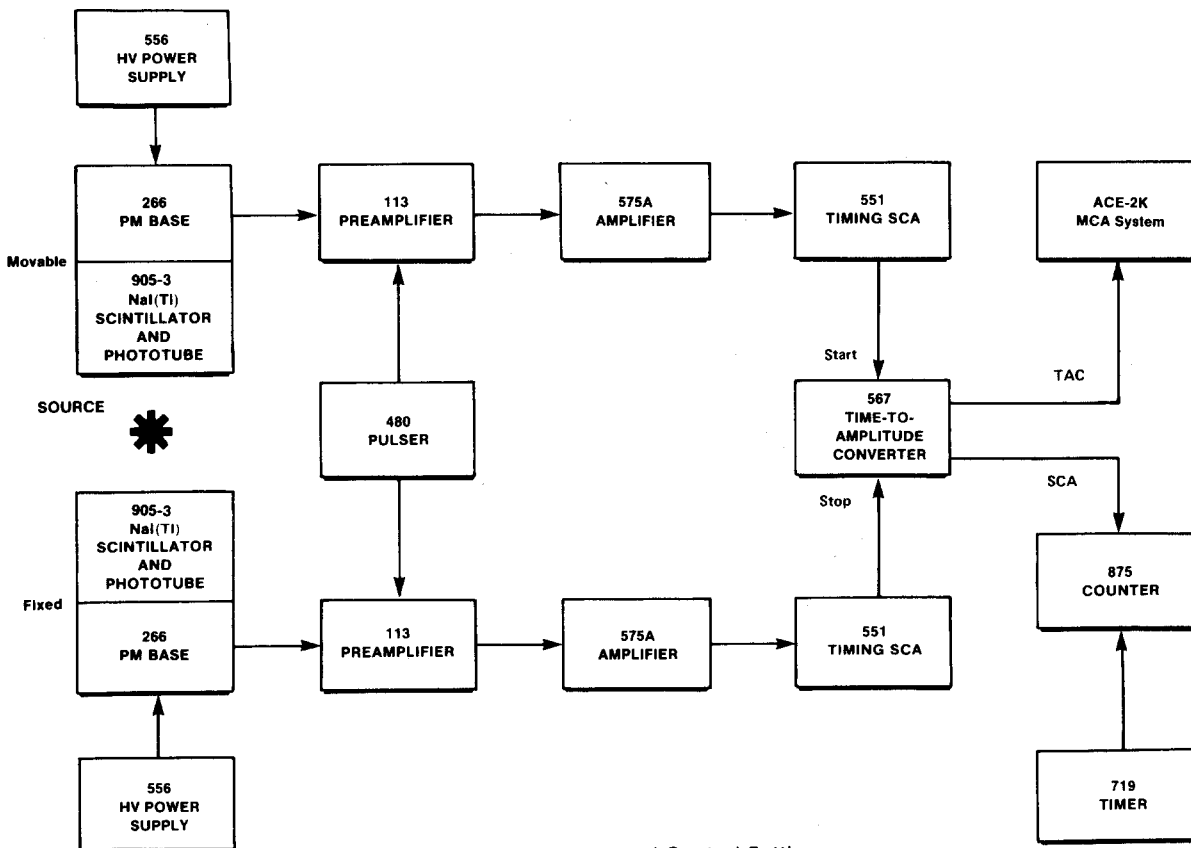
EXERCISE

- a. Determine the time resolution of the pulses from the 480 Pulser.

6. Turn off the pulser when the delays of the 551 SCAs are set for a 5- to 6-V output from the 567. Return the ²²Na source to its proper position as shown in Fig. 13.4. Measure the angular distribution of pulse rates from the system using the FWTM levels of the time spectrum and integrating the counts in the channels between these levels.

EXERCISES

- b. Plot your data on linear graph paper as in Experiment 13.1. Compare the count rates at $\theta = 0^\circ$.
- c. Determine the time resolution for the coincidence measurements from the MCA readout.



Module Connectors and Control Settings

575A Amplifiers: Negative Input, Bipolar Output.

551 Timing Single-Channel Analyzer on movable detector side: Integral mode, Lower Level = 40/1000,

Delay = 0.1 μ s, Neg Out to Start Input on 567.

551 Timing Single-Channel Analyzer on fixed detector side: Integral mode; Lower Level = 40/1000, Delay = 5 μ s,

Neg Out to Stop Input on 567.

567 TAC and SCA: Range 400 ns, TAC Out to MCA, SCA Out to 875.

480 Pulser: Attenuated output, negative polarity, power switch Off.

Fig. 13.7. Arrangement of Electronics for Experiment 13.3.

References

1. A. C. Melissinos, *Experiments in Modern Physics*, Academic Press, New York (1966).
2. H. A. Enge, *Introduction to Nuclear Physics*, Addison-Wesley (1966).
3. K. Seigbahn, *Alpha, Beta, and Gamma Spectroscopy*, North Holland Publishing Co., Amsterdam.
4. L. C. Biedenharn and M. E. Rose, *Rev. Mod. Phys.* **25**, 729 (1953).
5. R. D. Evans, *The Atomic Nucleus*, McGraw-Hill, New York (1955).
6. B. L. Cohen, *Concepts of Nuclear Physics*, McGraw-Hill, New York (1971).
7. C. E. Crouthamel, *Applied Gamma-Ray Spectrometry*, Pergamon, New York (1960).
8. C. M. Lederer and V. S. Shirley, Eds., *Table of Isotopes*, 7th Edition, John Wiley and Sons, Inc., New York (1978).
9. P. Quittner, *Gamma Ray Spectroscopy*, Halsted Press, New York (1972).
10. W. Mann and S. Garfinkel, *Radioactivity and Its Measurement*, Van Nostrand-Reinhold, New York (1966).

Nuclear Lifetimes and the Coincidence Method

EQUIPMENT NEEDED FROM EG&G ORTEC

- Two 113 Scintillation Preamplifiers
- Two 266 Photomultiplier Tube Bases
- Two Bins and Power Supplies
- 418A Universal Coincidence
- Two 551 Timing Single-Channel Analyzers
- 567 Time-to-Amplitude Converter and SCA
- Two 556 High Voltage Power Supplies
- 480 Pulser
- 875 Counter
- Two 575A Amplifiers
- 719 Timer

- 905-3 NaI(Tl) 2- by 2-in. Detector and PM tube
- ACE-2K MCA System including suitable IBM PC (other EG&G ORTEC MCAs may be used)

- Oscilloscope
- 20- μ Ci ^{57}Co source
- Source Kit SK-1G
- 905-1B Thin Window NaI(Tl) Detector with PM Tube
- ORC-14 Cable Set

OPTIONAL EQUIPMENT FOR EXPERIMENT 14.3

- GEM-10195 Coaxial Detector System
- SLP-06175 Si(Li) X-Ray Detector System

Purpose

This experiment will use the coincidence method of timing identification to measure the mean lifetime in the decay scheme of ^{57}Co .

Introduction

The measurement of the lifetimes of excited nuclear states constitutes an important experimental technique in nuclear physics. Many nuclear states remain excited for mean lifetimes that are measured easily with the techniques outlined in Experiment 9. The lifetime of a nuclear state is related to its width, (energy), by the uncertainty principle:

$$\Delta E \Delta t = \hbar, \tag{1}$$

where

- ΔE = uncertainty in energy associated with a state,
- Δt = uncertainty in time associated with the state,
- $\hbar = 1.054 \times 10^{-34}$ joules-s.

In general, for nuclear lifetimes, Eq. (1) becomes

$$\tau = \frac{\hbar}{\Gamma}, \tag{2}$$

where τ = mean life of a level of width Γ .

In this experiment several techniques are outlined for measuring the lifetime of the first excited state of ^{57}Fe . The accepted value for this lifetime is 98 ns, which is well within the measuring capabilities of the coincidence techniques discussed in Experiment 9.

The decay scheme for ^{57}Co is shown in Fig. 14.1. The decay of this isotope is essentially all by electron capture, (EC), to the 136-keV level of ^{57}Fe . Figure 14.2 shows a high-resolution x-ray spectrum of ^{57}Co , in which the K_{α_1} and K_{β_1} x rays resulting from the electron capture are shown. The decay of the 136-keV level of ^{57}Fe can occur by one of two principal modes: by a 136-keV gamma directly to the ground state or

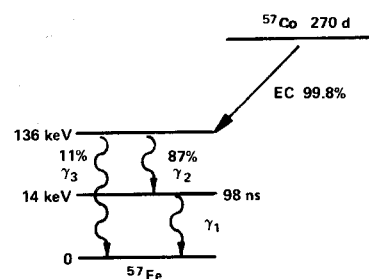


Fig. 14.1. Decay Scheme of ^{57}Co .

by branching through the 14-keV level to ground state. The 136-keV gamma, (γ_3), branch occurs 11% of the time. The 122-keV gamma, (γ_2), is 87% abundant. The 14-keV level, (γ_1), de-excites most of the time by internal conversion. The ratio of internal conversion to gamma decay, (e/γ), for this level is ~ 9.0 . The 14-keV gamma is also shown in Fig. 14.2. Figure 14.3 shows a high-resolution gamma spectrum of a ^{57}Co source. The lifetime of the 14-keV state can be measured by determining the time distribution of coincidence events between γ_2 and γ_1 .

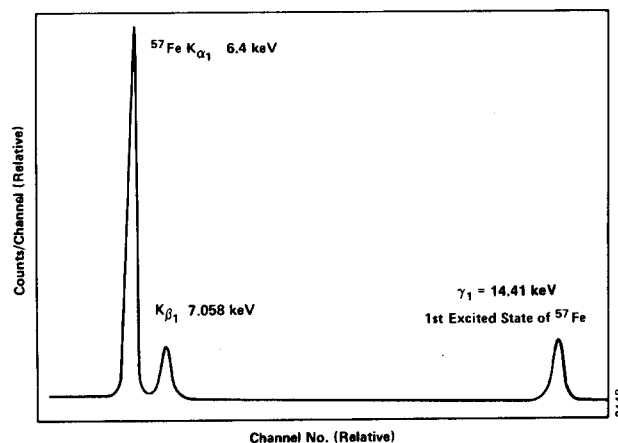


Fig. 14.2. Low-Energy Photon Spectrum from ^{57}Co .

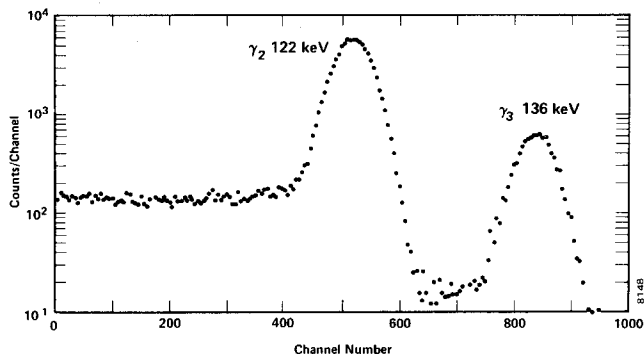


Fig. 14.3. High-Resolution Gamma Spectrum for ⁵⁷Co.

Experimentally the best way to do this delayed coincidence experiment is with a time-to-amplitude converter (TAC). In Experiment 9 the TAC was used to indicate pairs of coincident pulses and to measure the variation in their relative times of occurrence. In Experiment 14.1, γ_2 will be used to start a time measurement, and γ_1 will be used to stop the measurement. The output of the TAC will then provide a time distribution of the lifetime of the first excited state of ⁵⁷Fe, calibrated with known delays as in Experiment 9. In Experiment 14.2 the same information is obtained by measuring the γ_1 and γ_2 coincidence event rate with a fast coincidence circuit as a function of the delay in the γ_1 side of the circuit.

These techniques are repeated in Experiment 14.3 using detectors with different spectral response characteristics.

EXPERIMENT 14.1

Lifetime Measurement of the 14-keV State in ⁵⁷Fe Using the Time-to-Amplitude Converter Method

Procedure

1. Set up the electronics as shown in Fig. 14.4. The 905-3 NaI(Tl) detector will be used to detect the γ_2 events at 122 keV and to start a time measurement for each sensed event. The other NaI(Tl) detector, the one with the thin window, will be used to detect the γ_1 events at 14.41 keV and to stop the time measurements. Adjust each 556 High Voltage Power Supply to the voltage that is recommended for its detector.
2. Adjust the gain of the 575A Amplifier in the Start circuit in Fig. 14.4 so that the output pulses for the 122-keV gammas from ⁵⁷Co are ~5 V in amplitude. Use the bipolar output of the 575A to connect to the 551 Timing SCA in the Start circuit. For reference, Fig. 14.5 shows a typical spectrum of ⁵⁷Co as it will appear at the output of this amplifier. Note that the 122-keV and 136-keV lines are not resolved in the spectrum

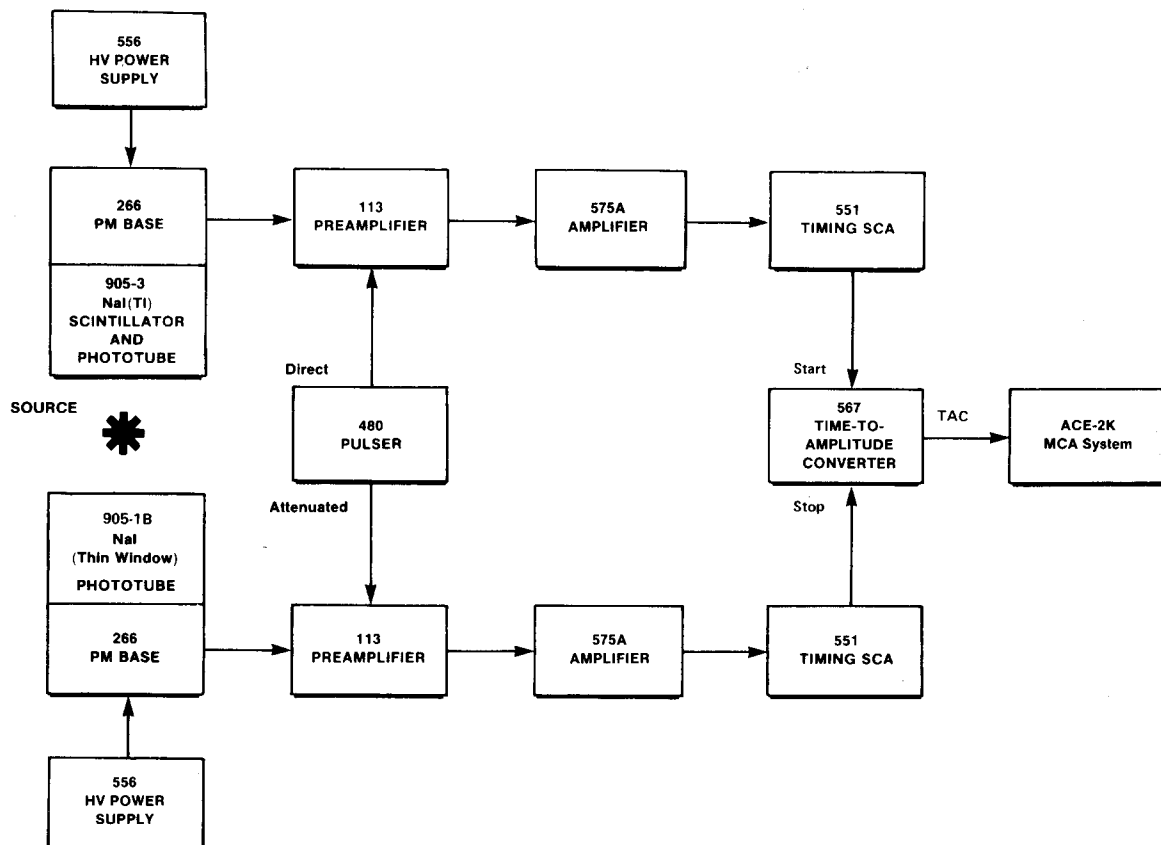


Fig. 14.4. Electronics for Lifetime Measurement with TAC.

taken with the NaL(Tl) detector as they were when taken with an HPGe detector (Fig. 14.3).

3. Set the 551 in the 2- x 2-in. NaI channel for a 400-ns delay (0.4 μ s). Adjust the Lower-Level control so that the lower-level threshold lies somewhere in the valley between the photopeaks and the Compton edge (in Fig. 14.5, this is about channel 50). Set the Upper-Level control fully clockwise and select the Normal mode. Connect the fast negative output to the Start input of the 567.
4. Adjust the gain of the 575A Amplifier in the Stop circuit in Fig. 14.4 so that the output pulses for the 14.41-keV gammas from ^{57}Co are ~ 5 V in amplitude. Use the bipolar output of the amplifier to connect to the 551 Timing SCA in the Stop circuit. For reference, Fig. 14.6 shows a typical spectrum of the 14.41-keV gammas from a thin-window NaL(Tl) detector. The ^{57}Fe $K\alpha_1$ and $K\beta_1$ x rays that are shown in Fig. 14.2 do not appear in Fig. 14.6. It is also interesting to note that the resolution of the spectrum obtained with the Si(Li) system is 16 times better than that of the same spectrum taken with the thin-window NaL(Tl).
5. Set the 551 in the thin-window NaI channel for minimum delay (100 ns). Adjust the Lower-Level dial so that the lower-level threshold corresponds to the valley in the pulse height spectrum (about channel 20 in Fig. 14.6). Set the Upper-Level control fully clockwise and select the Normal mode of

operation. Connect the fast negative output to the Stop input of the 567 TAC.

6. Set the 567 for its 400-ns range and Anticoincidence mode. Connect its output to the MCA.
7. Remove the ^{57}Co source and turn on the 480 Pulser. Set one X10 attenuator switch On and the other attenuator switches Off. Adjust the Pulse-Height dial and the Cal control as necessary to obtain an approximate 7-V amplitude out of the amplifiers (both amplifiers should have similar output levels ± 1 V). Both of the 551 Timing SCAs should now be counting the pulses from the 480, and thus should generate a time measurement with the 567. These time measurements should be ~ 200 ns, the difference in delays in the two circuits.
8. Feed the 567 TAC output to the MCA and accumulate for a period of time long enough to determine the position of the peak. Increase the delay on the 551 in the Stop channel to 600 ns and determine the new peak location on the MCA. Repeat for delays of 700, 800, 850, and 875 ns.

EXERCISE

Plot a curve of delay vs channel number for your data and determine the calibration in nanoseconds per channel. This technique was outlined in Experiment 9 (Fig. 9.9).

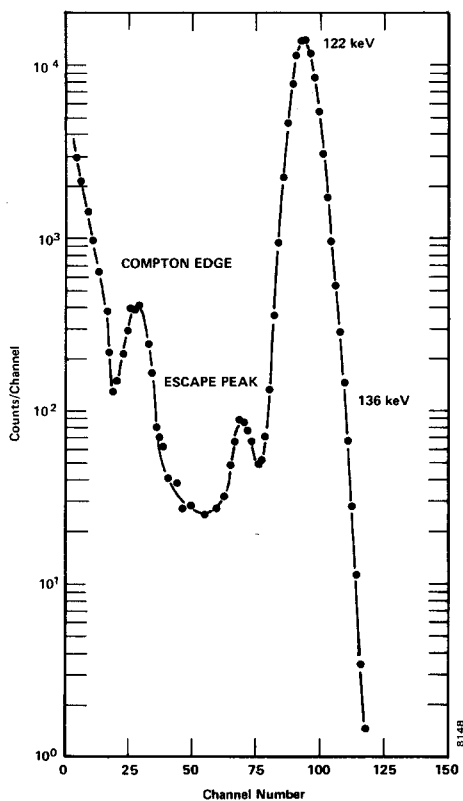


Fig. 14.5. Spectrum of ^{57}Co Taken with 2- by 2-in. NaI(Tl) Detector.

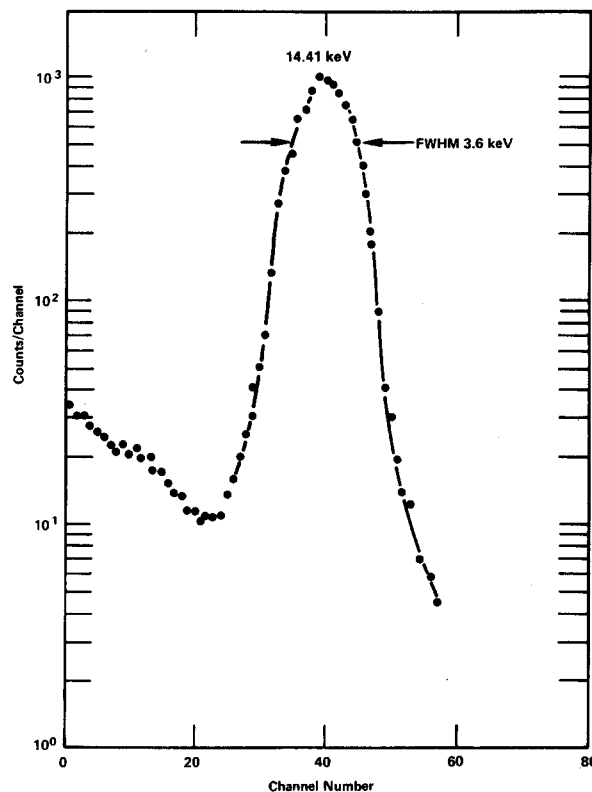


Fig. 14.6. Spectrum of 14.41-keV Gamma from ^{57}Co Taken with Thin-Window NaI(Tl) Detector.

9. Turn off the pulse generator and return the ^{57}Co source to its position as shown in Fig. 14.4. Return the delay on the 551 to 500 ns and accumulate a spectrum in the MCA. Figure 14.7 shows the results of a typical measurement that was made for this experiment. In order to smooth out the distribution, groups of ten channels were averaged and plotted. The slope of the delay vs channel number for Fig. 14.7 was 0.73 ns/channel. The lifetime of the state is therefore the product of the number of channels for half intensity times the 0.73 ns/channel. For the data in Fig. 14.7 this product is ~ 95

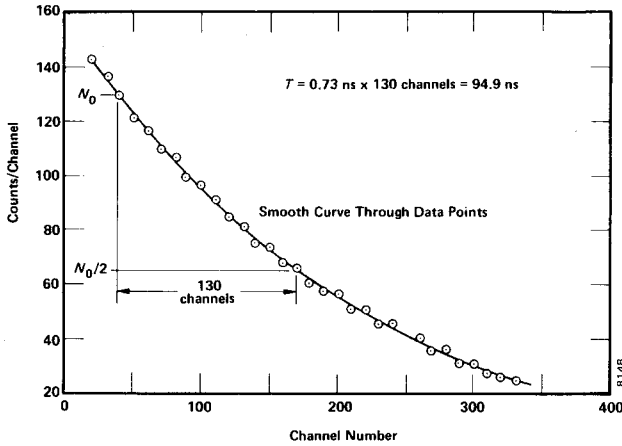


Fig. 14.7. Mean Lifetime Calculation.

ns, which is quite close to the accepted value of 98 ns. The data in Fig. 14.7 required a 2-h run. The electronic setup and time calibration also required ~ 2 h. Therefore the whole experiment should require a 4-h laboratory period.

EXPERIMENT 14.2

Lifetime Measurement of the 14-keV State in ^{57}Fe Using the Delayed Coincidence Method

This experiment is identical to Experiment 14.1 except for the instrument that is used to measure the lifetime. Where the TAC and MCA were used to make the measurements in the previous experiment, a fast coincidence circuit with controllable resolving time and a counter and a timer will be used in this experiment.

Procedure

1. Set up the electronics as shown in Fig. 14.8. Adjust the amplifier gains the same as in Experiment 14.1. Adjust the Lower-Level dials of both 551 Timing SCAs the same as in Experiment 14.1, with both the Upper-Level dials at 10 V.
2. Set the delay for the 551 in the A channel in Fig. 14.8 at 500 ns. Use its Pos Out for interconnection to the A Input on the 418A.

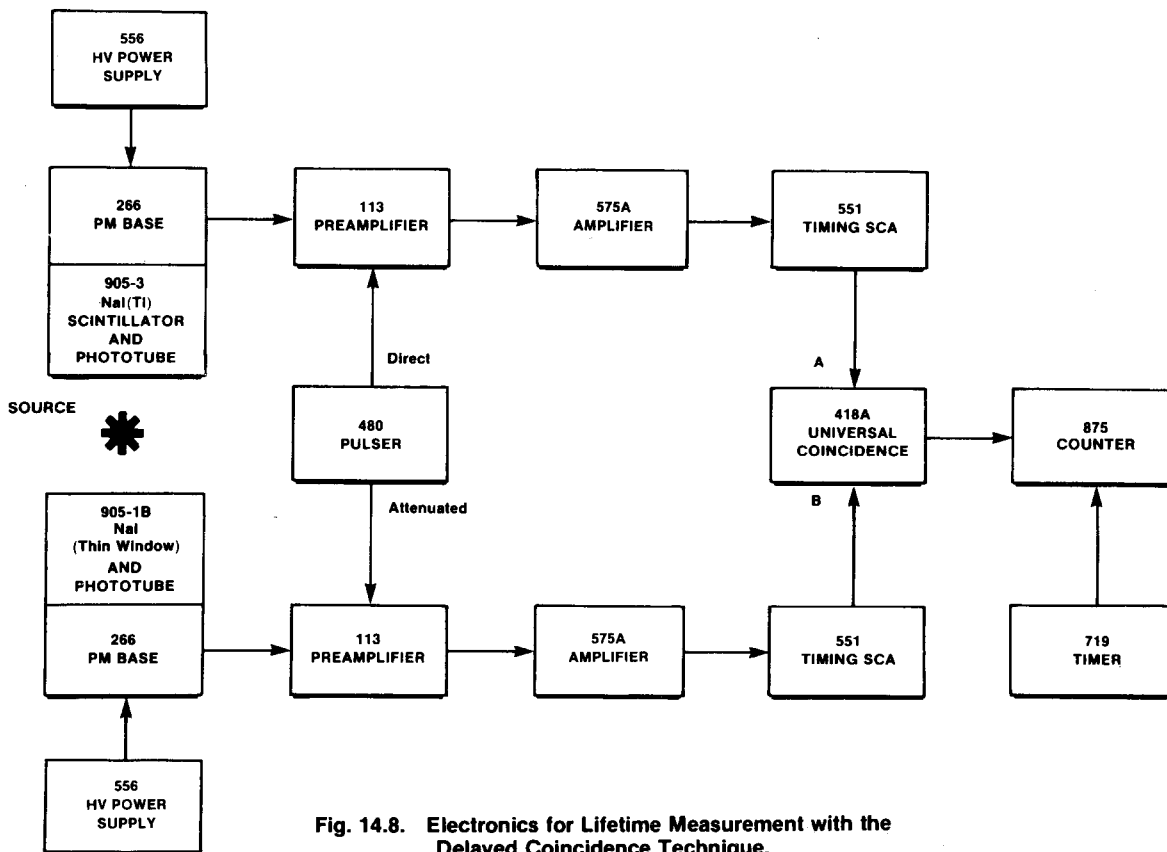


Fig. 14.8. Electronics for Lifetime Measurement with the Delayed Coincidence Technique.

- Set the delay for the 551 in the B channel in Fig. 14.8 at 500 ns. Use its Pos Out for interconnection to the B Input on the 418A.
- On the 418A, set the A and B switches at Coinc and the C, D, and E switches at Off. Set the Resolving Time of the 418A at maximum ($2 \mu\text{s}$). Select 2 for Coincidence Requirements.
- Remove the ^{57}Co source and turn on the 480 Pulser. Set the attenuation for X10 as in Experiment 14.1. Adjust the Pulse-Height and Cal controls as necessary to obtain an $\sim 7\text{-V}$ amplitude output for both amplifiers. Turn on the 875 Counter and observe the counting rate.
- Narrow the resolving time of the 418A to $1 \mu\text{s}$ and adjust the delay of the 551 in the B channel for a maximum counting rate. Since the delay in both circuits is about the same, this should not require much readjustment to obtain a maximum counting rate. Reduce the resolving time of the 418A to 100 ns and again maximize the counting rate with the delay on the same 551. The system is now set for 100-ns coincidence.
- Turn off the 480 Pulser and replace the ^{57}Co source in its operating position. Count for a time period, controlled by the 719 Timer, long enough to obtain reasonable statistics on the 875 Counter. Record the counting rate.
- Increase the delay in the 551 in the B channel by 20 ns and repeat the measurement. Continue for delay increases by 40, 60, 80, 100, 120, 140, 160, and 180 ns.

EXERCISE

Plot the counting rate as a function of delay change. The curve should be similar to that in Fig. 14.7. From these data determine the mean lifetime of the 14-keV state of ^{57}Fe as in Experiment 14.1.

EXPERIMENT 14.3

Alternate Detectors to be Used with the Electronics in Experiments 14.1 and 14.2

Purpose

In Experiments 14.1 and 14.2 the lifetime coincidence requirement was made between two NaI(Tl) detectors. The purpose of this experiment is to point out some other detectors that would be suitable for the measurements. The rest of the electronics can be exactly the same as those indicated in Experiments 14.1 and 14.2.

The Start Side (the 122-keV Gamma)

An HPGe detector could be used for the 122-keV gamma. Figure 14.3 shows a typical output spectrum for a germanium detector. For this measurement an SCA could be set to span the 122-keV peak. Other points with regard to HPGe

detectors are covered in Experiment 7. Additional information with regard to time measurements and germanium detectors can be obtained from EG&G ORTEC. Write for EG&G ORTEC's technical publication AN-42, *Principles and Applications of Timing Spectroscopy*.

An organic scintillator such as KL-236, NE-102, or Pilot B could be used to detect the 122-keV gammas. Figure 14.9 shows a spectrum of ^{57}Co obtained with an organic scintillator.

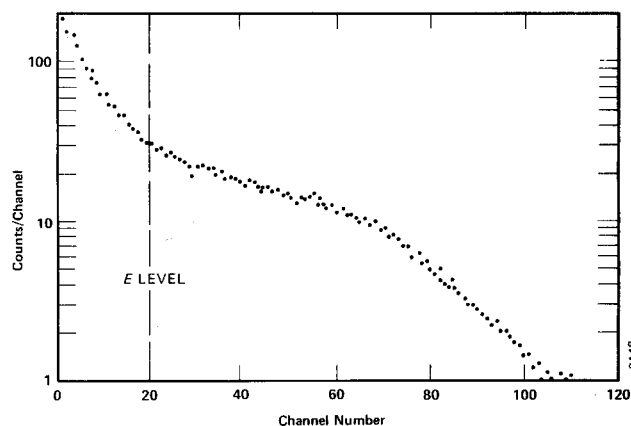


Fig. 14.9. Spectrum of ^{57}Co Obtained with an Organic Scintillator.

The organic scintillator has the advantage of being considerably faster than NaI(Tl) and hence better time resolution can be obtained. Figure 14.10 shows a typical output pulse from an EG&G ORTEC Timing Photomultiplier system and an organic detector.

The Stop Side (the 14-keV Gamma)

A Si(Li) detector could be used for the stop pulse. Figure 14.2 shows an output pulse-height spectrum for ^{57}Co that was taken with one of these high-resolution devices. These detectors also have good timing characteristics. Other features of these detectors are discussed in Experiment 8.

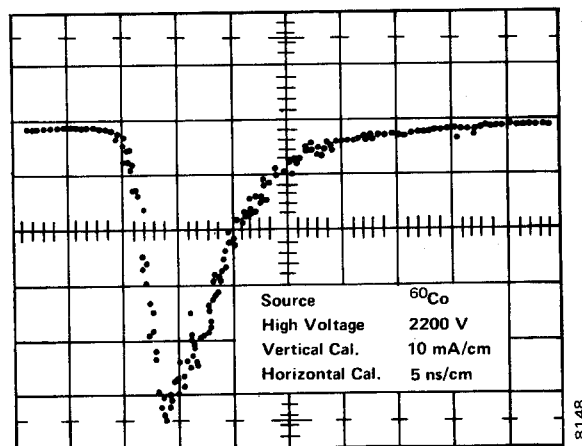


Fig. 14.10. Anode Output Pulse with EG&G ORTEC's 266 Photomultiplier Base and 905-5 Scintillation Detector.

References

1. K. Siegbahn, *Alpha, Beta, and Gamma Spectroscopy*, North Holland Publishing Co., Amsterdam.
2. R. D. Evans, *The Atomic Nucleus*, McGraw-Hill, New York (1955).
3. B. L. Cohen, *Concepts of Nuclear Physics*, McGraw-Hill, New York (1971).
4. H. A. Enge, *Introduction to Nuclear Physics*, Addison-Wesley (1966).
5. P. Marmier and E. Sheldon, *Physics of Nuclei and Particles*, 1 and 2, Academic Press, New York (1969).
6. A. C. Melissinos, *Experiments in Modern Physics*, Academic Press, New York (1966).
7. C. M. Lederer and V. S. Shirley, Eds., *Table of Isotopes*, 7th Edition, John Wiley and Sons, Inc., New York (1978).
8. P. Quittner, *Gamma Ray Spectroscopy*, Halsted Press, New York (1972).

Rutherford Scattering of Alphas from Thin Gold Foil

EQUIPMENT NEEDED FROM EG&G ORTEC

142B Preamplifier
Bin and Power Supply
428 Detector Bias Supply
480 Pulser
575A Amplifier
Surface Barrier Detector R-024-450-100
ACE-2K MCA System including suitable IBM PC (other EG&G ORTEC MCAs may be used)

Oscilloscope
1 mCi ^{241}Am source
Source Kit SK-1A
Target Kit M15
307 Rutherford Scattering Chamber
ORC-15 Cable Set

Purpose

In this experiment the effect of gold foil for scattering alpha particles will be measured, and the results will be interpreted as experimental cross sections which will be compared with theoretical related expressions.

Introduction

No experiment in the history of nuclear physics has had a more profound impact than the Rutherford elastic scattering experiment. It was Rutherford's early calculations based on the elastic scattering measurements of Geiger and Marsden that gave us our first correct model of the atom. Prior to Rutherford's work, it was assumed that atoms were solid spherical volumes of protons and that electrons intermingled in a more or less random fashion. This model was proposed by Thomson and seemed to be better than most other atomic models at that time.

Geiger and Marsden made some early experimental measurements of alpha-particle scattering from very thin hammered-metal foils. They found that the number of alphas that scatter as a function of angle is peaked very strongly in the forward direction. However, these workers also found an appreciable number of scattering events occurring at angles $>90^\circ$. Rutherford's surprise at this is this statement from one of his last lectures: "It was quite the most incredible event that has ever happened to me in my life. It was almost as incredible as if you fired a fifteen-inch shell at a piece of tissue paper and it came back and hit you."

Rutherford tried to analyze this angular dependence in terms of the atomic model that had been proposed by Thomson, but he observed that the Thomson model could not explain the relatively large back-angle cross section that had been found experimentally. Measurements by Geiger and Marsden revealed that 1 out of 8000 alpha particles incident on platinum foil experienced a deflection $>90^\circ$. This was in conflict with calculations based on the Thomson model which predicted that only 1 alpha in 10^{14} would suffer such a deflection.

With intense effort, coupled with his unusual physical insight, Rutherford proposed the nuclear model of the atom.

His calculations, based on Coulomb scattering from the proposed hard central core of charge, produced the required 10^{10} increase in cross section found by Geiger and Marsden. Of course, the cross section was very difficult to determine experimentally with the equipment available to these workers (an evacuated chamber with a movable microscope focused on a scintillating zinc sulfide screen). It was only through very careful and tedious measurements that the angular distribution was experimentally determined.

The term "cross section" mentioned above is a measure of the probability for the scattering reaction at a given angle. From a dimensional standpoint, cross section is expressed by units of area. This seems reasonable since the relative probability of an alpha striking a gold nucleus is proportional to the effective area of the nucleus. Cross sections are usually expressed in units called "barns," where one barn is $1 \times 10^{-24} \text{ cm}^2$. This is a very small effective area but is not unreasonable when one considers the size of the nucleus in comparison to the size of the atom.

For a Rutherford scattering experiment it is most convenient to express the results in terms of cross section per solid angle. The solid angle referred to is the solid angle that the detector makes with respect to the target and is measured in steradians, (sr). The solid angle, $(\Delta\omega)$, in steradians is simply A/R^2 , where A is the area of the detector and R is the distance of separation between the detector and the target. The measurement of cross section is expressed in barns/steradian or more conveniently millibarns/steradian. The cross section defined here is referred to as the differential cross section, and it represents the probability per unit solid angle that an alpha will be scattered at a given angle θ . The theoretical expression for the Rutherford elastic scattering cross section can be simplified to the following formula:

$$\frac{d\sigma}{d\Omega} = 1.296 \left(\frac{\text{mb}}{\text{sr}} \right) \left(\frac{Z_1 Z_2}{E_\alpha} \right)^2 \left[\csc^4 \left(\frac{\theta}{2} \right) - 2 \left(\frac{M}{A} \right)^2 \right] \quad (1)$$

where Z_1 and Z_2 are the atomic numbers of the projectile and target, E is the energy of the projectile in MeV, M is the mass

number of the projectile, and A is the mass number of the target nucleus. For our experiment, $^{197}\text{Au}(^4\text{He}, ^4\text{He})^{197}\text{Au}$, $Z_1 = 2$, $Z_2 = 79$, $E_\alpha = 5.8 \text{ MeV}$, $M = 4$, and $A = 197$. In alpha scattering from gold it is quite difficult to measure the cross section for scattering angles $>90^\circ$. The reason for this difficulty is that it takes a prohibitively long period of time to make a measurement at the back angles. Therefore the term $-2(M/A)^2$ is always quite small compared to $\csc^4(\theta/2)$ and hence can be ignored without much error. To a good approximation the differential cross section is then given by

$$\frac{d\sigma}{d\Omega} = 1.296 \left(\frac{\text{mb}}{\text{sr}}\right) \left(\frac{Z_1 Z_2}{E_\alpha}\right)^2 \csc^4\left(\frac{\theta}{2}\right). \quad (2)$$

The expression in Eq. (2) varies 4 orders of magnitude from $\theta = 0^\circ$ in the forward direction to $\theta = 90^\circ$. The purpose of this experiment is to show that the experimental cross section can be favorably compared with the theoretical expression in Eq. (2).

EXPERIMENT 15.1 The Rutherford Cross Section

Procedure

1. Set up the electronics as shown in Fig. 15.1 and the mechanical arrangement in Fig. 15.2.
2. Set $\theta = 0^\circ$ and remove the gold foil to calibrate the system. Adjust the gain of the 575A Amplifier so that the 5.8-MeV alphas from ^{241}Am are stored in the top quarter of the analyzer.
3. Calibrate the MCA with the ^{241}Am alphas and the 480 Pulser in the same manner as outlined for Experiments 4 and 5. Plot the analyzer calibration on linear graph paper.
4. Insert the gold foil at the target position at an angle of 45° to the collimated alpha beam. Measure the energy, E_f , that passes through the gold foil. Calculate the energy loss, (ΔE) , of the alphas in going through the foil (Experiment 5);

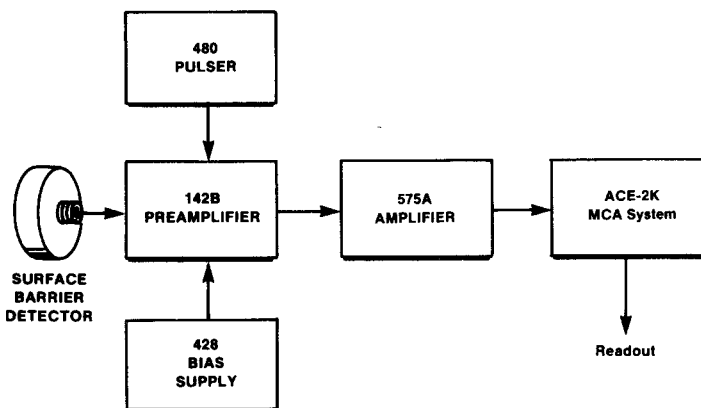
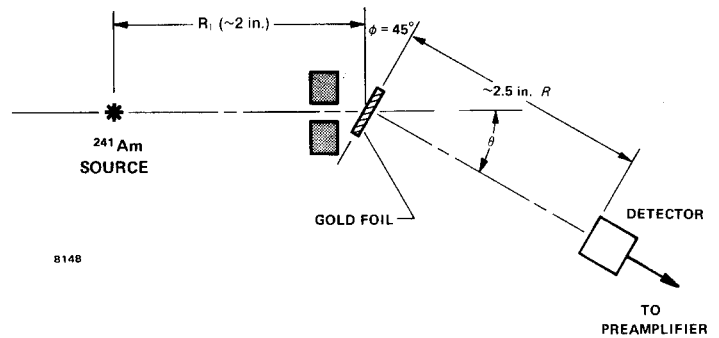


Fig. 15.1. Electronics for Rutherford Scattering Experiment.



This is done in a vacuum of at least $200 \mu\text{m}$.
The detector should rotate from $\theta = 0^\circ$ to $\theta = 90^\circ$.

Fig. 15.2. Experimental Arrangement for Rutherford Scattering Experiment Using an EG&G ORTEC 307 Chamber.

$\Delta E = E_0 - E_f$, where E_0 is 5.8 MeV for the source and E_f is the measured energy after the alphas pass through the gold foil.

EXERCISES

- a. From ΔE and Table 5.1, calculate the thickness of the gold foil in mg/cm^2 .
- b. The average energy of alphas in scattering from the foil is

$$E_{\text{av}} = \frac{E_0 + E_f}{2}, \quad (3)$$

Determine E_{av} for the measurements made in step 4. Use E_{av} as E_α in Eq. (3) and solve the equation for the values of $d\sigma/d\Omega$ (Theory) in Table 15.1 and fill in this column in the table.

- c. Plot $d\sigma/d\Omega$ (Theory) versus θ on 5-cycle semilog paper.

Table 15.1

θ (deg)	$d\sigma/d\Omega$ (Theory)	$d\sigma/d\Omega$ (Experimental)
10		
15		
20		
25		
30		
40		
50		
60		
70		
80		
90		

Calculate n_0 , the number of gold target nuclei per cm^2 from the following formula:

$$n_0 = \frac{(\text{g/cm}^2 \text{ of the target}) 6.023 \times 10^{23}}{197} \quad (4)$$

The value of the term n_0 will be used at a later time.

d. Calculate $\Delta\Omega$ from the formula

$$\Delta\Omega = \frac{\text{area of detector (cm}^2\text{)}}{R^2} \quad (5)$$

where R is the distance (in cm) from the detector to the gold foil.

5. Remove the gold foil and check the alignment of the apparatus by measuring the counting rates for the values in Table 15.2.

6. Plot the data in Table 15.2. If the instrument is properly aligned, the peak should be centered about zero degrees.

Table 15.2

Angle (deg)	Counts/m	Angle (deg)	Counts/m
0		0	
1		-1	
2		-2	
3		-3	
4		-4	
5		-5	
6		-6	
7		-7	

7. The number of alphas per unit time, (I_0), that impinge on the foil can be calculated from the following expression:

$$I_0 = \frac{(\text{activity of the source}) (\text{area of the foil}^*)}{4\pi R_1^2} \quad (6)$$

(See Fig. 15.2) The activity of the source can be determined by the methods outlined in Experiment 4.

8. You are now ready to measure the cross section. Replace the gold foil. Set the detector at 10° and count for a period of time long enough to get good statistics in the peak. Calculate the counting rate, (I), at 10° . Repeat for all of the values listed in Table 15.1. It should be obvious from the theoretical cross section that the counting time will have to be increased as θ increases. You should try to get at least 15% statistics for all points.

*Area of the foil projected perpendicular to the source which is not shadowed by the collimator.

EXERCISE

e. Calculate the experimental cross section for each of the points in step 8 by using the following formula:

$$\frac{d\sigma}{d\Omega} = \left(\frac{I}{I_0 \Delta\Omega n_0} \right) \left(\frac{\text{cm}^2}{\text{sr}} \right) \quad (7)$$

Since 1 barn = 10^{-24} cm^2 , the values calculated from Eq. (7) can be converted to millibarns per steradian and entered as $d\sigma/d\Omega$ (Experimental) in Table 15.1.

EXPERIMENT 15.2

The Z_2^2 Dependence of the Rutherford Cross Section

In this experiment alpha particles will be scattered from different foils to show the Z_2^2 dependence in Eq. (2). The foils used (which are included in the foil kit for this experiment) are aluminum ($Z_2 = 13$), nickel ($Z_2 = 28$), copper ($Z_2 = 29$), silver ($Z_2 = 47$), and gold ($Z_2 = 79$). The student will then plot this Z_2 dependence and show that it does agree with the theory.

Procedure

- Repeat procedures 1 through 4 in Experiment 15.1 for each of the foils. For each foil calculate n_0 as in Experiment 15.1, Exercise c.
- For each foil set $\theta = 45^\circ$ and accumulate a pulse height spectrum for a period of time long enough to get at least 1000 counts in the scattered peak. Determine I (the number of scattered alphas per second) for each sample.

EXERCISE

Plot I as a function of $n_0 Z_2^2$ for each sample. The curve should be a straight line. The slope of the line can be determined by equating the two expressions for cross section Eqs. (2) and (7) and solving for the product $n_0 Z_2^2$.

Therefore

$$1.296 \left(\frac{Z_1 Z_2}{E_\alpha} \right)^2 \csc^4 \left(\frac{\theta}{2} \right) \times 10^{-27} \frac{\text{cm}^2}{\text{sr}} = \frac{I}{I_0 \Delta\Omega n_0} \text{cm}^2/\text{sr}, \quad (8)$$

and hence

$$I = \left[\frac{1.296 Z_1^2 \csc^4 \left(\frac{\theta}{2} \right) I_0 \Delta\Omega \times 10^{-27}}{E_\alpha^2} \right] n_0 Z_2^2. \quad (9)$$

Since every term inside the brackets is a constant for all foils:

$$I = K n_0 Z_2^2.$$

Therefore our experimental intensity should plot as a straight line in this exercise. The slope of the curve K is the value that is calculated from Eq. (9).

References

1. A. C. Melissinos, *Experiments in Modern Physics*, Academic Press, New York (1966).
2. H. A. Enge, *Introduction to Nuclear Physics*, Addison-Wesley Publishing Co., Massachusetts (1966).
3. R. D. Evans, *The Atomic Nucleus*, McGraw-Hill, New York (1955).
4. B. L. Cohen, *Concepts of Nuclear Physics*, McGraw-Hill, New York (1971).
5. J. L. Duggan and J. F. Yegge, "A Rutherford Scattering Experiment," *J. Chem. Ed.*, **45** 85 (1968).
6. J. L. Duggan, *et.al.*, *Am. J. Phys.* **35**, 631 (1967).
7. C. M. Lederer and V. S. Shirley, Eds., *Table of Isotopes*, 7th Edition, John Wiley and Sons, Inc., New York (1978).
8. G. Marion and P. C. Young, *Tables of Nuclear Reaction Graphs*, John Wiley and Sons, New York (1968).

The Total Neutron Cross Section and Measurement of the Nuclear Radius

EQUIPMENT NEEDED FROM EG&G ORTEC

113 Scintillation Preamplifier
 266 Photomultiplier Tube Base
 Bin and Power Supply
 556 High Voltage Power Supply
 480 Pulser
 575A Amplifier
 905-5 Fast Plastic Scintillator and PM tube

ACE-2K MCA System including suitable IBM PC (other EG&G ORTEC MCAs may be used)
 Oscilloscope
 1- to 3-Ci Am-Be neutron source
 1 each AlRd-3, FeRd-1, CuRd-1, PbRd-1, PnRd-1 absorbers
 (see Appendix)
 High Transmission Stand, HTS-1
 ORC-16 Cable Set

Purpose

In this experiment the total cross section, σ_T , and the fundamental nuclear radius, R_0 , will be determined for several elements: aluminum, iron, copper, and lead.

Introduction

This experiment is based on the use of the 1-Ci Am-Be source, probably the most common of the neutron sources. The measurement of total cross section of an element is quite similar to the mass attenuation coefficient measurement made in Experiment 3. In this experiment (written in greater detail in ref. 5) the data for calculations will be obtained by measuring the intensities of the neutrons from the source both without an absorber and with an absorber placed between the source and the detector. Figure 16.1 shows the experimental arrangement of the source, absorber, and detector for this measurement.

The distance from the source to the detector should be ~ 100 cm, and the absorbers will be introduced, one at a time, at about the midpoint between the source and the detector. Handle the Am-Be source cautiously; 1 Ci of this material produces over 1×10^6 neutrons/s. It can be posi-

tioned by handling it with tongs at least 3-ft long or by a long string. Instructions for the safe handling of the neutron source are supplied by the manufacturer of the source. These instructions should be read carefully before using the source.

Figure 16.2 is a typical neutron source spectrum that was measured with a ^3He neutron spectrometer. It is obvious that the neutron spectrum from this source is rather complicated. For this experiment an electronic bias will be set on the neutron detector in order to eliminate response to neutron energies below ~ 7 MeV. The average neutron energy from 7 MeV to the end of the spectrum is ~ 8.5 MeV. A detailed analysis of the mathematical treatment of the neutron spectrum, as well as the total cross section, can be found in refs. 5 and 6. In this experiment the total neutron cross section will

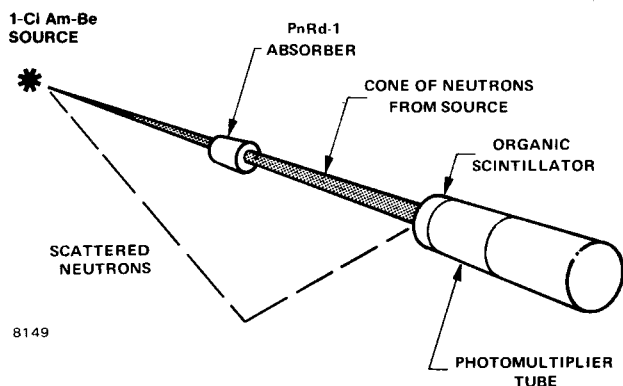


Fig. 16.1. System for Measuring Total Neutron Cross Section.

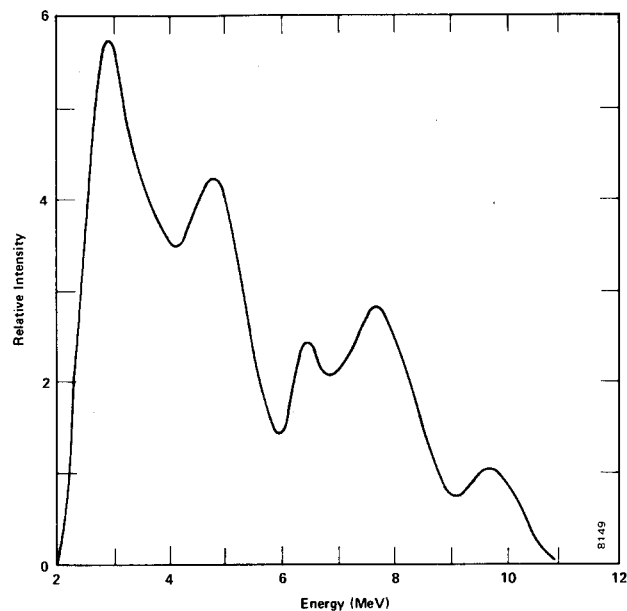


Fig. 16.2. Typical Neutron Source Spectrum Measured with a ^3He Semiconductor Spectrometer.

be measured for the several elements and for an average neutron energy of 8.5 MeV. The experimental values can then be compared with the accepted cross sections listed in ref. 1.

The Total Neutron Cross Section (TNCS)

The TNCS measurement is a transmission measurement. In Fig. 16.1 the number of neutrons, dN , that are removed from the initial beam by the absorber is given by

$$dN = \mu_t N dt, \tag{1}$$

where

- μ_t = linear absorption coefficient,
- N = initial number of neutrons without the absorber,
- dt = thickness of the absorber (in this case it is the length of the absorber in cm).

Hence, as for I_0 in Experiment 3,

$$N = N_0 e^{-\mu_t t} \tag{2}$$

The total cross section, σ_T , is defined from μ_t as

$$\sigma_T = \frac{\mu_t}{n}, \tag{3}$$

where n = number of nuclei/cm³ of the absorber.

If we substitute Eq. (3) back into (2), the following is obtained:

$$N = N_0 e^{-\sigma_T n t} \tag{4}$$

Since N/N_0 is equal to the transmission T ,

$$T = e^{-\sigma_T n t}, \tag{5}$$

and the total cross section, σ_T , is given by

$$\sigma_T = - \frac{\ln T}{nt}. \tag{6}$$

The samples to be used as absorbers are cylinders that are ~6 cm in diameter by a length, (t), of ~7 cm. The nt values for Eq. (6) can be calculated for each sample. These nt values are the number of nuclei/cm² for each absorbing sample. The transmission in Eqs. (5) and (6) is simply a ratio of the neutron counts with and without the absorber.

From the Optical Model Theory in ref. 4 the total cross section can be expressed:

$$\sigma_T = 2\pi(R + \chi)^2, \tag{7}$$

where

- $R = R_0 A^{1/3}$,
- R_0 = fundamental nuclear radius (~1.3 x 10⁻¹³ cm),
- A = atomic weight of scattering sample,
- χ = the de Broglie wavelength/2 π for 8.5 MeV neutrons (ref. 4).

Equation (7) can be written in two other forms:

$$\sigma_T = 2\pi (R_0 A^{1/3} + \chi)^2, \tag{8}$$

and

$$\sqrt{\sigma_T} = \sqrt{2\pi} (R_0 A^{1/3} + \chi). \tag{9}$$

The fundamental nuclear radius, R_0 , is therefore

$$R_0 = \frac{\sqrt{\sigma_T/2\pi} - \chi}{A^{1/3}} \tag{10}$$

If the $\sqrt{\sigma_T/2\pi}$ is plotted as a function of $A^{1/3}$ for the absorber, the slope of the line is R_0 . The purpose of this experiment is to measure σ_T for aluminum, iron, copper, and lead and to determine R_0 from the analysis derived above.

Procedure

1. Set up the electronics as shown in Fig. 16.3, and position the source and detector as shown in Fig. 16.1 separated by ~1 m and located on a common optical axis. The high transmission stand (HTS-1) that will hold the sample and the shadow bar should be placed half-way between the source and the detector. The source, stand, and detector can be aligned on axis with a tight string, or if available, a small laboratory laser. Do not put an absorber in the stand at this point.
2. Adjust the controls on the instruments as follows: set the 556 high voltage to the value that is recommended for the 905-5 detector; set the amplifier gain for a maximum bipolar output amplitude of ~5 V.
3. Accumulate a spectrum on the MCA. It should look like Fig. 16.4.
4. Set the Lower Level of the MCA so that it cuts out all pulses below the location marked E in Fig. 16.4. This corresponds to an energy level of ~7 MeV. Many of the pulses from the detector that represent energies below this level are gammas rather than neutrons, but most of the pulses for energies ~7 MeV represent neutrons only. The 7-MeV point in the spectrum can be determined by a linear extrapolation since the end point of the spectrum will be ~11 MeV.
5. Clear the analyzer to zero. Accumulate a spectrum in the MCA until there are ~3000 counts in the active portion of the spectrum.

EXERCISES

- a. Compare the spectrum with the portion of Fig. 16.4 above the 7-MeV level. Record the number of counts and the accumulation time, t_0 , in Table 16.1. Use the first line for "No absorber."
- b. Place the aluminum absorber in the stand (on the axis) as shown in Fig. 16.1 and repeat the measurement made in

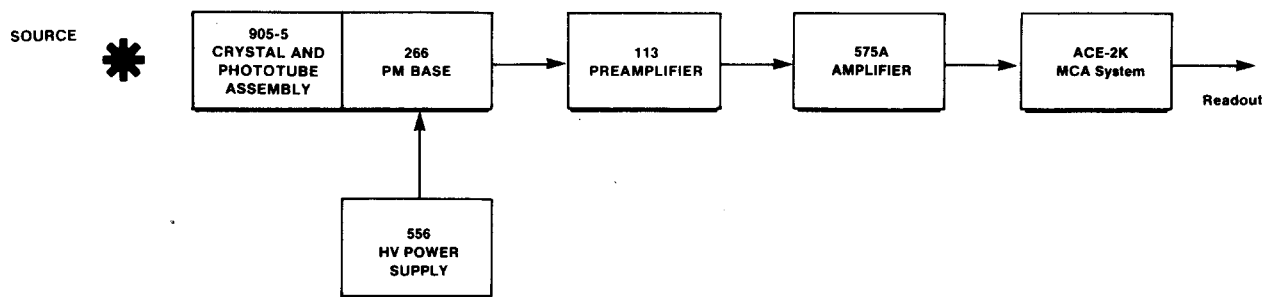


Fig. 16.3. Electronics for Total Neutron Cross-Section Measurements.

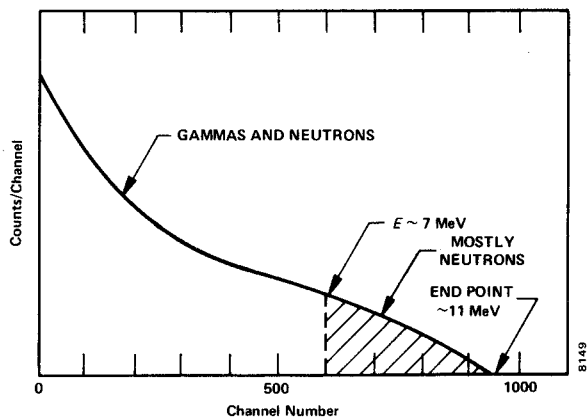


Fig. 16.4. Typical Neutron Spectrum Taken with an EG&G ORTEC 905-5 Detector.

step 5 for the same time, t_0 . Record the counts in Table 16.1. Repeat for each of the other absorbers and for the shadow bar. The shadow bar effectively attenuates all of the direct neutrons from the source, and any counts that are accumulated when it is in position will be those scattered from the floor or other surroundings into the detector. This is background, and the number of counts taken with the shadow bar must be subtracted from each of the other counts in Table 16.1 before these data are used.

c. Calculate σ_T from the corrected data in Table 16.1, using Eqs. (4), (5), and (6). Record these values in Table 16.1 as σ_T (measured). Look up the accepted values for $E_n = 8.5$ MeV in ref. 1 and record these in the last column of Table 16.1. Compare the measured values with the accepted values.

d. Plot $\sqrt{\sigma_T/2\pi}$ versus $A^{1/3}$ on linear graph paper and determine R_0 from the plot. Figure 16.5 shows some typical data that were measured by this method.

Additional Note: The conventional neutron long counter that is found in many laboratories could have been used to count the neutrons in this experiment. These counters can be set so that they are relatively insensitive to gammas, and the system can be operated to measure a wider portion of the spectrum than just the part from 7 to 11 MeV. The gamma

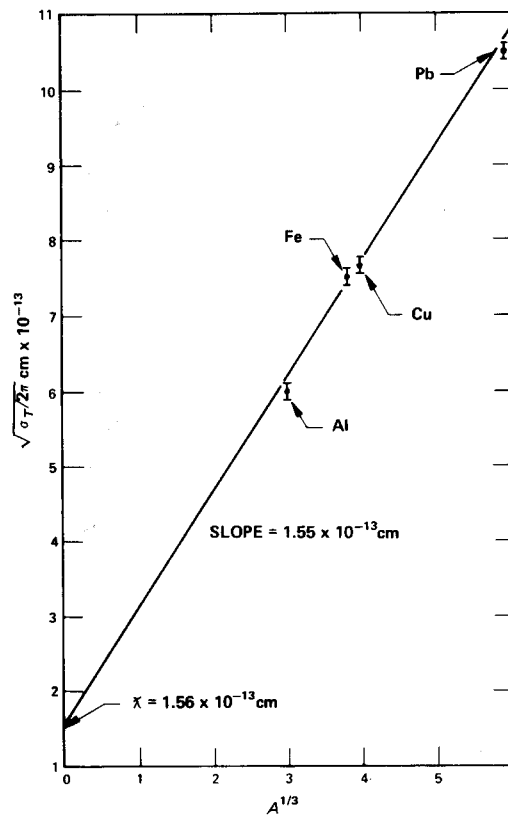


Fig. 16.5. Plot of $\sqrt{\sigma_T/2\pi}$ versus $A^{1/3}$ for Am-Be Neutron Energies (Electronic Bias at 7 MeV).

Table 16.1

Sample	Counts	Time, t_0	σ_T	
			Measured	Accepted (from ref. 1)
No absorber				
Aluminum				
Iron				
Copper				
Lead				
Shadow Bar				

problem can also be solved by using pulse shape discrimination with, for example, an organic scintillator and an EG&G ORTEC 458 Pulse Shape Analyzer.

References

1. D. J. Hughes and R. B. Schwartz, *Neutron Cross Sections*, **BNL-325**, 2nd Edition (Rev) (1958). Available from National Technical Information Service, U.S. Dept. of Commerce, Springfield, Virginia.
2. H. H. Barschall, "Studies of Intermediate and Heavy Nuclei with Neutrons," *Am. J. Phys.*, **22**(8), 517-523 (1954).
3. J. B. Marion and F. C. Young, *Nuclear Reaction Analysis*, John Wiley and Sons, New York (1968).
4. J. B. Marion and J. L. Fowler, Eds., *Fast Neutron Physics*, **1** and **2**, Interscience, New York (1960-1963).
5. T. C. Minor, *et. al.*, "Undergraduate Experiments to Find Nuclear Sizes by Measuring Total Cross-Section for Fast Neutrons," *Am. J. Phys.*, **37**(6), 649 (1969).
6. W. K. Robinson, J. L. Nagi, and J. L. Duggan, "A Time-of-Flight Neutron Experiment for the Undergraduate Laboratory," *Am. J. Phys.*, **37**(5), 482 (1969).
7. R. D. Evans, *The Atomic Nucleus*, McGraw-Hill (1955).

Neutron Activation Analysis (Slow Neutrons)

EQUIPMENT NEEDED FROM EG&G ORTEC

113 Scintillation Preamplifier
 266 Photomultiplier Tube Base
 Bin and Power Supply
 556 High Voltage Power Supply
 480 Pulser
 575A Amplifier
 905-3 2-in. x 2-in. or 905-4 3-in. x 3-in. NaL(Tl)
 Detector and PM Tube
 ACE-2K MCA System including suitable IBM PC (other
 EG&G ORTEC MCAs may be used)

Oscilloscope
 1- to 3-Ci Am-Be neutron source in howitzer
 308 Neutron Howitzer and Activation Chamber
 313 Activation Sample Set
 317 Activation Sample Set
 Model CD-17 Cadmium Shields
 Model V-17 Vanadium Saturation Factor Kit
 Model RE-17 Special Sample Set
 ORC-17 Cable Set
 Source Kit SK-1G (see Appendix)

Purpose

This experiment will demonstrate the principles of element identification using the technique of slow neutron activation.

Introduction

Neutron activation analysis is a very powerful technique for identifying many elements. Basically the technique is quite simple. A sample is irradiated by slow neutrons and becomes radioactive. By measuring the β^+ 's, γ 's, β^- 's, and half-life of the resulting sample, the elemental constituents of the sample and their relative concentrations can be identified.

Industrial activation analysis is usually done with slow neutrons from a reactor, where the neutron flux can be as high as 5×10^{13} neutrons/cm²/s, or with an accelerator with fast neutron fluxes of 10^{10} neutrons/cm²/s. When activation analysis is compared with other instrumental analyses such as gravimetric, colorimetric, spectrographic, or mass spectroscopy, its sensitivity is usually shown to be better by a factor of 10 than that of other methods. Activation analysis is used extensively in such fields as geology, medicine, agriculture, electronics, metallurgy, criminology, and the petroleum industry.

The Neutron Source

This experiment is described for 1 Ci of Am-Be for the neutron source, with the source located in the center of a paraffin howitzer. The samples are irradiated at a point ~4 cm from the source by the neutrons that have been moderated by the paraffin between that point and the source. Any of the commonly found isotopic neutron sources can be used for this experiment.

Neutron Activation Equations

Assume that the sample has been activated in the howitzer. At the instant when the activation has been terminated,

($t = 0$), the activity of the sample is given by the following expression:

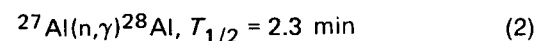
$$A_0 = \frac{\sigma m \eta \phi \alpha S}{w} \quad (1)$$

where

- A_0 = the number of disintegrations per second of the element in the sample at $t = 0$ (when irradiation stops),
- σ = cross section for the reaction, cm²,
- m = mass of the target element, grams,
- η = Avogadro's number, 6.023×10^{23} molecules/mole,
- ϕ = neutron flux, neutrons/cm²/s,
- α = fraction of the target isotope in the sample [e.g., with an ordinary copper sample producing the $^{63}\text{Cu}(n,\gamma)^{64}\text{Cu}$ reaction, $\alpha = 0.69$ since 69% of all natural copper is ^{63}Cu],
- S = saturation factor, $1 - e^{-\lambda t}$, where $\lambda = 0.693/T_{1/2}$ and $T_{1/2}$ is the half-life for the reaction,
- w = atomic weight of the element.

(Note: In the above definitions, t and $T_{1/2}$ must be in the same time units.)

Let us examine Eq. (1) in terms of our knowledge about a reaction. For example, if we were activating an aluminum sample, the following reaction would take place:



The cross section from ref. 13 is 0.21×10^{-24} cm². For our example then, we can determine everything in Eq. (1) except A_0 and ϕ . A_0 can be measured with a scintillation counter (the technique that is outlined), and ϕ will be determined in Experiment 17.1.

Table 17.1 is a list of common thermal neutron cross sections that is taken from ref. 11.

Table 17.1. Common Thermal Neutron Cross Sections.

Reaction	σ (barns)
1. $^{27}\text{Al}(n,\gamma)^{28}\text{Al}$	0.210 ± 0.020
2. $^{51}\text{V}(n,\gamma)^{52}\text{V}$	5.00 ± 0.010
3. $^{63}\text{Cu}(n,\gamma)^{64}\text{Cu}$	4.51 ± 0.23
4. $^{23}\text{Na}(n,\gamma)^{24}\text{Na}$	0.536 ± 0.010
5. $^{55}\text{Mn}(n,\gamma)^{56}\text{Mn}$	13.3 ± 0.2

After irradiation the sample is transferred immediately to the NaI(Tl) detector, and a spectrum is accumulated for a time, (t_1), long enough to get reasonable statistics under the photopeak. The time is usually at least one half-life. The true number of disintegrations, (N_0), that occurred during t_1 can be determined from the following:

$$N_d = \frac{\Sigma_p - \Sigma_\beta}{G\epsilon_p f} \quad (3)$$

where

- Σ_p = sum under the photopeak,
- Σ_β = background for the same counting period under the photopeak,
- $G = A/2\pi s^2$, where A = area of detector in cm^2 , and s = distance from source to detector in cm,
- ϵ_p = intrinsic peak efficiency for the gamma energy and the detector size used (Fig. 3.6, Experiment 3.6, or ref. 10 in Experiment 3),
- f = decay fraction of the unknown activity, which is the fraction of the total disintegrations in which the measured gamma is emitted (refs. 7 and 10 and Table 3.2 in Experiment 3.6).

From the decay equation, N_0 can be calculated:

$$N_d = N_0 (1 - e^{-\lambda t}) \quad (4)$$

$$A_0 = \lambda N_0 \quad (5)$$

where t is the time for which the sample was counted.

Therefore we have reduced Eq. (1) to one unknown, ϕ , which is the number of neutrons/cm²/s for our howitzer. The

secondary purpose of this experiment is to find ϕ for the howitzer, using the $^{27}\text{Al}(n,\gamma)^{28}\text{Al}$ reaction. We will also use that value of ϕ to determine the cross section for the $^{51}\text{V}(n,\gamma)^{52}\text{V}$ reaction.

EXPERIMENT 17.1 Neutron Flux Determination

Procedure

1. Set up the electronics as shown in Fig. 17.1. Use the bipolar output from the 575A to furnish pulses into the MCA.
2. Calibrate the system for full scale on the MCA of ~2 MeV. Use the ^{137}Cs and ^{60}Co gamma sources from the source kit for the calibration. Draw the calibration line (as in Experiment 3 or use the MCA energy calibrate feature).
3. Place the aluminum sample in the howitzer and activate it for 5 min. Transfer it immediately to the scintillation counting position and count it for a clock time [t_1 in the discussion preceding Eq. (3)] of 2 min.

EXERCISE

- a. Read the data out of the MCA and determine E_γ and the sum under the photopeak.
4. Remove the sample and count the background for 2 min. From your data determine N_d of Eq. (3).

EXERCISES

- b. Substitute the value for N_d into Eq. (4). Solve for N_0 and A_0 in Eqs. (4) and (5).
- c. Solve Eq. (1) for ϕ using the accepted cross section for the $^{27}\text{Al}(n,\gamma)^{28}\text{Al}$ reaction as $0.21 \times 10^{-24} \text{ cm}^2$.
5. Since the half-life for the reaction is 2.31 min, the sample activity will die out within ~20 min. After approximately this period of time, repeat the experiment and determine a second value for ϕ . If the work has been done carefully, the numbers should agree to within 5% of each other. Determine the average value of ϕ ; this will be used in Experiment 17.2.

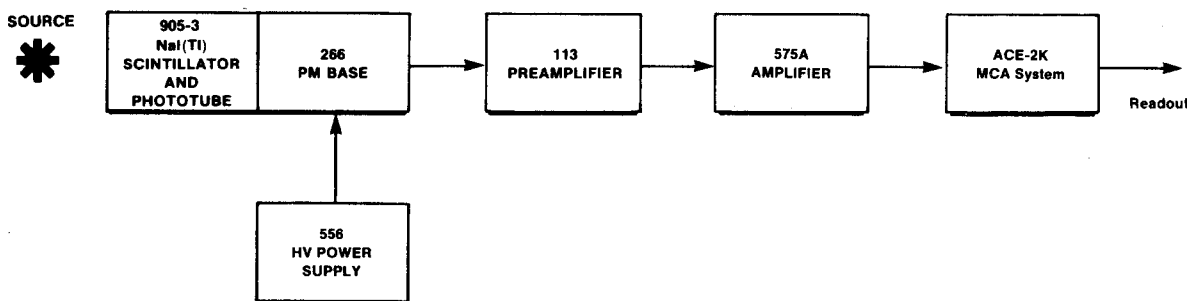


Fig. 17.1. Electronics Interconnections for Experiment 17.1.

EXPERIMENT 17.2

Measurement of the Thermal Neutron Cross Section for the $^{51}\text{V}(n,\gamma)^{52}\text{V}$ Reaction

Procedure

1. Use the same electronics setup as for Experiment 17.1.
2. Activate the vanadium sample for 5 min. Transfer it to the scintillation counting station and count for $t_1 = 2$ min.

EXERCISE

Use the average value of ϕ from Experiment 17.1 and the procedure discussed above to solve for σ , the cross section for the $^{51}\text{V}(n,\gamma)^{52}\text{V}$ reaction. The accepted value is 4.9×10^{-24} cm^2 . The measured gamma-ray energy for this reaction is 1.434 MeV. Do your results agree with this value?

EXPERIMENT 17.3

Determination of the Half-Life for the $^{27}\text{Al}(n,\gamma)^{28}\text{Al}$ Reaction

Procedure

1. Use the same electronics setup as for Experiment 17.1. Set the MCA Region of Interest, (ROI), so that it brackets the 1780-keV peak from the decay of ^{28}Al . See Fig. 17.2 for a typical spectrum from aluminum.

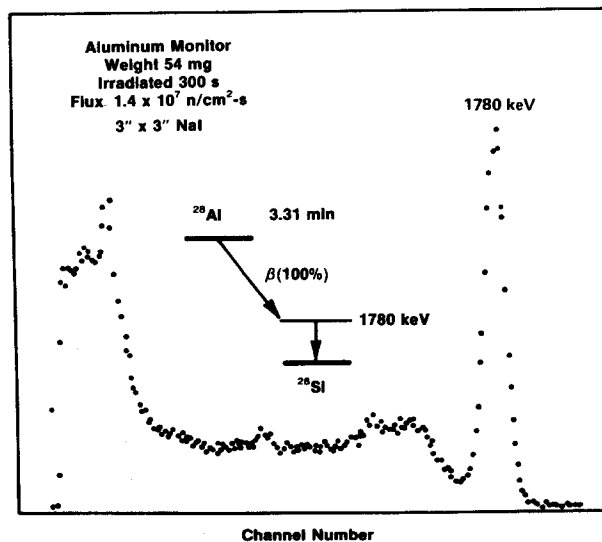


Fig. 17.2. Thermal Neutron Activation Spectrum of ^{28}Al .

2. Activate the aluminum sample (used in Experiment 17.1) for 5 min.
3. Transfer the sample and take 15-s counts every 45 s.

EXERCISE

Plot the data on semilog paper and determine $T_{1/2}$.

Note: Many other slow neutron reactions can be studied with the isotopic neutron source and the electronics of Experiment 17. Any of these can be made if the appropriate target materials are available. Reference 11 outlines many of these experiments. Table 17.2 (taken from ref. 11) is a rather com-

Table 17.2. Recommended Slow Neutron Reactions.

Element	Target Nuclide	Target Material	Product Nuclide	$T_{1/2}$	E_{γ} (MeV)
Aluminum	^{27}Al	Al, Al_2O_3	^{28}Al	2.30 m	1.78
Sodium	^{23}Na	Na_2CO_3	^{24}Na	15.0 h	2.75, 1.37
Vanadium	^{51}V	NH_4VO_3 or metal	^{52}V	3.77 m	1.43
Manganese	^{55}Mn	MnO_2	^{56}Mn	2.58 h	0.845, 1.81, 2
Cobalt	^{59}Co	CoO or foil	^{60m}Co	10.5 m	0.059
Copper	^{63}Cu	CuO or foil	^{64}Cu	12.9 h	$0.511 \gamma_{\pm}$
Gallium	^{71}Ga	Ga_2O_3	^{72}Ga	14.3 h	0.63, 0.83
Germanium	^{74}Ge	Ge (metal)	^{75}Ge	82 m	0.26, 0.20
Arsenic	^{75}As	As_2O_3	^{76}As	26.5 h	0.56, 0.66, 1
Bromine	^{79}Br	NH_4Br	^{80}Br	18 m	$0.62, 0.51 \gamma_{\pm}$
Indium	^{115}In	In (metal foil)	^{116m}In	54 m	0.40, 1.09, 1.27, 2.08
Tellurium	^{130}Te	Te	^{131}Te	25 m	0.15, 0.45
Iodine	^{127}I	NH_4I	^{128}I	25 m	0.46
Lanthanum	^{139}La	La_2O_3	^{140}La	40.2 h	0.48, 1.59
Tungsten	^{186}W	WO_3	^{187}W	24 h	0.480, 0.686, 0.134
Gold	^{197}Au	Au-Dowex-1 (gold foil)	^{198}Au	64.8 h	0.411

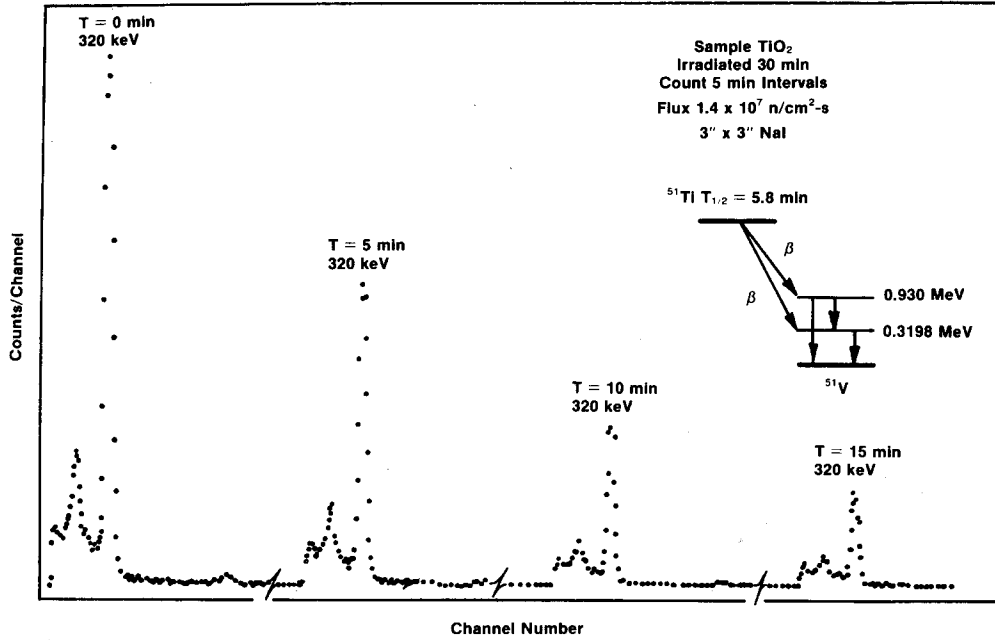


Fig. 17.3. Series of Four Pulse-Height Spectra for ^{51}Ti Showing the Fall-Off in Activity in Time.

plete listing of reactions that seem to work well for experiments by students. Figure 17.3 shows the fall-off in intensity of the 5.8-min ^{51}Ti activity displayed as four pulse-height spectra. If we were doing this experiment the ROI would be set to bracket the 320-keV photopeak. Table 17.2 shows a list of other recommended slow neutron reactions. Some of the resulting decay schemes are more complex than those we have studied in Experiments 17.1, 17.2, and 17.3. For example, Fig. 17.4 shows the decay of ^{187}W . Some of the gammas are listed in Table 17.2.

EXPERIMENT 17.4

The Saturation Factor in Neutron Activation Analysis

From the definitions at the beginning of Experiment 17, the saturation factor is given by:

$$S = 1 - e^{-\lambda t}$$

From this expression it can be seen that the activity at any time is given by:

$$A_t = A_s (1 - e^{-\lambda t}), \quad (6)$$

where A_s is the activity at saturation.

In this experiment we will verify Eq. (6) for the decay of ^{52}V (Fig. 17.5). Each of the vanadium samples in the Model V-17 Kit contains 2 g of NH_4VO_3 . In the experiment we will irradiate these identical samples for different times, (t), and plot the corresponding ^{52}V activity as a function of irradiation time.

Procedure

1. Use the electronics shown in Fig. 17.1. Set the ROI of the MCA so that it brackets the 1434-keV gamma line (Fig. 17.5). This can be done by irradiating one of the samples for 5 min and counting it directly against the face of the NaI(Tl) detector.

2. Irradiate samples for 2, 4, 6, 10, 15, and 25 min. Note: All of the ports of the neutron howitzer may be used, since the flux density, ϕ , is the same in all ports.

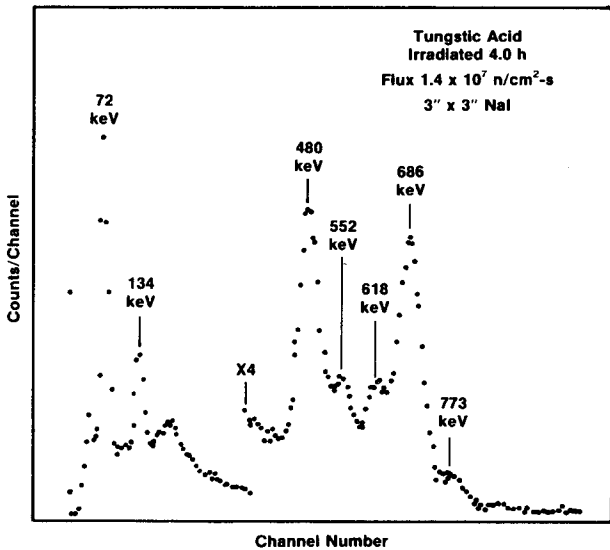


Fig. 17.4. Neutron Activation Spectrum of Tungsten.

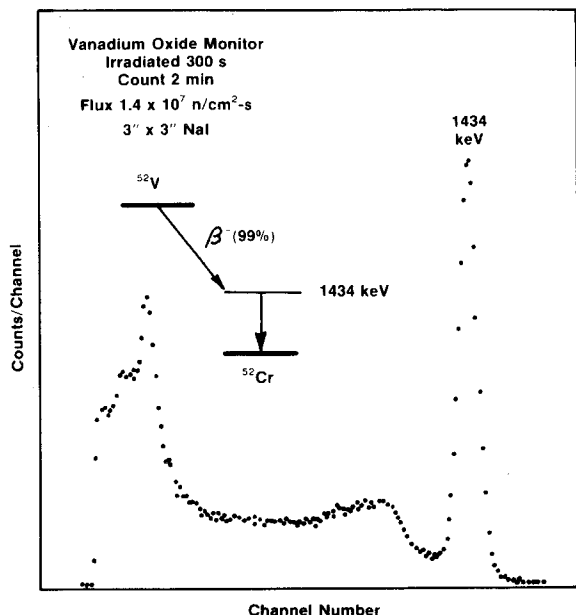


Fig. 17.5. Thermal Neutron Activation Spectrum of ⁵²V.

3. After irradiation, immediately transfer each sample to the counting station and count for exactly 100 s.

EXERCISE

Since the $T_{1/2}$ of the vanadium activity is 3.77 min, an irradiation time of 25 min will yield a value of A_0 from Eq. (6). Therefore we can call the count under the ROI 25 min = A_0 . For any other irradiation time, define the count under the ROI to be A_i .

On two-cycle graph paper make a plot of the experimental data A_i/A_0 versus irradiation time. Plot the theoretical function, $1 - e^{-\lambda t}$ on the same graph.

EXPERIMENT 17.5

The Study of a Complex Sample with Two Half-Lives Present

Ordinary silver has two pronounced isotopes, ¹⁰⁷Ag (51.35%) and ¹⁰⁹Ag (48.65%). If we activate a piece of silver, the following activities are produced: ¹⁰⁷Ag(n,γ)¹⁰⁸Ag ($T_{1/2} = 2.3$ min) and ¹⁰⁹Ag(n,γ)¹¹⁰Ag ($T_{1/2} = 24$ s). The purpose of this experiment is to determine these half lives by correcting the compound decay curve. ¹⁰⁸Ag has a 0.44-MeV gamma while ¹¹⁰Ag has gammas of 0.66 and 0.94 MeV.

Procedure

1. Obtain two silver samples from the Activation Sample Set No. 317. Set up the electronics as shown in Fig. 17.1.

Activate the first sample for 5 min and immediately place it against the face of the NaI(Tl) detector. Set the ROI of the analyzer so that it brackets the region from 0.44 MeV to 0.94 MeV. Under these conditions we are counting both half lives. This first sample is being irradiated so that we can set the ROI.

2. We are now ready to take data for the complex decay curve. Irradiate the second silver sample for a time of 10 min. Transfer the sample to the counting station and take 10-s counts every 30 s for 8 min. It is necessary that you record each ROI reading and erase quickly in preparation for the next reading.

EXERCISES

a. Plot the resulting data on a semilog scale. The straight line that represents the long-lived (2.3 min) component can easily be drawn on the curve by constructing a line through all points taken after 3.5 min. Determine the half life of the long-lived component.

b. Extrapolate the straight line for the 2.5-min activity back to zero time. Now subtract the straight line counts from this activity from all points from $t = 0$ to $t = 3.5$ min. Plot the resulting short-lived activity and determine the half life of the short-lived activity.

EXPERIMENT 17.6

Thermal Neutron Shielding

Introduction

In Experiment No. 3, we showed that the attenuation of gammas through a lead absorber is given by the following expression:

$$I = I_0 e^{-\mu x} \tag{7}$$

(See Eq. (8), Experiment 3.) A similar expression can be written for the attenuation of neutrons through an absorbing foil.

The equation takes the following form:

$$I = I_0 e^{-N\sigma x}, \tag{8}$$

where

- N = number of atoms/cm³ of the absorber,
- σ = thermal neutron cross section (in cm²),
- x = the absorber thickness (in cm).

In this experiment we will measure the reduction of the thermal neutron flux, ϕ , by placing a thin sheet of cadmium around the sample to be irradiated.

Procedure

1. Set up the electronics as shown in Fig. 17.1. Take two identical aluminum samples from the Activation Sample Set No. 317. Wrap one of the samples with a cadmium foil

Table 17.3. Recommended Activation Parameters for the Elements in Sample Kit RE-17.

Element	Reaction	σ_{barns}	$T_{1/2}$	Measured γ (keV)	Activation Time	Counting Time (s)
Indium	$^{115}\text{In}(n,\gamma)^{116}\text{In}$	210	54.2 min	1270	108 min	600
Copper	$^{65}\text{Cu}(n,\gamma)^{66}\text{Cu}$	2.10	5.1 min	1040	10 min	200
Germanium	$^{74}\text{Ge}(n,\gamma)^{75}\text{Ge}$	0.60	82 min	266	82 min	600
Tungsten	$^{184}\text{W}(n,\gamma)^{185}\text{W}$	2.0	1.7 min	171	6 min	100
Titanium	$^{50}\text{Ti}(n,\gamma)^{51}\text{Ti}$	0.140	5.8 min	322	12 min	200
Manganese	$^{55}\text{Mn}(n,\gamma)^{56}\text{Mn}$	13.3	2.58 h	845	4 h	1000

from the Cadmium Foil Set No. CD-17. The samples are now ready to irradiate.

2. Calibrate the MCA for 2 MeV full scale. Place the unshielded aluminum sample in the howitzer and irradiate for 8 min. By using the $^{27}\text{Al}(n,\gamma)^{28}\text{Al}$ cross section, (0.219 barns), and the techniques in Experiment 17.1 determine the flux, ϕ , in the howitzer. Define this flux to be ϕ_1 .

3. Repeat procedure 2 exactly for the aluminum sample that is wrapped with the cadmium foil. Determine the new value of flux and label it ϕ_2 .

EXERCISE

From Eq. (8) it can be seen

$$\frac{\phi_2}{\phi_1} = e^{-N\sigma x} \quad (9)$$

The density of cadmium is 8.65 g/cm³, and its atomic weight is 112.4. This gives $N = 4.651 \times 10^{22}$ atoms/cm³.

The value, x , of the cadmium foil is written on the foil. From Eq. (9) the thermal absorption cross section for cadmium can be determined. How does your value compare to the accepted value of 2500 barns? The effective shielding parameter for cadmium is given in Eq. (9) by ϕ_2/ϕ_1 .

EXPERIMENT 17.7

The Measurement of Thermal Neutron Activation Cross Sections of Elements with High Sensitivity Ratios

Introduction

A "Table of Relative Sensitivities of Elements to Thermal Neutron Activation" is given in the Appendix. In this experiment we will use the value of flux, ϕ , for the howitzer as determined by Experiment 17.1. From this value of ϕ we will calculate the cross section, σ , for several selected elements from the Special Sample Set RE-17.

Procedure

1. Set up the electronics as shown in Fig. 17.1. Calibrate the MCA for 2 MeV as in Experiment 17.1.

2. Place the indium sample in the howitzer and irradiate for two half lives ($T_{1/2} = 54.2$ min). Transfer it to the NaI counting station and count for 600 s.

EXERCISE

Sum under the 1270-keV peak and determine σ from Eqs. (1) through (5). How does your value compare with the accepted value of 210 barns (Table 17.3)?

3. Repeat for several of the other samples from the Special Sample Kit RE-17. In each case, the sample should be irradiated for at least two half lives. The counting time should be adjusted so that reasonable statistics are obtained under the peak of interest. Table 17.3 shows some recommended parameters for the samples in the RE-17 Kit.

References

1. L. K. Curtiss, *Introduction to Neutron Physics*, D. Van Nostrand Co., Inc., New York (1959).
2. W. S. Lyon, *A Guide to Activation Analysis*, D. Van Nostrand Co., Inc., New York (1964).
3. J. M. A. Lenihan and S. J. Thomson, Eds., *Activation Analysis—Principles and Applications*, Academic Press (1965).
4. C. M. Lederer and V. S. Shirley, Eds., *Table of Isotopes*, 7th Edition, John Wiley and Sons, Inc., New York (1978).
5. D. Gray, et al., "Determination of Trace Element Labels in Atmospheric Pollutants by Instrumental Neutron Activation Analysis," *IEEE Trans. Nucl. Sci.* **NS-19**(1), 194 (1972).
6. S. S. Brar and D. M. Nelson, *Modern Trends in Neutron Activation Analysis*, National Bureau of Standards, Special Publication 312, (1969). Available from the National Technical Information Service, Springfield, Virginia.
7. H. E. Palmer, "Instrumentation for 'In Vivo' Activation Analysis," *IEEE Trans. Nucl. Sci.* **NS-17**(1) (1970).
8. R. C. Koch, *Activation Analysis Handbook*, Academic Press, New York (1960).
9. K. S. Vorres, "Neutron Activation Experiments in Radiochemistry," *J. Chem. Ed.* **37**, 391 (1960).
10. D. Taylor, *Neutron Irradiation and Activation Analysis*, Van Nostrand, Princeton, New Jersey (1964).
11. G. I. Gleason, *Isotopic Neutron Source Experiments*, **ORAU-102** (1967). Available from Oak Ridge Associated Universities, P.O. Box 117, Oak Ridge, Tennessee 37830.

12. *Radiological Health Handbook* (1960), U.S. Dept. of Health, Education, and Welfare, PHS Publication 2016. Available from the National Technical Information Service, U.S. Dept. of Commerce, Springfield, Virginia.

13. *Chart of the Nuclides*, General Electric Company, modified by

Battelle-Northwest, Richland, Washington. Available from Supt. of Documents, GPO, Washington, D.C.

NOTE OF CREDIT: Some parts of this experiment were taken from ref. 11 by G. I. Gleason. This reference contains 18 excellent experiments that can be done in Activation Analysis.

Neutron Activation Analysis (Fast Neutrons)

EQUIPMENT NEEDED FROM EG&G ORTEC

113 Scintillation Preamplifier
 266 Photomultiplier Tube Base
 Bin and Power Supply
 556 High Voltage Power Supply
 480 Pulser
 575A Amplifier
 Source Kit SK-1G (see Appendix)

905-3 NaL(Tl) 2- x 2-in. Detector and PM Tube
 ACE-2K MCA System including suitable IBM PC (other
 EG&G ORTEC MCAs may be used)
 Oscilloscope
 1- to 3-Ci Am-Be neutron source
 Sample Set No. 318
 ORC-18 Cable Set

Purpose

This experiment will demonstrate the principles of element identification using the technique of fast neutron activation.

Introduction

In this experiment the same isotopic neutron source that was used in Experiment 17 will be used after it has been removed from the howitzer. The target samples will be irradiated by being placed in almost direct contact with the neutron source.

The spectrum of neutrons that results from an Am-Be isotopic neutron source is shown in Fig. 16.2. From this figure it is evident that the neutron energies are distributed from 2 to 11 MeV for the unmoderated source (with no paraffin or water moderator). The reaction that produces the neutrons in the source is



In Eq. (1) the 5.704-MeV energy is the Q value for the reaction. It is the effective mass, (Δm), that is converted into energy, where Δm is given by

$$\Delta m = (m_g + m_\alpha) - (m_n + m_{12}) , \quad (2)$$

and where m_g is the mass of ${}^9\text{Be}$, etc. Hence, $Q = \Delta mc^2$. Most of the alpha-emitting isotopes have alpha energies of ~ 5.5 MeV. Conservation of energy for Eq. (1) would be

$$E_\alpha + Q = E_n + E_{12C} . \quad (3)$$

From conservation of momentum the neutrons would get ~ 12 to 13 MeV ($\sim 92.5\%$) of the available energy ($E_n + Q$) for the reaction in the forward direction. Of course, the neutron energy would change as a function of its angle of departure relative to the direction of the incident alpha particle. It is therefore possible to produce neutrons with an upper energy value of ~ 11 MeV. The neutron energies in Fig. 16.2 are distributed as shown for the following reasons:

1. Alpha energy is lost in the source before a reaction is produced.

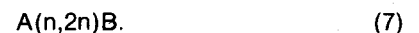
2. ${}^{12}\text{C}$ can be left in one of its excited states.
3. Neutron energies vary with the angles involved.

The activation in Experiment 17 was produced by slow neutrons. The spectrum of the neutrons from the isotopic source was thermalized by a paraffin moderator; the moderation could also have been produced by water. Slow neutron reactions are usually of the type



where *B usually decays by β^- emission followed by gamma radiation (see examples in Fig. 17.2).

For fast neutrons there are three types of reactions that predominate:



The reactions produced by Eq. (5) generally have neutron thresholds in the range of 1 to 3 MeV and therefore cannot be produced with thermal neutrons. The thresholds for Eqs. (6) and (7) are even higher and are usually in the range of 10 to 20 MeV.

An unmoderated isotopic neutron source can be used to produce only (n,p) reactions effectively.

WARNING

Do not physically contact the isotopic source at any time.

For the experiment the neutron source is usually removed from its container with tongs or by a string that will prevent the handler from getting any part of his body within 2 ft of the source. The neutron source is then placed in the center of a table that has been roped off and identified as a radiation hazard to ensure personnel isolation. Then the sample to

be activated can be moved to the chamber. Use tongs to place the sample in its position.

As in Experiment 17, each sample is normally activated for one half-life or longer.

EXPERIMENT 18.1 Gammas and Half-Lives from (n,p) Reactions

Procedure

1. Set up the electronics as shown in Fig. 18.1. Calibrate the MCA with gamma sources from SK-1G for an analyzer full scale of 2 MeV.
2. Place the aluminum target from Sample Set. No. 318 in contact with the Am-Be source for ~30 min. The reaction produced is $^{27}\text{Al}(n,p)^{27}\text{Mg}$ and the $T_{1/2}$ of the product will be 9.5 min (Fig. 18.2).
3. Transfer the sample to the NaI(Tl) detector and count for a period of time long enough to define the gamma groups for the reaction.

EXERCISE

- a. Measure the gamma energies. Do they agree with those shown for this reaction in Fig. 18.2?
4. Set the ROI of the MCA so that it brackets the 1.013-MeV gamma for the reaction. Preset for a counting time of 40 s. Take a 40-s count every 2 min until enough data have been obtained to plot a half-life curve. What is the measured $T_{1/2}$?
 5. Figure 18.2 shows that ~70% of the gammas are 0.842 MeV and that ~30% are 1.013 MeV. Irradiate a second aluminum sample for ~30 min to obtain a sample that will be used to check this ratio.
 6. Use the ROI of the MCA to set two regions of interest, one for 0.842 MeV and the other for 1.013 MeV. Transfer the sample to a counting position that is 9.3 cm from the face of

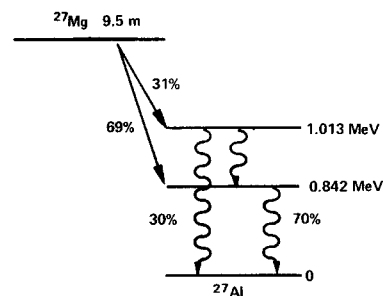


Fig. 18.2. Decay Scheme for Product of $^{27}\text{Al}(n,p)^{27}\text{Mg}$ Reaction.

the detector. Accumulate a spectrum in the MCA for a period of time long enough to have ~1500 counts under the 1.013-MeV peak.

EXERCISE

- b. Correct each of these sums by

$$\Sigma(\text{corrected}) = \frac{\Sigma}{\epsilon_p} \quad (8)$$

where ϵ_p is the intrinsic peak efficiency of the detector at that energy level (Fig. 3.6). The corrected sums should be in the ratio of 70% to 30% as stated above. Are they?

EXPERIMENT 18.2 Optional (n,p) Reactions that can be Studied

Procedure

Table 18.1 lists six (n,p) reactions from Sample Set No. 318 to be studied in the same manner as the $^{27}\text{Al}(n,p)^{27}\text{Mg}$ reaction of Experiment 18.1. All of the samples needed for the experiments outlined in Table 18.1 are contained in Sample Set No. 318.

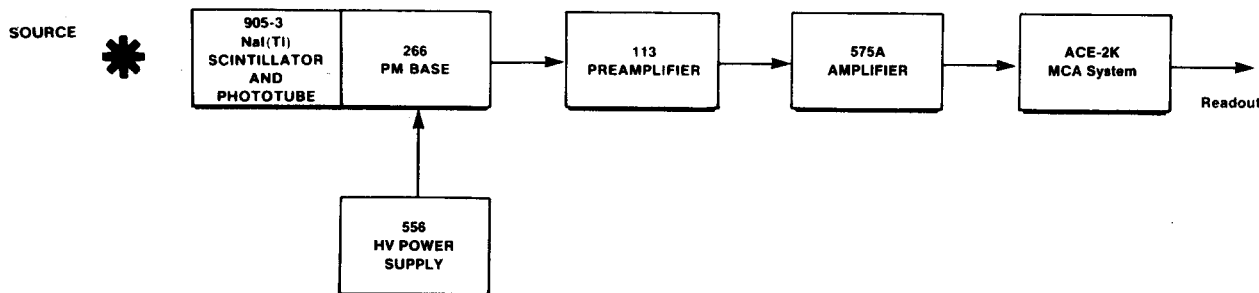


Fig. 18.1. Interconnection of Equipment for Experiment 18.

Table 18.1. Fast Neutron Activation Parameters for the Samples in Sample Set No. 318.

Element	Reaction	σ_{thms}	$T_{1/2}$	Measured γ (keV)	Activation Time	Counting Time (s)
Magnesium	$^{24}\text{Mg}(n,p)^{24}\text{Na}$	0.180	14.9 h	1370	4 h	1000
Sodium	$^{23}\text{Na}(n,p)^{23}\text{Ne}$	0.034	40.2 s	440	3 min	100
Silicon	$^{28}\text{Si}(n,p)^{28}\text{Al}$	0.220	2.3 min	1780	5 min	100
Vanadium	$^{51}\text{V}(n,p)^{51}\text{Ti}$	0.027	5.8 min	320,605	10 min	200
Iron	$^{56}\text{Fe}(n,p)^{56}\text{Mn}$	0.110	2.56 h	845,1810	4 h	1000
Chromium	$^{52}\text{Cr}(n,p)^{52}\text{V}$	0.080	3.76 min	1440	10 min	200

References

1. R. C. Koch, *Activation Analysis Handbook*, Academic Press, New York (1960).
2. D. S. Vorres, "Neutron Activation Experiments in Radiochemistry," *J. Chem. Ed.* **37**, 391 (1960).
3. W. S. Lyon, Ed., *A Guide to Activation Analysis*, D. Van Nostrand Co., Inc., New York (1964).
4. D. Taylor, *Neutron Irradiation and Activation Analysis*, D. Van Nostrand Co., Inc., New York (1964).
5. C. M. Lederer and V. S. Shirley, Eds., *Table of Isotopes*, 7th Edition, John Wiley and Sons, Inc., New York (1978).
6. *Chart of the Nuclides*, General Electric Co., modified by Battelle Northwest, Richland, Washington; available from Supt. of Documents, GPO, Washington, D.C.
7. G. I. Gleason, *Isotopic Neutron Source Experiments*, **ORAU-102** (1967). Available from Oak Ridge Associated Universities, P.O. Box 117, Oak Ridge, Tennessee 37830.
8. S. S. Nargolwalla and E. P. Przybylowicz, *Activation Analysis with Neutron Generators*, John Wiley and Sons, New York (1973).
9. H. E. Palmer, "Instrumentation for 'In Vivo' Activation Analysis," *IEEE Trans. Nucl. Sci.* **NS-17**(1) (1970).
10. J. M. A. Lenihan and S. J. Thomson, Eds., *Activation Analysis — Principles and Applications*, Academic, London (1965).

A Study of the Decay Scheme and Angular Correlation of ^{60}Co

EQUIPMENT NEEDED FROM EG&G ORTEC

- Two 113 Scintillation Preamplifiers
- Two 266 Photomultiplier Tube Bases
- Two Bins and Power Supplies
- 418A Universal Coincidence
- 426 Linear Gate
- 427A Delay Amplifier
- Two 556 High Voltage Power Supplies
- 480 Pulser
- Three 875 Counters
- Two 575A Amplifiers

- Two 551 Timing Single-Channel Analyzers
- 719 Timer
- Two 905-3 NaI(Tl) 2- x 2-in. Detectors with Phototubes
- ACE-2K MCA System including suitable IBM PC (other EG&G ORTEC MCAs may be used)
- Oscilloscope
- 10- μCi ^{60}Co gamma source
- Source Kit SK-1G
- 306 Gamma-Gamma Angular Correlation Table with fixed and rotating shield for the detectors
- ORC-19 Cable Set

Purpose

In this experiment the coincidence technique outlined in Experiments 9 and 13 will be used to study the gamma decay of ^{60}Co . Angular correlation concepts will also be introduced.

Introduction

There are two parts to Experiment 19: (1) a gamma-gamma coincidence experiment that will be performed to show that the two gammas from ^{60}Co are in coincidence and (2) measurement of the angular correlation of these two gammas and determination of the anisotropy and the coefficients of the correlation function. The decay scheme for ^{60}Co is shown in Fig. 19.1.

Note in Fig. 19.1 that the ^{60}Co beta decays to the 2.507-MeV level of ^{60}Ni and this de-excites by a gamma cascade through the 1.3325-MeV state. Since the lifetime of the 1.3325-MeV state is only 0.7 ps, the two gammas will appear to be in coincidence experimentally. Figure 19.2 shows an NaI(Tl) spectrum of ^{60}Co .

In order to verify that γ_1 and γ_2 are in coincidence, it is necessary to use the experimental techniques that were outlined in Experiment 13. Figure 19.3 shows the geometrical setup

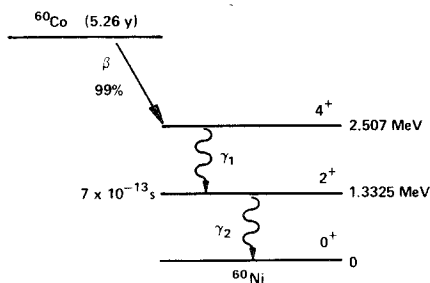


Fig. 19.1. Decay Scheme for ^{60}Co .

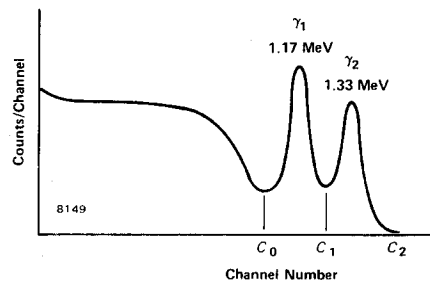


Fig. 19.2. NaI(Tl) Spectrum of ^{60}Co .

that will be used for both the γ_1 - γ_2 coincidence verification and the angular correlation measurement in this experiment.

Since the angular correlation of γ_1 and γ_2 is nearly isotropic, the angle θ in Fig. 19.3 can be set at any value for the coincidence verification. Usually the most convenient angle is 180° . A typical electronics setup for the measurement is shown in Fig. 19.4.

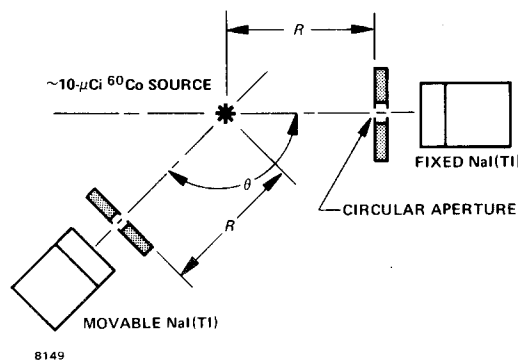


Fig. 19.3. Experimental Arrangement for Coincidence and Angular Correlation Measurements Using an EG&G ORTEC 306 Table.

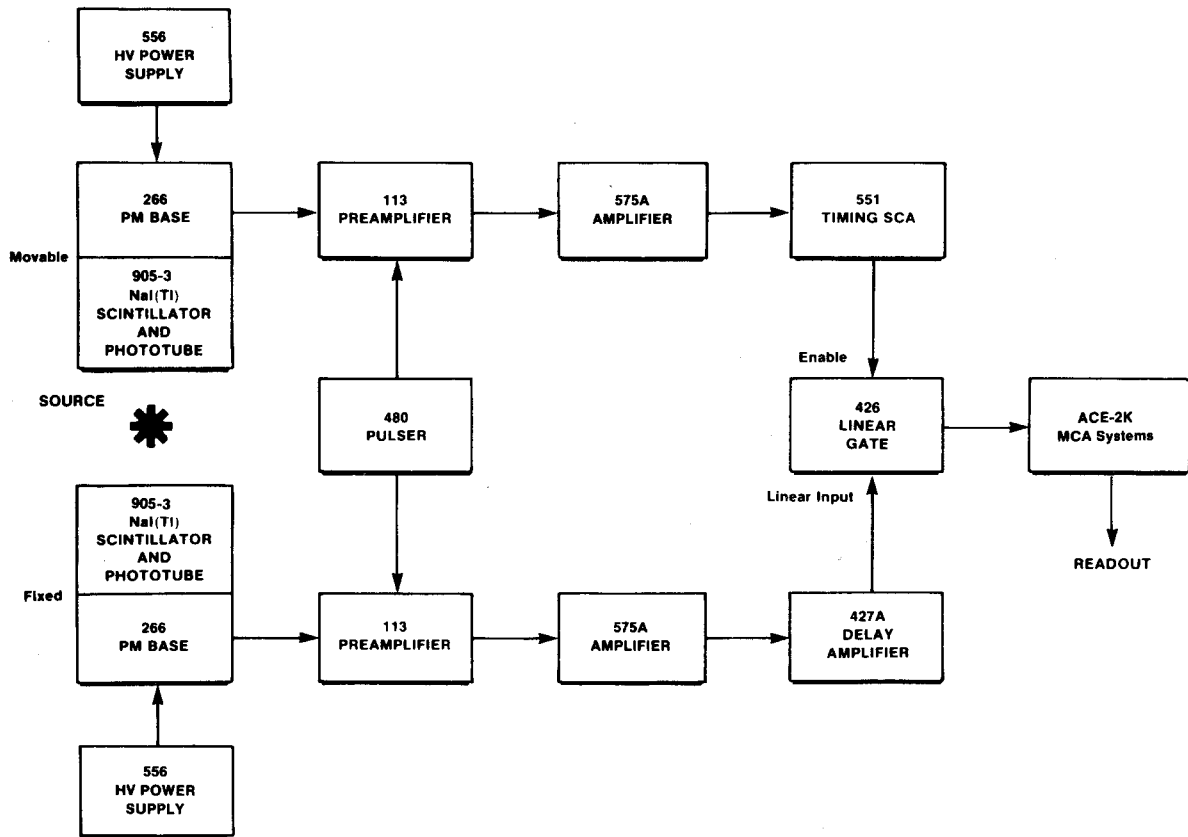


Fig. 19.4. Electronics for ⁶⁰Co Coincidence Experiment.

EXPERIMENT 19.1

Verification of the Gamma-Gamma Coincidence of ⁶⁰Co

Procedure

1. Set up the electronics as shown in Fig. 19.4. Adjust the 556 High Voltage Power Supplies to the values recommended for the 905-3 Detectors. Adjust the gain of each 575A Amplifier so that the 1.33-MeV gamma pulses at the output are ~6 V in amplitude. Figure 19.2 shows a typical spectrum that could be obtained from either amplifier output with an MCA.
2. Set the 551 Timing SCA for the Window mode and adjust its Lower- and Upper-Level controls to bracket the 1.17-MeV photopeak pulses. In Fig. 19.2, this is the region between C₀ and C₁. Use a 100-ns delay.
3. On the 426 Linear Gate, set the gate width at maximum (4 μs).
4. Turn on the pulse generator and adjust its pulse height, calibration, and attenuator controls to obtain output from the 551 Timing SCA.
5. Adjust the gate width on the 426 and the delay setting of the 427A so that the pulses out of the linear gate are similar

to Fig. 19.5. The combination will open the gate just before the linear input pulse arrives and will close it after ~2 μs. Turn off the pulse generator.

6. Accumulate a spectrum in the MCA. This spectrum should include only the 1.33-MeV peak and its Compton edge. The 1.17-MeV peak of Fig. 19.2 will be virtually eliminated. These results will show that the 1.17- and 1.33-MeV gammas are in coincidence because a 1.17-MeV gamma was required in the SCA in order to pass each 1.33-MeV pulse that was contributed into the spectrum.

7. Repeat the experiment with the 551 Timing SCA set to bracket the 1.33-MeV peak. Under these conditions, only the 1.17-MeV peak and its Compton should appear in the MCA spectrum. These two measurements verify that γ₁ and γ₂ in Fig. 19.1 are prompt cascade gammas. Experiment 19.2

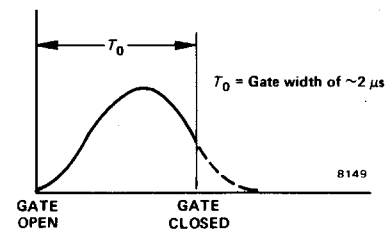


Fig. 19.5. Output of the Linear Gate.

describes the procedure necessary for studying their angular correlation.

EXPERIMENT 19.2

Angular Correlation of ⁶⁰Co

The Table of Isotopes (ref. 4) gives the spins of most of the nuclear levels that have been measured. Many of these spin assignments were made on the basis of angular correlation measurements. In the case of gamma-gamma angular correlation, an experimental arrangement similar to Fig. 19.3 is used. The fixed detector is set to measure only γ_1 , and the movable detector observes γ_2 . The number of coincidences between γ_1 and γ_2 is then determined as a function of θ (the angle between the two detectors). A plot of the number of coincidence events per unit time as a function of the angle, θ , is called the measured angular correlation. The measurement of γ_1 in a fixed direction determines nuclei which have an angular distribution of the resulting radiation, γ_2 , which is nonisotropic. This is a result of the nonisotropic distribution of spin orientations in ⁶⁰Co. Figure 19.1 shows that ⁶⁰Co beta decays to the 2.507-MeV, (4⁺) state which gamma branches through the 1.3325-MeV, (2⁺) state to the ground state, (0⁺), of ⁶⁰Ni.

These angular momenta determine the shape of the correlation function of the isotope. A complete discussion of the theoretical arguments associated with the angular correlation measurements is presented in refs. 1 and 2. The theoretical correlation function, $w(\theta)$, for ⁶⁰Co is given by

$$w(\theta) = a_0 + a_2 \cos^2\theta + a_4 \cos^4(\theta) , \quad (1)$$

where $a_0 = 1$, $a_2 = 1/8$, and $a_4 = 1/24$.

Table 19.1 shows the calculated values for $w(\theta)$ for angles between 90° and 180° in 10° increments for ⁶⁰Co.

It can be seen from Table 19.1 that the correlation function, $w(\theta)$, changes by only 17% from 90 to 180°. Therefore count-

Table 19.1. Angular Correlation Function $w(\theta)$ for ⁶⁰Co.

θ (deg)	$w(\theta)$
90	1.00000
100	1.00381
110	1.01519
120	1.03385
130	1.05876
140	1.08770
150	1.11719
160	1.14287
170	1.16042
180	1.16667

ing statistics of ~1% should be obtained when the experiment is performed.

The anisotropy, A, associated with an angular correlation measurement is defined as

$$A = \frac{w(180^\circ) - w(90^\circ)}{w(90^\circ)} . \quad (2)$$

A comparison of the experimental anisotropy with the theoretical value will reveal that angular correlation measurements are capable of rather high precision.

In this experiment the experimental angular correlation, $w(\theta)$, will be compared to Eq. (1) and the values shown in Table 19.1, and the calculated and measured anisotropy will be compared to Eq. (2).

Procedure

1. Set up the electronics as shown in Fig. 19.6. Adjust the gain of each 575A Amplifier for a bipolar output of ~6 V for the 1.33-MeV gamma pulses.
2. Set the resolving time of the 418A at 100 ns. Adjust the delays in the outputs of both 551 Timing SCAs so that the maximum coincidence counting rate is observed for pulses from the pulse generator. This technique is outlined in Experiments 9 and 13.
3. Set both 551 Timing SCAs for the Window mode and adjust the window widths. Set the window for pulses from the fixed detector so that it spans the 1.17-MeV peak. Set the window for the movable detector so that it spans the 1.33-MeV peak.
4. Set the angle, θ , carefully at 180° (Fig. 19.3). Turn off the pulse generator and accumulate a total count, N_T , through a period of time, t_i , that is long enough to obtain 1% statistics in the coincidence counter. Also measure the number of counts in the counters for the side channels. To determine the actual time coincidence rate a correction must be made for the number of accidental coincidence counts. Determine the accidental rate, N_{acc} , from the formula

$$N_{acc} = 2\tau N_1 N_2, \quad (3)$$

where

- τ = resolving time of the coincidence unit,
- N_1 = counting rate in the counter for the fixed detector,
- N_2 = counting rate in the counter for the movable detector.

The angular correlation function, $w(\theta)$, for 180° is then

$$w(\theta) = N_T - N_{acc} . \quad (4)$$

5. Repeat the measurements in step 4 and determine $w(\theta)$ for the other angles listed in Table 19.1. It is a good practice to repeat the measurement at 90° several times during the course of the experiment to ensure proper alignment of the system.

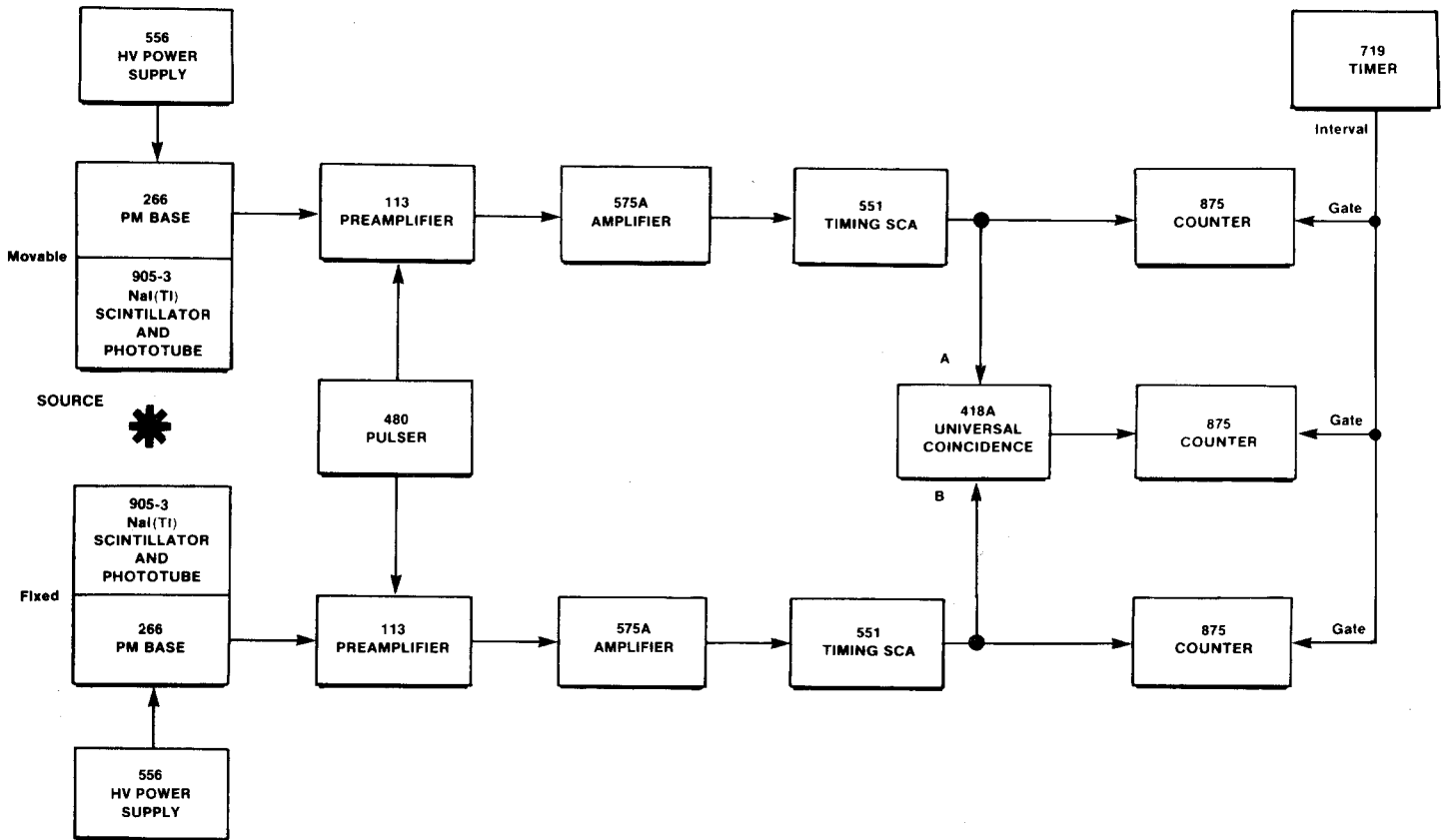


Fig. 19.6. Electronics for γ - γ Angular Correlation Measurements.

EXERCISES

a. In order to easily compare the experimental values with the theoretical values given by Eq. (1), it is more convenient to plot $G(\theta)$ vs θ , where $G(\theta)$ is calculated by

$$G(\theta) = \frac{w(\theta)}{w(90^\circ)} \quad (5)$$

Plot $G(\theta)$ experimental as a function of θ . Do the same for $G(\theta)$ theoretical from the data in Table 19.1. Figure 19.7 shows a typical set of experimental and theoretical data for this experiment.

b. Determine the anisotropy from the experimental data. How does this compare to the theoretical value?

c. Make a least-squares-fit to your data points and determine the experimental coefficients to the correlation function. How do your values compare with those in Eq. (1)?

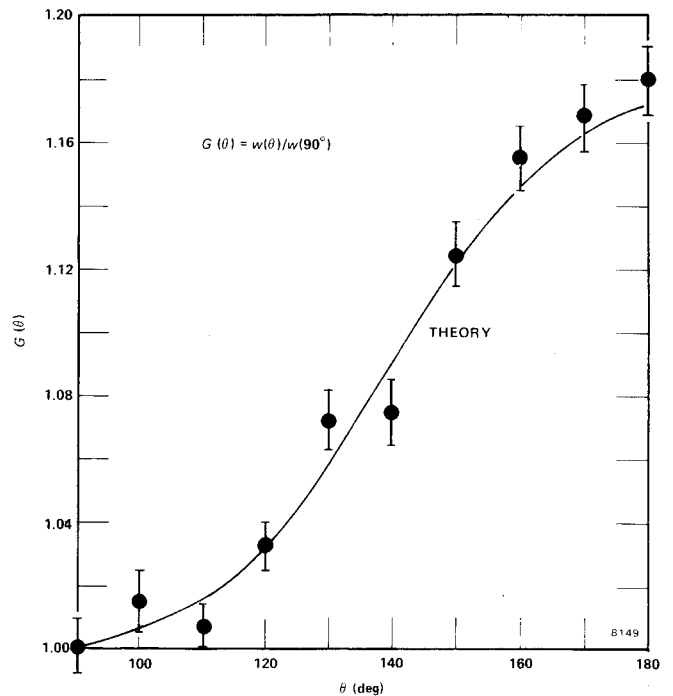


Fig. 19.7. Experimental and Theoretical Angular Correlation $w(\theta)$ from ^{60}Co .

References

1. A. C. Melissinos, *Experiments in Modern Physics*, Academic Press, New York (1966).
2. R. D. Evans, *The Atomic Nucleus*, McGraw-Hill, New York (1955).
3. H. A. Enge, *Introduction to Nuclear Physics*, Addison-Wesley, Massachusetts (1966).
4. C. M. Lederer and V. S. Shirley, Eds., *Table of Isotopes*, 7th Edition, John Wiley and Sons, Inc., New York (1978).
5. K. Siegbahn, Ed., *Alpha-, Beta-, and Gamma-Ray Spectroscopy*, North Holland Publishing Co., Amsterdam (1965).
6. P. Quittner, *Gamma Ray Spectroscopy*, Halsted Press, New York (1972).
7. W. Mann and S. Garfinkel, *Radioactivity and Its Measurement*, Van Nostrand-Reinhold, New York (1966).
8. G. F. Knoll, *Radiation Detection and Measurement*, John Wiley and Sons, New York (1979).
9. J. B. Marion and F. C. Young, *Nuclear Reaction Analysis*, John Wiley and Sons, New York (1968).

A Study of the Decay Scheme of ^{244}Cm by an Alpha X-Ray Coincidence Experiment

EQUIPMENT NEEDED FROM EG&G ORTEC

113 Scintillation Preamplifier
 142A Preamplifier
 266 Photomultiplier Tube Base Bin and Power Supply
 408A Biased Amplifier
 428 Detector Bias Supply
 556 High Voltage Power Supply
 480 Pulser
 Two 575A Amplifiers
 551 Timing Single Channel Analyzer
 427A Delay Amplifier

Surface Barrier Detector R-017-050-100
 ACE-2K MCA System including suitable IBM PC (other EG&G ORTEC MCAs may be used)
 Oscilloscope
 1 μCi ^{244}Cm
 905-1B Thin-Window NaI(Tl) Detector with PM Tube
 Mechanical Vacuum Pump
 305 Vacuum Can with Thin Plastic Window
 Source Kit SK-1X
 Source Kit SK-1A
 ORC-20 Cable Set

Purpose

This experiment demonstrates the technique of measuring the coincidence between alpha particles and x rays and verifies the alpha particle branching as indicated in ref. 4 for ^{244}Cm .

Introduction

Coincidence events such as (γ, γ) have been studied in previous experiments. The decay scheme of ^{244}Cm given in Fig. 20.1 shows that two alpha particle energies are present in the charged-particle spectrum. The energies are 5.806 MeV and 5.763 MeV. Figure 20.2 is a typical alpha spectrum of ^{244}Cm obtained with a surface barrier detector.

The details of making measurements with surface barrier detectors are covered in Experiment 4. The 43-keV level in Fig. 20.1 de-excites most of the time by internal conversion. The e_L/γ for this level is 760, which means there will be 760 conversion electrons for each 43-keV gamma. The internal conversion process has to be with the L or M electrons, since the binding energy of the K electron is 121.81 keV for ^{240}Pu . Therefore most of the time α_1 will be in coincidence with the L x rays resulting from the internal conversion process. This experiment will show that α_1 and only α_1 is coincident with the conversion electron x rays from this state.

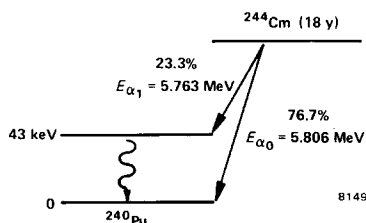


Fig. 20.1. Decay Scheme of ^{244}Cm .

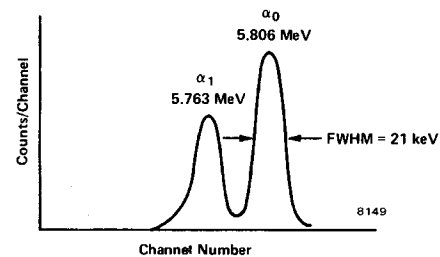


Fig. 20.2. Alpha Spectrum of ^{244}Cm .

Procedure

1. Connect the system as shown in Fig. 20.3. Connect the output of the 575A Amplifier on the NaI(Tl) detector side of the circuit to the MCA as shown by the broken line in the figure. Set the MCA Gate toggle switch at Off.
2. Adjust the 556 High Voltage as required for the thin-window NaI(Tl) detector and phototube.
3. Adjust the gain of the 575A Amplifier in the NaI(Tl) circuit so that the output will provide the spectrum on the MCA as shown in Fig. 20.4.

Note that the calibration points have been taken with the 6.4- and 14.4-keV lines from ^{57}Co and with the 32.2-keV x ray from ^{137}Cs . The x rays observed in Fig. 20.4 are the L conversion x rays resulting from the internal conversion of the 43-keV level in ^{240}Pu .

4. Set the 551 Timing Single Channel Analyzer for minimum delay of 0.1 μs . Adjust its window so that it brackets the 14.2- and 18.2-keV x-ray lines of Fig. 20.4. Use a calibrated 480 Pulser to aid in this adjustment.
5. Move the input connection for the MCA to the output of the 408A Biased Amplifier as shown by the solid line in Fig. 20.3. Leave the MCA Gate toggle switch at Off to permit calibration of the surface barrier detector side of the circuit.

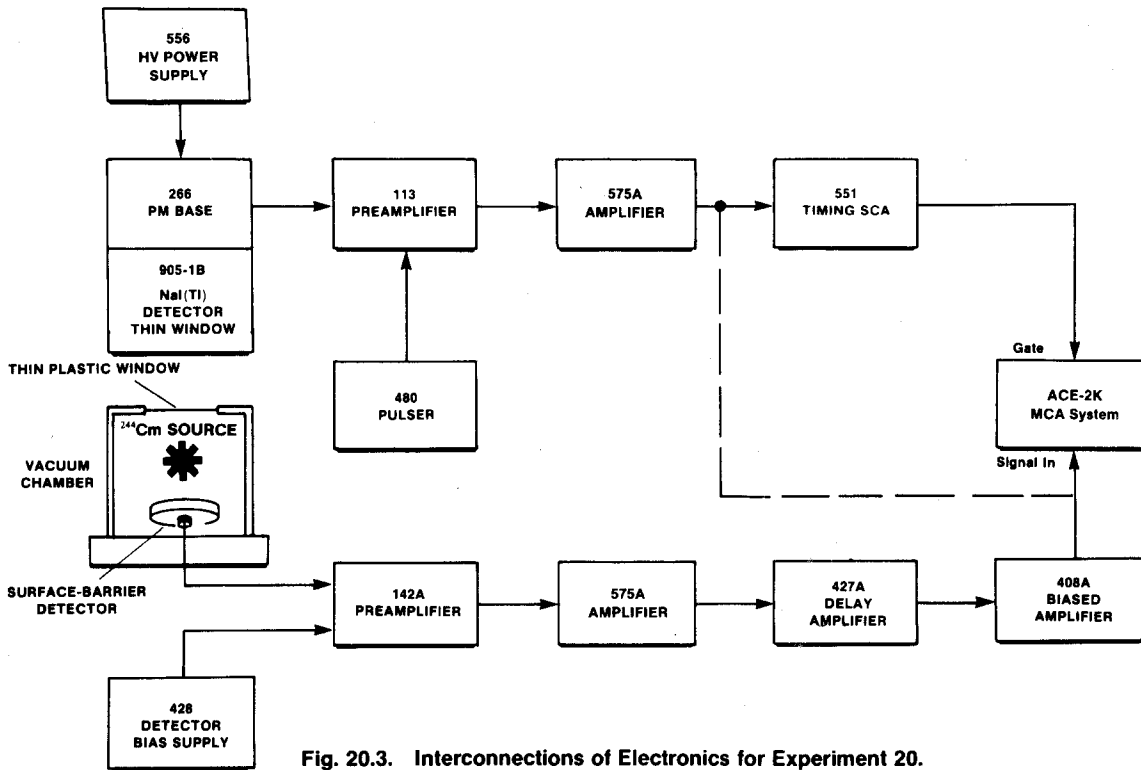


Fig. 20.3. Interconnections of Electronics for Experiment 20.

Remove the coincidence gate Input to the MCA as shown in Fig. 20.3. This allows for calibration of the surface barrier detector with the ²⁴⁴Cm lines.

6. Increase the 428 level slowly to the bias that is required for the surface barrier detector. Adjust the gain of the 575 Amplifier and the 408A Biased Amplifier on the surface barrier detector side of the circuit to obtain the alpha spectrum, similar to Fig. 20.2, in the MCA.

7. Reconnect the coincidence gate Input to the MCA.

8. Accumulate a spectrum on the MCA long enough to clearly see that the 5.806-MeV alpha is no longer present in

the spectrum. The resulting spectrum should resemble Fig. 20.5 because the 5.763-MeV alphas are in coincidence with the x rays and will be present in the spectrum but the 5.806-MeV alphas are not in coincidence with the x rays and are therefore not present in the spectrum.

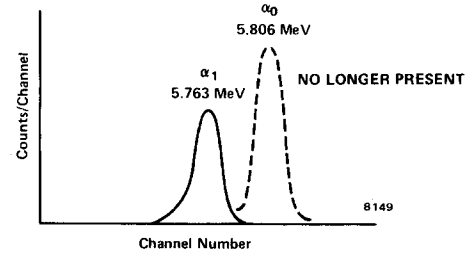


Fig. 20.5. Alpha Spectrum for ²⁴⁴Cm with X-Ray Coincidence Requirement.

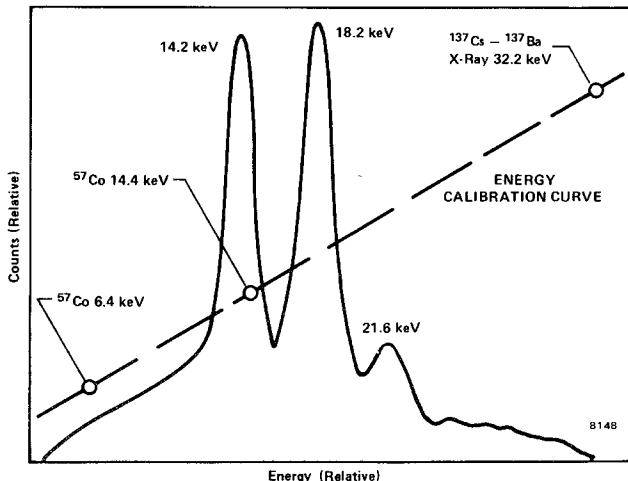


Fig. 20.4. Thin-Window NaI(Tl) Spectrum of ²⁴⁴Cm.

References

1. G. F. Knoll, *Radiation Detection and Measurement*, John Wiley and Sons, New York (1979).
2. K. Siegbahn, Ed., *Alpha-, Beta-, and Gamma-Ray Spectroscopy*, North Holland Publishing Co., Amsterdam (1965).
3. G. Dearnaley, "Nuclear Radiation Detection by Solid State Devices," *J. Sci. Instrum.*, **43**, 869 (1966).
4. C. M. Lederer and V. S. Shirley, Eds., *Table of Isotopes*, 7th Edition, John Wiley and Sons, Inc., New York (1978).
5. G. Bertolini and A. Coche, Eds., *Semiconductor Detectors*, American Elsevier Publishing Co., Inc. (1968).
6. R. D. Evans, *The Atomic Nucleus*, McGraw-Hill (1955).
7. A. C. Melissinos, *Experiments in Modern Physics*, Academic Press, New York (1966).

Alpha-Induced Innershell Ionization Studies with an ^{241}Am Source

EQUIPMENT NEEDED FROM EG&G ORTEC

Source Kits SK-1A and SK-1X

1 mCi ^{241}Am excitation source

Bin and Power Supply

Surface Barrier Detector A-016-100-100

Si(Li) Detector SLP-06175

142B Preamplifier

572 Amplifier

428 Bias Supply

Oscilloscope

480 Pulser

459 5-kV Detector Bias Supply

ACE-2K MCA System including suitable IBM PC (other EG&G ORTEC MCAs may be used)

Vacuum Pump

Model MAX-21 Chamber for innershell ionization studies with aluminum excitation foils and alpha absorber foils

807 Vacuum Chamber

ORC-21 Cable Set

Purpose

Alpha particles from an ^{241}Am source will be used to excite the characteristic x rays from an aluminum sample. Many of the techniques used in this experiment are the same as those used for Experiment 12, X-Ray Fluorescence. The major difference is that in Experiment 12, we used photons to excite the characteristic x rays whereas in this experiment alphas from an ^{241}Am source will be used. The experimental results of this experiment will be compared to theoretical calculations of Coulomb ionization for interaction of this type. We will also have to use the experimental techniques developed in Experiments 4, 5, and 8 to obtain the measurements in this experiment.

Introduction

The cross section for a reaction of a given type is defined to be the relative probability that an interaction will occur. In this experiment, alpha particles are allowed to bombard a thin foil of aluminum. As we saw in Experiment 5 (dE/dx measurements), the most probable event to occur when an alpha particle enters a foil is for it to lose energy by making Coulomb interactions with weakly-bound electrons. It is also possible for the alpha particle to interact with the more tightly bound K, L, or M electrons. If, for example, the Coulomb interaction occurs with the K shell electron, it can impart enough energy to completely remove this K shell electron. From the table of "X-Ray Critical Absorption and Emission Energies" in the Appendix of this manual, the binding energy of the K shell x ray in aluminum is only 1.559 keV. When this K shell electron is removed, the vacancy is immediately filled by an electron falling down from a higher orbit or an Auger transition. Auger electrons are given off when the energy difference between the two levels involved is used to eject electrons in outer-lying shells. The ratio of x rays emitted to vacancies produced is called the fluorescence yield. The probability of producing an x ray by alpha particle bombardment is quite high when it is compared to the probability of a nuclear interaction.

In this manual, one of the largest nuclear cross sections that we have dealt with is the slow neutron cross section, (5 barns), for $^{51}\text{V}(n,\gamma)^{52}\text{V}$ in Experiment 17. This is to be contrasted with Fig. 21.1 which shows that the ionization cross section for 5-MeV alphas on a manganese target is ~ 400 barns.

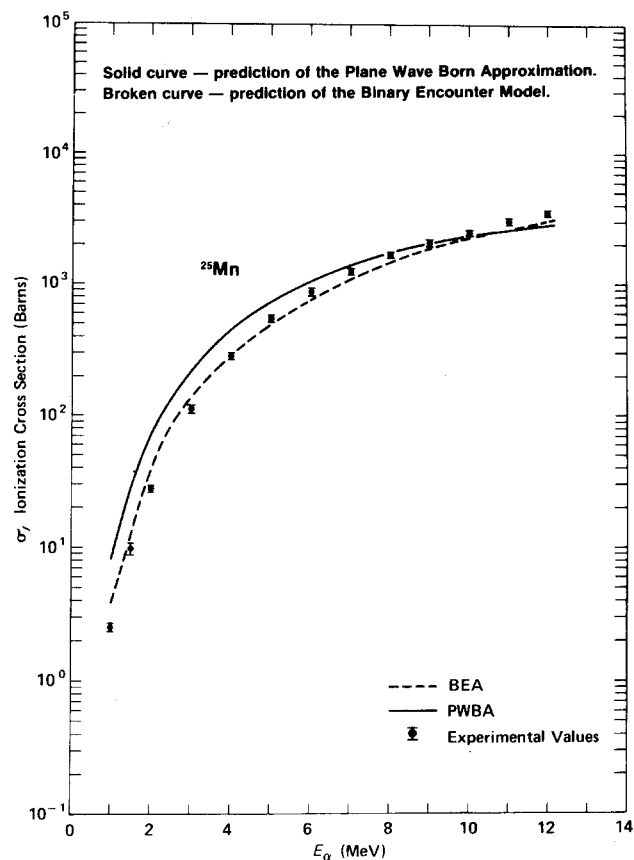


Fig. 21.1. K Shell Ionization Cross Section for Manganese by Alpha Impact.

EXPERIMENT 21.1

Innershell Ionization Induced by Alpha Particles

In this experiment it is necessary to measure the ionization cross section as a function of the alpha energy (Fig. 21.1).

The energy of the incident alpha particles from the source will be changed by inserting thin Mylar absorbers between the source and the target. These absorbers are supplied with the target chamber. Each foil has a thickness of $2.29 \times 10^{-4} \text{ g/cm}^2 \pm 5\%$. Our first problem is to find the energy of the alphas from the source. Figure 4.8 in Experiment 4 shows the spectrum of alphas from a thin ^{241}Am source. The maximum energy is 5.48 MeV. The spectrum will look quite different for the 1 mCi source used in this experiment. The 5.48-MeV alphas will be attenuated before they get out of this thick source. This attenuation is produced by dE/dx in the source material itself and the material that is used to seal the source. Therefore the alpha group will appear at ~ 4.5 MeV. In this experiment the exact energy of the alphas will be determined from the source and also their energy after they have been attenuated with Mylar foils.

Procedure

1. Set up the 807 vacuum can with the electronics used in Experiment 4 (Fig. 4.7). Place the ^{241}Am source from source kit SK-1A ~ 40 mm from the detector. Pump down, apply the bias, and adjust the gain of the 572 Amplifier so that the 5.48-MeV alpha is being stored in the upper quadrant of the MCA (approximately channel 800). Turn on the pulse generator and calibrate the pulser so that 548/1000 on the pulse-height dial corresponds to the same channel where the 5.48-MeV alpha peak was being stored. With the aid of the 480 Pulser, make a calibration curve for the MCA.

2. Turn off the bias, let the system up to air, and remove the weak ^{241}Am source from the chamber. Put the "hot" 1-mCi source in the 807 chamber and measure its spectrum. Reproduce the geometry that will ultimately be used in the innershell ionization studies (Fig. 21.2). The plane passing through the source should be 40 mm from the parallel plane

passing through the face of the detector. The source is off-axis by 18 mm. Under these conditions the source will be 44 mm from the center of the detector and the geometry of Fig. 21.2 has been reproduced. Evacuate the system and turn on the bias. Accumulate a spectrum in the MCA and determine the energy of the peak. Record this value; it will be our first excitation energy (no absorber) when we do the ionization experiment. We would also like to find the number of alphas/s that bombard the detector under these geometrical conditions. Note, the detector has been chosen, (100 mm^2), so that it is the same size as the aluminum target that will be used in the ionization experiment. From the MCA determine the number of alphas/s that are counted. Remember this is a "hot" source, so analyzer dead time corrections must be made. Record the number of alphas/s in Table 21.1.

3. Lower the bias to zero, let the system up to air, and place the first Mylar foil over the source. Pump down, turn on the bias, and determine the number of alphas/s and the energy of the peak. Repeat for all seven absorbers and record all data in Table 21.1. A plot of these peaks would look similar to Fig. 5.5 in Experiment 5.

EXPERIMENT 21.2

Efficiency of the Si(Li) Detector

In Experiment 8.2 the efficiency of a Si(Li) detector was measured. The student should read all of Experiment 8 before proceeding with this experiment. The sources that will be used for this calibration are the x-ray sources from source kit SK-1X, that is, ^{57}Co , ^{54}Mn , and ^{65}Zn .

Procedure

1. The chamber shown in Fig. 21.2 will be used for this experiment. Set up the electronics as shown in Fig. 21.2. Do not put the 1-mCi ^{241}Am source in the chamber. Place the ^{57}Co source from the source kit directly on top of the aluminum target in Fig. 21.2. Evacuate and adjust the gain of the 572 Amplifier so that the 5.9-keV peak is being stored at around channel 500. Figure 8.4 shows the spectrum. Determine the channel position of both peaks and the total num-

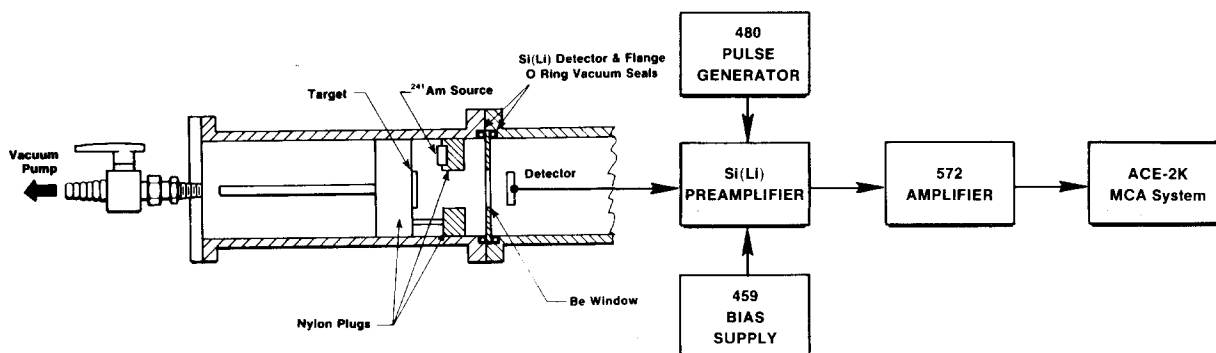


Fig. 21.2. Chamber for Innershell Ionization Studies with Electronics.

Table 21.1. Innershell Ionization Measurement Data.

Mylar Absorbers	E_α Measured	N_i Alphas/s (on the target)	Σ X Rays/s	σ_x Experimental	σ_x Theory
No Absorber					
1					
2					
3					
4					
5					
6					
7					

ber of x rays/s. Repeat for the ^{54}Mn and ^{65}Zn sources in the source kit.

2. Make an energy calibration curve. From the known number of x rays for each source (Table 21.2) and Experiment 8.2, plot the efficiency, E, for the three K_α lines for these isotopes. Please note that the intensity ratios, X/γ , shown in Table 21.2 include K_α and K_β in the summation.

Table 21.2. Energy and X-Ray Intensity Ratios of ^{54}Mn , ^{57}Co , and ^{65}Zn .

Nuclide	Energy of X-Rays and Low-Energy Gamma (keV)	Energy of High-Energy Gamma (keV)	Intensity Ratio X/γ
^{54}Mn	5.414 (K_α)	834.8	0.2514 ($\pm 0.5\%$) $K_\alpha + K_\beta$
	5.946 (K_β)		
^{57}Co	6.40 (K_α)	122.1	0.5727 ($\pm 2.0\%$)
	7.06 (K_β)		0.7861 ($\pm 2.9\%$)
	14.41 (γ)		0.112 ($\pm 1.8\%$)
^{65}Zn	8.04 (K_α)	1115.5	0.6596 ($\pm 0.8\%$)
	8.9 (K_β)		0.0911 ($\pm 2.0\%$)

3. The aluminum K_α line has an energy of 1.487 keV. The lowest point on the efficiency data above is 5.414 keV from the ^{54}Mn source. The efficiency of the detector can be calculated for the aluminum K_α line and normalized to the above experimental data to give the complete efficiency curve. This method has been described extensively in the literature (refs. 9 and 10). Figure 8.2 (Experiment 8) shows the window cutoff effect which completely dominates the efficiency at these low energies. For the detector used in this experiment the window attenuation can be calculated from the following:

$$I = I_0 \exp(-\Sigma \mu_i x_i), \quad (1)$$

where the μ_i are the linear absorption coefficients for the various window parameters and the x_i are the quoted thicknesses of these parameters from the detector specification sheets. For the detector used in this experiment these parameters consist of: the Be entrance window, the gold contact (2.2 μm), and the silicon dead layer (0.5 μm). There is also a Mylar entrance window (2.54 μm) on the chamber. The linear absorption coefficients of all of these materials are given in ref. 11.

Figure 21.3 shows an efficiency curve for a Si(Li) detector with a thick (10 mil) piece of Mylar between the target and the entrance window of the detector. The dashed portion of the curve is the part that was calculated with the attenuation equations. In our case the normalization would be to the ^{54}Mn K_α line at 5.414 keV.

For a typical 0.5×10^{-3} in. Be window detector, the efficiency, E, for the aluminum K_α was calculated to be 1.72×10^{-4} . The value that you calculate for your detector may be slightly different depending on the Be entrance window thickness, etc.

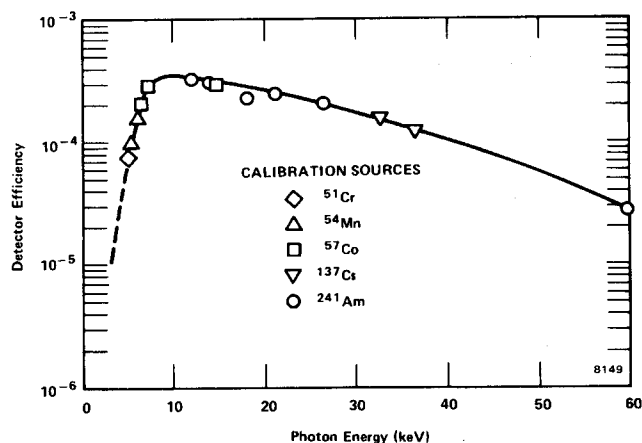


Fig. 21.3. Typical Si(Li) Detector Efficiency Curve (using 10-mil Mylar absorber).

EXPERIMENT 21.3

The Innershell Ionization Measurements

Procedure

1. Remove the x-ray calibration sources and place the 1-mCi ²⁴¹Am source in the chamber (no Mylar absorber). Pump back down and accumulate a spectrum for a time period long enough to record 2000 counts in the 1.48-keV aluminum K_α. Figure 21.4 shows a typical pulse height spectrum of an alpha excited aluminum K_α x ray. Record the number of x rays/s in Table 21.1.

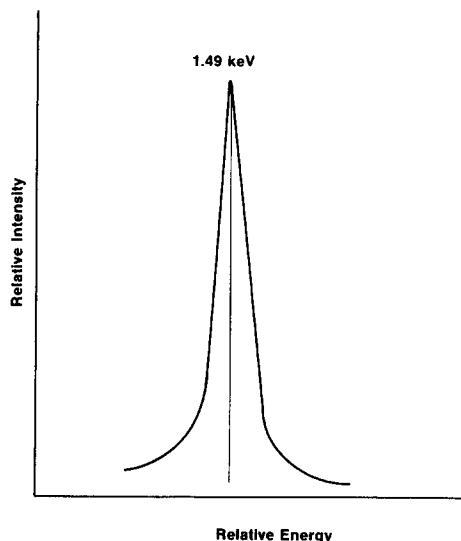


Fig. 21.4. Characteristic K X-Ray Spectrum for Alpha Particles on Aluminum.

- Open the vacuum system and place the first Mylar foil over the ²⁴¹Am source and accumulate a spectrum. Repeat for all the foils in the foil kit. Record the data in Table 21.1.
- At this time the experimental cross section can be calculated. The experimental x-ray production cross section is given by:

$$\sigma_x = \frac{\Sigma_x}{N_0 N_1 \epsilon} \quad (2)$$

where Σ_x is the number of aluminum x rays/s minus the background, N_0 is the number of target nuclei/cm², N_1 is the number of alphas/s that bombard the target, and ϵ is the Si(Li) detector efficiency. We have previously measured everything except N_0 . The aluminum target foil is 2.6×10^{-4} g/cm² which gives $N_0 = 5.9 \times 10^{18}$ atoms/cm². You can now calculate σ_x for all of the incident alpha energies that were used for the experiment. Record these values as σ_x (Experimental) in Table 21.1.

4. Table 21.3 shows the theoretical values for the x-ray production cross section for alphas on aluminum.

Table 21.3. σ_x (Theory) Plane Wave Born Approximation, (PBWA), Calculations.

[Cross sections are x-ray production, W_k , (Fluorescence Yield) = 0.039 for aluminum. (These calculations are easily done from the formulas outlined in refs. 5, 12, 13, and 14.)]

E_α (MeV)	σ_x (theory) (barns)
5.0	3.18×10^3
4.5	2.98×10^3
4.0	2.71×10^3
3.5	2.37×10^3
3.0	2.00×10^3
2.5	1.59×10^3
2.0	1.21×10^3
1.5	0.72×10^3
1.0	0.33×10^3

These theoretical cross sections are presented in the literature (refs. 5, 12, 13, and 14) in such a manner that a student can do the simple calculations and thus determine the values shown in Table 21.3. From Table 21.3 plot σ_x vs E_α (theory) and plot the measured σ_x vs E_α (experimental) from Table 21.1. The final plot, Fig. 21.5, compares the theoretical (PWBA) curve and the experimental points.

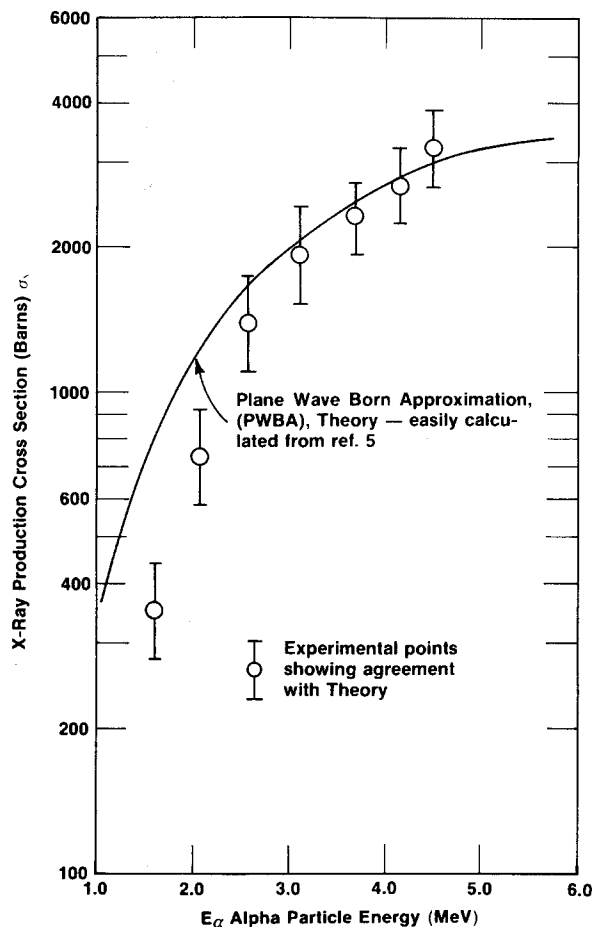


Fig. 21.5. Aluminum X-Ray Production Cross Section vs Alpha Particle Energy.

References

1. L. C. Northcliffe and R. F. Schilling, *Nuclear Data Tables* **A7**, 233, Academic Press, New York (1970).
2. J. L. Campbell and L. A. McNelles, *Nucl. Instrum. Methods* **125**, 205 (1975).
3. W. J. Gallagher and S. J. Cipola, *Nucl. Instrum. Methods* **122**, 405 (1974).
4. J. L. Duggan, W. D. Adams, R. J. Scroggs, and L. S. Anthony, *Am. J. Phys.* **35**, 631 (1967).
5. E. Merzbacher and H. W. Lewis, S. Flugge, Ed., *Handb. Phys.* **34**, 166, Berlin: Springer-Verlag (1958).
6. G. F. Knoll, *Radiation Detection and Measurement*, John Wiley and Sons, New York (1979).
7. R. J. Gehrke and R. A. Lokken, *Nucl. Instrum. Methods* **97**, 219 (1971).
8. R. H. McKnight, et. al., *Phys. Rev.* **A9**, 267 (1974).
9. G. Hubricht, B. Knaf, G. Presser, and J. Stahler, *Nucl. Instrum. Methods* **144**, 359 (1977).
10. B. Rosner, D. Gur, and L. Shabason, *Nucl. Instrum. Methods* **131**, 81 (1975).
11. W. J. Veigele, *Atomic Data* **5**, 51 (1973).
12. G. Basbas, W. Brandt, and R. Laubert, *Phys. Rev.* **A7**, 983 (1973).
13. G. Monigold, F. D. McDaniel, J. L. Duggan, et al., *Phys. Rev.* **A18**, 380 (1978).
14. G. S. Khandelwal, B. H. Chol, and E. Merzbacher, *Atomic Data* **1**, 103 (1969).

Acknowledgment

The author wishes to express his appreciation to Professor Dollard Desmarais of the University of Alberta, Canada for his work in helping to develop this experiment. Professor Desmarais and the author are publishing a detailed version of this experiment. The article will appear in the *American Journal of Physics* in the summer of 1984.

Measurements in Radiation Biology and Nuclear Medicine Training

EQUIPMENT NEEDED FROM EG&G ORTEC

Bin and Power Supply
 905-3 2- by 2-in. NaI(Tl) Crystal and Phototube
 266 Photomultiplier Tube Base
 556 High Voltage Power Supply
 113 Scintillation Preamplifier
 ACE-2K MCA System including suitable IBM PC (other EG&G ORTEC MCAs may be used)
 575A Amplifier
 719 Timer
 875 Counter
 903 End-Window Geiger Tube
 906 GM Inverter

Two pieces of PbPI-3 (see Appendix)
 Source Kit SK-1G (see Appendix)
 Ten pieces of PnPI-1 (see Appendix)
 25 μCi ^{131}I as sodium iodide for thyroid uptake test
 100 μCi ^{32}P as sodium phosphate for plant studies
 One large white laboratory rat (~300 g)
 Ten young bean plants with 7 or 8 leaves on each plant
 Miscellaneous radiobiological supplies such as syringes, pipettes, rubber gloves, filter paper, dissecting trays, animal boards, lead storage containers
 ORC-22 Cable Set
 Oscilloscope

Introduction

In radiation biology and nuclear medicine, as well as in radiation chemistry, it is often convenient to use radioisotope tracers. A radioisotope tracer is, generally, a chemical compound that contains at least one radioactive component. The amount of the radioactive chemical component that is present in the tracer should be related to the complexity and type of experiment that is to be performed. In terms of the atom, its chemical and biological behavior is determined for the most part by its orbiting electrons. Two isotopes, for example ^{12}C and ^{14}C , will enter into identical chemical reactions in a biological system because their electronic structure is the same. However, ^{14}C is radioactive, and so it can be traced as it goes through its complex biochemical reactions in the animal or plant system that is being studied.

Therefore, when it is necessary to study the behavior of a particular chemical or molecular configuration, a sample can be synthesized with a small fraction of one of the elements replaced by a radioactive element in an amount and with a half-life that is compatible with the necessary measurement for the experiment. The compound is then assayed for its specific activity and is introduced into the system being studied.

For most radiobiological and medical studies, isotopes that decay by betas or gammas are used. Gammas are quite penetrating and so, where applicable, gamma-emitting isotopes can be used in "in vivo" studies. This means, for example, an isotope is injected into a patient or an animal and a gamma counter is used to follow the rate and/or concentration of the isotope as a function of time. Normally, the activity rate of the tracers is so small that an animal or patient is not even aware of the fact that measurements are being made. On the other hand, particularly for beta-emitting isotopes, it is frequently necessary to perform "in vitro" measurements where a sample must be physically removed from a plant or animal and measured externally with a counter.

Table 22.1 lists the most commonly used radioisotopes for these studies.

In this series of experiments, we will study some geometrical considerations in radiobiological and medical applications and perform some simple plant and animal experiments with radioactive tracers.

Table 22.1. The Most Common Isotopes Used in Radiation Biology.

Isotope	Type of Radiation	Half-Life
^3H	beta	12.3 years
^{14}C	beta	5570 years
^{51}Cr	gamma	27.8 days
$^{99\text{m}}\text{Tc}$	gamma	6.0 hours
^{131}I	gamma	8.07 days
^{198}Au	gamma	2.7 days

EXPERIMENT 22.1

Geometrical Considerations in Radiobiological and Medical Experiments

Purpose

For many bio-tracer experiments the measurements can be made in vivo. For example, in Experiment 22.2 we will study the uptake of ^{131}I in the thyroid. For these measurements the major source of radioactivity is the thyroid gland, which is surrounded by flesh and tissue. There are also bones close to the gland, and they can cause Compton scattering and hence distort the measured spectra.

In this experiment, we will study some of the effects that are observed when there is material between the source and the detector or surrounding the source.

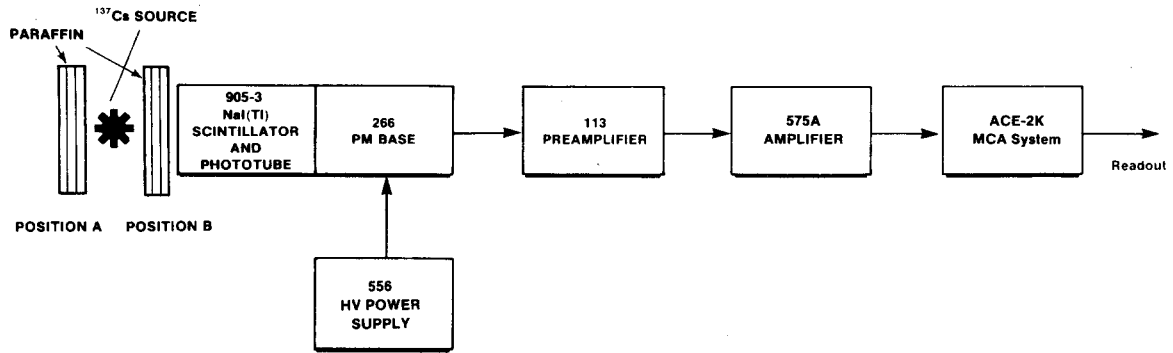


Fig. 22.1. Gamma-Spectra Measurements with Material Surrounding the Source.

Procedure

1. Set up the electronics and physical arrangement as shown in Fig. 22.1. Be sure to allow room between the source and the detector for inserting five pieces of 1/2-in. thick paraffin during the experiment.
2. Adjust the gain of the amplifier and the high voltage for the phototube so that the photopeak for ^{137}Cs (from the Source Kit) is near channel 300; this procedure was outlined in Experiment 3.
3. Store a spectrum in the MCA for a period of time long enough to obtain 1000 counts at the top of the photopeak. Figure 22.2 (the solid line) shows a typical ^{137}Cs spectrum. Read the data out of the MCA. Clear the analyzer to zero.
4. Place the first piece of paraffin in position A, Fig. 22.1, and store a spectrum for the same amount of time that was used in step 2. Read the data out of the analyzer and clear to zero.
5. Repeat step 4 with two, three, four, and then five pieces of paraffin in position A, Fig. 22.1.

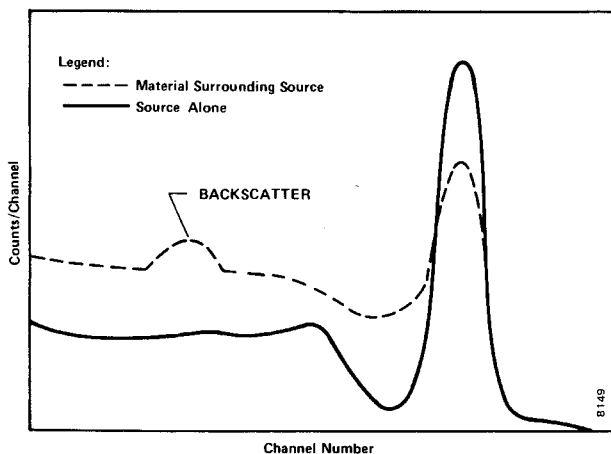


Fig. 22.2. NaI(Tl) Spectra with ^{137}Cs Source Alone and with Paraffin Surrounding the Source.

6. Without disturbing the paraffin in position A, place the first piece of paraffin in position B. Count for the same time period used in steps 2 and 3. Read the data out of the analyzer and clear to zero.
7. Repeat step 6 for two, three, four, and five pieces of paraffin in position B.

EXERCISES

- a. Plot on semilog paper the spectra recorded in step 2, with no paraffin. On the same graph paper, use different symbols and plot only the backscatter portion of the rest of the spectra measured in steps 2 and 3. Note that the photopeak remains the same for all spectra taken with paraffin in position A, but the backscatter is enhanced as the thickness of paraffin is increased.
- b. On another piece of semilog paper, plot again the spectrum taken with the source and with five pieces of paraffin in position A. On the same sheet, plot the spectrum that was taken with all five pieces of paraffin in position B. The broken line in Fig. 22.2 is a typical ^{137}Cs spectrum that was measured in this manner.
- c. Integrate the counts in the photopeaks of the spectra measured in steps 6 and 7 and make a linear plot of counts vs paraffin thickness.

Summary

In vivo biological and medical measurements almost always result in distorted scintillation measurements because materials between the source and the detector can be expected to eliminate some counts from the peak and also enhance the Compton scattering distribution. The distortion is produced by the photoelectric effect and Compton scattering in the material that surrounds the effective source in the biological sample that is being studied. However, by knowing the magnitude of these distortions, accurate biological measurements can still be made for most systems.

EXPERIMENT 22.2

 ^{131}I Uptake Studies in Rats

Purpose

A rather high percentage of the natural iodine in an animal's body is concentrated in the thyroid gland. If a solution of sodium iodide that is labeled with ^{131}I is injected into a rat, about 30% of it is accumulated quickly in the thyroid gland. Most of the remainder will be excreted as urine by the animal. A counter held over the thyroid will begin to register ^{131}I gammas almost immediately after injection of the animal. The purpose of this experiment is to study the concentration in the thyroid gland of the injected ^{131}I as a function of time. In vitro measurements will also be made to show the relative concentration of ^{131}I in other organs, compared to that in the thyroid.

Procedure

1. Pipette about $1\ \mu\text{Ci}$ of ^{131}I from your stock solution onto a counting card and dry it with a heat lamp. Cover the source with a thin piece of Mylar. This will be used as a calibration source.
2. Set up the electronics as shown in Fig. 22.1. Place the $1\text{-}\mu\text{Ci}$ source card 2 cm from the detector.
3. Set the 456 High Voltage for the value that is recommended for the phototube in the 905-3 detector. Adjust the amplifier gain so that a spectrum similar to Fig. 22.3 is obtained. For this experiment, the 364-keV and 280-keV lines will be used (see Fig. 22.4 for the decay scheme of ^{131}I to ^{131}Xe). Readjust the amplifier gain to place the 364-keV gamma line in about channel 200. Store a spectrum in the MCA for a period of time long enough to have the peak height in the 364-keV line at ~ 1000 counts. Read the data out of the analyzer. Do not clear to zero.

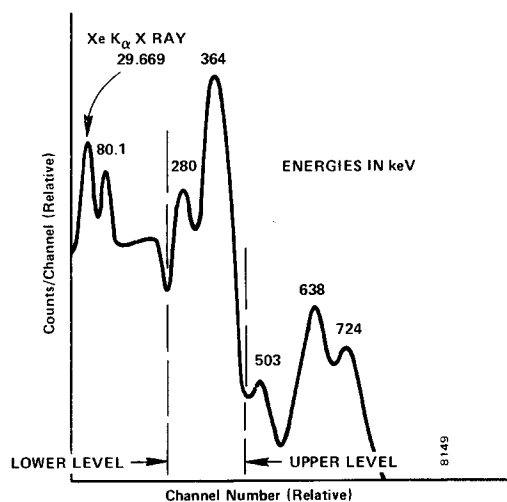


Fig. 22.3. Sodium Iodide Spectrum of ^{131}I Showing Major Lines and the ^{131}Xe X Rays.

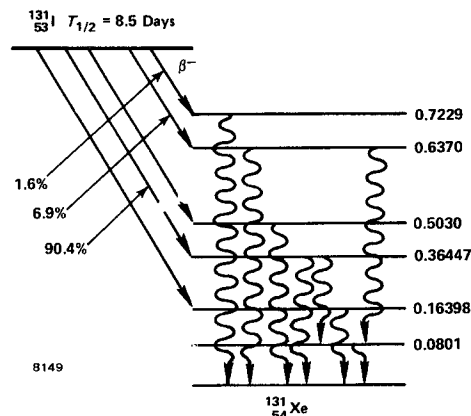


Fig. 22.4. Decay Scheme for ^{131}I Showing Major Gamma-Ray Energies.

4. Set the ROI of the MCA so that it brackets the 364- and 280-keV peaks (Fig. 22.3). You are now ready to do the ^{131}I uptake study with the rat.
5. Anesthetize the white rat carefully with ether. Fasten the rat to the dissecting tray on its back, using rubber bands to hold the legs to the tray.
6. Inject the animal intraperitoneally with about $5\ \mu\text{Ci}$ of the radioactive sodium iodide solution. Record the time of injection. From this point, it is necessary to keep the animal anesthetized only during counting intervals. Do not over-anesthetize the animal.
7. Support a 1-in. lead sheet over the animal's body to shield all but the neck area from the detector. Place the detector 3 in. above the neck of the animal, where the thyroid is located.
8. Set the preset time controls on the MCA for 80 seconds. Take spectra at 10-minute intervals, using 80 seconds for each accumulation. Read out the data and clear the analyzer after each counting period. Plot the number of counts as a function of time and continue to take counts until the counting rate has peaked and has fallen $\sim 10\%$ below the maximum.
9. Wait two hours after the above experiments have been completed and then sacrifice the animal with ether. Dissect it and remove the thyroid, kidney, liver, spleen, stomach, and heart. Dry the organs with blotting paper. Place them, one at a time, on counting planchets at a distance of 2 in. from the 905-3 crystal and count for 400 seconds. For each organ, determine the counts per minute per gram of organ.
10. Count the $1\text{-}\mu\text{Ci}$ standard ^{131}I card with the same geometry as was used for the organs (400 seconds).

EXERCISES

- a. From your plot of ^{131}I uptake as a function of time, determine the time required for maximum uptake for your animal.

b. Calculate the percentage of the original $5 \mu\text{Ci}$ of ^{131}I that is found in each of the organs. This can be done by comparing the total count for an organ to five times the count obtained on the $1\text{-}\mu\text{Ci}$ counting card since the injection was $5 \mu\text{Ci}$.

EXPERIMENT 22.3

Translocation of Radio-Phosphorus in Plants

The use of radioactive tracer techniques in agriculture and plant study has given us a rather accurate account of some of the basic physiological processes that occur during plant metabolism. The study of uptake of mineral elements by plants and their subsequent incorporation in plant tissues have also been advanced greatly by use of these tracer techniques. Measurements in the translocation of organic compounds elaborated during photosynthesis and respiration are now fairly well understood, at least partly because of radioactive tracer studies.

A plant, like any other organism, is not capable of distinguishing between different isotopes of the same element. It will therefore metabolize radioactive phosphorus exactly the same way it would the stable isotope of the element. For these studies, ^{32}P is an ideal isotope to use either *in vivo* or *in vitro*. It decays by pure beta emission directly to the ground state of ^{32}S . The half-life of ^{32}P is 14.3 days and its beta end-point energy is 1.707 MeV.

Purpose

To study the translocation of phosphorus in young bean plants by counting the 1.707-MeV betas from ^{32}P with a Geiger Mueller counting system.

Procedure

1. Young bean plants should be used for this experiment. The seeds should be germinated and grown in the proper

nutrient until the young plants have 7 or 8 leaves before they are ready for the experiment. Remove the plants carefully from the soil in which they were grown and wash all soil from the roots. Place a group of 5 plants in each of two flasks so that the root systems and stems are accommodated in the flasks and the leaves are outside the flasks.

2. Mix $20 \mu\text{Ci}$ of ^{32}P -labeled sodium phosphate with enough water to cover all of the plant roots in the flasks. Do not add the solution to the flasks until the counting system is ready for use.

3. Set up the electronics as shown in Fig. 22.5. Adjust the 556 High Voltage Power Supply to the level that is to be used for the 903 Geiger Tube and set the 719 Timer for 1-min. counting intervals. Test the system with a $1\text{-}\mu\text{Ci}$ ^{32}P counting card (see Experiment 22.2, step 1, for this procedure).

4. Position the 903 Geiger Tube ~ 1 cm from one of the large young plant leaves. Be sure that it is properly shielded from the solution that is added to the flasks to cover the roots at this time. Take 1-min. counts every 10 min. for ~ 3 h and record each count total.

5. After ~ 24 h, remove all plants from their radioactive solutions. Carefully wash the roots and prepare the plants for dissecting. From several of the plants that seem to have survived best, dissect roots, stems, and leaves, and keep the items separated.

6. Carefully weigh the roots and place them in a counting planchet. Use enough to cover an area of ~ 1 sq. in. on the planchet. Place the planchet 2 cm from the Geiger tube and take a 5-min. count. Repeat for other groups of roots. From these measurements determine the number of counts per minute per gram of roots.

7. Repeat step 5 for stems and then for leaves.

8. Place the $1\text{-}\mu\text{Ci}$ standard ^{32}P counting card 2 cm from the Geiger tube window and determine the number of counts per minute for the standard.

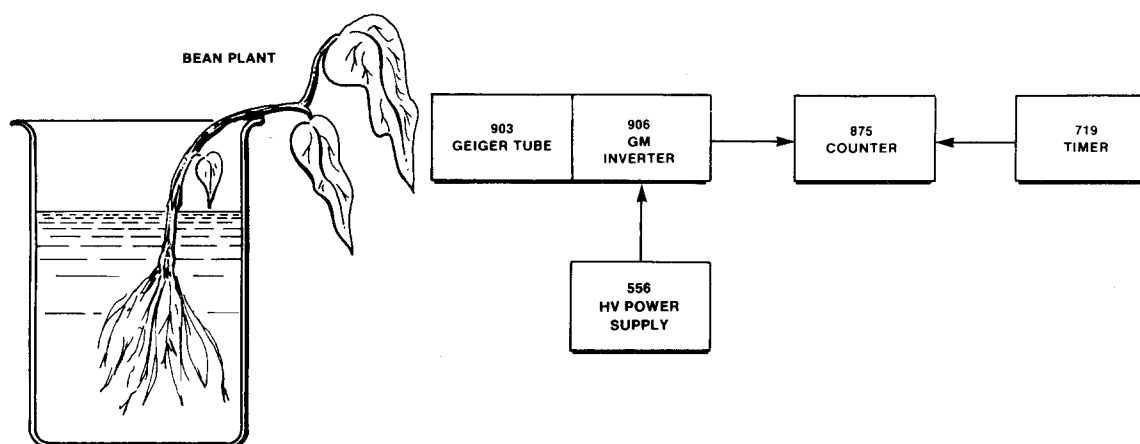


Fig. 22.5. Electronics for ^{32}P Studies in Plants.

EXERCISES

a. From the data that were taken in step 4, make a plot of the activity found in the leaves vs time.

b. From the data that were taken in steps 5, 6, and 7, determine the percentage of ^{32}P that was found in the roots of a given plant. This can be done by counting the roots of a plant and comparing the measurement to the 1- μCi counting card. Repeat the same comparison for stems and leaves by multiplying the counts per minute per gram by the total weight of the corresponding stems or leaves in one plant. From your measurements, summarize how long it takes phosphorus to be translocated to the leaves of the plant and how the phosphorus is distributed through the plant.

References

1. G. F. Knoll, *Radiation Detection and Measurement*, John F. Wiley and Sons, New York (1979).
2. A. C. Melissinos, *Experiments in Modern Physics*, Academic Press, New York (1966).
3. H. L. Andrews, *Radiation Biophysics*, Prentice-Hall, Inc., New Jersey (1974).
4. G. D. Chase and J. L. Rabinowitz, *Principles of Radioisotope Methodology*, 3rd Edition, Burgess Publishing Co., Minnesota (1967).
5. V. Arena, *Ionizing Radiation and Life*, The C. V. Mosby Co., Missouri (1971).
6. L. Cromwell *et al.*, *Biomedical Instrumentation and Measurements*, Prentice-Hall, Inc., New Jersey (1973).
7. *Radiological Health Handbook*, U.S. Dept. of Health, Education, and Welfare, PHS Publication 2016. Available from National Technical Information Service, U.S. Dept. of Commerce, Virginia.
8. Alison P. Casarett, *Radiation Biology*, Prentice-Hall, Inc., New Jersey (1968).
9. Z. M. Bacq and P. Alexander, *Fundamentals of Radiobiology*, Pergamon Press, New York (1961).
10. S. Silver, *Radioactive Nuclides in Medicine and Biology*, Lea and Febiger Publishing Co., Pennsylvania (1968).

Nuclear Techniques in Environmental Studies

EQUIPMENT NEEDED FROM EG&G ORTEC

Complete TEFA System
 311 Chamber for source-excited x-ray fluorescence
 SLP-06175 Si(Li) X-Ray Detector, CFG-SV, DWR-30
 Bin and Power Supply
 572 Spectroscopy Amplifier
 480 Pulser
 459 5-kV Detector Bias Supply
 ACE-2K System including suitable IBM PC (other
 EG&G ORTEC MCAs may be used)
 GEM-10195 Coaxial Detector System, CFG-SV, DWR-30

301 Air Pollution Filter Standards for x-ray fluorescence analysis
 302 Portable High-Velocity Air Filter Sample Collector
 308 Neutron Howitzer and Activation Chamber
 Excitation Sources for source-excited x-ray fluorescence:
 50 mCi each of ^{55}Fe , ^{109}Cd , and ^{241}Am
 X-Ray Source Kit SK-1X
 3 Ci Am-Be Neutron Source
 100 μg to 100 mg ^{252}Cf neutron source, $\sim 10^{12}$ neutrons/g
 Oscilloscope

Introduction

During the last several years many atomic and nuclear techniques have been developed to study environmental problems. These techniques have been applied to air and water pollution studies for the most part. The two techniques that have received the most attention are x-ray fluorescence (source- or tube-excited) and neutron activation analysis. Both of these methods can be nondestructive and, in many cases, show very good analytical sensitivity. Generally, sample preparation is simple and accuracies of $\pm 5\%$ are achievable with the proper standard samples.

There are about 20 elements for atmospheric samples that can be studied with neutron activation analysis, using thermal neutrons from a research reactor. This method has sensitivities for some of these elements as low as $0.01 \times 10^{-9} \text{ g/m}^3$ for air particulate material. Depending on the interferences in the spectra and local concentrations, it is also possible to observe and quantify 22 additional elements by this technique.

Source- and tube-excited x-ray fluorescence analysis is also being used commonly for atmospheric pollution studies. For thin air pollution samples, investigators have observed up to 18 elements in a given sample with concentrations high enough to quantify for the indicated measurement. In general, this method is not as sensitive as neutron activation analysis but for many studies it is an ideal analytic technique. It is rapid and, as was mentioned for air pollution studies, there is virtually no sample preparation. Many air pollution studies measure only a few selected elements for a large number of samples. In many cases this technique is the best analytical method that can be used.

Purpose

Experiment 23 is intended to point out the relevant techniques and also to encourage science departments in univer-

sities to become involved in environmental measurements using nuclear technology.

EXPERIMENT 23.1

A Study of Environmental Samples by Tube-Excited Fluorescence Analysis

Purpose

The purpose of this experiment is to study the applicability of tube-excited fluorescence analysis for trace environmental samples.

Procedure

1. Use the Model 302 Portable Air Filter Sample Collector to obtain air particulate samples for the area to be studied. These samples are usually collected for a 3- or 4-hour collection period. The flow rate meter on the Model 302 should be monitored periodically to assure an accurate air volume measurement.
2. The EG&G ORTEC TEFA System will be used to evaluate the elemental content and concentrations of the elements present on the filter sample. The main features of a TEFA system are shown in Fig. 23.1.

The TEFA system comes complete with a detailed set of instructions for energy calibration and determination of elemental concentration. It is assumed that the student performing this experiment is familiar with the TEFA system.

3. Adjust the excitation energy and calibration range of the TEFA system so that the main features of your spectrum can be observed for the air pollution filter sample. Table 23.1

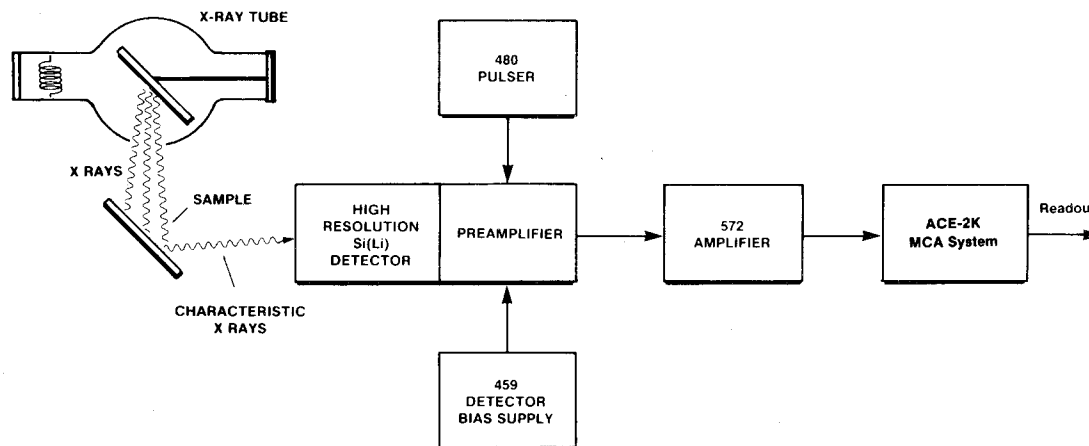


Fig. 23.1. Main Features of EG&G ORTEC's Tube-Excited X-Ray Fluorescence Analysis System.

Table 23.1. Typical Concentrations of Major Trace Elements of Airborne Particulates in an Industrial Area.

(Note: These numbers can change appreciably from one industrial area to another.)

Element	Concentration $\mu\text{g}/\text{m}^3$	Element	Concentration $\mu\text{g}/\text{m}^3$
Na	9.0	Zn	0.07
Al	0.75	As	1.0×10^{-4}
Si	1.00	Se	6×10^{-5}
Cl	5.00	Br	0.40
Ca	2.50	I	0.08
Sc	6.00×10^{-4}	Sb	5.0×10^{-4}
Ti	1.5×10^{-4}	Cs	4.0×10^{-4}
Cr	0.02	Ba	3×10^{-4}
Mn	0.50	La	7×10^{-4}
Fe	0.72	Ce	2×10^{-3}
Co	2.0×10^{-4}	Sm	2×10^{-4}
Ni	0.052	Eu	3×10^{-5}
Cu	0.80	Th	4×10^{-5}

shows typical concentrations of the major trace elements of airborne particulates in an industrial area.

Table 23.2 shows the presence of elements observed on atmospheric particulate samples by x-ray fluorescence.

4. Use the techniques outlined in the TEFA Instruction Manual to determine the elements present on your sample and the concentrations of each element.

In this measurement we have assumed that the pollution sample is thin. In other words, the matrix and attenuation corrections have been ignored. This is generally satisfactory for elements heavier than titanium for air filters. For lighter elements and thicker samples, refer to refs. 2, 3, and 9 for the necessary corrections to the data.

Table 23.2. Elements Observed on Atmospheric Particulate Samples.

X-RAY FLUORESCENCE	
Routinely	Marginal
K, Ca, Ti, Cr, Mn, Fe, Ni, Cu, Zn, As, Br, Rb, Cd, Br, Pb	Au, Hg, Sr
NEUTRON ACTIVATION ANALYSIS	
Na, Al, Ca, Sc, V, Mn, Fe, Co, Cu, Zn, Se, Br, Sb, La, Ce, Sm, Eu, Hf, Th	Mg, S, Cl, Ti, Cr, Ni, Ga, As, Mo, Ag, In, I, Cs, Ba, Yb, Lu, W, Re, Ir, Au, Hg

Figure 23.2 is a spectrum similar to that which might be measured in this experiment. The technique outlined above for air pollution studies is equally applicable for water pollution data or any number of environmental measurements. Figure 23.3 is a spectrum that was measured on whole blood from a patient who showed lead poisoning symptoms. This tube-excited sample showed that the patient had several times the normal concentration of lead in his blood, indicating lead poisoning.

Figure 23.4 shows the results of some experiments studying the heavy element environmental pollution of mercury in fish. This figure is a good example of the ability of this state-of-the-art technique to do multielement analysis of an environmental sample in counting times of only 10 minutes.

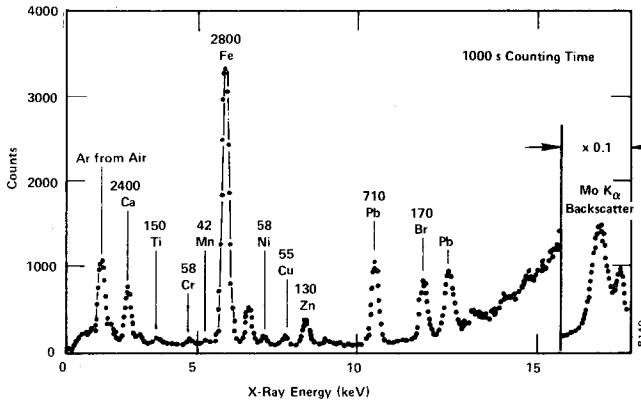


Fig. 23.2. Tube-Excited X-Ray Fluorescence Spectrum for an Air Pollution Filter. The numbers above the peaks are the measured concentrations in ng/cm² (taken from ref. 9).

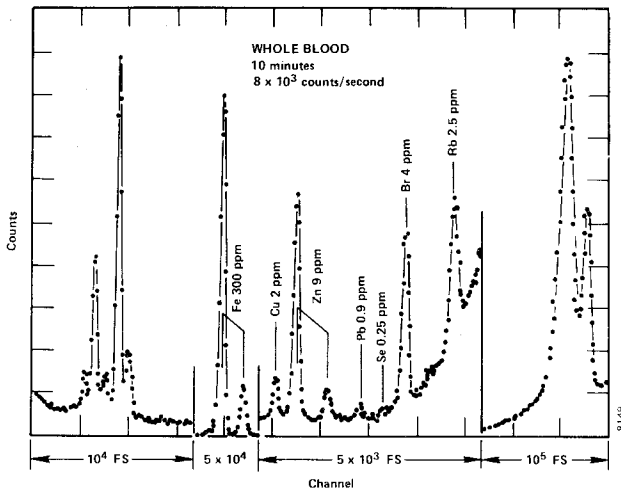


Fig. 23.3. Tube-Excited X-Ray Fluorescence Spectrum of a Whole Blood Sample. In this spectrum the measured concentration of lead is several times normal, indicating lead poisoning (taken from ref. 9).

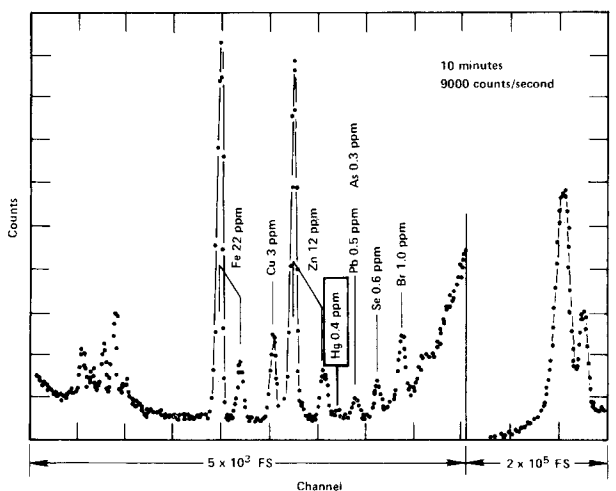


Fig. 23.4. Tube-Excited X-Ray Fluorescence Spectrum of a Fish taken from Water that has a High Mercury Content (taken from ref. 9).

EXPERIMENT 23.2

A Study of Environmental Samples by Source-Excited Fluorescence Analysis

Purpose

The purpose of this experiment is to study the applicability of source-excited x-ray fluorescence for trace analysis of environmental samples.

Description

The only difference between this experiment and Experiment 23.1 is the source of x rays. Sample preparation and other data comparative techniques are the same. Figure 23.5 shows the experimental arrangement for the EG&G ORTEC SEFA electronics, the MCA, and some detail of the method by which the sample is irradiated and fluoresced.

In order to produce the maximum sensitivity for trace analysis studies, it is necessary to select the excitation source carefully. Figure 23.6 shows a plot of photoelectric excitation cross section vs energy. As is expected from the theory, the maximum cross section for the K-shell excitation occurs at an energy equal to the K-shell binding energy for that element. For example, assume that all elements lighter than vanadium in our sample are to be studied with maximum sensitivity. The maximum photoelectric cross section for vanadium occurs at 5.463 keV (Fig. 23.6). Therefore, from a theoretical point of view, we would like to have an excitation source with exactly that energy. However, because of Compton scattering from the sample and other experimental reasons, it is best to have the excitation photons a little higher in energy than the binding energy listed above. For this problem, a source of ⁵⁵Fe, which emits photons of 5.895 keV, would be the best source. A general rule of thumb would

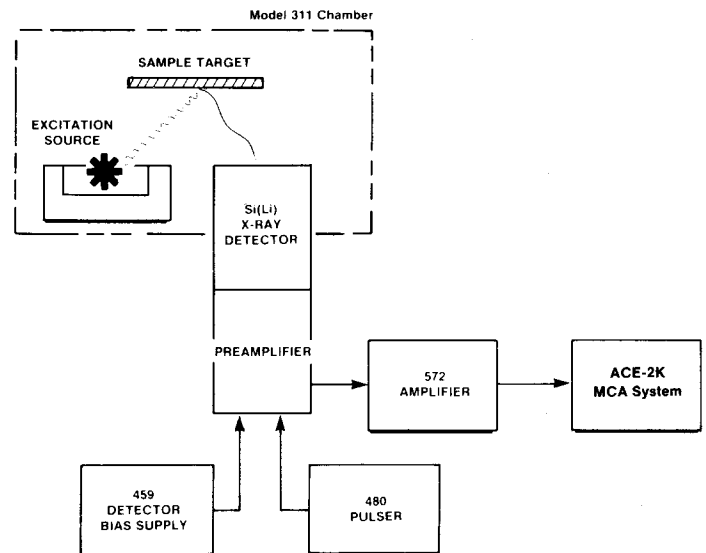


Fig. 23.5. Equipment Arrangement for Experiment 23.2.

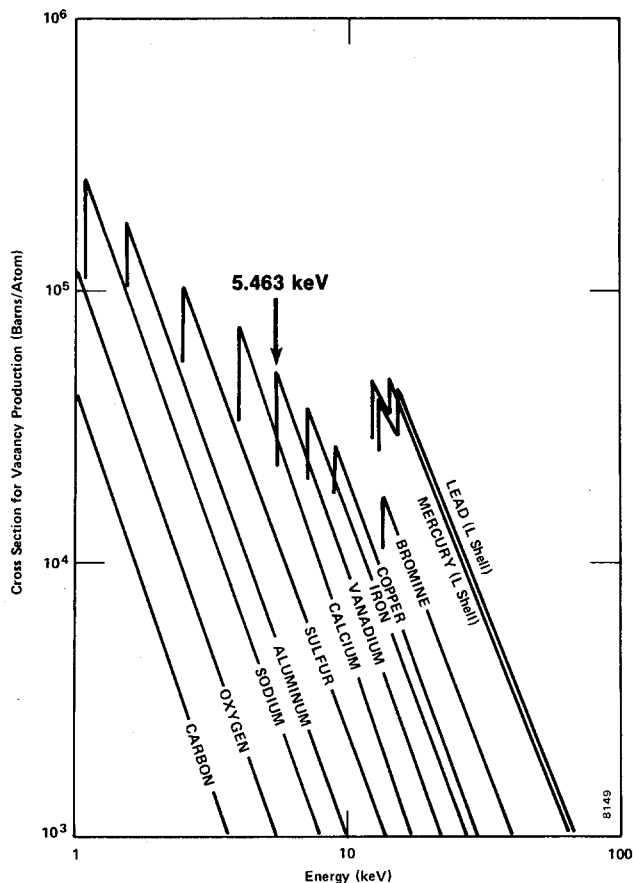


Fig. 23.6. Photoelectric Excitation Cross Sections for Twelve Elements Plotted as a Function of Energy.

say that the excitation photons from the source should be ~2 keV higher in energy than the K_{α} peak from the heaviest element in the environmental sample being studied. From the preceding statements and a careful analysis of Fig. 23.6, it should be obvious that it is advisable to study any given sample with several different excitation sources. The low-energy sources give maximum sensitivity for low-atomic-number elements, while the higher-energy sources, such as ^{109}Cd , are quite effective for heavier elements.

Procedure

1. Set up the electronics as shown in Fig. 23.5. Use the techniques learned in Experiment 12 to calibrate the system over the desired range with Source Kit SK-1X.
2. You may now fluoresce your first air- or water-pollution sample. For air pollution samples the Model 302 Portable High Velocity Air Filter Sample Collector can be used as outlined in Experiment 23.1. For the techniques of preparing other samples, refs. 2, 7, and 9 are helpful.
3. Figure 23.7 shows a typical source-excited x-ray fluorescence spectrum of residue from water that was taken from a municipal treatment plant.

The concentrations of each element in the spectrum can be determined by comparing the peak area to that of a standard

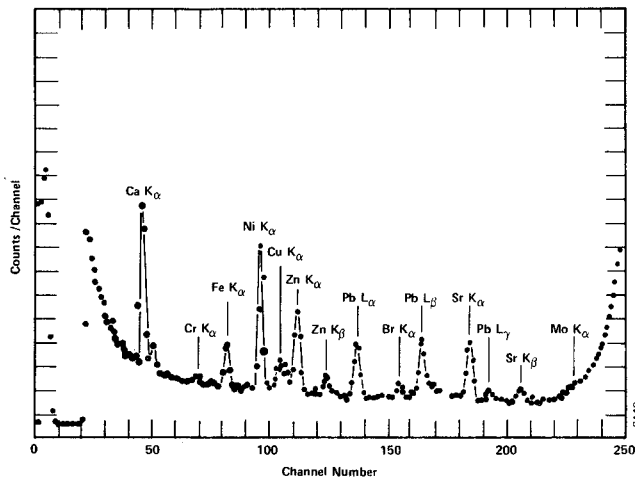


Fig. 23.7. ^{109}Cd Source-Excited X-Ray Fluorescence Spectrum of a Water Filter from the Effluent Water of a Municipal Treatment Plant.

that was fluoresced for the same conditions. For some of the major elements, the Model 301 Filter Standards can be used in this comparative mode.

EXPERIMENT 23.3

A Study of Environmental Samples using Neutron Activation Analysis and High-Resolution Gamma Spectrometry

Purpose

To study the applicability of neutron activation analysis with HPGe detectors to trace analysis measurements.

Discussion

There are four sources of neutrons that can be used for this experiment. These are: neutrons from research reactors, isotopic neutron sources, ^{252}Cf sources, or accelerator-produced neutrons. For thermal neutron cross-section measurements, the neutrons from any of the above sources will have to be thermalized before being used. A neutron howitzer, such as the EG&G ORTEC 308, can be used for this thermalization as well as to provide an activation chamber for the experiment. Figure 16.2 shows the spectrum of neutrons that must be thermalized for a typical isotopic source such as Am-Be. Figure 23.8 shows the fission spectrum of neutrons from the ^{252}Cf sources that have become popular. Most accelerators that are used for neutron activation analysis are Cockcroft-Walton machines that use 14-MeV neutrons from the $^3\text{H}(d,n)^4\text{He}$ reaction. These fast neutrons can be thermalized with the 308 Howitzer, or they can be used directly, depending on the elements being studied in the environmental sample.

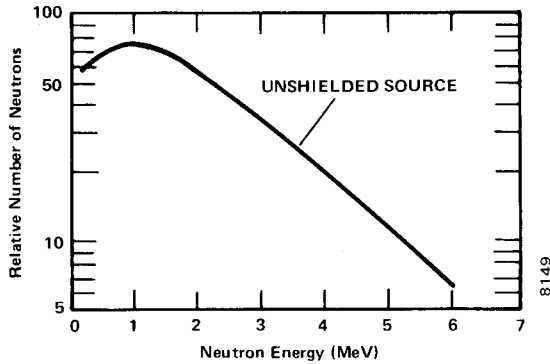


Fig. 23.8. Typical Fission Neutron Distribution from an Unshielded ²⁵²Cf Source.

Procedure

1. Set up the electronics as shown in Fig. 23.9. Use the procedures outlined in Experiment 7 to calibrate the electronics system so that 2 MeV falls near full scale, using 1024 channels in the analyzer.
2. Determine the proper activation and counting times for the first environmental sample. Use the data in Experiment 17 and in Table 17.2 as a guide.
3. Activate the samples in the irradiation facility and count for the best calculated times. Identify the elements present by the calibration curve and the Table of the Isotopes (ref. 8).
4. To quantify the elements in the sample, irradiate the standards of the observed trace elements under the same conditions as for the environmental samples and compare the peak measurements. These techniques are outlined in Experiment 23.2 and refs. 4 and 6.

Figure 23.10 shows an air filter sample that was measured using this technique by the scientists at Battelle Memorial Institute in Richland, Washington. For comparison, the same sample's spectrum is also shown as it was analyzed with a 3-in. x 5-in NaI detector. Figure 23.11 is a spectrum of an Alaskan caribou liver (courtesy of Battelle Memorial Institute) with the observed isotopes.

Many other environmental, biological, medical, etc. spectra have been studied with this technique as well as with x-ray fluorescence. The student is encouraged to read the references listed for this experiment in order to appreciate the state-of-the-art contributions that these techniques have made to trace element analysis.

Table 23.2 lists elements that have been identified with both x-ray fluorescence and neutron activation techniques. Table 23.3 lists the major elements found in air filter samples that were obtained in Los Angeles, California.

Table 23.3. Typical Sources of Trace Elements on Air Pollution Filters.

(This is data for Los Angeles taken from ref. 7.)

Source	Source Strength	Major Elements
Power Plant and Petro Chemical	36%	S, V, Ni
Automotive	28%	Pb, Br, Fe, Si, S, Ca, Cl, Al, Zn, K, Cu
Airborne Soil	25%	Si, Fe, Al, Ca, K, Ti, Mn
Sea Salt	7%	Na, Cl, Mg, S
Other	5%	K, Zn, Mg, Ti, Mn, Cu

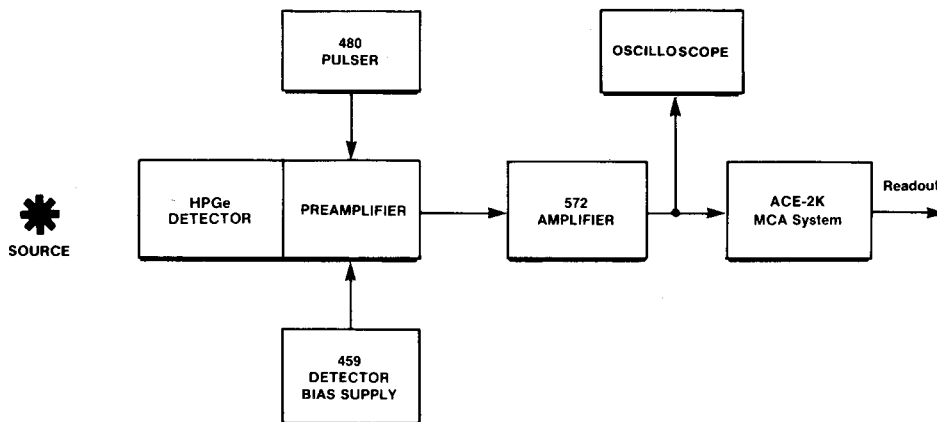


Fig. 23.9. Electronics Connections for Experiment 23.3.

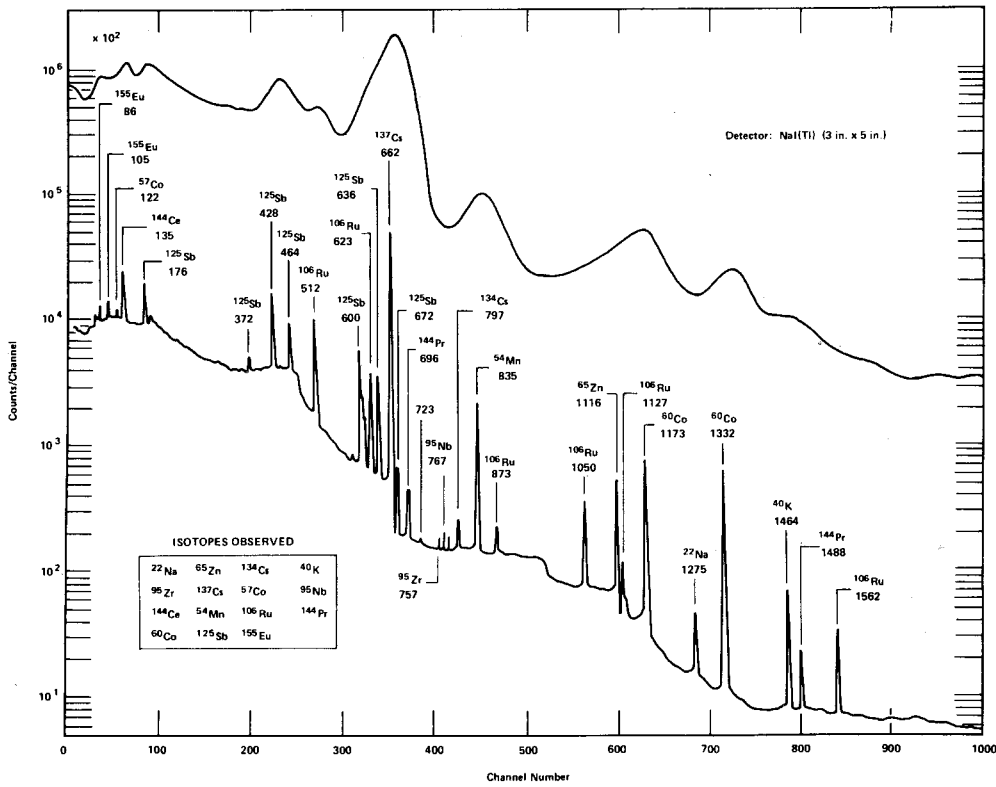


Fig. 23.10. High-Resolution Germanium Spectrum of an Air Filter Sample. Shown also on the figure for comparison is the 3-in. x 5-in. NaI spectrum of the same sample. (Courtesy of Battelle Memorial Institute.)

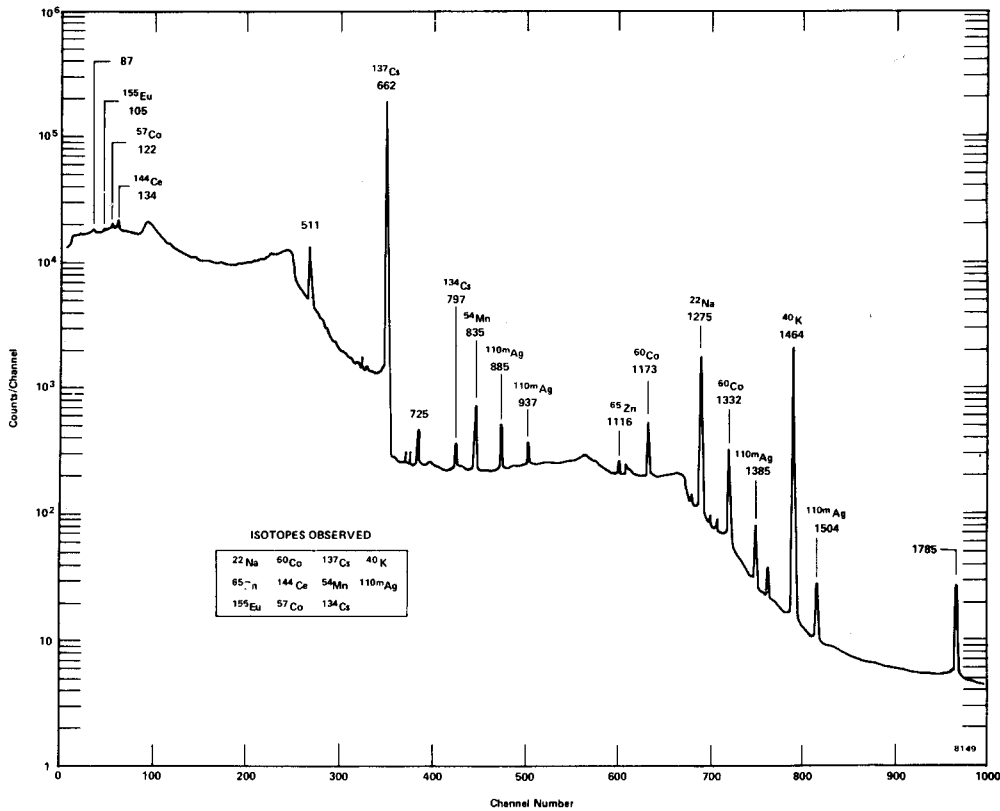


Fig. 23.11. High-Resolution Germanium Spectrum of Alaskan Caribou Liver Showing Isotopes Observed. (Courtesy of Battelle Memorial Institute.)

References

1. G. F. Knoll, *Radiation Detection and Measurement*, John Wiley and Sons, New York (1979).
2. J. M. Jaklevic and F. S. Goulding, "Semiconductor Detector X-Ray Fluorescence Spectrometry Applied to Environmental and Biological Analysis, *IEEE Trans. Nucl. Sci.* **NS-19** (1972).
3. R. Dams, J. A. Robins, K. A. Rahn, and J. W. Winchester, "Non-Destructive Neutron Analysis of Air Pollution Particles," *Anal. Chem.* **42**, 861-867 (1970).
4. W. H. Zoller and G. E. Gordon, "Instrumental Neutron Activation Analysis of Atmospheric Pollutants Utilizing Ge(Li) Gamma-Ray Detectors, *Anal. Chem.* **42**, 257 (1970).
5. J. V. Lagerwesff and A. W. Spech, "Contamination of Roadside Soil and Vegetation with Cadmium, Nickel, Lead, and Zinc," *Environ. Sci. and Tech.* **4**, 583 (1970).
6. D. Gray *et al.*, "Determination of Trace Element Labels in Atmospheric Pollutants by Instrumental Neutron Activation Analysis," *IEEE Trans. Nucl. Sci.* **NS-19**(1), 194 (1972).
7. J. W. Nelson *et al.*, Report of the Workshop on Nuclear Techniques for Environmental Trace Element Information Relative to Energy Production and Consumption (1974). National Technical Information Services, Dept. of Commerce, Springfield, Virginia.
8. C. M. Lederer and V. S. Shirley, Eds., Table of Isotopes, 7th Edition, John Wiley and Sons, New York (1978).
9. R. D. Giaugue and J. M. Jaklevic, "Rapid Quantitative Analysis of Air Pollution Particles," available as Report No. LBL-204 from Lawrence Berkeley Laboratory, Berkeley, California.

Measurements in Health Physics

EQUIPMENT NEEDED FROM EG&G ORTEC

Bin and Power Supply
 905-3 2- by 2-in. NaI(Tl) Crystal and Phototube
 266 Photomultiplier Tube Base
 556 High Voltage Power Supply
 113 Scintillation Preamplifier
 575A Amplifier
 ACE-2K MCA System including suitable IBM PC (other EG&G ORTEC MCAs may be used)
 875 Counter
 719 Timer
 903 End-Window Geiger Tube
 906 GM Inverter
 Surface Barrier Detector A-015-025-1500
 142A Preamplifier

Oscilloscope
 807 Vacuum Chamber
 428 Detector Bias Supply
 905-5 Plastic Scintillator and Phototube
 Mechanical Vacuum Pump
 10 sheets each: PbPI-2, CdPI-1, SIPI-1, AIPi-1, PnPI-2
 4 each AIFI-1, AIFI-2, AIFI-3, AIFI-4
 2 each AIFI-5
 8 each PbPI-3
 Source Kit SK-1G
 25 μCi ^{137}Cs
 3 Ci Am-Be Neutron Source
 Portable Geiger-Mueller Health Physics Survey Instrument
 ORC-24 Cable Set

Purpose

To study some of the basic concepts associated with radiation protection and good health physics practices.

The field of health physics is very broad, encompassing various facets of the nature of radiation effects in living animals. The primary concern is one of protection against exposure. This experiment is an attempt to inform the student of the merits of various types of shielding against common forms of radiation encountered in laboratory situations and does not exhaust the field of health physics. It is not meant to fully qualify the student in the discipline of health physics. For additional information and applicable regulatory guidelines on this subject matter, consult the references for this experiment and the local pertinent authorities.

Introduction

In any laboratory where radioactive sources are used, everyone should be aware of, and use, good health physics practices. Most of the radioactive sources that are used for the experiments in this manual are sealed and have low activity, so they do not present a real health physics problem. For the experiments that require higher activity sources, we have carefully explained the particular safety techniques that should be used in setting up and performing the experiment. The main goal of any health physics program is to reduce personal exposure, both external and internal, to a minimum.

Assume that a fairly "hot" source must be used in an experiment. There are three general ways to minimize exposure when using this source. These are:

1. Do not stay in the vicinity of the source any longer than necessary.
2. Remember the $1/R^2$ relationship that is valid for all isotopic radiation sources; stay as far away from the source as is practical during the experiment.

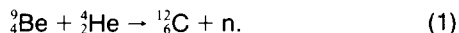
3. Where necessary, use shielding between the source and yourself. The amount of shielding and the type of shielding material depends on the type of radiation that the source is emitting.

Alpha particles lose energy rapidly in any medium because of their high specific ionization. Therefore, as was shown in Experiment 5, even a thin foil will stop most alphas. But there is another very important consideration; most alpha sources will decay not only to the ground state of the daughter nucleus, but also to excited states. The de-excitation of these levels can result in gammas or x rays from internal conversion. The attenuation of gammas and x rays were studied briefly in Experiments 3 and 11. For low-energy gammas or x rays, the most pronounced attenuation mechanism is the photoelectric effect. Since the cross section for this process varies as Z^5 , where Z is the atomic number of the absorber, the best shielding material for low-energy photons is something heavy like lead.

In Experiment 6 we were concerned with beta sources and internal conversion electron sources. The process by which betas lose energy in absorbers is similar to that of alphas. The beta particle is not as massive and, hence, its specific ionization is not as great as for alphas. In air, alphas travel only a few centimeters where betas will generally travel many feet. The thickness and choice of material for shielding betas depends on the end-point beta energy of the isotope and on the Bremsstrahlung radiation that is always present for a beta source. In general, the shielding thickness that is necessary to stop betas of a given end-point energy will decrease with increasing density of the shield. For example, 0.1 in. of aluminum will stop 1.5-MeV betas. For lead, 0.024 in. will do the same job. The Bremsstrahlung production in the shielding must also be considered. This production rate increases with the atomic number of the absorber. So, for this reason, aluminum or even glass might be

the best and cheapest effective shield in the case of a pure beta emitting isotope. As for alphas, most beta-emitting isotopes also have gammas in their decay schemes and the shielding is done best with heavier atomic number materials such as lead.

A neutron source was used in Experiments 16, 17, 18, and 23, and will be used in this experiment. Shielding against these neutron sources presents a rather unique set of problems. Neutrons from these isotopic neutron sources are produced from the following reaction:



In some of these reactions the ${}^{12}_6\text{C}$ nucleus is left in an excited state. When the state de-excites, high-energy gammas are produced. Gammas are also produced by slow and fast neutron activation analysis in the source material as well as in the surroundings. Therefore these isotopic neutron sources also carry a rather heavy inventory of gammas. The gammas are attenuated quite effectively by lead, but this is not the case for neutrons. The most effective shielding material for neutrons is one that contains a large amount of hydrogen. The most practical common materials of this nature are paraffin and water. The reason that neutrons are effectively shielded by hydrogenous materials is that neutrons have a large scattering cross section with hydrogen. Fast neutrons therefore make a lot of billiard ball collisions with the protons in the shielding material. Each collision causes the neutron to lose some energy; on the average, about one-half its energy is lost per collision. Therefore, after ten collisions, the neutron is thermalized and can be captured by the large thermal cross section for hydrogen. So, in summary, a good shield for an isotopic neutron source is a combination of lead and a hydrogenous material such as paraffin.

In this series of experiments some of the properties of various shielding materials will be studied, accompanied by time, distance, and radiation protection parameters.

EXPERIMENT 24.1

Gamma Intensity as a Function of Distance

Purpose

To study the $1/R^2$ (or R^{-2}) relationship of 0.662-MeV gammas from ${}^{137}\text{Cs}$, typical for any gamma emitter.

Procedure

1. Set up the electronics as shown in Fig. 24.1. Adjust the voltage for the phototube to the recommended value.
2. Obtain the ${}^{137}\text{Cs}$ source from the source kit ($E_\gamma = 0.662$ MeV). Place this at a distance of 2 cm from the face of the NaI(Tl) crystal detector. Adjust the gain of the amplifier so that the 0.662-MeV photopeak from the ${}^{137}\text{Cs}$ is stored in about channel 350.
3. Adjust the Region of Interest of the MCA at about the center of the Compton distribution range in the analyzer spectrum. Figure 24.2 shows the approximate Upper- and Lower-Level settings.

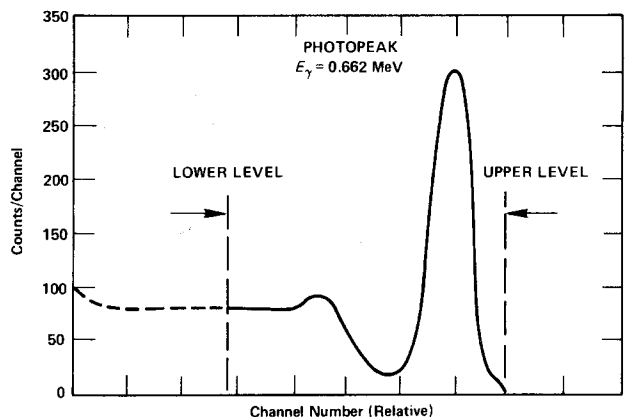


Fig. 24.2. ${}^{137}\text{Cs}$ Spectrum with the MCA ROI Lower Level Set at the Middle of the Compton Distribution.

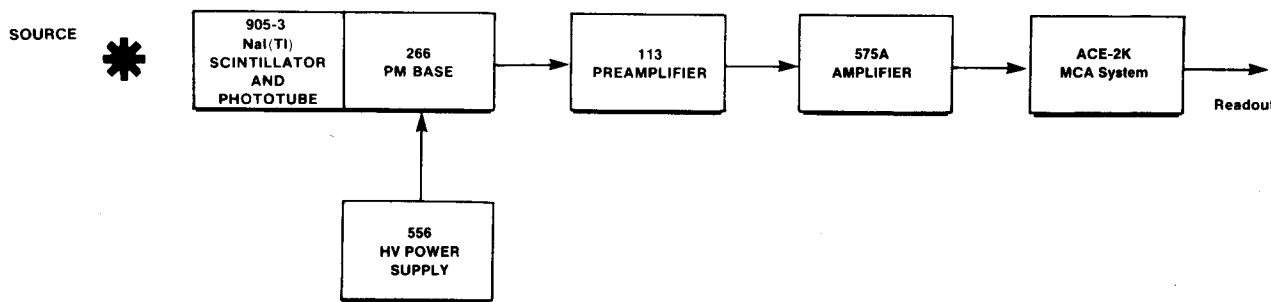


Fig. 24.1. Electronic Block Diagram for Gamma-Ray Spectrometry System with a Linear Gate for $1/R^2$ Studies.

4. Remove the 1- μCi ^{137}Cs source and run a background spectrum for 400 s. Integrate the number of counts in the portion of the spectrum that is included in the ROI.
5. Handle the 25- μCi ^{137}Cs source carefully with tongs or forceps, and place it at a distance of 4 m from the detector. Accumulate a spectrum at this distance for 400 s and integrate the total number of counts in the MCA. Repeat for each of the other distances listed in Table 24.1.

Table 24.1. $1/R^2$ Studies for ^{137}Cs Gammas.

Distance (Meters)	Time (Minutes)	Integrated MCA Counts	Counting Rate Minus Background (cpm)	Theoretical Intensity
4				
3.5				
3.0				
2.5				
2.0				
1.5				
1.0				
0.5				
0.25				

NOTE: In this experiment, support the source and detector so that external scattering from the surroundings is minimized, and be sure to remove all other sources from the area.

EXERCISES

- a. Record the data in Table 24.1. Calculate the counting rate in cpm from the integrated count and the preset time (400 s). Subtract the background and record the true counting rate in column 4 of Table 24.1.
- b. For an isotopic gamma source, the following relations are valid provided there is minimum external scattering.

$$I_1 = \frac{I_0}{R_1^2}, \tag{2}$$

$$I_2 = \frac{I_0}{R_2^2}, \tag{3}$$

where I_1 is the gamma intensity at a distance R_1 , and I_2 is the corresponding intensity at a distance R_2 .

$$\frac{I_1}{I_2} = \frac{R_2^2}{R_1^2}, \tag{4}$$

$$I_1 = I_2 \frac{R_2^2}{R_1^2}. \tag{5}$$

Now, define I_2 to be the counting rate at 4 m as recorded in column 4 of Table 24.1. To get the rest of the theoretical values, simply multiply this 4-m rate by the ratio of the square of the corresponding distance for each value as in Eq. (5) above. Record these theoretical values in column 5 of Table 24.1.

- c. Plot this theoretical intensity vs distance. On the same plot, record your experimental data points.

EXPERIMENT 24.2

Gamma Intensity Measured with a Geiger Counter

Purpose

This experiment is similar to Experiment 24.1 except that a hand-held Geiger Mueller Counter is used instead of the more sensitive 2- by 2-in. NaI(Tl) detector.

Procedure

NOTE: Observe health physics principles carefully when using a hand-held detector in this measurement; the source has a high enough activity level that prolonged exposure at close range can result in unnecessary exposure.

1. Remove all radioactive sources from the room. Take a background count and record the count rate from the GM counter.
2. Support the 25- μCi ^{137}Cs source in a position so that scattering is minimized. Starting at a distance of 4 m from the source, record the counting rate at all of the distances listed in Table 24.1.

EXERCISES

- a. Subtract the background from the measured counting rates and record these in a table similar to Table 24.1 as counting rate minus background.
- b. Normalize the theoretical intensity to the experimentally determined value at 2 m. Normalization at 2 m, rather than at 4 m, is recommended because the GM counter is not as sensitive as the NaI(Tl) detector and statistics are usually better at 2 m.
- c. Calculate the rest of the theoretical values in Table 24.1 by multiplying the counting rate at 2 m by the ratio of the

square of distances as in Experiment 24.1. Plot a curve of the theoretical counting rate as a function of distance. Plot the experimental points on the same curve.

d. From the definition of the Curie (3.7×10^{10} dps) and R^{-2} relationship, calculate the number of disintegrations/min/cm² that your source should produce at a distance of 2 m. Divide your observed counting rate by the approximate area of your detector window and compare the answer with the calculated intensity. What does this tell you about the efficiency of your GM counter for ¹³⁷Cs?

EXPERIMENT 24.3

Shielding Effectiveness of Different Materials for Gammas

Purpose

The purpose of this experiment is to investigate the shielding properties of various materials for 0.662-MeV gammas from ¹³⁷Cs.

Procedure

1. Set up the electronics the same as for Experiment 24.1 and set the MCA ROI at the center of the Compton region as in Fig. 24.2.
2. Place the ¹³⁷Cs source from the source kit at a distance of 8 cm from the face of the crystal. Count for 400 s and record the integrated count total from the analyzer.
3. Place the first PbPI-2 absorber at a distance of 4 cm from the detector and count for 400 s. Repeat for the other lead absorber thicknesses listed in Table 24.2.
4. Remove the lead absorbers, ($Z = 82$), and replace them with the CdPI-1 cadmium absorbers. Make another table

similar to Table 24.2 and record the measurements made with cadmium absorbers in this table.

5. Repeat the above procedure using iron, ($Z = 26$), and then aluminum, ($Z = 13$). Since these materials are supplied in 1/8-in. thicknesses, instead of the 1/16-in. thicknesses for PbPI-2 and CdPI-1, it is only necessary to make half as many measurements for these two absorber types. Make tables similar to Table 24.2 and fill in the data for iron and aluminum.

6. Place four pieces of PnPI-2 (1-in. thick paraffin) between the source and the detector and count for 400 s. Calculate the counting rate, (cpm), when using this 4-in. layer of paraffin as an absorber.

7. Remove the source and all absorbers and determine a background counting rate for the room. Subtract the background counting rate from each of the uncorrected counting rates recorded in the tables. Record these corrected values in column 5 of each data table.

EXERCISES

- a. On semilog graph paper, plot the corrected counting rate for lead as a function of absorber thickness. This technique was outlined in Experiment 3.7. Calculate the effective half value layer, (HVL), for lead as shown in Experiment 3.7.
- b. From the data for cadmium, iron, and aluminum, determine the effective HVL values for these materials.
- c. On semilog graph paper, plot the HVL for each material as a function of the atomic number of the material.
- d. For the measurement made with 4 in. of paraffin, calculate the percent of attenuation. Is paraffin a very effective shield for gammas?

Table 24.2. Shielding Properties of Different Absorbers for Gammas.

Run No.	Absorber Thickness (1/16 in.)	Time (Seconds)	Integrated MCA Counts	Counting Rate Minus Background (cpm)
1	Zero	200		
2	1.0	200		
3	2.0	200		
4	3.0	400		
5	4.0	400		
6	5.0	400		
7	6.0	400		
8	7.0	400		
9	8.0	400		

EXPERIMENT 24.4

Attenuation of Betas in Aluminum by the Geiger Mueller Method

Purpose

To study the absorption of betas in order to determine the necessary parameters associated with beta shields.

Procedure

1. Set up the electronics as shown in Fig. 24.3. Without an absorber, adjust the voltage of the GM tube to its proper value. The techniques associated with Geiger tube counting were carefully outlined in Experiment 2.
2. Position the ²⁰⁴Tl source from the source kit ~3 cm from the window of the GM tube. Be sure that the absorbers can be inserted between the source and the detector without disturbing the geometry.
3. Take a 400-s count without an absorber. Record the count in Table 24.3. Place the first aluminum absorber (2 mg/

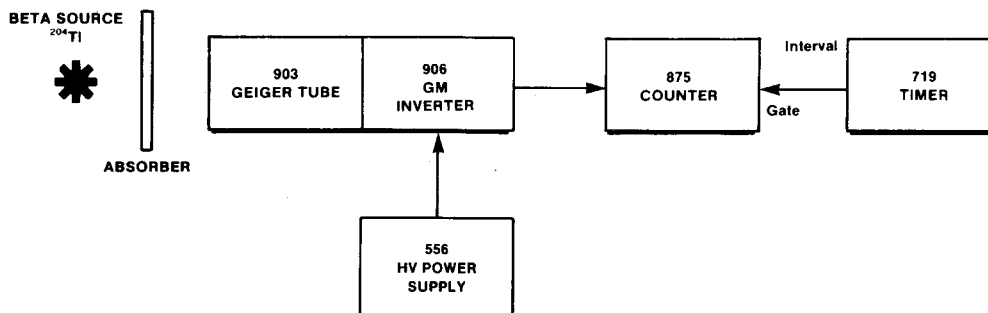


Fig. 24.3. Electronics for Beta Attenuation Experiment with a GM Counter.

cm²) in position between the source and the GM tube and count for 400 s. Continue for the other absorber thicknesses and times as listed in Table 24.3.

4. Remove the source and obtain a background count for 1000 s.

Table 24.3. Beta Absorption in Aluminum.

Run No.	Thickness (mg/cm ²)	Time (Seconds)	Counts	Counting Rate Minus Background (cps)
1	0.00	400		
2	2.00	400		
3	4.00	400		
4	6.00	400		
5	10.00	400		
6	20.00	400		
7	60.00	400		
8	80.00	800		
9	100.00	800		
10	120.00	1000		
11	140.00	1000		

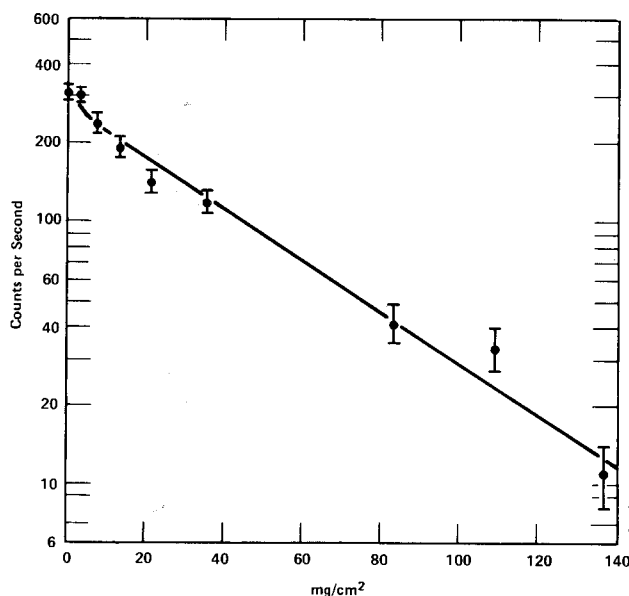


Fig. 24.4. Attenuation of the 0.766-MeV Betas from ²⁰⁴Tl by Aluminum Absorbers.

Table 24.4. Approximate Range of Electrons of Various Energies in Aluminum.

Energy (MeV)	Range (mg/cm ²)
0.010	0.20
0.020	0.75
0.030	1.40
0.040	2.60
0.050	4.00
0.080	9.00
0.100	12.00
0.200	40.00
0.300	80.00
0.400	120.00
0.500	160.00
1.000	500.00
2.000	900.00

EXERCISES

a. Subtract the background counting rate, (cps), from each of the measured counting rates and record the corrected values in column 5 of Table 24.3.

b. Make a plot on semilog graph paper of the corrected counting rate as a function of absorber thickness. Figure 24.4 shows some typical data that were obtained for this experiment. The experiment can be repeated with other beta sources if desired. Table 24.4 lists the approximate range of electrons of various energies in aluminum.

EXPERIMENT 24.5

Attenuation of Betas in Aluminum by the Surface Barrier Detector Method

Purpose

To measure absorption of the true beta portion in aluminum by measuring the events with a surface barrier detector.

Discussion

Surface barrier detectors are rather insensitive to gammas. So, if an isotope has gammas in its decay scheme, the true beta portion of the absorption can be measured with these detectors. Most isotopes that decay by beta emission will, in fact, decay to excited levels in the residual nucleus which, in turn, gamma-decay to the ground state of the daughter nucleus.

Procedure

1. Set up the electronics as shown in Fig. 24.5. Place the ^{204}Tl source from the source kit in the vacuum chamber so that all of the absorbers that will be used can be placed between the source and the detector (Table 24.3). Evacuate the chamber and set the detector bias voltage to its recommended value. These techniques were outlined in Experiment 6.
2. Adjust the gain of the amplifier so that the end point of the ^{204}Tl spectrum falls in about channel 350. The spectrum will be similar to Fig. 6.1.
3. Count for 200 s, or a time period long enough to obtain ~ 5000 counts in the entire spectrum. Since the background should be essentially zero, the counting rate can be calculated directly and entered into column 5 of a table similar to Table 24.3.
4. Repeat for each value of aluminum absorber shown in Table 24.3.

EXERCISE

Plot the data and compare with the values obtained in Experiment 24.4.

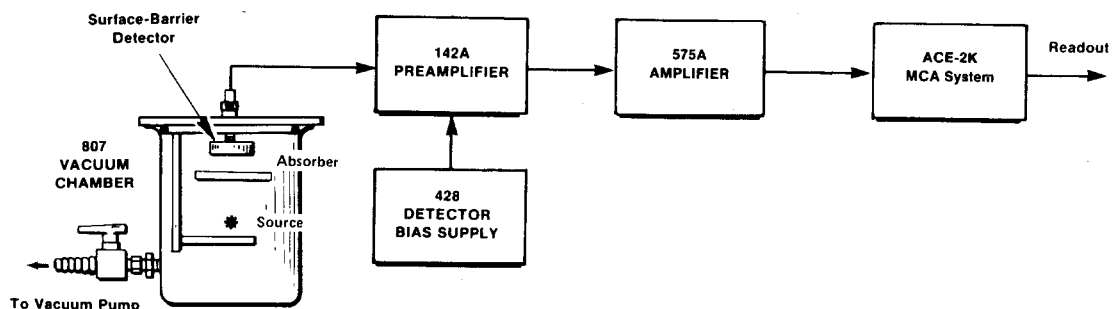


Fig. 24.5. Electronic Arrangement for Attenuation of Betas by the Surface Barrier Detector Method.

EXPERIMENT 24.6

A Study of Paraffin as a Neutron Shielding Material

Purpose

To study the properties of paraffin and lead as shielding materials for the fast neutrons that are produced from an isotopic neutron source (Am-Be).

Procedure

1. Set up the experimental arrangement shown in Fig. 24.6. Adjust the amplifier gain so that the end-point of the neutron spectrum is in about channel 550 (Fig. 24.7).
2. Remove the Am-Be source and place the $1\text{-}\mu\text{Ci } ^{60}\text{Co}$ source (from the source kit) at a distance of 1 cm from the 905-5 Plastic Scintillation Detector. Adjust the Lower Level of the MCA to cut out the steep slope in the lower portion of the spectrum as shown in Fig. 24.7.
3. Remove the ^{60}Co source and return the 1-Ci Am-Be source 100 cm from the detector as shown in Fig. 24.6.
4. Place the ten sheets of PbPI-2 (1/16-in. thick lead) at a position 10 cm from the Am-Be source. This lead helps shield the gammas from the plastic scintillator. The total lead thickness is 0.625 in., but the experiment will prove that this does little to attenuate the neutrons from the source.
5. Accumulate a neutron spectrum in the MCA for a time period long enough to have ~ 50 counts in each channel in the flat portion of the curve in Fig. 24.7.
6. Integrate the counts in the MCA spectrum and operate for a period of time long enough to record ~ 5000 total counts. Record the time and the number of counts. Place the first PnPI-2 paraffin absorber in its proper position and count for the same time used for the measurement without the absorber.
7. Continue making measurements while adding 1-in. increments of paraffin up to 10 in. It is probably wise to increase the time for the thicker absorbers so that the number of counts recorded stays above 3000. The live time for each accumulation is recorded in channel zero in the MCA.

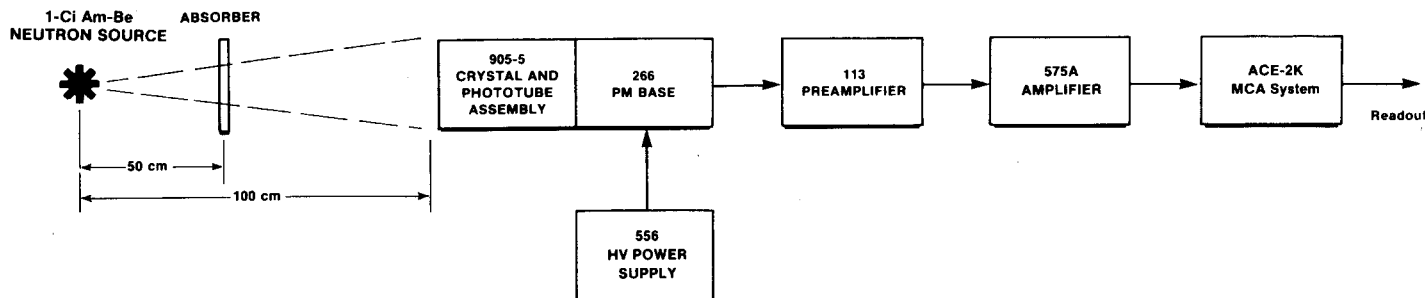


Fig. 24.6. Experimental Arrangement for Neutron Shielding Materials Study.

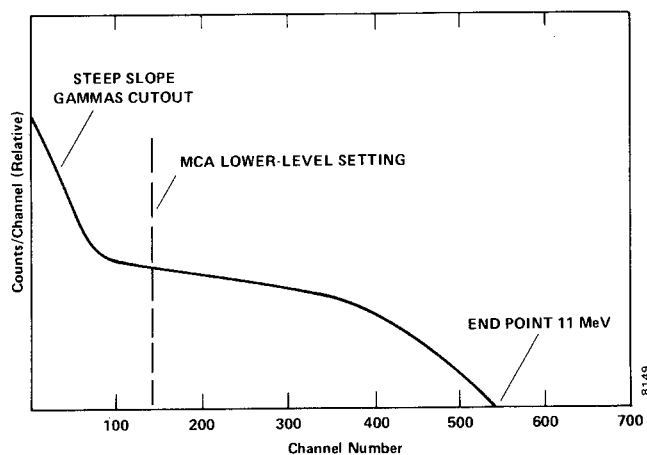


Fig. 24.7. Neutron Spectrum from Plastic Scintillator for Shielding Studies.

8. Remove the Am-Be source and take a background count for 400 s.

EXERCISES

- a. Calculate the counting rates for each measurement made. Determine the background counting rate and subtract it from each of the other measurements.
- b. Plot the corrected counting rate on semilog graph paper as a function of the paraffin absorber thickness. Calculate the effective half value layer, (HVL), for paraffin.

EXPERIMENT 24.7

A Study of Lead as a Neutron Shielding Material

Purpose

To study the absorption properties of lead for neutrons.

Procedure

1. Use the experimental arrangement and format of Experiment 24.6 for this experiment. Follow steps 1 through 5 in Experiment 24.6.

2. Place the first PbPI-3 (1-in. thick lead) absorber in position and count for a long enough period of time to accumulate ~5000 integrated counts in the analyzer spectrum.
3. Add one 1-in. thickness of lead and count for the same time period. Add each of the remaining lead shields, one at a time, and repeat this procedure.
4. Measure the background as in Experiment 24.6 and subtract it from each of the counting rates found above.

EXERCISES

- a. Plot the corrected counting rate on semilog graph paper as a function of lead thickness.
- b. From the projected straight line extrapolation on the curve, calculate the HVL of lead for neutrons from the Am-Be source. From the HVL of paraffin established in Experiment 24.6, calculate the ratio of the HVL values for paraffin and lead.

References

1. G. F. Knoll, *Radiation Detection and Measurement*, John Wiley and Sons, New York (1979).
2. G. D. Chase and J. L. Rabinowitz, *Principles of Radioisotope Methodology*, 3rd Edition, Burgess Publishing Co., Minnesota (1967).
3. V. Arena, *Ionizing Radiation and Life*, The C. V. Mosby Co., Missouri (1971).
4. H. L. Andrews, *Radiation Biophysics*, Prentice-Hall, New Jersey (1974).
5. C. M. Lederer and V. S. Shirley, Eds., *Table of Isotopes*, 7th Edition, John Wiley and Sons, New York (1978).
6. *Radiological Health Handbook*, U.S. Dept. of Health, Education, and Welfare, PHS Publication 2016. Available from National Technical Information Services, U.S. Dept. of Commerce, Springfield, Virginia.
7. W. Mann and S. Garfinkel, *Radioactivity and Its Measurement*, Van Nostrand-Reinhold, New York (1966).

Time-of-Flight Spectroscopy

EQUIPMENT NEEDED FROM EG&G ORTEC FOR EXPERIMENT 25.1

Two Bins and Power Supplies
 Transmission Detector TD-25-25-15
 Surface Barrier Detector A-019-300-100
 Two 142B Preamplifiers
 480 Pulser
 428 Bias Supply
 574 Timing Amplifier
 Two 473A Constant-Fraction Discriminators
 457 Time-to-Amplitude Converter
 572 Amplifier
 ACE-2K MCA System including suitable IBM PC
 (other EG&G ORTEC MCAs may be used)
 M367 Alpha Time-of-Flight Chamber
 DB463 Delay Box
 ORC-25 Cable Set
 1 μCi ^{241}Am
 Source Kit SK-1A
 Vacuum Pump
 Oscilloscope
 459 5-kV Detector Bias Supply

Copper Absorber Kit MCU-5
 Aluminum Absorber Kit MAL-25

EQUIPMENT NEEDED FROM EG&G ORTEC FOR EXPERIMENT 25.2

Two Model 905-11-S 8850 PM Tubes with 1-in. x 1-in.
 Pilot U Plastic Scintillator
 Two 265-S PM Bases
 Two 556 High Voltage Power Supplies
 Two 583 Constant-Fraction Differential Discriminator/SCAs
 DB463 Delay Box
 414A Fast Coincidence
 457 Time-to-Amplitude Converter
 ACE-2K MCA System including suitable IBM PC (other
 EG&G ORTEC MCAs may be used)
 Two MT-624 Stands for Photomultiplier Tubes and Source
 10 μCi ^{22}Na Source
 Source Kit SK-1G
 MT050 Splitter
 Two Bins and Power Supplies
 ORC-25 Cable Set

Purpose

State-of-the-art, fast-timing techniques will be used to do two time-of-flight experiments. In the first experiment, the time-of-flight of alphas from an ^{241}Am source will be measured. This technique will be used to measure the energy loss of alphas after they pass through thin foils (as in Experiment 5). In the second experiment time-of-flight techniques will be used to measure the flight time of a gamma over a known flight path, and the velocity of the gamma, and therefore the velocity of light, can be determined.

EXPERIMENT 25.1

Alpha Particle Time-of-Flight and Energy Loss Measurements

A block diagram of the electronics used for this experiment is shown in Fig. 25.1. Alphas from the ^{241}Am source are allowed to pass through the ΔE detector and are completely stopped in the E detector. The experiment is done in a chamber that is evacuated with a fore pump. The ΔE detector is a thin, transmission detector $\sim 15 \mu\text{m}$ thick. Alphas from ^{241}Am will deposit on the order of 2 MeV in the ΔE detector. Since alphas from the source have an energy of 5.48 MeV, those passing through the ΔE detector will have an energy of ~ 3.48 MeV. The energy of this group of alphas can easily be measured by calibrating the 572 amplifier and the MCA as outlined in Experiment 4.

The chamber is designed so that the source and the ΔE detector can be moved together towards the E detector. The

start pulse for the time-to-amplitude converter, (TAC), is derived from the ΔE detector. The stop pulse comes from the E detector. When properly set up and calibrated (see Procedure), the TAC output into the MCA shows a single isolated peak in a specified channel. Next the source and the ΔE detector are moved a few centimeters closer to the E detector. The peak moves a number of channels, ΔC , in the MCA.

From the calibration of the TAC, the time difference, Δt , for this flight path difference, Δx , is measured. The velocity of the alpha particle group is determined by taking the ratio $\Delta x/\Delta t$.

This same procedure is used to measure the velocity of the alpha group after it has passed through a thin copper foil that is placed just in front of the ΔE detector. The energy loss of the alpha group is determined by this time-of-flight technique. This procedure will be repeated for various foils of different thicknesses as in Experiment 5. The results will be compared to the theoretical semiempirical calculations from the literature.

Before attempting this experiment, the student should have completed Experiments 4, 5, and 13. Experiments 4 and 5 deal with surface barrier detectors and energy loss, and Experiment 13 is an introduction to fast timing and the TAC.

Procedure

1. Set up the electronics as shown in Fig. 25.1. The interconnecting cables for all of the fast timing portions of Fig. 25.1 should be 50- Ω cable. These cables are provided in the

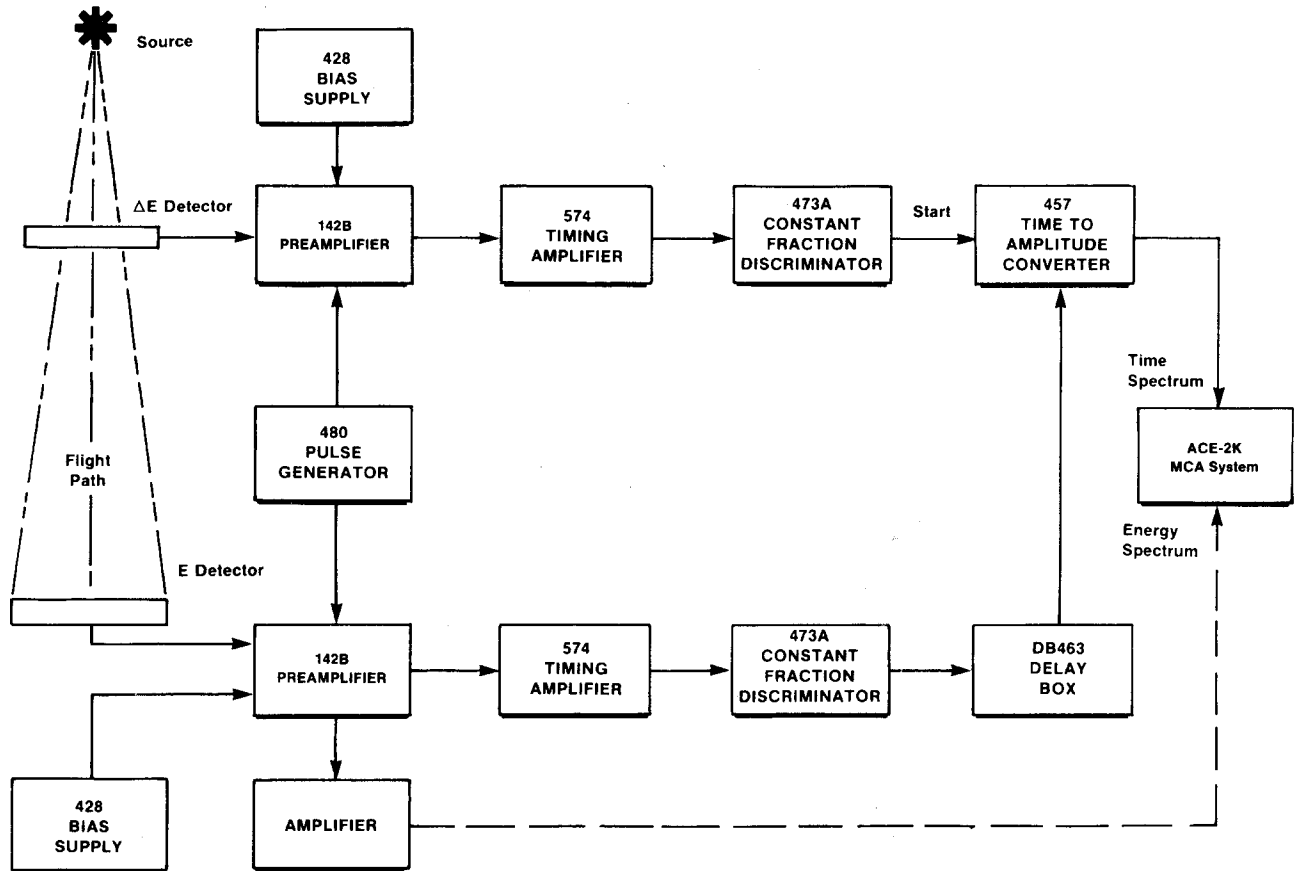


Fig. 25.1. Block Diagram of Electronics for the Alpha Particle Time-of-Flight Experiment.

ORC-25 Cable Set. The timing output of the 142B Preamplifier is connected to the input of the 574 Timing Amplifier for both the ΔE and E detectors. For the E detector the energy output, (E), of the 142B Preamplifier is fed into the 572 Amplifier for pulse-height analysis processing as in all of the previous experiments.

2. In this experiment the transmitted energy of the alphas from the source are measured in two ways: (1) directly, by calibrating the E detector, and (2) by measuring the velocity of the alphas by time-of-flight techniques. In order to measure the transmitted energy directly, it is necessary to calibrate the E detector with the ^{241}Am source. This is done by removing the ΔE detector and calibrating the E detector by normalizing the 480 pulse generator as in Experiment 4.

Make the calibration so that full scale on the MCA is ~ 6.0 MeV. Figure 4.9 shows the decay scheme for ^{241}Am and Fig. 4.8 shows a typical pulse height spectrum for the alphas from the source. Now that the E detector is calibrated, the ΔE detector can be replaced in its holder.

3. The timing output of the 142B ΔE Preamplifier should be fed into one of the inputs of the 574 Timing Amplifier. Adjust the 142B for minimum rise time. This procedure is outlined in the Operating and Service Manual. The 574 is a single-width

NIM module that contains four independent direct-coupled amplifiers packaged in a single module. The E preamplifier timing output is fed into one of the other amplifiers on the 574. The output of the 574 is connected to the input of the 473A Constant-Fraction Discriminator for both the start and stop channels. The controls of the 473A should be set as follows: Scint 2 shaping mode, constant fraction timing mode. The output pulses from the 473A are fast negative logic pulses. These pulses are fed into the 457 TAC in the start channel and in the stop channel they go into the DB463 Delay Box. The output of the DB463 goes into the stop side of the TAC.

4. The 480 pulse generator was calibrated in step 2. Set the 480 at 1 MeV and adjust the discriminator level (both start and stop sides) of the 473A so that fast negative output pulses are seen with a scope. The TAC settings should be as follows: 50 ns range, anticoincidence, TAC output. In the stop channel, set all delays out in the DB463 Delay Box except the 22-ns delay. Connect the output of the TAC into the MCA. The MCA should show a single peak in the lower quarter of the analyzer. The TAC can now be calibrated by changing the delay in the DB463 Delay Box and observing the corresponding shift in channel number for the MCA. Figure 25.2 shows a typical MCA spectrum that was taken for

22, 26, 30, and 34 ns delays. Take enough delay settings so that the time per channel can be determined.

5. Determine the time resolution of the system by multiplying the slope of this calibration curve by the FWHM of any of the pulser peaks. In Fig. 25.2 this value is shown to be 0.99 ns.

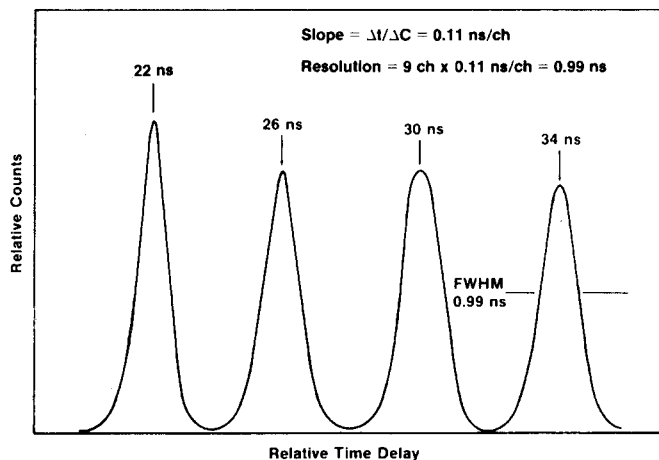


Fig. 25.2. Time-to-Amplitude Converter Calibration with the 480 Pulse Generator.

6. We are now ready to measure the time-of-flight of the alpha group after it has passed through the ΔE detector. Place the ΔE detector back in its original position as shown in Fig. 25.1. Evacuate the system and apply the bias to both detectors. Accumulate a spectrum in the MCA for a period of time long enough to accurately determine the peak position. Adjust the DB463 delay until this group is in the middle range of the MCA. Count for a period of time long enough to accurately determine its position. Record this channel, turn the

bias down on both detectors, and move the ΔE detector and source in towards the E detector 3 cm. Evacuate the system with bias on, and count for a period of time long enough to determine the new peak location. From the time calibration, determine Δt . The velocity of the group is simply $\Delta x/\Delta t$. From this velocity calculate the transmitted alpha energy.

7. Measure the energy of the alpha particle directly and compare the results with those of step 6. Connect the output of the 572 Amplifier into the MCA and accumulate for a period of time long enough to determine the centroid of the peak. From the energy calibration curve of the MCA, determine the energy of this transmitted alpha group. How does it compare with the time-of-flight results? Record both of these values in Table 25.1.

8. Open the vacuum system, move the ΔE detector back to its original position and place the thinnest aluminum foil directly in front of the ΔE detector. Evacuate and determine the channel position of the peak in the time-of-flight spectrum as above. Open the system, move the ΔE detector and foil 3 cm towards the E detector and evacuate. Accumulate a spectrum and determine Δt , v , and E as in step 6. Record this value of E under E (time-of-flight) in Table 25.1.

9. Measure the energy of the group directly as in step 7. Record this value in Table 25.1. Repeat for all of the foils in both foil kits and fill in Table 25.1. Figure 25.3 shows the direct energy measurement for the ^{241}Am source and the various combinations of aluminum absorbers on the same drawing.

EXERCISE

From the dE/dx values in ref. 8 and the procedures in Experiment 5, calculate the theoretical energy loss that would be expected for the transmitted alpha group. Remember, for our case, E_0 is the energy that the alpha group has when it enters

Table 25.1. Alpha Particle Time-of-Flight and Energy Loss Data.

Foil Thickness* (mg/cm ²)	E (direct) (MeV)	E (time-of-flight) (MeV)	Energy Loss (time-of-flight)	Energy Loss (theory)	% Difference
Aluminum Z = 13					
0.250					
0.500					
0.750					
Copper Z = 29					
2.00					
4.00					
6.00					
Silver Z = 47					
0.400					
0.600					
0.800					

*The foils listed are nominal thicknesses. The actual thicknesses in the kit may be slightly different. The quoted thickness value on the actual foils in the kit will be accurate to $\pm 5\%$.

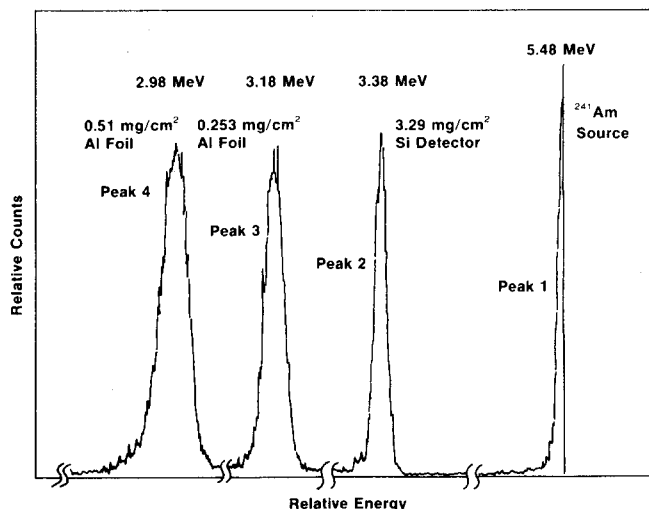


Fig. 25.3. Direct Energy Measurement.

NOTE: Peak 1 is the ²⁴¹Am source; Peak 2 is the transmitted spectrum through only the ΔE detector; Peak 3 is the transmitted spectrum through the ΔE detector plus 0.253 mg/cm² of Al; Peak 4 is the transmitted spectrum through the ΔE detector plus 0.51 mg/cm² of Al.

the foil (~3.4 MeV). This is shown in Table 25.1 as E (time-of-flight) with zero foil thickness. Record these values in Table 25.1 as energy loss (theory). From the data recorded in Table 25.1 determine the measured energy loss from the time-of-flight spectra. Calculate the percentage difference and record in Table 25.1.

EXPERIMENT 25.2

Gamma Ray Time-of-Flight and the Speed of Light

Figure 25.4 is a block diagram of the fast-timing coincidence system that will be used in this experiment. Under proper conditions, it will give the best time resolution possible.

The constant-fraction discriminators generate the timing information and determine the energy range of interest simultaneously. If the two gamma flashes fall within the selected energy range and are coincident within the resolving time set on the 414A Fast Coincidence unit, the TAC will

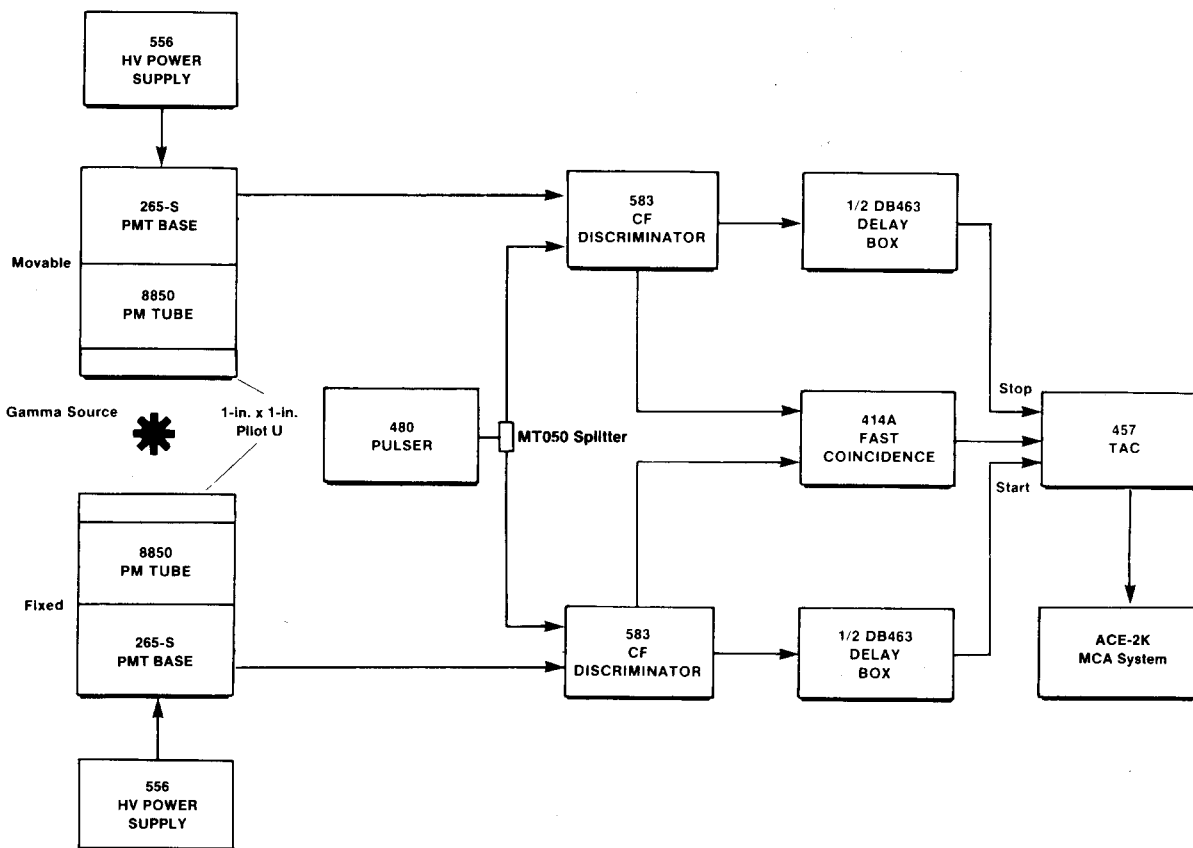


Fig. 25.4. Electronics Setup for the Gamma Ray Time-of-Flight Experiment.

be gated on and record the event. This experiment is similar to Experiment 25.1 in that the TAC will first be calibrated with a pulse generator and then the γ - γ coincidence of the 0.511-MeV γ 's from ^{22}Na will be measured. Read Experiment 13 and study Fig. 13.5 before starting this experiment.

The fixed detector will be used to start the TAC and it will be stopped by the movable detector. Next the movable detector will be moved a known flight path and the time difference recorded from the MCA. The velocity of the γ will be calculated from $v = \Delta x / \Delta t$. This measurement will be repeated for several different flight paths.

Figure 3.10 shows the decay scheme of ^{22}Na . Keep in mind that when the β^+ decays, two annihilation γ 's of 0.511 MeV are given off with an angular separation of 180° . In this experiment one of these γ 's will be used to start the time converter and the other to stop it.

If the pulse-height spectrum from the anode of either of the 265 Photomultiplier Bases is viewed, only the Compton distribution is seen. The reason for this is that the Pilot U scintillator is plastic. Therefore, it is basically a hydrocarbon, a low Z (atomic number) material. Remember that the photoelectric cross section is proportional to Z^5 . Since Z is low, the photoelectric effect is essentially nonexistent. The pulse-height distribution will look similar to the neutron distribution shown in Fig. 16.4.

Procedure

1. Set up the electronics as shown in Fig. 25.4. Set the 556 High Voltage Power Supplies to the values recommended in the Operating and Service Manual. Be sure to use the 50- Ω cable which is provided in the cable package for all fast timing connections. The long cable bundle is for the movable detector. These cables are long enough to change the flight path of the movable detector by 6 m. Initially the stands that hold the two phototubes should be placed about 50 cm apart with the source stand midway between the two. Don't put the ^{22}Na source in the stand. This will be done after the system has been calibrated.

2. Connect the output of the phototubes (anodes) to the inputs of the 583 Constant-Fraction Discriminators. Use one of the timing outputs of the 583 to connect to the input of the DB463 nanosecond Delay Box. On the start side, set the delay on the DB463 at 100 ns. Set the DB463 at delays for a sum of 120 ns on the stop side. Connect a piece of 50- Ω cable (~0.40 m in length) between the two delay outputs of the 583. This sets the required constant-fraction shaping delay for the unit. Repeat for the other 583.

3. The other controls on the 583 should be set as follows: Differential mode, constant-fraction timing mode, lower level (starting) 10%, upper level (starting) 90%. Set the walk adjustment to -0.5 mV.

4. The 480 pulse generator should be on negative, attenuated output. For the 414A Fast Coincidence use the two coincidence inputs on the left. These two toggle switches

should be In and the remaining two Out. Use either output of the 414A to gate the TAC. Set the resolving time of the 414A at 40 ns.

5. Set the 457 TAC to the 50-ns range, coincidence mode. Use the TAC output to the MCA.

6. Turn on the 480 Pulser and adjust the pulse height until the TAC output is being stored in the MCA. It should appear in the lower quadrant of the MCA.

7. We will now determine a delay vs pulse height curve for the TAC and the MCA as in Experiment 25.1. Change the DB463 delay on the stop side by 4 ns and record the new peak position. Continue for as many delay values as you wish, to determine the delay vs pulse height curve. Calculate the slope of the curve and determine the resolution of any of the pulser peaks.

8. Figure 25.5 shows two typical pulser peaks for delays of 4 ns and 12 ns. Both peaks in the figure have an FWHM of 8 channels, showing 0.94-ns time resolution for the pulser peaks. Turn off the pulse generator and place the ^{22}Na source in the holder in preparation for the time-of-flight data.

9. Clear the MCA and set the stop delay at 12 ns. Accumulate a spectra in the MCA for the γ - γ coincidence. It should appear in the lower quadrant of the MCA. The resolving time of the 414A can now be lowered and the upper and lower levels of the 583 adjusted for optimum resolution. When both the counting rate and the resolution are satisfactory, lock the dials down. Clear the MCA.

10. Accumulate a spectrum in the MCA for a period of time long enough to accurately determine the peak location. Record the centroid of this peak. Increase the flight path of the movable detector by 1 m and accumulate another spectrum. It should take ~25 times as long to get the same statistics as those obtained for the first measurement.

11. Determine the peak position and the channel shift. Calculate Δt from the slope of the calibration curve. Calculate $C = \Delta x / \Delta t$. How close is your value to the speed of light, $3 \times$

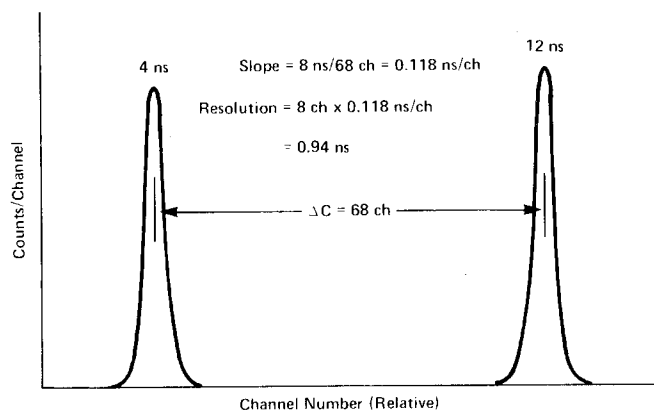


Fig. 25.5. Typical Pulser Peaks Showing the Calculation of Time/Channel for the MCA.

10^8 m/s? For the calibration shown in Fig. 25.5, ΔC should have been about 28 channels. This would give 3.3 ns, which is the correct value.

12. Repeat for flight path changes of 2, 3, and 4 m and calculate the γ velocity for each measurement. The 4-m data might take a few hours, but it should give the most accurate value for C since the major uncertainty in this experiment is in Δx , the flight path difference.

Note of Credit Parts of Experiment 25.1 were developed by Professor Dollard Demarais of the University of Alberta, Canada. A detailed experiment, "Alpha Particle Time-of-Flight" by Professor Demarais and the author, will appear in the *American Journal of Physics* in the summer of 1984.

References

1. "Principles and Applications of Timing Spectroscopy," EG&G ORTEC Application Note AN-42, available from EG&G ORTEC.
2. "Silicon Charged Particle Radiation Detectors," EG&G ORTEC Instruction Manual, available from EG&G ORTEC.
3. T. J. Paulus, R. D. McKnight, and T. L. Mayhugh, "Experimental Characterization of the Timing Properties of Detector Preamplifier System for Charged Particle Detectors Using a Laser Pulser," *IEEE Trans. Nucl. Sci.* **NS-24**(1), 335 (1977).
4. G. J. Wozniak, et al. "Time-Walk Characteristics of an Improved Constant-Fraction Discriminator," *Nucl. Instrum. Methods* **180**, 509-519 (1981).
5. M. Moszynski and B. Bengtson, "Status of Timing with Plastic Scintillation Detectors," *Nucl. Instrum. Methods* **158** 1-31 (1979).
6. S. Sanyal, et al., "Sub-Nanosecond Timing Studies with Plastic Scintillation Detectors," *Nucl. Instrum. Methods* **136**, 157 (1976).
7. J. F. Ziegler, *The Stopping Power and Ranges of Ions in Matter*, Pergammon Press, New York (1977).
8. L. C. Northcliffe and R. F. Schilling, *Nuclear Data Tables A7*, 233 (1970).
9. M. O. Bedwell and T. J. Paulus, "A Constant Fraction Differential Discriminator for Use in Fast Timing Coincidence Systems," *IEEE Trans. Nucl. Sci.* **NS-26**(1), 442 (1979).
10. M. O. Bedwell and T. J. Paulus, "A New High Rate Positron Lifetime Measurement System," Proceedings of the Fifth International Conference on Positron Annihilation, Lake Yamanaka, Japan, 375 (April 1979).
11. M. O. Bedwell and T. J. Paulus, "A New Constant Fraction Timing System with Improved Time Derivation Characteristics," *IEEE Trans. Nucl. Sci.* **NS-23**(1), 234 (1976).
12. See also the references for Experiments 4 and 5.

Fission Fragment Energy Loss Measurements from ²⁵²Cf

EQUIPMENT NEEDED FROM EG&G ORTEC

Heavy-Ion Detector Model F-025-300-60
 5- μ Ci ²⁵²Cf Fission Oil and Source Kit SK-1A
 142B Preamplifier
 Bin and Power Supply
 575A Amplifier
 428 Detector Bias Supply
 480 Pulser

ACE-2K MCA System including suitable IBM PC (other EG&G ORTEC MCAs may be used)
 Mechanical Pump
 Model 3C52 Fission Chamber with Rotating Foil Wheel
 Foil Set MC252
 Oscilloscope
 ORC-26 Cable Set

Introduction

In 1938 O. Hahn and F. Strassman discovered fission. In these studies they bombarded uranium with neutrons and produced nuclides which were chemically indistinguishable from elements in the middle range of the periodic table. Later scientists realized that the energetics of this process could be used as a power source. Theoretically, the fission process is not as well understood as most other nuclear reactions. Nevertheless, because of the energy potential of this process it has received more attention than any other nuclear reaction. As fossil fuel supplies are used the world is, and will continue to be, dependent on fission as a source of energy until alternate dependable sources such as fusion, solar, etc. are developed.

The advent of the high-flux isotope reactor has given a wealth of heavy isotopes that decay by spontaneous fission. ²⁵²Cf is now readily available from commercial vendors as a fission foil source and an ideal candidate to be used in the study of the fission process.

Figure 26.1 shows a production diagram for ²⁵²Cf. It is necessary to have a high-flux reactor to produce ²⁵²Cf. Most of the species shown in Fig. 26.1 would rather decay to an appro-

appropriate daughter than absorb a neutron. The high-flux isotope reactors produce such a high neutron flux that absorption occurs before the isotope can decay. Thus ²⁵²Cf is ultimately produced. Table 26.1 shows some of the physical properties of ²⁵²Cf. Figure 26.2 shows a typical spectrum that will be measured in the laboratory for this experiment. If the kinematics of this fission are studied there is ~200 MeV available to the fission products. Conservation of momentum will give the light group about 30% more energy than the heavy group.

Table 26.1. Physical Properties of ²⁵²Cf.

Alpha particle energy	: 6.12 MeV
Effective half life	: 2.65 years
Alpha decay half life	: 2.73 years
Spontaneous fission half life	: 85.5 years
Gamma emission rate	: 1.37×10^7 photons/ μ g
Specific activity	: 500 μ Ci/ μ g
Average neutron energy	: 2.35 MeV
Average neutrons per fission	: 3.76
Neutron emission rate	: 2.34×10^6 neutrons/s/ μ g
Fission rate	: 6.2×10^5 /s/ μ g

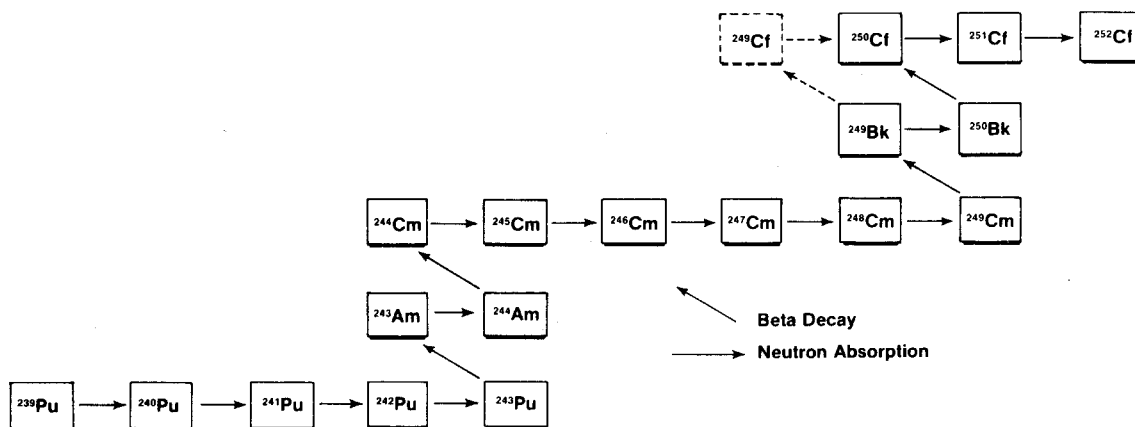


Fig. 26.1. Diagram Showing the Production of ²⁵²Cf.

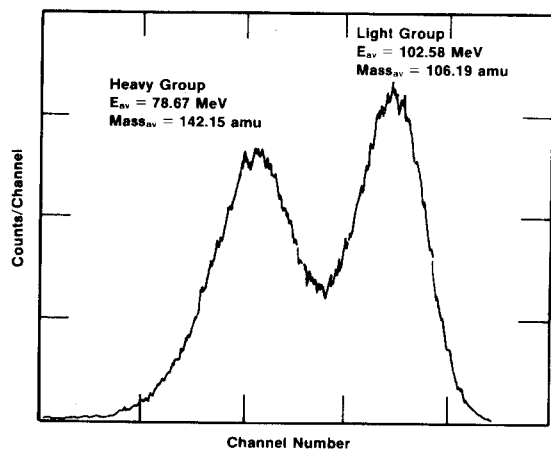


Fig. 26.2. Typical Pulse Height Spectrum for a Thin ²⁵²Cf Fission Foil Source.

This energy difference is sufficient to easily separate the groups and perform energy loss measurements on both groups independently.

EXPERIMENT 26.1

Energy Calibration for Fission Fragments

In all of the experiments in this manual the energies measured were <10 MeV. In this experiment heavy ions will be measured having energies >100 MeV.* When the energy of a fast moving heavy ion is studied with a surface barrier detector, the measured number is always less than the theoretical value. This phenomenon is called the pulse-height defect. For alpha- and beta-particle measurement the effect is also present, but it is so insignificant that it is usually

*See Detector Manual for comments on detector damage rates for neutrons, etc.

ignored. For heavy ions this pulse-height defect is produced by the following: entrance window effects, nuclear collision effects, and plasma effects. The entrance window effect is ~0.4 MeV for this experiment. It is accounted for by the dE/dx of the fission fragments in the gold entrance window of the detector. For 6-MeV alphas this loss would be ~4 keV. In the nuclear collision effect the fission fragment can interact with the nucleus with a fairly high probability. The average energy produced during this collision is lost to the production of electron hole pairs and a decrease in pulse height results.

The final decrease in pulse height is produced by the plasma effect. When the fission fragment enters the surface barrier detector it loses energy very rapidly, creating a dense cloud of electron hole pairs in a narrow region. This plasma tends to cancel out, for a short period of time, the electric field that is trying to separate the electron hole pairs and produce a pulse. During this short time a small fraction of the electron hole pairs can recombine with a subsequent loss in pulse height.

Many papers have been written on this phenomenon. Reference 9 is a good summary of measurements in regard to this effect. For ²⁵²Cf the average pulse height defect is 16 MeV for both the heavy and light fission products.

Procedure

1. Set up the electronics as shown in Fig. 26.3. There are four positions on the foil wheel. Place the three aluminum absorbers in three of these positions. Line up the remaining open port with the detector and source. Evacuate the chamber with the vacuum pump and apply the recommended bias.
2. Adjust the gain of the 575A Amplifier so the 6.12-MeV alpha from the source is being stored in the first quarter of the MCA. Record the position of the peak. Turn on the 480 Pulse Generator and enter a X10 with one of the attenuators. Set the pulse height dial at 612/1000. Normalize the pulse

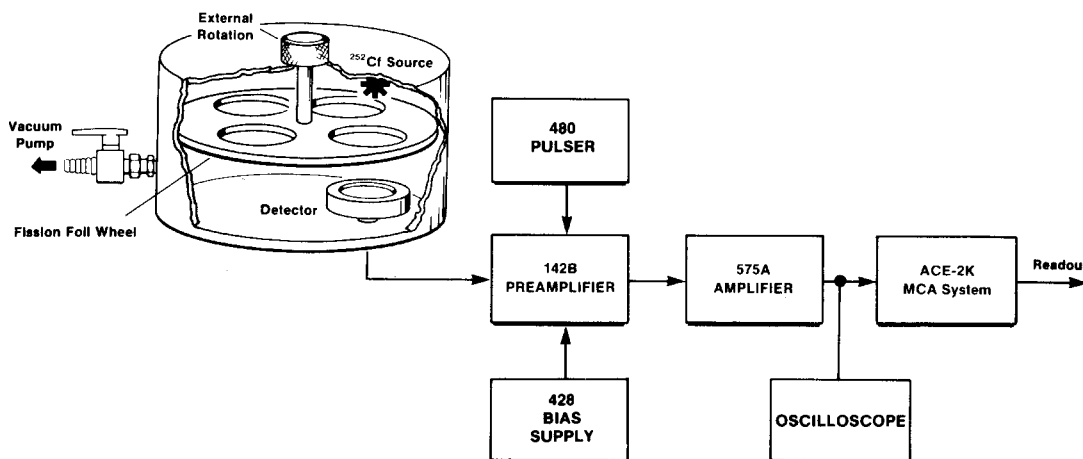


Fig. 26.3. Electronics Arrangement for Fission Fragment Energy Loss Experiment.

generator with the Cal control so that the pulser peak falls in the same channel as the 6.12-MeV alpha. This technique was carefully outlined in Experiment 4. The 480 is now calibrated for 10-MeV full scale. In order to change this calibration to 100-MeV full scale, it is only necessary to change the attenuator from X10 to X1. Now 500/1000 on the pulse height dial corresponds to 50 MeV, etc.

3. Set the 480 Pulser at 50 MeV and adjust the 575A Amplifier so the pulse is being stored in approximately channel 400. Make a calibration curve for 20, 40, 60, 80, and 100 MeV. Plot the calibration curve as in Experiment 4.

4. Turn off the 480 and accumulate a spectrum for the fission fragments from the ²⁵²Cf source. The spectrum should resemble Fig. 26.2. Readout the MCA and plot the spectrum. Determine the centroid energy for both the light and heavy groups. What is your measured pulse height defect?

5. Rotate the foil wheel and place the thinnest aluminum foil between the source and the detector. Accumulate a spectrum and determine the centroids for the two peaks. From your calibration curve determine ΔE, the energy loss for both groups. Record these values in a data table as ΔE (measured) for both the light and heavy groups. Continue for the rest of the aluminum foils in the absorber kit. Your data table should also have an entry for ΔE (theoretical) for each foil and each group. This value is calculated in the exercise that follows.

6. Turn the bias down and carefully let the system up to air. Remove the aluminum absorbers and replace them with the copper absorbers. Pump back down, turn the bias on, and repeat step 5 for these copper foils.

EXERCISES

Figure 26.4 shows the mass distribution of the fission fragments from ²⁵²Cf. To compare our experimental data to the theory, assume that the light fragment has a mass of 106 amu and use the theoretical dE/dx tables for ¹⁰⁶Pd. For the heavy mass the average is 142 amu, and therefore, the dE/dx for

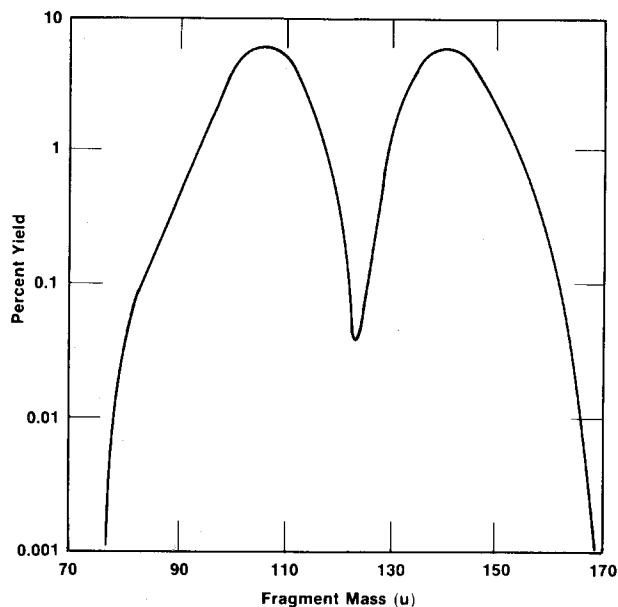


Fig. 26.4. Mass Distribution of Fission Fragments for ²⁵²Cf.

¹⁴²Nd will be used. From ref. 6, the dE/dx (theory) of ¹⁰⁶Pd at 102.58 MeV is 44.05 MeV-cm²/mg.

Assuming that the light mass passes through a 0.250 mg/cm² aluminum foil, the theoretical energy loss would be:

$$\Delta E \text{ (theory)} = 44.05 \text{ MeV-cm}^2/\text{mg} \times 0.250 \text{ mg/cm}^2 = 11.01 \text{ MeV.}$$

These procedures were covered in Experiment 5. Calculate ΔE/Δx (theory) for the rest of the aluminum foils and all of the copper foils. Record these values in your data table and calculate the percentage difference between your experimental values and the theoretical calculations. The dE/dx (theory) values for the fragment and foils used in this experiment are shown in Table 26.2.

Table 26.2. dE/dx (theory) (from ref. 6).

Fragment	Energy	dE/dx (theory) Aluminum	dE/dx (theory) Copper
Light ¹⁰⁶ Pd	102.58	44.05 MeV-cm ² /mg	30.77 MeV-cm ² /mg
Heavy ¹⁴² Nd	78.67	43.99 MeV-cm ² /mg	28.6 MeV-cm ² /mg

Note of Credit This experiment was developed primarily by Professor Dollard Desmarais of the University of Alberta, Canada and the author. A detailed "Fission Fragment Energy Loss" experiment will appear in the *American Journal of Physics* in the summer of 1984.

References

1. G. Bertolini and A. Coche, Eds, *Semiconductor Detectors*, Sections 4.1.1 and 4.2.1 to 4.2.4, American Elsevier Publishing Co., New York (1968).
2. G. F. Knoll, *Radiation Detection and Measurement*, John Wiley and Sons, New York (1979).
3. H. W. Schmitt and F. Pleasonton, *Nucl. Instrum. Methods* **40**, 204 (1966).
4. S. Parker and H. N. Steiger-Shafrin, *Nucl. Instrum. Methods* **91**, 557 (1971).
5. H. L. Adair, *Nucl. Instrum. Methods* **100**, 467 (1972).
6. L. C. Northcliffe and R. F. Schilling, *Nuclear Data Tables* **A7**, 233, Academic Press, New York (1970).
7. H. Henschel, *et al.*, *Nucl. Instrum. Methods* **190**, 125 (1981).
8. "Heavy Ion Spectroscopy with Silicon Surface Barrier Detectors," *EG&G ORTEC Application Note AN-40*. Available from EG&G ORTEC.
9. E. C. Finch and A. L. Rodgers, "Measurements of the Pulse Height Defect and its Mass Dependence for Heavy Ion Silicon Detectors," *Nucl. Instrum. Methods* **113**, 29 (1973).

This appendix contains information of general interest to help explain some of the details of discussions where the terms used to explain nuclear events may not be too well known. It also lists the definitions of the coded items that are used in various experiments in this manual.

Linear and Logic Signal Standards in EG&G ORTEC NIM Instruments

Introduction to NIM

EG&G ORTEC has established itself as the leading manufacturer of NIM modules and related products since the introduction of the Standardized Nuclear Instrument Module (NIM). We offer the largest selection of NIM electronics available anywhere, and all modules conform to the standards outlined in AEC (adopted by DOE) Report TID-20893 (Rev) which ensures compatibility between instruments provided by various manufacturers. Specifications and testing of EG&G ORTEC NIM modules are made in accordance with "IEEE Standard Test Procedures for Amplifiers and Preamplifiers for Semiconductor Radiation Detectors for Ionizing Radiation" where applicable.

LINEAR AND LOGIC STANDARDS AND CONNECTIONS

Since many EG&G ORTEC instruments utilize both linear and logic signals it is always important to distinguish between linear and logic connections when setting up NIM equipment. The amplitude of a linear signal contains information about the energy of a detected event. Therefore, linear signals vary over a range of amplitudes, and the analysis of linear signal amplitudes from an instrument reveals the energy spectrum of the photon source. By contrast, logic signals have a fixed amplitude and shape. They are used to provide timing information and to control the function of subsequent instruments in a system. Both linear and logic signal connections are made by coaxial cables and standard BNC connectors.

LINEAR SIGNALS Linear signals from EG&G ORTEC NIM modules conform to the NIM-standard preferred practices for 0 to 10 V spans.

Standard polarity and span do not apply to the linear signal between the preamplifier and the amplifier. This signal must be variable in span and polarity to accommodate particular applications. However, all EG&G ORTEC preamplifiers are standardized with respect to the output pulse shape and typically furnish a 50 μ s or greater time-constant tail pulse to the main amplifier. The main amplifier accommodates this standardized input pulse with a compatible pole-zero-cancellation facility. In addition, EG&G ORTEC main amplifiers accommodate either input polarity.

Linear Signal Interconnections EG&G ORTEC instruments always provide linear output signals through a very low source impedance, typically $<1 \Omega$. Some instruments also provide the output signals through a second circuit with 93- Ω source impedance.

The low impedance ($<1 \Omega$) allows connection of almost any load without loss of signal span due to internal loss in the source impedance itself. For instance, a 100- Ω load may be driven to the full 10 V span. If a 93- Ω source must drive a 93- Ω or 100- Ω load, half of the span will be lost. For these reasons, the low-impedance outputs are simpler to use. They also permit paralleled multiple loads without loss of span. A potential problem with the low-impedance output is oscillation due to reflections from unterminated cables more than 5 ft long. For this reason cables should be terminated at the receiving end or connected to the 93- Ω output if it is available. The 93- Ω outputs may be used for full-span signal transfer only if the receiving end of the output cable is essentially an open circuit, meaning 1000 Ω or more in practice. If a lower impedance is encountered, the span will be reduced. The chief virtue of the 93- Ω output is absolute stability for variable cable conditions, obtained at the expense of variable span dependent on load impedance.

LOGIC SIGNALS All EG&G ORTEC instruments use standardized (positive and fast negative) logic signals to provide full interunit compatibility.

Positive Logic Signals The standard positive logic signal is used for slow- to medium-speed logic signals with repetition rates from dc to 20 MHz. The NIM-standard Preferred Practice provisions define this signal by the following amplitude limits:

	Output (must deliver)	Input (must respond to)
Logic 1	+4 to +12 V	+3 to +12 V
Logic 0	+1 to -2 V	+1.5 to -2 V

In addition, EG&G ORTEC imposes further standards on the positive logic signal:

Pulse width: 0.5 μ s nominally.

Source impedance: 10 Ω or less nominally.

Input impedance: 1000 Ω or more nominally.

Connection of the positive logic sources and loads should be made with 93- Ω coaxial cables. RG-62A/U cables with UG-260/U (BNC) connectors are recommended.

For cable lengths under 5 ft, impedance-matching cable termination is not usually required since reflections are not a problem. In longer cable lengths, proper termination with a 100- Ω terminator is advisable to prevent cable reflections.

Fast Negative Logic Signals The standard fast negative logic signal is used when rise time or repetition rate requirements exceed the capability of the standard positive logic pulses. The NIM Preferred Practice provisions define this signal as one that is furnished into a 50- Ω impedance with the following characteristics:

	Output (must deliver)	Input (must respond to)
Logic 1	-14 to -18 mA	-12 to -36 mA
Logic 0	-1 to +1 mA	-4 to +20 mA

Because of the fast rise time, the fast negative logic signal must be used with properly terminated cables to prevent reflections. Therefore 50- Ω cables and terminations such as RG-58C/U cables with UG-88/U connectors are recommended.

The rise time of the fast negative logic pulse is not specified in the NIM Preferred Practice provisions. In EG&G ORTEC instruments the rise time is typically 2 ns. The leading edge is normally used for all triggering, and width is unimportant except for repetition and rate considerations.

Equipment and Supplies Identified by Code

Source Kits

SK-1G	Sealed Solid Disk Gamma-Ray Sources ~ 1 μ Ci, ^{137}Cs , ^{60}Co , ^{22}Na , ^{65}Zn , ^{54}Mn .
SK-1X	Sealed X-Ray Sources (Disk Type) 1-5 μ Ci, ^{57}Co , ^{55}Fe , ^{65}Zn .
SK-1A	Unsealed Alpha Sources (Disk Type) 0.01-0.1 μ Ci, ^{241}Am , ^{210}Po , ^{244}Cm .
SK-1B	Sealed Beta and Conversion Electron Sources (Disk Type) 1-5 μ Ci, ^{204}Tl , ^{207}Bi , ^{137}Cs , ^{113}Sn .
OT8	RaD and E Split Check Source Set; ^{210}Pb and ^{210}Bi , ~ 1 μ Ci, includes blank-half to retain geometry when using either half alone.

Detector Stands and Housings

M-Nal-3	Stand for 2- x 2-in. NaI Tube; 6 counting levels.
MPM-9	Stand for 2- x 2-in. Phototube; supports the Phototube above the 305 Vacuum Chamber.
MGM-5	Stand for GM Counter; contains GM Tube and stand with 6 counting levels.

MT-624 Three Stands for the Gamma Time-of-Flight Experiment. One stand is used for positioning the ^{22}Na source; the other two are for mounting the phototubes on axis with the source coincident gamma rays.

Absorber Kits and Target Kits

PbAl-23	Contains 10 lead absorbers from 800 to 8000 mg/cm^2 and 20 aluminum absorbers from 0 to 3000 mg/cm^2 .
3-Z2	Contains 3 foils each of the following: Al, Fe, Cu, Mo, Sn, Ta, and Pb. Thicknesses range from 400 mg/cm^2 to 1500 mg/cm^2 .
MCU-5	10 copper absorbers in the range from 1.25 mg/cm^2 to 7.05 mg/cm^2 .
MNI-5	10 nickel absorbers in the range from 1.5 mg/cm^2 to 8.25 mg/cm^2 .
M-12	Sample set for x-ray fluorescence includes: Fe, Ni, Cu, Zn, Mo, Cd, Ag, Ge, and Zr plus 3 composite samples.
M-15	Rutherford Scattering Target Kit; contains thin foils of Cu, Al, Au, and Ag.
313	Neutron Activation Sample Set; contains 3-gm sample of high-purity metal: V, Al, Ge, Mn, and Cu.
317	Neutron Activation Sample Set; contains; Ag, Ti, W, Na, and Co.
V-17	Contains 10 each vanadium samples used for Experiment 17.4.
RE-17	Contains elements with high activation cross section samples of In, La, Br, and I.
Cd-17	Six (6) each cadmium shields for Experiment 17.6.
318	Contains 6 samples with high cross sections for fast neutrons: Mg, Na, Si, V, Fe, and Cr.
MC252	Six (6) each Ag foils for fission fragment time-of-flight energy loss.
MAL-25	Six (6) each Ag foils for alpha particle energy loss by time-of-flight.
301	Air Pollution Filter Standards; to be used with either Model 311 or 312 Chambers for standardization; contains: Si, Ca, Fe, Cu, and Ag.

Individual Absorbers and Shields

AIFI-1	Aluminum Foil, 2 x 2 in. x 2 mg/cm^2
AIFI-2	Aluminum Foil, 2 x 2 in. x 5 mg/cm^2
AIFI-3	Aluminum Foil, 2 x 2 in. x 10 mg/cm^2
AIFI-4	Aluminum Foil, 2 x 2 in. x 20 mg/cm^2
AIFI-5	Aluminum Foil, 2 x 2 in. x 50 mg/cm^2

AIP1-1 Aluminum Plate, 4 x 4 x 1/8 in.	309	Compton Scattering Apparatus, 36 in. x 46 in. x 30-in. high. Rotating shield for 2 x 2 in. NaI detector. Angular accuracy $\pm 0.10^\circ$. The lead shield for the ^{137}Cs source can be locked for student safety.
AIRd-1 Aluminum Rod, 0.5 in. diam x 4 in. long		
AIRd-2 Aluminum Rod, 2 cm diam x 1 cm long (~10 g)		
AIRd-3 Aluminum Rod, 6 cm diam x 7 cm long		
AuFI-1 Gold Foil, 200 $\mu\text{g}/\text{cm}^2$		
AuFI-x Gold Foil, 1.31 to 27.1 mg/cm^2	310	Proportional Counter Chamber; vacuum chamber 8-in. diam x 3-in. deep. Four sample positions which can be indexed under vacuum. Primarily designed for x-ray attenuation measurements.
CdPI-1 Cadmium Plate, 4 x 4 x 1/16 in.		
CuRd-1 Copper Rod, 6 cm diam x 7 cm long		
NiFI-1 Nickel Foil, 2 x 2 in. x 5 mg/cm^2		
NiFI-x Nickel Foil. 0.74 to 13.46 mg/cm^2		
PbPI-1 Lead Plate, 3 x 3 x 1/16 in.	311	Chamber for X-Ray Fluorescence Measurements with a Si(Li) Detector; 8-in. diam x 3-in. deep. Designed to fit onto an upright Si(Li) detector. Four each selectable sample positions under vacuum.
PbPI-2 Lead Plate, 4 x 4 x 1/16 in.		
PbPI-3 Lead Plate, 4 x 4 x 1 in.		
PbRd-1 Lead Rod, 6 cm diam x 7 cm long		
PnPI-1 Paraffin Plate, 4 x 4 x 1/2 in.	312	Chamber for X-Ray Fluorescence with a Proportional Counter. Same as Model 311 except it is designed to be used with a high-resolution proportional counter.
PnPI-2 Paraffin Plate, 4 x 4 x 1 in.		
FeRd-1 Iron Rod, 6 cm diam x 7 cm long		
PnRd-1 Paraffin Shadow Bar Rod, 6 cm diam x 7 cm long		
SIPI-1 Steel Plate, 4 x 4 x 1/8 in.		
Chambers, Howitzers, Angular Correlation Tables, Filter Sample Collectors		
302		Portable, High-Velocity Filter Collector for collecting air pollution samples. Air flow rates up to 70 cubic feet per minute.
305		Vacuum Can with Thin Plastic Window, 4 in. diam x 6 in. high. Most α and β experiments can be done in this chamber and also α, γ or β, γ coincidence experiments.
306		Angular Correlation Table, 46 in. x 46 in. x 30 in. high. Contains lead shields for fixed and movable 2 x 2 in. NaI detectors. The angular settings are accurate to $\pm 0.1^\circ$.
307		Rutherford Scattering Chamber, 11-3/4-in. diam x 5-1/4-in. high; polished aluminum. The detector can be moved under vacuum with an accuracy of $\pm 0.25^\circ$.
308		Neutron Howitzer, 3 ft x 3 ft x 3 ft; contains four each 1-in. activation ports for neutron sources up to 10 Ci. The source can be locked in the chamber for safety while the students are doing the experiment.
	M367	Alpha Particle Time-of-Flight Chamber; 11-3/4 in. diam x 5-1/4-in. high. Provisions for movable source and detectors. Flight paths up to 22.5 cm are possible. High vacuum tested to 1×10^{-6} mm of Hg.
	3C52	Fission Fragment Studies Chamber; 8-in. diam x 3-in. deep. Four sample positions which can be indexed under vacuum. The fission source and solid-state detector are precisely aligned on axis with the absorber foils.
	MAX 21	Chamber for Innershell Ionization Studies. The chamber is coupled to a Si(Li) x-ray detector with high vacuum techniques. The source, foils, and center line of the detector are all precisely aligned for geometrical purposes. The system can be evacuated to 1×10^{-6} mm of Hg.
	HTS-1	High Transmission Stand Set for the Total Neutron Cross Section Experiment. The stands are Webb designed for minimum neutron scattering.

Glossary

Absorption Coefficient: Fractional decrease in the intensity of a beam of x- or gamma-radiation per unit thickness (linear absorption coefficient), per unit mass (mass absorption coefficient), or per atom (atomic absorption coefficient) of absorber, due to deposition of energy in the absorber. The total absorption coefficient is based on the sum of individual energy absorption processes (Compton effect, photoelectric effect, and pair production).

Absorption Coefficient, Atomic: The linear absorption coefficient of a nuclide divided by the number of atoms per unit volume of the nuclide. It is equivalent to the nuclide's total cross section for the given radiation.

Absorption Coefficient, Compton: That fractional decrease in the energy of a beam of x- or gamma-radiation due to the deposition of the energy to electrons produced by Compton effect in an absorber. (See also Scattering, Compton.)

Absorption Coefficient, Linear: A factor expressing the fraction of a beam of x- or gamma-radiation absorbed in unit thickness of material. In the expression $I = I_0 e^{-\mu x}$, I_0 is the initial intensity, I is the intensity of the beam after passage through a thickness, x , of the material, and μ is the linear absorption coefficient.

Absorption Coefficient, Mass: The linear absorption coefficient per cm divided by the density of the absorber in grams per cm^3 . It is frequently expressed as μ/ρ , where μ is the linear absorption coefficient and ρ the absorber density.

Alpha Particle: A helium nucleus, consisting of two protons and two neutrons, with a double positive charge.

Analysis, Activation: A method of chemical analysis, especially for small traces of material, based on the detection of characteristic radionuclides following a nuclear bombardment.

Analysis, Feather: A technique for the determination of the range in aluminum of the beta particles of a radio-element by comparison of the absorption curve with the absorption curve of a reference series, usually ^{210}Bi (range 501 mg/cm^2).

Angstrom Unit (\AA): One angstrom unit equals 10^{-8} cm .

Atomic Number: The number of orbital electrons surrounding the nucleus of a neutral atom and according to present theory the number of protons in the nucleus (Symbol: Z).

Attenuation: The process by which a beam of radiation is reduced in intensity when passing through some material. It is the combination of absorption and scattering processes and leads to a decrease in flux density of the beam when projected through matter.

Attenuation Coefficient, Compton: The fractional number of photons removed from a beam of radiation per unit thickness of a material through which it is passing as a result of Compton effect interactions.

Attenuation Factor: A measure of the opacity of a layer of material for radiation traversing it; the ratio of the incident intensity to the transmitted intensity. It is equal to I_0/I , where I_0 and I are the intensities of the incident and emergent radiation, respectively. In the usual sense of exponential absorption ($I = I_0 e^{-\mu x}$) the attenuation factor is $e^{-\mu x}$, where x is the thickness of the material, and μ is the absorption coefficient.

Auger Effect: The emission of an electron from the extranuclear portion of an excited atom when the atom undergoes a transition to a less excited state.

Average Life (Mean Life): The average of the individual lives of all the atoms of a particular radioactive substance. It is 1.443 times the radioactive half-life.

Avogadro's Number (6.025×10^{23} physical scale): Number of atoms in a gram atomic weight of any element; also the number of molecules in the gram molecular weight of any substance.

Backscattering: The deflection of radiation by scattering processes through angles $>90^\circ$ with respect to the original direction of motion.

Barn: Unit expressing the probability of a specific nuclear reaction taking place in terms of cross-sectional area. Numerically it is 10^{-24} cm^2 .

Beta Particle: Charged particle emitted from the nucleus of an atom and having a mass and charge equal in magnitude to those of the electron.

Branching: The occurrence of two or more modes by which a radionuclide can undergo radioactive decay. For example, RaC can undergo α and β decay, ^{64}Cu can undergo β^- , β^+ , and electron capture decay. An individual atom of a nuclide exhibiting branching disintegrates by one mode only. The fraction disintegrating by a particular mode is the branching fraction for that mode. The branching ratio is the ratio of two specified branching fractions (synonym: multiple disintegration).

Bremsstrahlung: Secondary photon radiation produced by deceleration of charged particles passing through matter.

Capture, Electron: A mode of radioactive decay involving the capture of an orbital electron by its nucleus. Capture from a particular electron shell is designated as K-electron capture, L-electron capture, etc.

Capture, K-Electron: Electron capture from the K shell by the nucleus of the atom. Also loosely used to designate any orbital electron-capture process.

Capture, Radiative: The process by which a nucleus captures an incident particle and loses its excitation energy immediately by the emission of gamma radiation.

Compton Effect: An attenuation process observed for x- or gamma-radiation in which an incident photon interacts with an orbital electron of an atom to produce a recoil electron and a scattered photon of energy less than the incident photon.

Conversion, Internal: A mode of radioactive decay in which the gamma rays from excited nuclei cause the ejection of orbital electrons from the atom. The ratio of the number of internal conversion electrons to the number of gamma quanta emitted in the de-excitation of the nucleus is called the "conversion ratio."

Cosmic Rays: High energy particulate and electromagnetic radiations which originate outside of the earth's atmosphere.

Coulomb: Unit of electrical charge in the practical system of units. A quantity of electricity equal to 3×10^9 electrostatic units of charge.

Cross Section, Nuclear: The probability that a certain reaction between a nucleus and an incident particle or photon will occur. It is expressed as the effective "area" that the nucleus presents for the reaction. (See Barn.) Macroscopic cross section refers to the cross section per unit volume (preferably) or per unit mass. Microscopic cross section is the cross section of one atom or molecule.

Decay, Radioactive: Disintegration of the nucleus of an unstable nuclide by the spontaneous emission of charged particles and/or photons.

Delta Ray: Any secondary ionizing particle ejected by recoil when a primary ionizing particle passes through matter.

Deuterium: A heavy isotope of hydrogen having one proton and one neutron in the nucleus (Symbol: D or ${}^2\text{H}$).

Disintegration, Constant: The fraction of the number of atoms of a radioactive nuclide which decay in unit time; λ in the equation $N = N_0 e^{-\lambda t}$, where N_0 is the initial number of atoms present and N is the number of atoms present after some time, t .

Disintegration, Nuclear: A spontaneous nuclear transformation (radioactivity) characterized by the emission of energy and/or mass from the nucleus. When numbers of nuclei are involved, the process is characterized by a definite half-life.

Electron: Negatively charged particle which is a constituent of every neutral atom. Unit of negative electricity equal to 4.8×10^{-10} electrostatic units or 1.6×10^{-19} coulomb. Its mass is 0.000549 atomic mass units.

Electron Volt (eV): A unit of energy equivalent to the amount of energy gained by an electron in passing through a potential difference of 1 volt. Larger multiple units of the electron volt are frequently used, viz: keV for thousand or kilo electron volts, MeV for million electron volts, and BeV for billion electron volts; $1 \text{ eV} = 1.6 \times 10^{-12}$ erg.

Element: Pure substance consisting of atoms of the same atomic number which cannot be decomposed by ordinary chemical means.

Emulsion, Nuclear: A photographic emulsion specially designed to permit observation of the individual tracks of ionizing particles.

Energy: Capacity for doing work. Potential energy is the energy inherent in a mass because of its position with reference to other masses. Kinetic energy is the energy possessed by a mass because of its motion; cgs units: $\text{g-cm}^2/\text{s}^2$ or ergs.

Energy, Binding: The energy represented by the difference in mass between the sum of the component parts and the actual mass of the nucleus.

Energy, Excitation: The energy required to change a system from its ground state to an excited state. With each different excited state there is associated a different excitation energy.

Energy, Ionizing: The average energy lost by ionizing radiation in producing an ion pair in a gas. For air it is about 33 eV.

Energy, Radiant: The energy of electromagnetic waves, such as radio waves, visible light, x rays and gamma rays.

Energy, Reaction (Nuclear): In the disintegration of a nuclear reaction, it is equal to the sum of the kinetic or radiant energies of the reactants minus the sum of the kinetic or radiant energies of the products. (If any product of a specified reaction is in an excited nuclear state, the energy of subsequently emitted gamma radiation is not included in the sum.) The ground-state nuclear reaction energy is the reaction energy when all reactant and product nuclei are in their ground states (Symbol: Q_0).

Excitation: The addition of energy to a system, thereby transferring it from its ground state to an excited state. Excitation of a nucleus, an atom, or a molecule can result from absorption of photons or from inelastic collisions with other particles.

Fluorescence: The emission of radiation of particular wavelengths by a substance as a result of absorption of radiation of shorter wavelength. This emission occurs essentially only during the irradiation.

Flux: For electromagnetic radiation, the quantity of radiant energy flowing per unit time. For particles and photons,

the number of particles or photons flowing per unit time.

Gamma Ray: Short wavelength electromagnetic radiation of nuclear origin with a range of wavelengths from about 10^{-8} to 10^{-11} cm, emitted from the nucleus.

Geiger Region: In an ionization radiation detector, the operating voltage interval in which the charge collected per ionizing event is essentially independent of the number of primary ions produced in the initial ionizing event.

Geiger Threshold: The lowest voltage applied to a counter tube for which all pulses produced in the counter tube are of substantially the same size, regardless of the size of the primary ionizing event.

Geometry, Good: In nuclear physics measurements, an arrangement of source and detecting equipment so that the use of finite source size and finite detector aperture introduces little error.

Gram Atomic Weight: A mass in grams numerically equal to the atomic weight of an element.

Half-Life, Radioactive: Time required for a radioactive substance to lose 50% of its activity by decay. Each radionuclide has a unique half-life.

Half Value Layer (Half Thickness): The thickness of any particular material necessary to reduce the intensity of an x-ray or gamma-ray beam to one-half its original value.

Ionization: The process or the result of any process by which a neutral atom or molecule acquires either a positive or a negative charge.

Ionization, Total: The total electric charge of one sign on the ions produced by radiation in the process of losing all of its kinetic energy. For a given gas, the total ionization is closely proportional to the initial ionization and is nearly independent of the nature of the ionizing radiation. It is frequently used as a measure of radiation energy.

Ion Pair: Two particles of opposite charge, usually referring to the electron and positive atomic or molecular residue resulting after the interaction of ionizing radiation with the orbital electrons of atoms.

Isobar: One of two or more different nuclides having the same mass number but differing in atomic number. Originally called isobares but the name "isobars" is now generally employed.

Isomer: One of several nuclides having the same number of neutrons and protons but capable of existing, for a measurable time, in different quantum states with different energies and radioactive properties. Commonly, the isomer of higher energy decays to one with lower energy by the process of isomeric transition.

Isotope: One of several nuclides having the same number of protons in their nuclei, and hence having the same atomic

number, but differing in the number of neutrons, and therefore in the mass number. Almost identical chemical properties exist between isotopes of a particular element. The use of this term as a synonym for nuclide is to be discouraged.

Isotope, Stable: A nonradioactive isotope of an element.

keV: The symbol for 1000 electron volts, or 10^3 eV.

Mass Number: The number of nucleons (protons and neutrons) in the nucleus of an atom.

MeV: The symbol for 1 million electron volts, or 10^6 eV.

Micron: Unit of length equal to 10^{-6} meter. Preferred usage is "micrometer." Use of "micron" is discouraged by IUPAP.

Mil: Linear measurement unit equal to one-thousandth of an inch.

Neutrino: A neutral particle of very small rest mass postulated to account for the continuous distribution of energy among the particles in the beta-decay process and to allow for conservation of momentum in beta decay.

Neutron: Elementary nuclear particle with a mass approximately the same as that of a hydrogen atom and electrically neutral; its mass is 1.008982 mass units. Neutrons are commonly divided into sub-classifications according to their energies as follows: thermal, around 0.025 eV; epithermal, 0.1 eV to 100 eV; slow, <100 eV; intermediate, 10^2 to 10^5 eV; fast, >0.1 MeV.

Nucleon: Common name for a constituent particle of the nucleus; applied to protons and neutrons, but will include any other particle found to exist in the nucleus.

Nucleus (Nuclear): That part of an atom in which the total positive electric charge and most of the mass are concentrated.

Nuclide: A species of atom characterized by the constitution of its nucleus. The nuclear constitution is specified by the number of protons, Z , number of neutrons, N , and energy content; or, alternatively, by the atomic number Z , mass number $A = (N + Z)$, and atomic mass. To be regarded as a distinct nuclide, the atom must be capable of existing for a measurable time; thus nuclear isomers are separate nuclides, whereas promptly decaying excited nuclear states and unstable intermediates in nuclear reactions are not so considered.

Pair Production: An absorption process for x- and gamma-radiation in which the incident photon is annihilated in the vicinity of the nucleus of the absorbing atom with subsequent production of an electron and positron pair. This reaction only occurs for incident photon energies exceeding 1.02 MeV.

Photoelectric Effect: A process by which a photon ejects an electron from an atom. All the energy of the photon is absorbed in ejecting the electron and in imparting kinetic energy to it.

Photon: A quantity of electromagnetic energy whose value in ergs is the product of its frequency in cycles/s and Planck's constant. The equation is: $E = h\nu$.

Planck's Constant: A natural constant of proportionality, (h), relating the frequency of a quantum of energy to the total energy of the quantum:

$$h = \frac{E}{\nu} = 6.624 \times 10^{-27} \text{ erg-s.}$$

Positron: Particle equal in mass to the electron and having an equal but opposite charge.

Power, Stopping: A measure of the effect of a substance upon the kinetic energy of a charged particle passing through it.

Rare Earth: Any of the series of very similar metals ranging in atomic number from 57 through 71.

Reaction (Nuclear): An induced nuclear disintegration, that is, a process occurring when a nucleus comes into contact with a photon, an elementary particle, or another nucleus. In many cases the reaction can be represented by the symbolic equation: $X + a \rightarrow Y + b$ or, in abbreviated form, $X(a,b)Y$, in which X is the target nucleus, a is the incident particle or photon, b is an emitted particle or photon, and Y is the product nucleus.

Roentgen: An exposure dose of x- or gamma-radiation such that the associated corpuscular emission per 0.001293 gram of air produces, in air, ions carrying 1 electrostatic unit of quantity of electricity of either sign (abbreviated R).

Scattering: Change of direction of subatomic particle or photon as a result of a collision or interaction.

Scattering, Compton: The inelastic scattering of a photon through interaction with atomic electrons, accompanied by ejection of a recoil electron from the atom with which the interaction occurred. Compton-scattered photons carry away a fraction of the incident photon energy, ranging from an average of about 85% of the initial energy for a 0.1-MeV photon to an average of about 30% for a 10-MeV photon. Sometimes referred to as incoherent scattering.

Scattering, Elastic: Scattering effected through the agency of elastic collisions and therefore with conservation of kinetic energy of the system. Rayleigh scattering is a form of elastic scattering.

Scattering, Inelastic: The type of scattering which results in the nucleus being left in an excited state and the total kinetic energy being decreased.

Time Units: Standardized abbreviations for time units are:

1 y = 1 year

1 d = 1 day

1 h = 1 hour

1 min = 1 minute

1 s = 1 second

1 ms = 1 millisecond = 10^{-3} s

1 μ s = 1 microsecond = 10^{-6} s

1 ns = 1 nanosecond = 10^{-9} s

1 ps = 1 picosecond = 10^{-12} s

Tritium: (^3_1H or T) The hydrogen isotope having one proton and two neutrons in the nucleus.

X-Rays: Penetrating electromagnetic radiations having wavelengths shorter than those of visible light. They are usually produced by bombarding a metallic target with fast electrons in a high vacuum. In nuclear reactions it is customary to refer to photons originating in the nucleus as gamma rays and those originating in the extranuclear part of the atom as x rays. These rays are sometimes called roentgens, after their discoverer, W. C. Roentgen.

Relative Sensitivities of Elements to Thermal Neutron Activation

The following table of neutron activation analysis sensitivities, taken from ORAU Report 102, Isotopic Neutron Source Experiments, by G. I. Gleason, should be quite useful to schools that have either an isotopic neutron source such as Am-Be or a small ^{252}Cf neutron source. The numbers in the table are equally valid for thermalized accelerator neutron sources. Information can be extracted from this table in regard to unknowns that are used in the activation analysis experiments in this manual.

Experimentally determined sensitivities are relative and are based on the sensitivity of aluminum. If the irradiation and counting system is capable of measuring the results from 1 milligram of aluminum, then it is capable of measuring the listed quantity of each element in milligrams. In each case, the reaction product and gamma energy have been selected to give the best interference-free sensitivity.

Irradiation to saturation is assumed for nuclides having half-lives in seconds or minutes. An overnight, (16-h), irradiation is assumed for longer-lived nuclides.

Measurements of the activities were made with NaI(Tl) scintillation detectors. Sensitivity was assigned on the basis of the amount of the element required to produce a discharge count rate of 100 net counts per minute in the photopeak for the product nuclide. The listed relative sensitivities would be approximately the same for measurement with a Ge(Li) detector. With Ge(Li), longer counting periods are necessary because of their lower efficiencies; hence, very short half-life activities can be expected to show a decreased sensitivity. The higher resolution of the Ge(Li) detector, however, is an advantage when interferences are present.

Neutron Activation Sensitivities

Atomic Number	Element	Product Nuclide	Half-Life	Measured E_{γ} (keV)	Relative Sensitivity*	Atomic Number	Element	Product Nuclide	Half-Life	Measured E_{γ} (keV)	Relative Sensitivity*
9	Fluorine	^{20}F	11.6 s	1634	60.	49	Indium	$^{116\text{m}}\text{In}$	53.7 m	1293	0.006
11	Sodium	^{24}Na	15.0 h	2754	1.5	50	Tin	$^{125\text{m}}\text{Sn}$	9.5 m	331	15.
12	Magnesium	^{27}Mg	9.46 m	844	35.	51	Antimony	^{122}Sb	64.3 h	564	0.7
13	Aluminum	^{28}Al	2.32 m	1779	1.0	52	Tellurium	^{131}Te	24.8 m	150	5.7
17	Chlorine	^{38}Cl	37.3 m	2168	8.	53	Iodine	^{128}I	25.0 m	443	0.3
19	Potassium	^{42}K	12.4 h	1525	28.	55	Cesium	$^{134\text{m}}\text{Cs}$	2.9 h	127	0.4
20	Calcium	^{49}Ca	8.8 m	3084	260.	56	Barium	^{139}Ba	83.0 m	166	3.2
21	Scandium	$^{46\text{m}}\text{Sc}$	18.7 s	143	0.03	57	Lanthanum	^{140}La	40.2 h	1597	0.8
22	Titanium	^{51}Ti	5.79 m	320	18.	58	Cerium	^{143}Ce	33.7 h	293	14.
23	Vanadium	^{52}V	3.75 m	1434	0.07	59	Praseodymium	^{142}Pr	19.2 h	1576	5.
24	Chromium	^{51}Cr	27.8 d	320	85.	60	Neodymium	^{149}Nd	104.0 m	211	5.
25	Manganese	^{56}Mn	2.58 h	847	0.015	62	Samarium	^{153}Sm	46.8 h	103	0.07
27	Cobalt	$^{60\text{m}}\text{Co}$	10.5 m	59	0.23	63	Europium	$^{152\text{m}}\text{Eu}$	9.3 h	963	0.008
28	Nickel	^{65}Ni	2.53 h	1482	130.	64	Gadolinium	^{161}Gd	3.6 m	360	—
29	Copper	^{66}Cu	5.10 m	1039	6.	65	Terbium	^{160}Tb	72.0 d	299	4.
30	Zinc	$^{69\text{m}}\text{Zn}$	14.1 h	439	23.	66	Dysprosium	^{165}Dy	2.32 h	95	0.01
31	Gallium	^{72}Ga	14.1 h	834	0.32	67	Holmium	^{166}Ho	26.8 h	81	0.2
32	Germanium	$^{75\text{m}}\text{Ge}$	48.0 s	140	5.2	68	Erbium	^{171}Er	7.52 h	308	0.36
33	Arsenic	^{76}As	26.4 h	559	0.32	69	Thulium	^{170}Tm	129.0 d	84	90.
34	Selenium	$^{77\text{m}}\text{Se}$	17.4 s	162	0.27	70	Ytterbium	^{175}Yb	101.0 h	396	1.5
35	Bromine	^{80}Br	16.8 m	616	0.8	71	Lutetium	$^{176\text{m}}\text{Lu}$	3.7 h	88	0.2
37	Rubidium	$^{86\text{m}}\text{Rb}$	1.02 m	556	5.	72	Hafnium	$^{179\text{m}}\text{Hf}$	18.6 s	214	0.05
38	Strontium	$^{87\text{m}}\text{Sr}$	2.83 h	389	3.	73	Tantalum	^{182}Ta	115.0 d	1121	35.
39	Yttrium	$^{89\text{m}}\text{Y}$	16.1 s	909	23.	74	Tungsten	^{187}W	24.0 h	686	0.4
42	Molybdenum	^{101}Tc	14.2 m	307	8.	75	Rhenium	^{188}Re	16.7 h	155	0.07
44	Ruthenium	^{105}Ru	4.4 h	724	12.	76	Osmium	^{193}Os	31.5 h	139	35.
45	Rhodium	$^{104\text{m}}\text{Rh}$	4.3 m	51	0.03	77	Iridium	^{192}Ir	74.2 d	317	0.3
46	Palladium	$^{109\text{m}}\text{Pd}$	4.7 m	189	5.5	78	Platinum	^{199}Pt	31.0 m	543	25.
47	Silver	$^{110\text{m}}\text{Ag}$	24.0 s	658	0.35	79	Gold	^{198}Au	64.7 h	412	0.027
48	Cadmium	$^{111\text{m}}\text{Cd}$	49.0 m	245	18.	80	Mercury	^{197}Hg	65.0 h	78	1.2

*The numbers in this column indicate the number of units (weight) of an element that provide a count rate equal to the count rate furnished from irradiation of one unit weight of aluminum.

X-Ray Critical-Absorption and Emission Energies in keV

By S. FINE and C. F. HENDEE
Philips Laboratories
Irvington on Hudson, New York

Increased use of energy-proportional detectors for x rays has created a need for a table of energy values of K and L absorption and emission series.

The table presented here includes all elements. Most values were obtained by a conversion to keV of tabulated experimental wavelength values (1-3); some are from previous energy-value compilations (4,5). Where a choice existed, the value chosen was the one derived from later work. Certain values were determined by interpolation, using Moseley's law. (All this is annotated in footnotes.)

The conversion equations relating energy and wavelength used are (6)

$$E(\text{keV}) = (12.39644 \pm 0.00017)/\lambda(\text{\AA}) \\ = 12.39644/1.002020 \lambda(\text{kX unit})$$

In computing values the number of places retained sufficed to maintain the uncertainty in the original source value. The values in the table have been listed uniformly to 1 eV. However, chemical form may shift absorption edges as much as 10-20 eV (4,5).

To discover computational errors a fit was made to Moseley's law. In general the values were consistent, however there were a few irregularities due to the deviation of some input values (1). These were retained in the body of the table but a set of values calculated to fit better are footnoted.

* * *

The authors wish to express their appreciation to W. Parrish for helpful suggestions and to H. Kasper for performing the computation in connection with this work.

BIBLIOGRAPHY

1. Y. Cauchois, H. Hulubei, "Tables de Constantes et Donnees Numeriques, I, Longueurs D'Onde des Emissions X et des Discontinuites D'Absorption X" (Hermann et Cie, Paris, France, 1947).
2. A. H. Compton and S. K. Allison, "X-Rays in Theory and Experiment" (D. Van Nostrand Co., Inc., New York, 1951).
3. C. E. Moore, "Atomic Energy Levels," NBS 467 (National Bureau of Standards, U.S. Department of Commerce, Washington, D.C., 1949).
4. Y. Cauchois, J. phys. radium **13**, 113 (1952).
5. R. D. Hill, E. L. Church, and J. W. Mihelich, Rev. Sci. Instr. **23**, 523 (1952).
6. J. W. M. DuMond, E. R. Cohen, Phys. Rev. **82**, 555 (1951).

X-Ray Critical-Absorption and Emission Energies in keV

Atomic Number	Element	K series					L series							
		K _{ab}	K _{β₂}	K _{β₁}	K _{α₁}	K _{α₂}	L _{Iab}	L _{IIab}	L _{IIIab}	L _{γ₁}	L _{β₂}	L _{β₁}	L _{α₁}	L _{α₂}
1	Hydrogen	0.0136†												
2	Helium	0.0246†												
3	Lithium	0.055				0.052								
4	Beryllium	0.116‡				0.110								
5	Boron	0.192†				0.185								
6	Carbon	0.283				0.282								
7	Nitrogen	0.399				0.392								
8	Oxygen	0.531				0.523								
9	Fluorine	0.687†				0.677								
10	Neon	0.874*				0.851‡	0.048†	0.022†	0.022†					
11	Sodium	1.08*		1.067		1.041	0.055‡	0.034‡	0.034‡					
12	Magnesium	1.303		1.297		1.254	0.063	0.050	0.049					
13	Aluminum	1.559		1.553	1.487	1.486	0.087	0.073**	0.072**					
14	Silicon	1.838		1.832	1.740	1.739	0.118*	0.099**	0.098**					
15	Phosphorus	2.142		2.136	2.015‡	2.014‡	0.153*	0.129‡	0.128‡					
16	Sulphur	2.470		2.464	2.308	2.306	0.193*	0.164**	0.163**					
17	Chlorine	2.819‡		2.815	2.622	2.621	0.238*	0.203‡	0.202‡					
18	Argon	3.203		3.192‡	2.957	2.955	0.287*	0.247**	0.245**					
19	Potassium	3.607		3.589	3.313	3.310	0.341*	0.297**	0.294**					
20	Calcium	4.038		4.012	3.691	3.688	0.399*	0.352	0.349			0.344	0.341	
21	Scandium	4.496		4.460	4.090	4.085	0.462*	0.411**	0.406**			0.399	0.395	
22	Titanium	4.964		-4.931	4.510	4.504	0.530*	0.460**	0.454**			0.458	0.452	
23	Vanadium	5.463		-5.427	4.952	4.944	0.604*	0.519**	0.512**			0.519	0.510	
24	Chromium	5.988		-5.946	5.414	5.405	0.679*	0.583**	0.574**			0.581	0.571	
25	Manganese	6.537		6.490	5.898	5.887	0.762*	0.650**	0.639**			0.647	0.636	
26	Iron	7.111		7.057	6.403	6.390	0.849*	0.721**	0.708**			0.717	0.704	
27	Cobalt	7.709		7.649	6.930	6.915	0.929*	0.794**	0.779**			0.790	0.775	
28	Nickel	8.331	8.328	8.264	7.477	7.460	1.015*	0.871**	0.853**			0.866	0.849	
29	Copper	8.980	8.976	8.904	8.047	8.027	1.100*	0.953	0.933			0.948	0.928	
30	Zinc	9.660	9.657	9.571	8.638	8.615	1.200*	1.045	1.022			1.032	1.009	
31	Gallium	10.368	10.365	10.263	9.251	9.234	1.30*	1.134**	1.117**			1.122	1.096	
32	Germanium	11.103	11.100	10.981	9.885	9.854	1.42*	1.248**	1.217**			1.216	1.186	
33	Arsenic	11.863	11.863	11.725	10.543	10.507	1.529	1.359	1.323			1.317	1.282	
34	Selenium	12.652	12.651	12.495	11.221	11.181	1.652	1.473	1.434			1.419	1.379	
35	Bromine	13.475	13.465	13.290	11.923	11.877	1.794‡	1.599**	1.552**			1.526	1.480	
36	Krypton	14.323	14.313	14.112	12.648	12.597	1.931‡	1.727**	1.675**			1.638‡	1.587**	
37	Rubidium	15.201	15.184	14.960	13.394	13.335	2.067	1.866	1.806			1.752	1.694	1.692
38	Strontium	16.106	16.083	15.834	14.164	14.097	2.221	2.008	1.941			1.872	1.806	1.805
39	Yttrium	17.037	17.011	16.736	14.957	14.882	2.369	2.154	2.079			1.996	1.922	1.920
40	Zirconium	17.998	17.969	17.666	15.774	15.690	2.547	2.305	2.220	2.302	2.219	2.124	2.042	2.040

Atomic Number	Element	K series					L series							
		K_{ab}	$K\beta_2$	$K\beta_1$	$K\alpha_1$	$K\alpha_2$	L_{Iab}	L_{IIab}	L_{IIIab}	$L\gamma_1$	$L\beta_2$	$L\beta_1$	$L\alpha_1$	$L\alpha_2$
41	Niobium	18.987	18.951	18.621	16.614	16.520	2.706	2.467**	2.374	2.462	2.367	2.257	2.166	2.163
42	Molybdenum	20.002	19.964	19.607	17.478	17.373	2.884	2.627	2.523	2.623	2.518	2.395	2.293	2.290
43	Technetium	21.054§	21.012§	-20.585¶	18.410¶	18.328¶	3.054§	2.795§	2.677§	2.792§	2.674§	2.538§	2.424§	2.420§
44	Ruthenium	22.118	22.072	21.655	19.278	19.149	3.236§	2.966	2.837	2.964	2.836	2.683	2.558	2.554
45	Rhodium	23.224	23.169	22.721	20.214	20.072	3.419	3.145	3.002	3.144	3.001	2.834	2.696	2.692
46	Palladium	24.347	24.297	23.816	21.175	21.018	3.617	3.329	3.172	3.328	3.172	2.990	2.838	2.833
47	Silver	25.517	25.454	24.942	22.162	21.988	3.810	3.528	3.352	3.519	3.348	3.151	2.984	2.978
48	Cadmium	26.712	26.641	26.093	23.172	22.982	4.019	3.727	3.538	3.716	3.528	3.316	3.133	3.127
49	Indium	27.928	27.859	27.274	24.207	24.000	4.237	3.939	3.729	3.920	3.713	3.487	3.287	3.279
50	Tin	29.190	29.106	28.483	25.270	25.042	4.464	4.157	3.928	4.131	3.904	3.662	3.444	3.435
51	Antimony	30.486	30.387	29.723	26.357	26.109	4.697	4.381	4.132	4.347	4.100	3.843	3.605	3.595
52	Tellurium	31.809	31.698	30.993	27.471	27.200	4.938	4.613	4.341	4.570	4.301	4.029	3.769	3.758
53	Iodine	33.164	33.016	32.292	28.610	28.315	5.190	4.856	4.559	4.800	4.507	4.220	3.937	3.926
54	Xenon	34.579	34.446¶	33.644	29.802¶	29.485¶	5.452	5.104	4.782	5.036§	4.720§	4.422§	4.111§	4.098§
55	Cesium	35.959	35.819	34.984	30.970	30.623	5.720	5.358	5.011	5.280	4.936	4.620	4.286	4.272
56	Barium	37.410	37.255	36.376	32.191	31.815	5.995	5.623	5.247	5.531	5.156	4.828	4.467	4.451
57	Lanthanum	38.931	38.728	37.799	33.440	33.033	6.283	5.894	5.489	5.789	5.384	5.043	4.651	4.635
58	Cerium	40.449	40.231	39.255	34.717	34.276	6.561	6.165†	5.729	6.052	5.613	5.262	4.840	4.823
59	Praseodymium	41.998	41.772	40.746	36.023	35.548	6.846	6.443	5.968	6.322	5.850	5.489	5.034	5.014
60	Neodymium	43.571	43.298¶	42.269	37.359	36.845	7.144	6.727	6.215	6.602	6.090	5.722	5.230	5.208
61	Promethium	45.207§	44.955§	-43.945¶	38.649¶	38.160¶	7.448§	7.018§	6.466§	6.891§	6.336§	5.956	5.431	5.408§
62	Samarium	46.846	46.553¶	45.400	40.124	39.523	7.754	7.281¶	6.721	7.180	6.587	6.206	5.636	5.609
63	Europium	48.515	48.241	47.027	41.529	40.877	8.069	7.624	6.983	7.478	6.842	6.456	5.846	5.816
64	Gadolinium	50.229	49.961	48.718	42.983	42.280	8.393	7.940	7.252	7.788	7.102	6.714	6.059	6.027
65	Terbium	51.998	51.737	50.391	44.470	43.737	8.724	8.258	7.519	8.104	7.368	6.979	6.275	6.241
66	Dysprosium	53.789	53.491	52.178	45.985	45.193	9.083	8.621¶	7.850¶	8.418	7.638	7.249	6.495	6.457
67	Holmium	55.615	55.292**	53.934§	47.528	46.686	9.411	8.920	8.074	8.748	7.912	7.528	6.720	6.680
68	Erbium	57.483	57.088	55.690	49.099	48.205	9.776	9.263	8.364	9.089	8.188	7.810	6.948	6.904
69	Thulium	59.335¶	58.969**	57.576¶	50.730	49.762	10.144	9.628	8.652	9.424	8.472	8.103	7.181	7.135
70	Ytterbium	61.303	60.959	59.352	52.360	51.326	10.486	9.977	8.943	9.779	8.758	8.401	7.414	7.367
71	Lutecium	63.304	62.946	61.282	54.063	52.959	10.867	10.345	9.241	10.142	9.048	8.708	7.654	7.604
72	Hafnium	65.313	64.936	63.209	55.757	54.579	11.264	10.734	9.556	10.514	9.346	9.021	7.898	7.843
73	Tantalum	67.400	66.999	65.210	57.524	56.270	11.676	11.130	9.876	10.892	9.649	9.341	8.145	8.087
74	Tungsten	69.508	69.090	67.233	59.310	57.973	12.090	11.535	10.198	11.283	9.959	9.670	8.396	8.333
75	Rhenium	71.662	71.220	69.298	61.131	59.707	12.522	11.955	10.531	11.684	10.273	10.008	8.651	8.584
76	Osmium	73.860	73.393	71.404	62.991	61.477	12.965	12.383	10.869	12.094	10.596	10.354	8.910	8.840
77	Iridium	76.097	75.605	73.549	64.886	63.278	13.413	12.819	11.211	12.509	10.918	10.706	9.173	9.098
78	Platinum	78.379	77.866	75.736	66.820	65.111	13.873	13.268	11.559	12.939	11.249	11.069	9.441	9.360
79	Gold	80.713	80.165	77.968	68.794	66.980	14.353	13.733	11.919	13.379	11.582	11.439	9.711	9.625
80	Mercury	83.106	82.526	80.258	70.821	68.894	14.841	14.212	12.285	13.828	11.923	11.823	9.987	9.896
81	Thallium	85.517	84.904	82.558	72.860	70.820	15.346	14.697	12.657	14.288	12.268	12.210	10.266	10.170
82	Lead	88.001	87.343	84.922	74.957	72.794	15.870	15.207	13.044	14.762	12.620	12.611	10.549	10.448
83	Bismuth	90.521	89.833	87.335	77.097	74.805	16.393	15.716	13.424	15.244	12.977	13.021	10.836	10.729
84	Polonium	93.112	92.386	89.809	79.296	76.868	16.935	16.244	13.817	15.740	13.338	13.441	11.128	11.014
85	Astatine	95.740	94.976	92.319	81.525	78.956	17.490	16.784	14.215	16.248	13.705	13.873	11.424	11.304
86	Radon	98.418	97.616	94.877	83.800	81.080	18.058	17.337	14.618	16.768	14.077	14.316	11.724	11.597
87	Francium	101.147	100.305	97.483	86.119	83.243	18.638	17.904	15.028	17.301	14.459	14.770	12.029	11.894
88	Radium	103.927	103.048	100.136	88.485	85.446	19.233	18.481	15.442	17.845	14.839	15.233	12.338	12.194
89	Actinium	106.759	105.838	102.846	90.894	87.681	19.842	19.078	15.865	18.405	15.227	15.712	12.650	12.499
90	Thorium	109.630	108.671	105.592	93.334	89.942	20.460	19.688	16.296	18.977	15.620	16.200	12.966	12.808
91	Protactinium	112.581	111.575	108.408	95.851	92.271	21.102	20.311	16.731	19.559	16.022	16.700	13.291	13.120
92	Uranium	115.591	114.549	111.289	98.428	94.648	21.753	20.943	17.163	20.163	16.425	17.218	13.613	13.438
93	Neptunium	118.619	117.533	114.181	101.005	97.023	22.417	21.596	17.614	20.774	16.837	17.740	13.945	13.758
94	Plutonium	121.720	120.592	117.146	103.653	99.457	23.097	22.262	18.066	21.401	17.254	18.278	14.279	14.082
95	Americium	124.876	123.706	120.163	106.351	101.932	23.793	22.944	18.525	22.042	17.677	18.829	14.618	14.411
96	Curium	128.088	126.875	123.235	109.098	104.448	24.503	23.640	18.990	22.699	18.106	19.393	14.961	14.743
97	Berkelium	131.357	130.101	126.362	111.896	107.023	25.230	24.352	19.461	23.370	18.540	19.971	15.309	15.079
98	Californium	134.683	133.383	129.544	114.745	109.603	25.971	25.080	19.938	24.056	18.980	20.562	15.661	15.420
99		138.067	136.724	132.781	117.646	112.244	26.729	25.824	20.422	24.758	19.426	21.166	16.018	15.764
100		141.510	140.122	136.075	120.598	114.926	27.503	26.584	20.912	25.475	19.879	21.785	16.379	16.113

For $Z \leq 69$, values without symbols are derived from (1). Values prefixed with a - sign are $K\beta_{1,2}$.
 For $Z \geq 70$, absorption-edge values are from (4) in the case of $Z = 70-83, 88, 90$, and 92; remaining absorption edges to $Z = 100$ are obtained from these by least-squares quadratic fitting. All emission values for $Z \geq 70$ are derived from the preceding absorption edges, and others based on (4), using the transition relations $K\alpha_1 = K_{ab} - L_{III}$, $K\alpha_2 = K_{ab} - L_{II}$, $K\beta_1 = K_{ab} - M_{III}$, etc.
 * Obtained from R. D. Hill, E. L. Church, J. W. Mihelich (5). † Derived from Compton and Allison (2). ‡ Derived from C. E. Moore (3).
 ¶ Values derived from Cauchois and Hulubei (1) which deviate from the Moseley law. Better-fitting values are: $Z = 17$, $K_{ab} = 2.826$; $Z = 43$, $K\alpha_1 = 18.370$, $K\alpha_2 = 18.250$, $K\beta_1 = 20.612$; $Z = 54$, $K\alpha_1 = 29.779$, $K\alpha_2 = 29.463$, $K\beta_2 = 34.398$; $Z = 60$, $K\beta_2 = 43.349$; $Z = 61$, $K\alpha_1 = 38.726$, $K\alpha_2 = 38.180$, $K\beta_1 = 43.811$; $Z = 62$, $K\beta_2 = 46.581$, $L_{II} = 7.312$; $Z = 66$, $L_{II} = 8.591$, $L_{III} = 7.790$; $Z = 69$, $K_{ab} = 59.382$, $K\beta_1 = 57.487$.
 § Calculated by method of least squares. ** Calculated by transition relations.

Timing Single-Channel Analyzer

- Single-channel analyzer and timing signal derivation
- Trailing-edge constant-fraction timing provides walk $\leq \pm 3$ ns for 100:1 dynamic range
- Integral, normal, and window modes
- Separate lower-level and upper-level discriminator outputs
- DC-coupled
- Adjustable delay 0.1 to 11 μ s
- Provision for external baseline sweep



The EG&G ORTEC Model 551 Timing Single-Channel Analyzer performs the dual functions of single-channel pulse-height analysis and timing signal derivation.

The patented* trailing-edge constant-fraction timing technique provides unexcelled timing on either unipolar or bipolar signals and shows better results than are possible with conventional leading-edge discriminators.

With SCAs that utilize leading-edge timing, the rise time of the input pulses causes degradation of time resolution because the pulses have varying amplitudes.

Constant-fraction timing compensates for varying amplitudes and essentially eliminates this timing shift, giving consistently better timing results.

For the internally set 50% fraction, the output occurs soon after the midpoint on the linear input trailing edge to facilitate gating and accumulation of data at very high input rates. This technique also minimizes timing shift and dead time when used with sodium iodide, silicon, and germanium detectors, thereby allowing better system time resolution and higher counting rates.

The constant-fraction technique makes it possible to realize significant improvements in time resolution in most timing applications. Notice that analysis is made of the main amplifier output. This

technique allows optimization of time resolution and extension of dynamic range for neutron-gamma discrimination and other timing applications. Walk of < 3 ns for 100:1 dynamic range using input pulses from a pulser is possible.

The Model 551 is versatile, with three basic operating modes provided. In the Window mode, the unit operates as a high-resolution, narrow (0 to 10%) window, single-channel analyzer. For wide-window applications, the Normal mode is used. In this mode the upper-level and lower-level controls are independently variable from 0 to 10 V, and an output is generated for pulses analyzed between the levels. Through use of the separate rear-panel LL Out and UL Out outputs, the unit can operate as a dual wide-dynamic-range integral discriminator for leading-edge timing or for pulse routing.

The dc-coupled input of the Model 551 makes it possible to take full advantage of the baseline restoration of the main amplifier for maximum performance at widely varying counting rates.

The continuously adjustable output delay (two ranges covering 0.1 to 11 μ s) makes it possible to align output signals that have actual time differences without a need for additional delay devices or modules. Alternatively an External strobe input can be used to cause an SCA output at the desired time.

For an application where it is desirable to scan an entire spectrum, an external base-line sweep input is provided via the rear-panel LL Ref Ext BNC connector. In this mode of operation, the baseline (lower-level threshold) on which a window is riding is swept through an energy range and the count rate is recorded as a function of energy.

*U.S. Patent No. 3,714,464.

Specifications

PERFORMANCE

DYNAMIC RANGE 200:1.

PULSE-PAIR RESOLVING TIME Output pulse width plus Delay (as selected by the front-panel Delay controls), plus 100 ns for fast NIM output or plus 200 ns for positive NIM output. Minimum resolving time for negative output 220 ns; for positive output 800 ns.

THRESHOLD TEMPERATURE

INSTABILITY $\pm 0.01\%/^{\circ}\text{C}$ of full scale, 0 to 50°C using a NIM Class A power supply (referenced to -12 V).

DISCRIMINATOR NONLINEARITY $\pm 0.25\%$ of full scale (integral) for both discriminators.

DELAY TEMPERATURE INSTABILITY $\pm 0.03\%/^{\circ}\text{C}$ of full scale, 0 to 50°C .

DELAY NONLINEARITY $< \pm 2\%$ of delay range.

WINDOW WIDTH CONSTANCY $\pm 0.1\%$ variation of full-scale window width over the linear range 0 to 10 V.

MINIMUM INPUT THRESHOLD 50 mV for lower-level discriminator.

TIME SHIFT vs PULSE HEIGHT (WALK)

Walk (ns)		Dynamic Range
System A	System B	
± 1.0	± 2.0	10:1
± 2.5	± 4.0	50:1
± 3.0	± 8.0	100:1

System A: Using an EG&G ORTEC Model 460 Amplifier, single delay-line mode, integrate 0.1 μs with 1- μs delay line.

System B: Using an EG&G ORTEC Model 570, 571, or 572 Amplifier, unipolar output with 0.5- μs shaping time. Input from EG&G ORTEC Model 419 Pulser.

CONTROLS

LOWER LEVEL Front-panel 10-turn potentiometer adjustable from 0 to 10 V; when the rear-panel LL Ref mode switch is set on Int, determines the threshold setting for the lower-level discriminator. When the LL REF mode switch on the rear panel is in the EXT position, this control is ineffective.

WINDOW OR UPPER LEVEL Front-panel 10-turn potentiometer determines the window width (0 to +1 V) in the Window mode or the upper-level (0 to +10 V) threshold in the Normal mode. This control is disabled in the Integral mode.

INT/NOR/WIN Front-panel 3-position locking toggle switch selects one of three operating modes:

Integral LL sets a single-discriminator threshold (0 to +10 V) and UL is disabled.

Normal UL and LL are independently adjustable levels (0 to +10 V).

Window LL sets the baseline level (0 to +10 V) and UL sets the window width (0 to +1 V).

DELAY RANGE Front-panel locking toggle switch selects delay ranges of 0.1 to 1.1 μs or 1.0 to 11 μs .

DELAY Front-panel 10-turn potentiometer for continuous adjustment of output delay over selected range. In the external strobe mode the delay control adjusts the automatic reset time from 5 μs to 50 μs .

WALK ADJUST Front-panel screwdriver adjustment for precise setting of walk compensation.

LL REF MODE Rear-panel 2-position locking toggle switch selects either the front-panel LL potentiometer or the voltage signal applied to the rear-panel LL REF EXT connector as the LL discriminator reference threshold.

STROBE Rear-panel 2-position locking toggle switch selects either Internal or External source for the SCA output signal strobe function.

INPUTS

SIGNAL INPUT Front-panel dc-coupled BNC connector accepts positive unipolar or bipolar signal, 0 to +10 V linear range, $\pm 12\text{ V}$ maximum; width 100 ns; 1000- input impedance. Rear-panel ac-coupled BNC connector accepts positive unipolar or bipolar signal, 0 to +10 V linear range, $\pm 100\text{ V}$ maximum; width 0.2 to 10 μs ; 1000- input impedance.

LL REF EXT When the rear-panel LL REF mode switch is on EXT, the rear-panel LL REF EXT BNC connector accepts the lower-level biasing (an input of 0 to -10 V on this connector corresponds to a range of 0 to 10 V for the lower-level discriminator setting). Input protected to $\pm 24\text{ V}$.

EXT STROBE INT When the rear-panel EXT/INT STROBE locking toggle switch is in EXT, the rear-panel EXT STROBE IN BNC connector accepts a positive NIM-standard input, nominally +5 V, 500 ns wide, to cause an output to occur from the SCA. The external strobe should be given within 5 μs (or 50 μs as determined by the front-panel Delay control) of the linear input. At the end of this period, the Model 551 resets its internal logic without producing an output signal.

OUTPUTS

SCA POS OUT Front- and rear-panel BNC connectors provide positive NIM-standard output, nominally +5 V; 500 ns wide; 10- output impedance. For internal strobe the output occurs at the midpoint of the linear input trailing edge plus the output Delay as selected by the front-panel controls. For external strobe the output occurs at the time of strobe signal.

SCA NEG OUT Front-panel BNC connector provides fast NIM-standard output, nominally -16 mA (-800 mV on 50- load); width 20 ns; rise time 5 ns; 10- output impedance. Output occurs at the mid-point of the linear trailing edge plus the output Delay as selected by the front-panel controls.

LL OUT Rear-panel BNC connector provides positive NIM-standard output, nominally +5 V, 500 ns wide; 10- output impedance. Output occurs as leading edge of linear input crosses the LL threshold.

UL OUT Rear-panel BNC connector provides NIM-standard output, nominally +5 V, 500 ns wide; 10- output impedance. Output occurs as leading edge of linear input crosses the UL threshold.

ELECTRICAL AND MECHANICAL

POWER REQUIRED +12 V, 160 mA; -12 V , 110 mA; +24 V, 90 mA; -24 V , 50 mA.

WEIGHT

Net 1.1 kg (2.5 lb).

Shipping 2.25 kg (5.0 lb).

DIMENSIONS NIM-standard single-width module 3.43 X 22.13 cm (1.35 X 8.714 in.) per DOE/ER-0457T.

Related Equipment

The Model 551 is compatible with all EG&G ORTEC amplifiers and other amplifiers having a 0 to 10 V positive, linear output range.

Ordering Information

To order, specify:

Model	Description
551	Timing Single-Channel Analyzer

480 Pulser

The EG&G ORTEC Model 480 Pulser simulates the output signal from a solid-state or scintillation detector and provides a means of checking electronic instruments in a pulse processing system. It has 1% overall accuracy, good stability as a function of temperature and time, and front-panel controls that allow the instrument to be calibrated to read directly in terms of equivalent energy deposited in a detector. The Model 480 has a stable internal reference voltage that is effectively independent of any modular power supply or ac line voltage changes. Four toggle switches in a pi-attenuator arrangement in the attenuated output line provide a maximum attenuation of 1000:1. The direct output precedes the attenuator switches and provides a means of stable oscilloscope triggering. A charge terminator and a 100- Ω voltage terminator are provided with this instrument. The use of the charge terminator allows the voltage pulse to be converted to a charge pulse for subsequent amplification by a charge-sensitive preamplifier. The use of the voltage terminator allows the voltage pulse to be input directly to other instruments such as amplifiers, discriminators, and ADCs. A holder is provided on the rear panel to store the charge terminator when it is not in use.

The Model 480 Pulser is designed to meet the interchangeability standards of DOE/ER-0457T. An EG&G ORTEC NIM bin and power supply provides all necessary power through the rear module connector. All signal levels and impedances are compatible with all other EG&G ORTEC NIM-standard modules.

Specifications

PERFORMANCE

TEMPERATURE INSTABILITY $\leq \pm 0.01\%/^{\circ}\text{C}$, 0 to 50 $^{\circ}\text{C}$.

LINE VOLTAGE INSTABILITY $\leq \pm 0.005\%$ per 10% change in line voltage.

RIPPLE AND NOISE 0.003% of pulse amplitude.

NONLINEARITY $\leq \pm 0.25\%$ of full scale.

RISE TIME Exponential waveform, 610 ns (10 to 90%).

FALL TIME Exponential decay with 200- or 400- μs time constant (depending on whether or not the direct output is terminated).

CONTROLS

CAL 22-turn potentiometer on front panel covers 62:1 amplitude span for normalization of Pulse Height control to read directly in equivalent energy.

PULSE HEIGHT Front-panel potentiometer controls output pulse height from 0 V to the maximum determined by the Attenuator switches, the Cal control setting, and the termination load.

ATTENUATOR Front-panel switches provide step attenuation over 1000:1 range with 1% resistors (X2, X5, X10, X10).

OFF/ON Front-panel slide switch allows internal relay to be driven from the ac line.

NEG/POS Front-panel slide switch determines polarity of the output signal.

OUTPUTS

ATTEN Front-panel BNC connector provides positive or negative attenuated dc-coupled output with an impedance of 100 Ω . Amount of attenuation is set by the Attenuator switches.

DIRECT Front-panel BNC connector provides positive or negative dc-coupled 0 to 10 V pulse into a high impedance and 0 to 5 V maximum pulse into 100 Ω . This is equivalent to a range of 0 to 220-MeV energy referred to a silicon detector, when used with associated charge terminator.

ELECTRICAL AND MECHANICAL

POWER REQUIRED +24 V, 60 mA; -24 V, 60 mA; +12 V, 0 mA; -12 V, 0 mA; 117 V ac, 8 mA (used only to drive relay).

WEIGHT

Net 0.9 kg (2.1 lb).

Shipping 1.8 kg (4.1 lb).

DIMENSIONS NIM-standard single-width module 3.43 X 22.13 cm (1.35 X 8.714 in.) per DOE/ER-0457T.

Included Accessories

VOLTAGE TERMINATOR A standard 100- Ω resistive terminator is attached to the Direct Output connector on the front panel to terminate the output correctly when only the Attenuated Output is being used.

CHARGE TERMINATOR A specially constructed terminator is mounted in a rear-panel clip and should be used to properly terminate the pulser output and feed a charge signal into the signal input of a charge-sensitive preamplifier when the output pulses are being furnished for this type of test.

Ordering Information

Model	Description
480	Pulser

- Simulates detector output signals
- May be calibrated to read directly in terms of equivalent energy deposition in semiconductor detectors
- Exponential pulse shape with <10-ns rise time and 200- or 400- μs decay time constant
- Line frequency pulse rate
- Positive or negative polarity
- Direct 0 to 10-V output
- Attenuated output with 1000:1 attenuation range

